Coordination of Reproductive Shoot Architecture in Cereals in Response to Resource Availability

Alex Michael Wakeman

Submitted in accordance with the requirements for the degree of Doctor of Philosophy

University of Leeds
Faculty of Biological Sciences

October 2024

The candidate confirms that the work submitted is his own and that appropriate credit has been given where reference has been made to the work of others.

Nec requies, quin aut pomis exuberet annusaut fetu pecorum
aut Cerealis mergite culmi, proventuque oneret sulcos atque horrea vincat.

No respite! still the year o'erflows with fruit,
Or young of kine, or Ceres' wheaten sheaf,
With crops the furrow loads, and bursts the barns.

Acknowledgements

The following is stated with the greatest extent of sincerity and gratitude that I can communicate through written language.

I give thanks to the people and communities who have contributed to this thesis, via their support, conversation and patience. Adjacency to the passion, pulse and power of such people has allowed me with freest action to form this work and myself as a scientist.

Dr Tom Bennett would deserve unceasing gratitude solely for his practical guidance on experimental design, data analysis and the writing of this thesis. However, his role as a supervisor has extended to encompass not only the development of my scientific output, but my development as a scientist and thinker. Through him, I am fortunate to have developed the invaluable insight that a PhD is a Doctor of *Philosophy*.

I could not ask for a more nurturing community in which to grow, learn and work than the Bennett lab and I owe thanks to every past and current member. However, it would be a disservice to not specifically thank Dr Catriona Walker for her singular kindness and support. Through her, an entire lab has been furnished with a model example of a PhD student, postdoctoral researcher and leader which we might aspire towards.

Finally, my untempered gratitude must be directed towards the wider community of PhD students and researchers in Leeds and across the world, whom I have befriended and collaborated with. There is not the space to list every intelligent, diligent and kind-hearted person I have encountered in the past four years, suffice to say I am both overwhelmed and energised by their abundance. In particular, any attempts to properly express my appreciation for the tenacity and brilliance of Dr Iain Lawson, India Lacey, Dr Katherine O'Connor and Jillian Schacher would be insufficient; fortunately, their similarly exemplary kindness and humility renders the need for such words superfluous.

Abstract

The successful development and maturation of seed is essential for determining the reproductive success of almost all angiosperms and is therefore also an essential determinant of yield in many of the world's most consumed crops, including wheat and barley. The development of structures such as tillers, ears and spikelets that constrain final seed set is under tight developmental control in both space and time. Evidence from various species indicates that this developmental control is heavily influenced by resource availability (including nutrient availability and soil volume availability), but is also subject to feedback control between different structures on the shoot. The mechanisms underlying the resource-related coordination of shoot architecture are generally poorly characterised in cereals but likely utilise long-distance hormonal signalling. Here, I investigate how shoot architecture in wheat is coordinated in response to environmental and endogenous stimuli and try to understand the hormonal signalling mechanisms by which this occurs. I show that actively developing spikelets repress tiller outgrowth in wheat and barley, in a previously unreported mechanism of correlative inhibition. I further show that cytokinin is likely to coordinate this feedback alongside the development of paired spikelets. Cytokinin and strigolactone are shown to delay and accelerate SAM development respectively, in a mechanism which could coordinate tiller and spikelet number distinct from previously reported genetic networks. Additionally, I report how wheat responds to environmental resource restriction by prioritizing its developmental effort in a small number of the earliest emerging tillers and suggest that strigolactone may be an essential hormone in coordinating this response. This work develops species-specific understanding of the distribution of perceived resource availability between different aspects of shoot architecture and supports the growing academic consensus that manipulation of hormone levels in time and space could result in improved crop yields without the need for increased resource inputs.

List of abbreviations

6-BA	6-benzylaminopurine
ANOVA	Analysis of Variance
APO1	*ABERRANT PANICLE ORGANIZATION1*
ARF	AUXIN RESPONSE FACTOR
ATS	*Arabidopsis thaliana* salts
BA1	*BARREN STALK1*
BD1	*BRANCHED SILKLESS1*
BRC1	*BRANCHED1*
$Ca(NO_3)_2$	Calcium Nitrate
CCD7/8	CAROTENOID CLEAVAGE DIOXYGENASE 7/8
cDNA	Complementary DNA
CLV	CLAVATA
COM	COMPOSITUM
Ctrl.	Control
CK	Cytokinin
CKX	Cytokinin dehydrogenase
cZ	*Cis*-Zeatin
DaP	Days after planting
D3/10/14/53	DWARF3/10/14/53
FC1	FINE CULM1
FM	Floret meristem
FZP	FRIZZY PANICLE
FT1/FT2	FLOWERING LOCUS T1/2
GT1	Grassy tillers1
GRF	Growth regulating factor
High[N]	High nitrate
*Hv_*	*Hordeum vulgare* (Barley)
hb	*highly branched*
IAA	Indole-3-acetic acid
IM	Inflorescence meristem
INT-C	INTERMEDIUM-C

IPT	*ISOPENTENYL TRANSFERASE*
KNO_3	Potassium Nitrate
LOG	LONELY GUY
Low[N]	Low nitrate
MAX	More axillary growth
Mid[N]	Mid nitrate
MOC1	*MONOCULM1*
miRNA	Micro RNA
mRNA	messenger RNA
n	Number of samples
*Os_*	*Oryza sativa* (rice)
PIN	PIN-FORMED
PRR	Pseudo-response regulator
Ppd-1	Photoperiod-1
qPCR	quantitative polymerase chain reaction
R^2	Coefficient of determination
SAM	Shoot apical meristem
SD	Standard deviation
SM	Spikelet meristem
SPL	*SQUAMOSA PROMOTER-BINDING-LIKE*
SVA	Soil volume availability
SL	Strigolactone
*Ta_*	*Triticum aestivum* (Bread wheat)
TB1	Teosinte Branched1
TF	Transcription factor
TFL1	*TERMINAL FLOWER1*
TGA1	*TEOSINTE GLUME ARCHITECTURE1*
TSM	Triple spikelet meristem
Type-A RRA/Type-B RRA	Type-A/Type-B ARABIDOPSIS RESPONSE REGULATOR
tZ	*trans*-Zeatin
VM	Vegetative meristem
VRN1	*Vernalization1*
vrs1	*SIX-ROWED SPIKE1*

WT	Wild-type
WPS1	WHEAT PAIRED SPIKELETS 1
WUS	WUSCHEL

Contents

List of Figures

Chapter 1 – General Introduction

Chapter 2 – Materials and Methods

Chapter 3 – Spikelet-Tiller feedback in wheat and barley

Chapter 5 – Coordination of reproductive shoot architecture in cereals with soil volume availability

Chapter 6 – Discussion

Chapter 1

General Introduction

1.1 General Introduction

Bread wheat (*Triticum aestivum*) is one of the most widely consumed crops on the planet, providing approximately 20% of global calories and protein (Reynolds *et al.*, 2009, p. 20). Global population increases and predicted climate change-driven losses of arable land have led to the conclusion that wheat yields must increase significantly beyond current levels (Pequeno *et al.*, 2021). Creating new wheat varieties with improved yield potential will ultimately involve increasing either the size or number of grains produced by elite wheat varieties. However, after rapid yield increases during the 'Green Revolution' in the 1960s, global crop yields are now failing to increase at a rate predicted to be necessary to maintain or improve food security (Ray *et al.*, 2013). New insights into the grain-formation and filling processes are therefore needed to overcome this yield plateau.

The production of the grain in wheat is dependent on the development of many precursor structures, such as branches (called tillers in wheat and other grasses), inflorescences and flowers. The spatio-temporal production of these underpinning structures is referred to as 'reproductive architecture' (Walker, Wheeldon and Bennett, 2021). Reproductive architecture in wheat (and indeed other flowering plants) is highly sensitive to the resources available to the plant; mineral nutrient concentration (Luo, Zhang and Xu, 2020), water availability (Ha *et al.*, 2014) and soil volume (Wheeldon *et al.*, 2020) have all been linked to reproductive architecture development. This allows plants to match their seed-set to prevailing environmental conditions. However, since plants normally exist in an environment where resource availability is highly variable, they do not *maximize* their seed production relative to resource availability. This is reflected by the relatively poor nutrient use efficiency in crops, which do not fully utilise the resources available (Reynolds *et al.*, 2009; Mitchell and Sheehy, 2018; Schils *et al.*, 2018). This suggests that there is significant scope to improve crop yields by increasing the responsiveness of reproductive architecture to resource availability.

1.2 Reproductive Architecture and Decision Making

Despite a vast range of morphologies, angiosperms share common features in the development of their reproductive architecture. The development of higher plants is organised using ‘phytomers’: simple repeating units, providing a predictable underlying uniformity, from which variations may arise (McSteen and Leyser, 2005). The most common model used defines the basic phytomer unit as a length of stem, a leaf, and a secondary ‘axillary’ shoot meristem. The behaviour of these secondary meristems is typically a major source of developmental variation between plants of the same and different species. During vegetative growth, the activation of axillary meristems leads to new vegetative axes of growth (i.e. branches, or tillers in grasses). At the initiation of the reproductive phase active vegetative shoot apical meristems (VMs) convert into reproductive inflorescence meristems (IMs) (Koppolu and Schnurbusch, 2019). From these, a sequence of meristems sequentially form, leading to the development of hierarchical subunits. IMs form inflorescences, from which spikelet meristems (SMs) form, which produce further floral meristems (FMs) (Schultz and Haughn, 1991). Each floral meristem produces a single flower which, upon fertilisation, gives rise to a seed-containing fruit. Final seed set therefore reflects the hierarchical production of reproductive shoots, inflorescences and flowers during reproductive development.

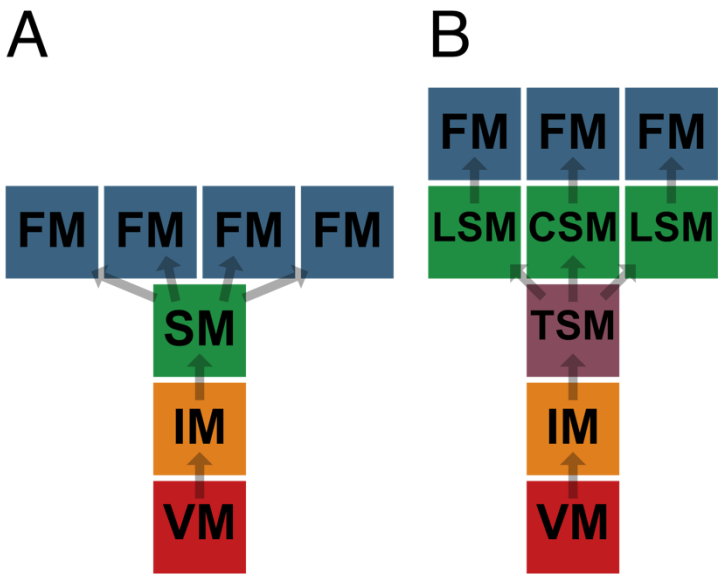

Figure 1.01: Shoot apical meristem progression
(A) Wheat **(B)** Barley.
Vegetative Meristem is represented in red (VM); Inflorescence Meristem is represented in orange (IM); Triple Spikelet Meristem (barley only) is represented in purple (TSM); Spikelet Meristems are represented in green (SM), including central spikelet meristems and lateral spikelet meristems in barley; Floret Meristems are represented in blue (FM).

The temporal separation of this hierarchical sequence of structures presents an issue for linking seed development with resource availability (Walker and Bennett, 2018). To maximise seed-set, plants need to maximise the production of earlier structures. However, when reproductive development begins, the plant cannot 'know' what resources will be available at the point of seed-set, making it difficult to 'predict' the optimal reproductive architecture for maximum seed-set. As such, reproductive architecture tends to be a cautious under-estimation, based on currently available information (Walker and Bennett, 2018).

The model plant Arabidopsis has been shown to respond to this uncertainty by determining the overall scale of reproductive development very soon after flowering. The number of secondary inflorescences (inflorescences initiated by axillary meristems along the primary inflorescence) is determined very shortly after the

beginning of flowering and has been shown to be a key determinant of the overall reproductive effort of Arabidopsis. This process is underpinned by a series of negative feedbacks between stages of development, preventing over-investment early on. These feedbacks thus produce a homeostatic system, where new organs may form in response to loss elsewhere in the system. This early determination can be mitigated by a flexible adjustment to environmental conditions by increases or decreases in tertiary inflorescence number, though these produce smaller fruits and have low impact on final seed production (Walker, Wheeldon and Bennett, 2021). It was further shown that in oilseed rape (*Brassica napus*) the reproductive architecture present immediately after flowering in April directly predicted final fruit number and seed mass in July (Walker, Wheeldon and Bennett, 2021). These findings indicate the inclination for plants to determine their production early on, potentially under-utilising later resource availability.

The production of structures across the plant such as branches and fruits are not independent events but have been shown to be interconnected. Correlative inhibition refers to a set of mechanisms in which older organs suppress the development of newer ones on the same plant. Currently identified correlative inhibition mechanisms include apical dominance (the prevention of new branch formation by current branches) and carpic dominance (the prevention of new fruit formation by current fruit), both of which have a significant function in determining how many of each structure develops (Figure 1.02). Apical dominance is the most studied of the correlative inhibitions and is regulated by long-distance phytohormones, including cytokinin, strigolactone and auxin (section 1.3.2). The production of reproductive structures in Arabidopsis is tightly controlled by a series of homeostatic feedback mechanisms that limit the production of reproductive structures relative to resource availability (Figure 1.02). Currently, we do not understand the molecular mechanisms that underpin these feedbacks. However, because of their phenomenological similarity to apical dominance, it has been speculated that they may operate on similar principles (Walker, Wheeldon and Bennett, 2021).

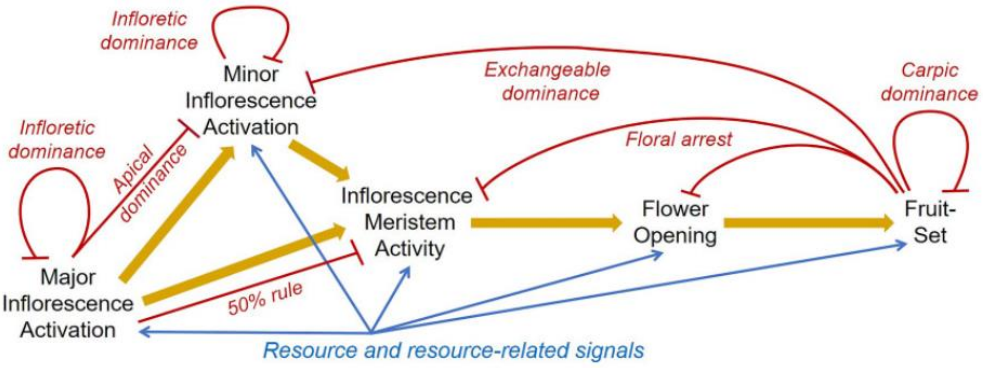

Figure 1.02: The spatio-temporal regulation of shoot architecture development in *Arabidopsis* (taken from (Walker, Wheeldon and Bennett, 2021))

Interrelationships between developmental processes are shown in gold, negative feedbacks are shown in red, positive feedbacks from resource-related signals are shown in blue.

1.3 Shoot branching as a model for architecture control

1.3.1 Shoot branching and axillary meristems

Shoot branches arise from axillary shoot meristems. After formation, axillary meristems exist as dormant vegetative buds, until their outgrowth is triggered, which may occur shortly after formation, or significantly later. In this way branching is an essentially binary process, comprising of initiation and outgrowth. Shoot branching is a highly plastic process, adapting to a range of external cues. Nutritional availability has been shown to alter shoot branching. For instance, the sensing of high levels of available nitrogen and phosphorus by the roots results in increased shoot branching (Umehara *et al.*, 2010; de Jong *et al.*, 2019), and light availability has also been shown to increase branching (Xie *et al.*, 2020). Additionally, shoot branching can be modulated by internal stimuli. For instance, apical dominance is the process by which previously developed shoot branches repress further branching. As with the response of branching to external stimuli, apical dominance appears to be the result of active signalling through hormonal signals (Bangerth, 1989; Booker, Chatfield and Leyser, 2003).

In its coordination by internal and external stimuli, the regulation of shoot branching thus demonstrates the same general principles as the control of reproductive architecture. The regulation of shoot branching has been intensively studied, resulting in a detailed understanding of the underlying mechanisms. Key to this is the interaction of three hormones: auxin, cytokinin and strigolactone.

1.3.2 The role of auxin, cytokinin and strigolactone in apical dominance

Auxin has been established as a regulator of apical dominance since the 1930s. Excision of actively growing shoot meristems causes activation of previously dormant axillary meristems, but auxin prevents this effect when placed upon excised shoot apices, ultimately demonstrating that active meristems export auxin, which causes apical dominance (Thimann and Skoog, 1933). However, auxin is not transported into the dormant buds and direct application of auxin to dormant buds does not maintain their dormancy, indicating the role of auxin is not direct (Prusinkiewicz *et al.*, 2009). Several models have been proposed to explain this. The canalization model proposes that growth of a branch is linked to its capacity to export auxin. Export of auxin by active branches weakens the stem's function as an auxin 'sink', preventing outgrowth of additional branches. Alternative models have proposed that auxin is merely a primary signal, which triggers a downstream change in the levels of other hormones, which directly promote or repress branching (Bangerth, 1989; Xu *et al.*, 2015). Candidates for 'second messengers' include cytokinin and strigolactone. Cytokinin synthesis is downregulated in both the root and the shoot in response to auxin (Nordström *et al.*, 2004; Tanaka *et al.*, 2006), and cytokinin (Sachs and Thimann, 1967) directly promotes bud outgrowth (Wickson and Thimann, 1958). Conversely, strigolactone has also been shown to repress bud outgrowth (Gomez-Roldan *et al.*, 2008; Umehara *et al.*, 2008; Domagalska and Leyser, 2011; Khuvung, Silva Gutierrez and Reinhardt, 2022) and its synthesis is promoted by auxin in the root and the shoot (Arite *et al.*, 2007; Hayward *et al.*, 2009).

Whilst some models treat these solely as secondary signals, triggered by levels of auxin, newer theories treat their role in branching control as separate, primary signal

mechanisms (Yuan *et al.*, 2023). All these models are consistent with observations on branching control and are supported by experimental evidence. It is quite possible that no one theory is solely correct and that the essential hormones auxin, cytokinin and strigolactone act as generalized signals, through which many different messages are transmitted, and which accomplish their signalling role in multiple different ways.

1.3.3 BRC1 as an integrator of shoot branching signals

BRANCHED1 (*BRC1*), which encodes a TCP-family transcription factor, has been proposed as a central coordinator of shoot branching in Arabidopsis. The BRC1 protein acts to repress bud outgrowth (Aguilar-Martínez, Poza-Carrión and Cubas, 2007), and *BRC1* expression is downregulated in the presence of cytokinin and upregulated by strigolactone (Sachs and Thimann, 1967; Umehara *et al.*, 2008; Dun *et al.*, 2012). *BRC1* therefore provides hormones observed controlling shoot branching with a genetic gateway to regulate outgrowth of new branches. The function of BRC1 also provides a possible solution to auxin's role in branching repression without being transported into repressed buds. By reducing cytokinin and increasing strigolactone levels (as discussed in section 1.3.2) auxin can indirectly upregulate *BRC1* and its repressive function (Dun *et al.*, 2012). Although proposed as a crucial central coordinator of the response of branching to environmental nutrient availability and the presence of other branches (M. Wang *et al.*, 2019), BRC1 has been shown to be neither necessary nor sufficient to solely explain all the observed activities of auxin, cytokinin and strigolactone (Seale, Bennett and Leyser, 2017). It is likely that BRC1 is simply one (albeit major) piece in a much larger system that integrates the same small group of universal hormonal signals, possibly acting to determine a bud's activation potential, rather than solely determining its outgrowth. Strigolactone in particular, appears to repress bud outgrowth largely independently of *BRC1* (Seale, Bennett and Leyser, 2017) and expression of the rice homologue *FINE CULM 1* (*FC1*) is insensitive to strigolactone (Minakuchi *et al.*, 2010).

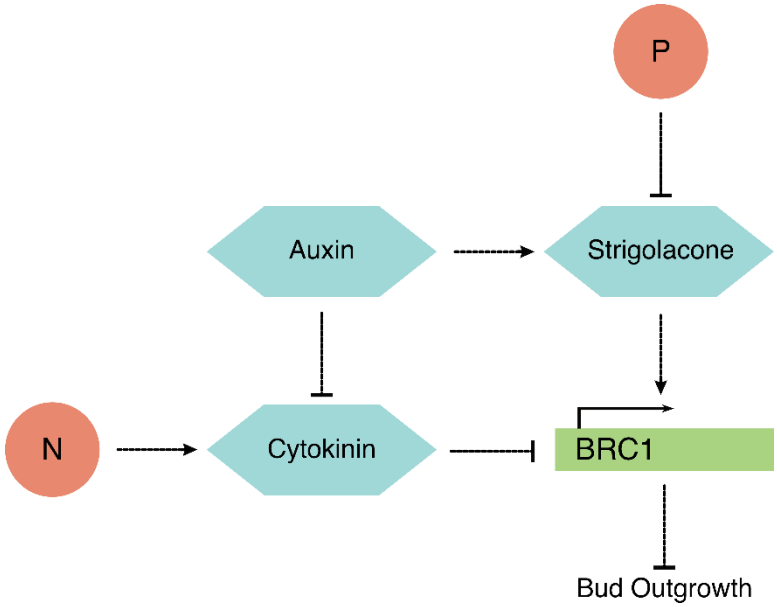

Figure 1.03: Summary of BRC1 mediated branching control

Genes are represented as green rectangles. Hormones are represented as blue hexagons. Nutrients are represented as red circles. Pointed arrows represent positive regulation, flat headed arrows represent negative regulation.

1.3.4 Interactions of auxin, cytokinin and strigolactone

Complicating our understanding of branching is the fact that auxin, cytokinin and strigolactone interact and modulate each other. In Arabidopsis auxin downregulates cytokinin levels by repressing expression of *ISOPENTENYL TRANSFERASE (IPT)* and *LONELY GUY (LOG)* genes, both essential for cytokinin biosynthesis (Zhang *et al.*, 2018). Cytokinin also modulates auxin transport by upregulating abundance of auxin transporter proteins PIN3, PIN4 and PIN7 – potentially increasing auxin sink capacity in the stem (Waldie and Leyser, 2018). Similarly, auxin has been shown to have clear regulatory control over strigolactone levels. The CAROTENOID CLEAVAGE DIOXYGENASE 7 (CCD7) and CCD8 enzymes are essential in the synthesis of strigolactone (Booker, Chatfield and Leyser, 2003; Sorefan *et al.*, 2003), and in numerous plant species the CCD7 and CCD8 genes have been shown to be upregulated by auxin (Ishikawa *et al.*, 2005; Zou *et al.*, 2006; Arite *et al.*, 2007). Strigolactone has been shown to downregulate abundance of auxin efflux protein

PIN1, reducing auxin transport through the stem (Shinohara, Taylor and Leyser, 2013). These data imply that negative feedback loops between hormones with antagonistic effects may form a detailed network that regulates shoot branching. Low shoot strigolactone levels increase the flow of auxin into the shoot, in turn increasing strigolactone synthesis, and conversely high cytokinin levels increase the flow of auxin, in turn decreasing cytokinin synthesis – and increasing strigolactone synthesis. Strigolactone is also known to directly downregulate cytokinin levels. In rice it upregulates expression of the *OsCKX9* gene, which encodes a cytokinin dehydrogenase/oxidase, which breaks down cytokinin molecules (Duan *et al.*, 2019). Thus, although strigolactones and cytokinins can directly regulate branching through BRC1, they can also indirectly regulate branching through their effect on each other, and through their effects on auxin. Overall, the network regulating shoot branching seems to consist of interlocking feedback loops that might act to prevent over- or under-response to external or internal stimuli.

1.3.5 Hormonal regulation of SAM development

The CLAVATA-WUSCHEL pathway regulates the development of stem cells to ultimately determine meristem growth (Somssich *et al.*, 2016), which ultimately determines the possible shoot architecture by mediating the number of branches and inflorescences. This important role has therefore been extensively studied in *Arabidopsis* and orthologous components have been identified in maize and rice.

In *Arabidopsis,* cytokinin has been shown to work antagonistically with *CLAVATA1 (CLV1)* (Whitewoods *et al.*, 2018) and to promote SAM formation by inducing *WUSCHEL (WUS)* expression (Meng *et al.*, 2017; Cammarata, Roeder and Scanlon, 2019). Furthermore, *WUS* has been shown to repress type-A RRA cytokinin receptors and thus cytokinin signalling in *Arabidopsis* (Leibfried *et al.*, 2005), whilst in rice, mutation of a cytokinin biosynthesis *LOG* gene results in a phenotype resembling that of *wus* mutants (Chickarmane *et al.*, 2012). Cytokinin signalling receptors have also been implicated, with type-B RRAs *ARR1* and *ARR12* directly activating *WUS* expression, and indirectly repressing *CLV3* (Liu *et al.*, 2020). It has

also been shown that meristem developmental defects in the maize mutant *tls1 (tassel-less1)* coincided with altered activity of the *CLV1* orthologue *td1 (thick tassel dwarf)* and altered cytokinin signalling (Matthes *et al.*, 2022).

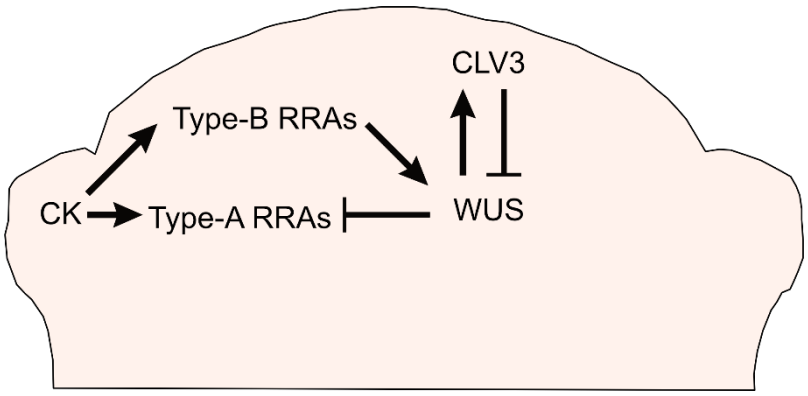

Figure 1.04: Summary of effects of cytokinin on CLAVATA-WUSCHEL meristem maintenance.

Another known regulator of meristem development is *FT1 (FLOWERING LOCUS T1)*, which integrates several signals to regulate the timing of reproductive development of the SAM in wheat. RNAi induced repression of *FT1* results in further downregulation of *FT2* and *FT5* as well as a 2-4 week delay in flowering (Lv *et al.*, 2014). More recent work showed that different alleles of *FT-B1* result in different final spikelet numbers, independent of the effect on flowering time (which may be more dependent on alleles of VRN-A1) (Brassac *et al.*, 2021). *FT2*, a paralogue of *FT1* has also been suggested to be involved in the initiation of reproductive SAM development. RNAi interference of *FT2* resulted in an increase in spikelet number, potentially as a result of the additional mutant effect of increased flowering time (Shaw *et al.*, 2019), and natural alleles of *FT-A2* affected grain number per ear (Glenn *et al.*, 2022).

1.3.6 Resource regulation of hormonal signals in shoot branching control

The regulation of shoot branching by long-distance hormonal signals allows plants to coordinate developmental events in the shoot with stimuli detected elsewhere in the plant. In *Arabidopsis*, high nitrogen levels trigger synthesis of cytokinin in the roots, which is then transported shootward (Takei *et al.*, 2001; Müller *et al.*, 2015). Recent work has shown that there is extensive natural plasticity in how Arabidopsis responds to changes in nitrogen, with more nitrogen-sensitive lines producing a more extreme difference in branching between high and low nitrogen conditions (de Jong *et al.*, 2019). It has been proposed that the plasticity of a plant's nitrogen response depends on the underlying hormone network, with extreme phenotype lines being the result of differences in cytokinin or strigolactone synthesis, transport or sensing (de Jong *et al.*, 2019). High phosphate levels repress the biosynthesis of strigolactone in the roots, reducing the amount transported to the shoots (Kapulnik and Koltai, 2016). Thus, the auxin-cytokinin-strigolactone network likely allows plants to activate an optimal number of shoot branches with response to nitrogen (cytokinin) and phosphate (strigolactone) availability, and to the number of actively growing branches (auxin). Clearly then, shoot architecture is both responsive to resource availability and responsive to feedback from existing organs. It is possible then that the common hormonal networks that underlie these nutrient responses also control reproductive architecture. This idea has previously been proposed (Walker and Bennett, 2018), however there is currently a lack of evidence clearly linking the development of reproductive architecture with hormones, resource availability, and already existing structures. However, there are some signs that this hypothesis is valid. For instance, recent work has shown that floral arrest in Arabidopsis is the result of auxin export from the inflorescence and older work has implicated auxin as being a key driver of carpic dominance (Bangerth, 1989; Ware *et al.*, 2020). Ultimately, branching is one of the most important and well-studied aspects of shoot development. Almost no study of shoot development can entirely ignore it, and my research focuses on it as a fundamental method through which cereals respond to internal and external stimuli.

1.4 Reproductive Architecture in Cereals

1.4.1 Wheat and barley reproductive architecture

Arabidopsis is a useful model for understanding many aspects of development, such as meristem fate and hormone signalling. However, all the world's major cereals are grasses, with architectural features unseen in Arabidopsis. Grass inflorescences are referred to as spikelets, which act as the basic unit of the reproductive architecture and are further divided into one or multiple seed producing florets, depending on the species. These spikelets are arranged either in a distichous phyllotaxy (such as in wheat (*Triticum aestivum*) and barley (*Hordeum vulgare*)) in which spikelets develop from two parallel rows of nodes along a central rachis, as a polistichous phyllotaxy, in which nodes of spikelet growth are arranged along primary and secondary branches, (such as in rice (*Oryza sativa*) and maize (*Zea mays*)) (Sakuma and Schnurbusch, 2020). In grasses, a typical reproductive effort first involves the formation of multiple vegetative tillers. After floral transition, some proportion of tiller meristems are converted to reproductive shoot meristems and initiate the development of grain-bearing 'spikes' – also commonly referred to as 'ears'. The axillary meristems initiated along the spike give rise to spikelets, and the axillary meristems within the spikelets initiate florets. Each fertile floret may produce a single grain. Some grass species (e.g. barley) will only ever produce a single floret per spikelet, while others (e.g. wheat) may initially produce up to 12 florets per spikelet, though typically many of these will senesce or be infertile, typically reducing the final number of grain producing florets to between one and four. Variations on number of ears per plant, spikelets per ear and florets per spikelet thus determine potential grain output. Although typically only one spikelet may develop from a spikelet node, some mutant lines have been identified that significantly increase number of spikelets per ear by disrupting this, by producing supernumerary spikelets. A well-established instance of supernumerary spikelet formation in wheat is the paired spikelet phenotype, in which a second spikelet develops at the node, directly beneath the main spikelet (Figure 1.05C-D).

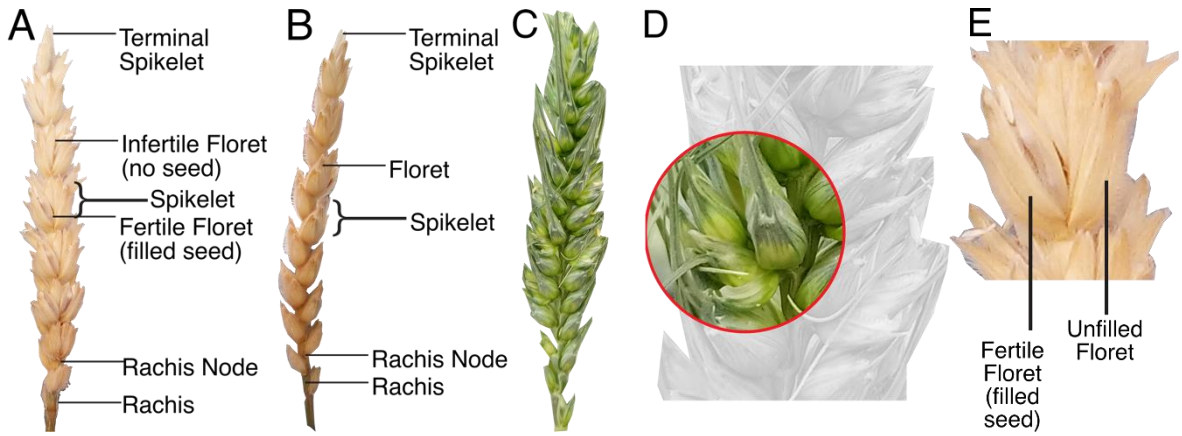

Figure 1.05: The architecture of emerged wheat ears.

(A) Labelled ear of elite wheat variety Cadenza. **(B)** Lateral view of an ear of elite wheat variety Cadenza. **(C)** Lateral view of an ear of the paired spikelet forming *hb* wheat mutant. **(D)** Highlighted view of paired spikelet developing at rachis node, directly beneath a regular wheat spikelet. **(E)** Single wheat spikelet containing multiple florets.

1.4.2 Regulation of shoot branching in cereals

The previously discussed hormones of strigolactone, cytokinin and auxin have all been implicated in controlling tiller formation in grasses, particularly in rice, where tillering is a key yield determinant.

Elevated strigolactone levels, as a result of phosphate restriction, have been shown to repress bud outgrowth in rice where suppression of tiller bud outgrowth is not seen in strigolactone insensitive mutants (Arite *et al.*, 2007; Umehara *et al.*, 2010). Another rice gene *GROWTH-REGULATING FACTOR 7 (OsGRF7)* has been shown to regulate gibberellin and auxin metabolism and to negatively regulate tillering by targeting the promoter of *NODULATION SIGNALING PATHWAY 2 (OsNSP2)* (Chen, Dan and Li, 2020), whose proper function is required for strigolactone synthesis (though any potential additional roles of *GRF7* involving gibberellin and auxin in branching are yet to be elucidated).

In rice, the *dwarf and low tillering 10 (Osdlt10)* mutant, which exhibits reduced tillering, was associated with increased expression of PIN proteins, linking the

mutation with the low tillering phenotype via increased local auxin concentration (Wen *et al.*, 2020). This conclusion is supported by other studies which have implicated PIN proteins (and thus auxin concentration) with tillering directly, such as OsPIN9, the overexpression of which results in increased tillering, whereas the *Ospin9* mutant produced fewer tillers (Hou *et al.*, 2021). Also of interest is the finding that *OsPIN9* is upregulated by ammonium availability, but not nitrate availability, suggesting another system by which nutritional availability is tethered to shoot development via common signalling hormones (Hou *et al.*, 2021).

Cytokinin levels also appear to be involved in tiller formation. Downregulation of cytokinin degradation protein OsCKX2 results in increased cytokinin levels and was shown to increase tiller number (Yeh *et al.*, 2015). Additionally, overexpression of the nitrate transporter encoding *OsNPF7.2* was shown to increase tillering and transcription of cytokinin production genes such as IPTs, LOGs and ARRs (J. Wang *et al.*, 2018), clearly indicating a conserved role for cytokinin in communicating nitrate levels with tillering.

MONOCULM 1 (*MOC1*) (the orthologue of Arabidopsis *LATERAL SUPRESSOR* (*LAS*)) encodes a GRAS family transcriptional regulator. *OsMOC1* has been proposed as a regulator of axillary meristem formation, as it is seen to be highly expressed in the axillary bud at vegetative and reproductive stages and the *Osmoc1* mutant almost entirely stops tillering (Shao *et al.*, 2019). Wheat haplotype analysis identified orthologous *TaMOC1-7A* has recently been shown to regulate spikelet number per spike in wheat (Zhang *et al.*, 2015).

1.4.3 BRC1-class genes in cereal reproductive architecture

The *BRC1*-class of genes was originally identified through analysis of the *Teosinte Branched1* gene in maize, where an overexpression allele was found to be essential in the domestication of the wild – highly branched – teosinte to modern cultivated maize. In addition to repressing vegetative branch outgrowth, TB1 also appears to be a regulator of inflorescence development. TB1 directly regulates *TEOSINTE*

GLUME ARCHITECTURE1 (*TGA1*) which further coordinates an array of MADS-box transcription factors, known to impact inflorescence morphology by influencing a cascade of organ identity transcriptional regulators (Bommert *et al.*, 2005; Studer, Wang and Doebley, 2017). This suggests another possible developmental context in which *BRC1/TB1* acts as a central gateway between hormone signals and a downstream network of architecture-influencing genes.

Orthologues of BRC1 have been identified as crucial regulators of shoot architecture in most major cereal crops: FINE CULM 1 (FC1) in rice (*Oryza sativa*) (Arite *et al.*, 2007); TEOSINTE BRANCHED 1 (TB1) in maize (*Zea mays*) (Aguilar-Martínez, Poza-Carrión and Cubas, 2007); TB1 in wheat (*Triticum aestivum*) (Dixon *et al.*, 2018); TB1 in sorghum (*Sorghum bicolor*) (Kebrom, Burson and Finlayson, 2006) and INTERMEDIUM-C (INT-C, aka VRS5) in barley (Bull *et al.*, 2017). However, the roles each of these proteins fulfil is only partially similar to AtBRC1, and changes in their expression often result in changes to other grass specific structures (e.g. spikelets) as well as tillers, highlighting the necessity to experiment outside of Arabidopsis in the investigation of reproductive architecture.

Extensive work on *TB1* in maize laid the foundation for study of the orthologous wheat gene *TaTB1*. As in maize, *TaTB1* encodes a class II TCP transcription factor, which in addition to the expected repression of bud outgrowth also regulates spikelet development, tillering and height (Dixon *et al.*, 2018; Dixon, Pasquariello and Boden, 2020). Crucially, *TB1* expression has been shown to cause an increase in spikelet number, by causing the development of a supernumerary spikelets called ‘paired spikelets’ (Boden *et al.*, 2015; Dixon *et al.*, 2018). *TaTB1 w*as also shown to interact with *FT1*, suggesting that it could influence spikelet development by modulating flowering time (Boden *et al.*, 2015; Dixon *et al.*, 2018). *tb1* mutants reduce expression of FT1-activated meristem identity genes, leading to the paired spikelets phenotype and an increased total number of spikelets. More recent work identified low levels of *TB1* expression in main culm nodes pre-elongation and that increased levels of expression resulted in elongation repression, producing overall shorter

plants, whereas reduced *TB1* expression (e.g. in the loss-of-function allele *tb-B1b*) resulted in taller plants (Dixon, Pasquariello and Boden, 2020).

1.4.4 Regulation of reproductive architecture in cereals

The regulation of shoot branching in cereals and Arabidopsis share fundamental similarities. This raises the prospect that other aspects of reproductive architecture may also be systemically coordinated by similar mechanisms. Correlative inhibition mechanisms have not been especially well-studied in grasses, though their presence in the diverse families of plants that have been studied, suggests these mechanisms also exist in cereals (Bangerth, 1989).

Reproductive architecture in grasses has mostly been studied from the perspective of single locus mutations that produce significant changes in morphology. For instance, *BRANCHED SILKLESS1*/*FRIZZY PANICLE* (*BD1*/*FZP*) modulates spike branching in maize and rice (Komatsu *et al.*, 2001; Chuck *et al.*, 2002) and the wheat orthologue *TaFZP* has been shown to regulate development of multirow spikelet phenotypes (Dobrovolskaya *et al.*, 2015; Y. Li *et al.*, 2021).

Several characterised reproductive architecture genes in grasses are significant to the comparison with Arabidopsis and associated with changes in meristem development. The rice *RCN (RICE CENTRORADIALIS)* gene is a regulator of inflorescence meristem identity, and overexpression leads to delay of transition to the reproductive phase, resulting in plants with more secondary branches and denser panicles (Nakagawa, Shimamoto and Kyozuka, 2002; Kaneko-Suzuki *et al.*, 2018). Overexpression of the wheat orthologue of *TERMINAL FLOWER1 (TaTFL1-2D)* increases the numbers of spikelets, florets, and seeds per spike, as well as leading to extension of the double-ridge and floret stages of meristem development (J. Sun *et al.*, 2023), indicating a role in regulation of both spike complexity transition of meristem states. Another example is the rice genes *ABERRANT PANICLE ORGANIZATION 1 (APO1)* and *APO2,* required for regulating meristem size; both *apo1* and *apo2* mutants produce fewer primary branches, and smaller panicles

(Ikeda *et al.*, 2007; Ikeda-Kawakatsu *et al.*, 2012). *WHEAT ORTHOLOGUE OF APO1 (WAPO1)* has recently been proposed as the candidate gene for a QTL shown to effect spikelet number (Kuzay *et al.*, 2019; Muqaddasi *et al.*, 2019).

Another potentially important reproductive architecture gene is *PHOTOPERIOD-1* (*PPD-1*) (Boden *et al.*, 2015). PPD-1 is a pseudo-response regulator protein, which controls photoperiod response in wheat by interacting with central flowering protein *FLOWERING LOCUS T1 (FT1)*. When this interaction produces a weak signal (either due to naturally weaker alleles, or by intentional knockout (such as with the deletion of *TaFT-B1*) spikelet number is seen to increase (Brassac *et al.*, 2021). The increase in flowering time which allows additional spikelet development is produced by a shortening of the vegetative stages of development.

Our current literature therefore indicates that the molecular regulation of final reproductive architecture can likely be better understood through the study of meristem development.

1.4.5 Regulation of spikelet development in wheat

Several genes have been identified as regulators of spikelet development in wheat and barley, which also influence meristem development.

Transcription factors *TaPDB1 (photoperiod-1-dependent bZIP1)* and *HvALOG1 (Arabidopsis thaliana LSH1 and Oryza G1)* affect spikelet number in wheat and barley respectively and both have been proposed to function downstream of flowering gene *PPD-1 (photoperiod-1)* (Gauley *et al.*, 2024). Overexpression of MicroRNA156 (miR156) in wheat resulted in greatly increased tillers and greatly reduced spikelets, which is likely achieved by the miR156 repressing a group of *SPL (SQUAMOSA PROMOTER BINDING PROTEIN-LIKE)* genes. In these plants, *TB1* and *BA1 (BARREN STALK1)* expression was significantly reduced (Liu *et al.*, 2017b).

Liu *et al*., 2017 is also one of the examples we currently have of the involvement of phytohormonal signalling in architecture and meristem development. Strigolactone

signalling repressor *D53* was shown to interact with the miR156-SPL3/17 module (Liu *et al.*, 2017b), to repress *TB1* and *BA1* expression and thus regulate wheat shoot development. Furthermore, work comparing the changing transcriptome of the developing wheat meristem showed that auxin and cytokinin biosynthesis genes were upregulated later in spike development (Ai *et al.*, 2024). Investigation of the potential role of cytokinin and strigolactone signalling in coordinating reproductive architecture is a primary aim of this thesis and our current understanding of both is discussed in sections 1.4.7 and 1.4.8.

In addition to the multiple genes known to regulate spikelet development, a small number have been identified as regulators of paired spikelet development and continue to implicate hormonal signalling in the coordination of reproductive architecture development.

PPD-1 and *TB1* have both been shown to regulate paired spikelet formation via their regulatory effect on *FT1* in a process that is independent of *FT1* regulation of flowering time (Boden *et al.*, 2015; Dixon *et al.*, 2018). Furthermore, *WPS1 (WHEAT PAIRED SPIKELETS1)* encodes a TF which appears to prevent paired spikelet formation and *wps1* produced significantly more paired spikelets than the wild-type. Further analysis showed that in the *wps1* mutant, auxin-related genes (including PINs, Aux/IAAs and ARFs) were upregulated, whilst cytokinin-related genes (including type-B ARRs and a putative LOG gene) were downregulated (Zhang *et al.*, 2022). This has led to the suggestion that paired spikelet formation in the *wps1* mutant may be the result of disordered hormonal balance.

1.4.6 *VRS* genes and six-rowed barley

Barley produces its spikelets in a distichous phyllotaxy, in which two rows of spikelet producing rachis nodes are arranged in parallel along a single unbranched rachis. At each rachis node three uni-floreted spikelets may develop, consisting of a central spikelet, flanked on either side by a lateral spikelet. In two-row barley, the two lateral spikelets are infertile, leaving only a single fertile central spikelet at each node. In

six-row barley, the lateral spikelets are fertile, producing three spikelets per node (though the lateral spikelets are typically smaller than the central spikelet). The reproductive architecture of both two-row and six-row barley is shown in Figure 1.06.

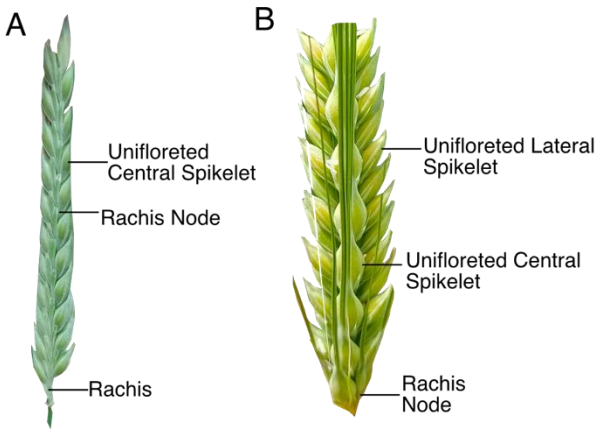

Figure 1.06: The architecture of emerged two-row and six-row barley ears.

(A) Ear of two-row barley line Bowman, with fertile central spikelets and infertile lateral spikelets. **(B)** Ear of six-row of *vrs1* mutation in Bowman background line, with fertile central and lateral spikelets.

Five separate *VULGARE ROW TYPE SPIKE (VRS1-VRS5)* genes that regulate lateral spikelet fertility have been identified in barley. All *vrs* mutants have a six-row phenotype. Mutant alleles in *VRS1* are the principal cause of current commercial six-row barley and it appears to be a central regulator for a short VRS pathway, with VRS3, VRS4 and VRS5 all shown to function by modulating *VRS1* expression (Zwirek, Waugh and McKim, 2019). *VRS2* encodes a SHORT INTERNODES (SHI) transcription factor (Youssef *et al.*, 2017). The SHI family have previously been linked to auxin biosynthesis in Arabidopsis, a function that may be conserved in barley, as *VRS2* loss of function is associated with a reductions in auxin concentration and an increase in cytokinin levels. *VRS3* appears to be the only *VRS* gene that does not encode a transcription factor, instead encoding a histone demethylase. Associative transcriptomics suggest that *VRS3* modifies the chromatin of the other *VRS* genes, promoting their expression (Bull *et al.*, 2017; van Esse *et al.*, 2017). *VRS4* encodes a LATERAL ORGAN BOUNDARY (LOB) transcription

factor, orthologous to *Ramosa2* (which has already been established as an essential regulator of branch architecture in maize), and has been shown to induce *VRS1* expression (Bortiri *et al.*, 2006; Koppolu *et al.*, 2013). *VRS5* is also known as INTERMEDIUM-C (INT-C) (Ramsay *et al.*, 2011). VRS5 works upstream of *VRS1* and is induced by VRS3 and VRS4. Intriguingly, *VRS5* is the barley orthologue of *BRC1/TB1.* The *int-c.a* allele has been linked to paired spikelet formation and alongside *vrs1* promotes increased lateral spikelet size (compared to plants with only a *vrs1* mutation). In addition to affecting spikelet morphology, *int-c* loss-of-function mutations have been associated with reduced tillering (Ramsay *et al.*, 2011). An observed phenotype of *vrs1* barley (in addition to the increased spikelet number) is a reduced number of tillers. This role for *VRS5/INT-C* presents an interesting question: is the reduction in tillering the result of conserved bud outgrowth repressive function, or some other feedback mechanism that reduces tiller number as a response to increased spikelet number?

VRS1 is orthologous to the maize protein Grassy Tillers1 (GT1) (Dong *et al.*, 2019; Gallagher *et al.*, 2023), which inhibits bud outgrowth downstream of TB1. Similarly, VRS1 has been shown to inhibit lateral spikelet fertility downstream of the TB1 orthologue VRS5 (Ramsay *et al.*, 2011). Despite the increased fertile spikelet number of six-row *vrs1* barley, decreased tiller number, decreased number of rachis nodes and decreased grain weight all accompany the six-row phenotype, dampening the theoretical potential 3-fold yield increase of six-row barley (Ramsay *et al.*, 2011; Zwirek, Waugh and McKim, 2019). Hence, *vrs1* presents a fascinating line for study, since it displays a change in reproductive architecture accompanied changes in other architectural parameters, a trade-off which I hypothesise could be driven by correlative inhibition (section 1.2).

1.4.7 Cytokinin coordination of reproductive architecture in cereals

Auxin, cytokinin and strigolactone are the main hormones coordinating shoot architecture in *Arabidopsis* (section 1.3). Although the roles of these phytohormones are less well characterised in cereals, their importance is beginning to be understood.

The role of auxin in cereal reproductive architecture remains the most elusive, due to the difficulty of studying the hormone directly, and the lack of suitable genetic tools. However, there is now a strong body of evidence that implicates cytokinin as one of the key regulators of cereal shoot architecture development. Several genes essential in coordinating cytokinin levels have been shown to affect cereal reproductive architecture, however, several gaps in our understanding remain.

CYTOKININ DEHYDROGENASE/OXIDASE (CKX) proteins act in the catabolism of cytokinin and changes in their expression and activity have resulted in observed changes in grain number per spike, grain weight, spikelet number and root growth (Zhang *et al.*, 2011; Ogonowska *et al.*, 2019; Jablonski *et al.*, 2021). Several *CKX* genes (such as *TaCKX2.1* and *TaCKX2.*2 in wheat) are highly expressed in young spikes, implying a potential role in maintaining proper spike morphogenesis (Zhang *et al.*, 2011). However, *CKX* genes exist in large multi-gene families, with differing expression profiles and roles between members. For instance, in barley, different expression levels of *HvCKX1-HvCKX9* results in varying effects on seed development when disrupted (Zalewski *et al.*, 2014). A similar complexity exists for the cytokinin biosynthesis *LOG (LONELY GUY)* genes. 11 functional LOGs have been found in wheat and most are highly expressed in the developing inflorescence, suggesting the involvement of cytokinin in shoot development (Chen *et al.*, 2022). Similarly, 11 CKX families have been identified in wheat, which vary in expression patterns between tissues and points in development (Jain *et al.*, 2022), implicating the involvement of cytokinin in regulating development. CKX7 and CKX10 were found to be expressed at very low levels in the spike during reproductive development (Jain *et al.*, 2022). Silencing of CKX genes in wheat (Jablonski *et al.*, 2021) and barley (Zalewski *et al.*, 2010) has shown improved yield.

Another outstanding problem is that while *CKX* genes have been identified and related to reproductive architecture in many cereals, the function and expression of orthologous genes don’t necessarily match up. In rice, *OsCKX2* is associated with grain weight and grain number, whereas its wheat orthologue *TaCKX6-D1* has been shown to regulate grain weight, but studies have failed to show it having any impact

on grain number (Zhang *et al.*, 2012). Instances such as these illustrate the limitations of inferring information from even very similar model plants and indicates the need to study each cereal as an individual system.

As discussed in section 1.3.5 and 1.4.4, final reproductive architecture is highly determined by meristem development. Therefore, developing and understanding of how cytokinin might regulate meristem development is particularly important. Levels of hormones including cytokinin were found to vary along the length of developing meristem and between meristem developmental stages, suggesting their crosstalk could regulate progression through development (Youssef and Hansson, 2019). Furthermore, the *COMPOSITUM (COM)* genes have been shown to regulate meristem determinacy in cereals. *COM1* encodes a class II TCP TF and *COM2* (*FRIZZY PANICLE* in rice) encodes an AP2-ERF (Poursarebani *et al.*, 2015). Single mutants of both genes saw a loss of meristem identity, and the development of full spikes in place of spikelets (Sakuma and Koppolu, 2023). The same phenotype was also observed in *HvVrs4* mutants, which may regulate *COM1* and *COM2* in barley inflorescence development (Poursarebani *et al.*, 2015). Also in barley, *HvMADS1* was shown to maintain regular inflorescence development. Interestingly, the SEPALLATA TF encoded by *HvMADS1* was shown to target not only inflorescence differentiation genes, but cytokinin signalling genes, particularly *HvCKX3* (Y. Li *et al.*, 2021). This recently developed body of work strongly supports the involvement of cytokinin with the coordination of cereal shoot development. Accordingly, modulation of cytokinin levels via manipulation of CKXs (Chen *et al.*, 2020) and LOGs (Rathore *et al.*, 2024) has therefore been suggested as a promising potential method of improving cereal yields.

1.4.8 Strigolactone coordination of reproductive architecture in cereals

Strigolactones have been shown to play conserved roles in the regulation of shoot branching in rice, maize and barley (Minakuchi *et al.*, 2010; Guan *et al.*, 2012; Song *et al.*, 2017; H. Wang *et al.*, 2018). However, there are relatively few studies

investigating the potential role of strigolactones in regulating aspects of cereal reproductive architecture development besides shoot branching.

Wheat *oligo-tillering* mutant *ot1* has significantly reduced tillering and spike length, but increased grain weight, independent of the previously reported effects of *TB1*. Strigolactone biosynthesis genes *D27, D17, D10 and MAX1* and signal transduction genes *D14* and *D53* were all shown to be upregulated in *ot1*, suggesting strigolactone concentration was involved in causing these developmental effects (Bai *et al.*, 2024). Furthermore, mutation of the strigolactone receptor *TaD14* was associated with increased tillering and an increased thousand grain weight (Liu *et al.*, 2021a). An optimal balance between *TaD14* haplotypes may have been selected for in modern wheat varieties (Liu *et al.*, 2021a), illustrating the potentially significant role of strigolactone in multiple aspects of reproductive architecture.

S*QUAMOSA PROMOTER-BINDING-LIKE 14 (SPL14)* is an *IPA1* orthologue in wheat (Jian *et al.*, 2024). *SPL14* overexpression results in reduced tiller number and increased grain weight in wheat. *SPL14 is* downstream of the SL signalling gene *D53* (Song *et al.*, 2017) and itself regulate the downstream expression of auxin transport genes *PIN1b* and *PILS6b* in rice, suggesting another mechanism for strigolactone influencing cereal shoot development (Li *et al.*, 2022; Feng *et al.*, 2023).

This small number of studies suggests that strigolactone may be involved in not only tillering, but also spike and grain development and is justified as a subject of further inquiry into the regulation of cereal reproductive architecture.

1.5 Nitrate Response

As discussed in section 1.3.6, it is well established that resource availability is communicated by hormonal signals to modulate shoot branching (Takei *et al.*, 2001; Müller *et al.*, 2015; de Jong *et al.*, 2019). However, it is less well understood how nitrate availability affects all of reproductive shoot architecture, especially in cereals.

As a major world crop, the effect of fertiliser application on many aspects of wheat development has been studied extensively, particularly the effect on grain yield and grain quality (Abedi, Alemzadeh and Kazemeini, 2011; Duan *et al.*, 2018; Zörb, Ludewig and Hawkesford, 2018; Peng *et al.*, 2022). However, many studies investigate the effect of nutritional increase generally, via fertiliser application or nitrogen increase, even though specific forms of nitrogen have been shown to elicit distinct developmental responses via different signalling pathways (Andrews, Raven and Lea, 2013). For instance, in rice, *OsPIN9* was shown to increase tillering in response to ammonium, but not to nitrate (Hou *et al.*, 2021). Meanwhile, in wheat, levels of root-shoot cytokinin translocation (and subsequent tillering) differed significantly between treatments of nitrate, ammonium and urea (Bauer and von Wirén, 2020).

What remains under-investigated is how nitrate availability affects the development of specific aspects of shoot architecture development in wheat, such as spikelet development and shoot apical meristem determinacy. Some wheat-specific work has indicated that soil nitrogen levels influence aspects of architecture besides tillering, such as spikelet and floret development (Ewert and Honermeier, 1999; Oscarson, 2000; Z. Zhang *et al.*, 2021). However, this work does not distinguish any specific nitrogen form from another and only goes as far as to report observed phenotypic effects. What is ultimately needed is a specific understanding of how nitrate affects shoot architecture in wheat and the molecular network that coordinates the response. This increased understanding would allow for improved breeding efforts of crops that could better utilise the nutrients available to them, potentially creating greater yields, without the need for increased fertiliser use.

Studies into nitrate response in Arabidopsis nd rice suggest rational lines of enquiry into how wheat might coordinate shoot development with nitrate availability. Increased nitrogen in the soil is well established as resulting in increased synthesis of tZ cytokinins in the root and their subsequent transport to the shoot system (Takei *et al.*, 2001, 2004; Hirose *et al.*, 2008; Poitout *et al.*, 2018), where it subsequently encourages tiller bud outgrowth (Yuan *et al.*, 2023). This has been confirmed in

wheat, where nitrogen fertilisation results in increased active trans-Zeatin and decreased inactive cis-Zeatin forms of cytokinin (Garnica *et al.*, 2010) and that cytokinin has a conserved role in the upregulation of tillering in wheat, which is encouraged by increased levels of several nitrogen forms (Bauer and von Wirén, 2020).

Additionally, there is a smaller body of evidence that also supports the theory that strigolactones coordinate response to nitrogen and nitrate availability in several species, including *Arabidopsis* (de Jong, Ongaro and Ljung, 2014) and rice (Sun *et al.*, 2014; J. Sun *et al.*, 2023). Additionally, nitrate fertilisation of rice was shown to increase tillering via the strigolactone synthesis MAX1 orthologue *Os1900* and mutations to this gene resulted in increased tillering sensitivity to nutritional increase (Cui *et al.*, 2023). Whilst nitrate-induced levels and activity of strigolactone in the wheat shoot system are not well understood, nitrogen deficiency does result in increased strigolactone exudation in the root system, implying at least some link between nitrogen and strigolactone in wheat (Yoneyama *et al.*, 2012).

As discussed in sections 1.4.7 and 1.4.8, both cytokinin and strigolactone have the capacity to modulate the development of wheat shoot architecture. Therefore, in chapter 4, both hormones are investigated for their potential as coordinators of shoot development with nitrate availability.

1.6 Soil Volume Availability Response

Plant development responds to soil volume, however there is relatively little research into how this process is coordinated. Restriction of soil volume has been shown to elicit shoot developmental responses in several species, including tomato (Bar-Tal *et al.*, 1995), cotton (Yong *et al.*, 2010), bean (Carmi and Heuer, 1981), and wheat (Wheeldon *et al.*, 2020). Importantly, modulation of shoot architecture in response to soil volume has been shown to occur independently of associated changes to nutrients (Hess and De Kroon, 2007; Poorter *et al.*, 2012; Wheeldon *et al.*, 2020). However, it appears that SVA affects different aspects of shoot development

depending on the species, including shifting towards vegetative development, shifting towards reproductive development, and altered flowering time, (McConnaughay and Bazzaz, 1991) indicating the need for species-specific research.

Several species-specific effects of soil volume and planting density (the effects of which have been proven to be interchangeable) (Wheeldon *et al.*, 2020), have been reported in wheat. Denser planting results in decreased seed size, primarily by reducing the size of seeds produced on the middle spikelets of ears (Liu, Liao and Liu, 2021). Furthermore, in the elite spring wheat line ‘Mulika’, increased SVA resulted in a significant increase in peak tiller number and dry shoot biomass (Wheeldon *et al.*, 2020).

Although this small body of evidence is sufficient to show that wheat plants modulate shoot development in response to growing volume, it remains to be determined *how* shoot architecture development is coordinated with perceived SVA. This coordination is likely performed by long distance phytohormones, as is established for shoot developmental response to nutrient availability in *Arabidopsis* and cereals (Takei *et al.*, 2001; de Jong, Ongaro and Ljung, 2014; Müller *et al.*, 2015). There is little work on potential hormonal coordinators of SVA response, but strigolactones are a likely candidate. Firstly, they act as root exudates, with important roles in sensing soil volume in the root system in pea (Wheeldon *et al.*, 2022) and rice (Yoneyama *et al.*, 2022). Secondly, they are already shown to act as root-shoot signals to modulate shoot development in response to root sensing, in particular, phosphate availability, including in wheat (Umehara *et al.*, 2010; Kohlen *et al.*, 2011; de Souza Campos *et al.*, 2019). Thirdly, they have already been shown capable of influencing shoot architecture development in wheat (section 1.4.8). Thus, a pathway of root sensing, root-shoot transport and shoot modulation could be achieved through the involvement of strigolactone in each of these steps. Further encouraging this theory is the finding that changes in strigolactone levels in winter wheat were shown to correlate with decreases in tillering and increases in grain number under denser planting conditions (P. Liu *et al.*, 2023). Therefore, in chapter

5, I investigate the involvement of strigolactone in the coordination of wheat shoot architecture development with soil volume.

1.7 Aims

The principal aim of this thesis is to investigate how internal and external stimuli result in changes to cereal reproductive architecture development and to explore the involvement of cytokinin and strigolactone in this coordination. Specifically, I investigate the coordination of reproductive architecture with perceived resource availability, resulting from nitrate restriction, soil volume restriction or increased developmental demand from an increased number of spikelets.

Furthermore, I investigate the phytohormonal mechanisms that underlie this coordination. Utilising knowledge from better understood model systems including Arabidopsis and rice, I identify cytokinin and strigolactone as candidates for coordinating wheat and barley shoot developmental response to resource availability and investigate their potential involvement in three interrelated developmental phenomena:

1. Spikelet-tiller feedback

Lines of wheat and barley with a high number of spikelets per ear are often reported as also having a reduced number of tillers per plant. I hypothesise that this is not an unlinked genetic effect, but a linked feedback response, similar to the observed feedback between inflorescences in *Arabidopsis.* Two high-spikelet, low-tiller lines are studied: the wheat *hb* line, which produces a high number of additional, ‘paired’ spikelets and the barley *vrs1* line, which is a six-row line, producing three spikelets per node instead of one.

2. Shoot developmental response to nitrate availability

Wheat shoot development is sensitive to nitrate availability. I investigate the specific effects of nitrate restriction on tiller, spikelet and shoot meristem development in wheat. Research in *Arabidopsis* and rice suggests the involvement of cytokinin and strigolactone in these species' nitrate response. These two phytohormones are therefore investigated to determine the extent to which they coordinate the observed shoot developmental responses to nitrate restriction.

3. Shoot developmental response to soil volume availability

Plants respond to soil volume availability (SVA) in a manner that is distinct from their response to the change in nutrients that coincides with soil volume. I investigate the specific effect SVA restriction has on wheat shoot architecture development, with particular focus on tiller, spikelet and shoot meristem development. Informed by the reported function of strigolactone as a soil volume sensing root exudate and as root to shoot phytohormone than can modulate shoot architecture, I investigate the extent to which strigolactone coordinates the observed developmental effects.

1.8 References

Abedi, T., Alemzadeh, A. and Kazemeini, S.A. (2011) ‘Wheat yield and grain protein response to nitrogen amount and timing’. AJCS. 5(3), pp. 2330-336.

Aguilar-Martínez, J.A., Poza-Carrión, C. and Cubas, P. (2007) ‘Arabidopsis BRANCHED1 Acts as an Integrator of Branching Signals within Axillary Buds’, The Plant Cell, 19(2), pp. 458–472.

Ai, G. et al. (2024) ‘Dissecting the molecular basis of spike traits by integrating gene regulatory networks and genetic variation in wheat’, Plant Communications, 5(5), p. 100879.

Andrews, M., Raven, J. a. and Lea, P. j. (2013) ‘Do plants need nitrate? The mechanisms by which nitrogen form affects plants’, Annals of Applied Biology, 163(2), pp. 174–199.

Arite, T. et al. (2007) ‘DWARF10, an RMS1/MAX4/DAD1 ortholog, controls lateral bud outgrowth in rice’, The Plant Journal, 51(6), pp. 1019–1029.

Bai, J. et al. (2024) ‘Strigolactone and abscisic acid synthesis and signaling pathways are enhanced in the wheat oligo-tillering mutant ot1’, Molecular Breeding : New Strategies in Plant Improvement, 44(2), p. 12.

Bangerth, F. (1989) ‘Dominance among fruits/sinks and the search for a correlative signal’, Physiologia Plantarum, 76(4), pp. 608–614.

Bar-Tal, A. et al. (1995) ‘Root restriction and N-NO3 solution concentration effects on nutrient uptake, transpiration and dry matter production of tomato’, Scientia Horticulturae, 63(3), pp. 195–208.

Bauer, B. and von Wirén, N. (2020) ‘Modulating tiller formation in cereal crops by the signalling function of fertilizer nitrogen forms’, Scientific Reports, 10, p. 20504.

Boden, S.A. et al. (2015) ‘Ppd-1 is a key regulator of inflorescence architecture and paired spikelet development in wheat’, Nature Plants, 1.

Bommert, P. et al. (2005) ‘Genetics and evolution of inflorescence and flower development in grasses’, Plant and Cell Physiology, 46(1), pp. 69–78.

Booker, J., Chatfield, S. and Leyser, O. (2003) ‘Auxin Acts in Xylem-Associated or Medullary Cells to Mediate Apical Dominance’, The Plant Cell, 15(2), pp. 495–507.

Bortiri, E. et al. (2006) ‘ramosa2 encodes a LATERAL ORGAN BOUNDARY domain protein that determines the fate of stem cells in branch meristems of maize’, Plant Cell, 18(3), pp. 574–585.

Brassac, J. et al. (2021) ‘Linkage mapping identifies a non-synonymous mutation in FLOWERING LOCUS T (FT-B1) increasing spikelet number per spike’, Scientific Reports, 11(1), p. 1585.

Bull, H. et al. (2017) ‘Barley SIX-ROWED SPIKE3 encodes a putative Jumonji C-type H3K9me2/me3 demethylase that represses lateral spikelet fertility’, Nature Communications, 8(1).

Cammarata, J., Roeder, A.H. and Scanlon, M.J. (2019) ‘Cytokinin and CLE signaling are highly intertwined developmental regulators across tissues and species’, Current Opinion in Plant Biology, 51, pp. 96–104.

Carmi, A. and Heuer, B. (1981) ‘The Role of Roots in Control of Bean Shoot Growth’, Annals of Botany, 48(4), pp. 519–527.

Chen, L. et al. (2020) ‘Cytokinin dehydrogenase: a genetic target for yield improvement in wheat’, Plant Biotechnology Journal, 18(3), pp. 614–630.

Chen, L. et al. (2022) ‘The LONELY GUY gene family: from mosses to wheat, the key to the formation of active cytokinins in plants’, Plant Biotechnology Journal, 20(4), pp. 625–645.

Chen, Y., Dan, Z. and Li, S. (2020) ‘Rice GROWTH-REGULATING FACTOR 7 controls tiller number by regulating strigolactone synthesis’, Plant Signaling and Behavior, 15(11).

Chickarmane, V.S. et al. (2012) ‘Cytokinin signaling as a positional cue for patterning the apical-basal axis of the growing Arabidopsis shoot meristem’, Proceedings of the National Academy of Sciences of the United States of America, 109(10), pp. 4002–4007.

Chuck, G. et al. (2002) ‘The Control of Spikelet Meristem Identity by the branched silkless1 Gene in Maize’, Science, 298(5596), pp. 1238–1241.

Cui, J. et al. (2023) ‘Fertilization controls tiller numbers via transcriptional regulation of a MAX1-like gene in rice cultivation’, Nature Communications, 14(1), p. 3191.

Dixon, L.E. et al. (2018) ‘TEOSINTE BRANCHED1 regulates inflorescence architecture and development in bread wheat (Triticum aestivum)’, Plant Cell, 30(3), pp. 563–581.

Dixon, L.E., Pasquariello, M. and Boden, S.A. (2020) ‘Teosinte branched1 regulates height and stem internode length in bread wheat’, Journal of Experimental Botany, 71(16), pp. 4742–4750.

Dobrovolskaya, O. et al. (2015) ‘Frizzy panicle drives supernumerary spikelets in bread wheat’, Plant Physiology, 167(1), pp. 189–199.

Domagalska, M.A. and Leyser, O. (2011) ‘Signal integration in the control of shoot branching’, Nature Reviews Molecular Cell Biology, 12(4), pp. 211–221.

Dong, Z. et al. (2019) ‘The regulatory landscape of a core maize domestication module controlling bud dormancy and growth repression’, Nature Communications, 10(1).

Duan, J. et al. (2018) ‘Grain number responses to pre-anthesis dry matter and nitrogen in improving wheat yield in the Huang-Huai Plain’, Scientific Reports, 8(1), p. 7126.

Duan, J. et al. (2019) ‘Strigolactone promotes cytokinin degradation through transcriptional activation of CYTOKININ OXIDASE/ DEHYDROGENASE 9 in rice’,

Proceedings of the National Academy of Sciences of the United States of America, 116(28), pp. 14319–14324.

Dun, E.A. et al. (2012) ‘Antagonistic action of strigolactone and cytokinin in bud outgrowth control’, Plant Physiology, 158(1), pp. 487–498.

van Esse, G.W. et al. (2017) ‘Six-rowed spike3 (VRS3) is a histone demethylase that controls lateral spikelet development in Barley’, Plant Physiology, 174(4), pp. 2397–2408.

Ewert, F. and Honermeier, B. (1999) ‘Spikelet initiation of winter triticale and winter wheat in response to nitrogen fertilization’, European Journal of Agronomy, 11(2), pp. 107–113.

Feng, F. et al. (2023) ‘OsPIN2 is involved in OsSPL14/17-inhibited tiller bud outgrowth in response to phosphate deficiency in rice’, Environmental and Experimental Botany, 209, p. 105297.

Gallagher, J.P. et al. (2023) ‘GRASSY TILLERS1 (GT1) and SIX-ROWED SPIKE1 (VRS1) homologs share conserved roles in growth repression’, Proceedings of the National Academy of Sciences of the United States of America, 120(51), p. e2311961120.

Garnica, M. et al. (2010) ‘The signal effect of nitrate supply enhances active forms of cytokinins and indole acetic content and reduces abscisic acid in wheat plants grown with ammonium’, Journal of Plant Physiology, 167(15), pp. 1264–1272.

Gauley, A. et al. (2024) ‘Photoperiod-1 regulates the wheat inflorescence transcriptome to influence spikelet architecture and flowering time’, Current Biology, 34(11), pp. 2330-2343.e4.

Glenn, P. et al. (2022) ‘Identification and characterization of a natural polymorphism in FT-A2 associated with increased number of grains per spike in wheat’, Theoretical and Applied Genetics, 135(2), pp. 679–692.

Gomez-Roldan, V. et al. (2008) ‘Strigolactone inhibition of shoot branching’, Nature, 455(7210), pp. 189–194.

Guan, J.C. et al. (2012) ‘Diverse Roles of Strigolactone Signaling in Maize Architecture and the Uncoupling of a Branching-Specific Subnetwork’, Plant Physiology, 160(3), pp. 1303–1317.

Ha, C.V. et al. (2014) ‘Positive regulatory role of strigolactone in plant responses to drought and salt stress’, Proceedings of the National Academy of Sciences of the United States of America, 111(2), pp. 851–856.

Hayward, A. et al. (2009) ‘Interactions between auxin and strigolactone in shoot branching control’, Plant Physiology, 151(1), pp. 400–412.

Hess, L. and De Kroon, H. (2007) ‘Effects of rooting volume and nutrient availability as an alternative explanation for root self/non-self discrimination’, Journal of Ecology, 95(2), pp. 241–251.

Hirose, N. et al. (2008) ‘Regulation of cytokinin biosynthesis, compartmentalization and translocation’, Journal of Experimental Botany, 59(1), pp. 75–83.

Hou, M. et al. (2021) ‘OsPIN9, an auxin efflux carrier, is required for the regulation of rice tiller bud outgrowth by ammonium’, New Phytologist, 229(2), pp. 935–949.

Ikeda, K. et al. (2007) ‘Rice ABERRANT PANICLE ORGANIZATION 1, encoding an F-box protein, regulates meristem fate’, The Plant Journal, 51(6), pp. 1030–1040.

Ikeda-Kawakatsu, K. et al. (2012) ‘ABERRANT PANICLE ORGANIZATION 2/RFL, the rice ortholog of Arabidopsis LEAFY, suppresses the transition from inflorescence meristem to floral meristem through interaction with APO1’, The Plant Journal, 69(1), pp. 168–180.

Ishikawa, S. et al. (2005) ‘Suppression of Tiller Bud Activity in Tillering Dwarf Mutants of Rice’, Plant and Cell Physiology, 46(1), pp. 79–86.

Jablonski, B. et al. (2021) ‘Genotype-Dependent Effect of Silencing of TaCKX1 and TaCKX2 on Phytohormone Crosstalk and Yield-Related Traits in Wheat’, International Journal of Molecular Sciences, 22(21), p. 11494.

Jain, P. et al. (2022) ‘Genome-Wide Analysis and Evolutionary Perspective of the Cytokinin Dehydrogenase Gene Family in Wheat (Triticum aestivum L.)’, Frontiers in Genetics, 13, p. 931659.

Jian, C. et al. (2024) ‘The TaGW2-TaSPL14 module regulates the trade-off between tiller number and grain weight in wheat’, Journal of Integrative Plant Biology.

de Jong, M. et al. (2019) ‘Natural variation in Arabidopsis shoot branching plasticity in response to nitrate supply affects fitness’, PLoS Genetics, 15(9), pp. 1-31.

de Jong, M., Ongaro, V. and Ljung, K. (2014) ‘Auxin and Strigolactone Signaling are Required for Modulation of Arabidopsis Shoot Branching by Nitrogen Supply’, Plant Physiology, 166(1), pp. 384–395.

Kaneko-Suzuki, M. et al. (2018) ‘TFL1-Like Proteins in Rice Antagonize Rice FT-Like Protein in Inflorescence Development by Competition for Complex Formation with 14-3-3 and FD’, Plant and Cell Physiology, 59(3), pp. 458–468.

Kapulnik, Y. and Koltai, H. (2016) ‘Fine-tuning by strigolactones of root response to low phosphate’, Journal of Integrative Plant Biology, 58(3), pp. 203–212.

Kebrom, T.H., Burson, B.L. and Finlayson, S.A. (2006) ‘Phytochrome B Represses Teosinte Branched1 Expression and Induces Sorghum Axillary Bud Outgrowth in Response to Light Signals’, Plant Physiology, 140(3), pp. 1109–1117.

Khuvung, K., Silva Gutierrez, F.A.O. and Reinhardt, D. (2022) ‘How Strigolactone Shapes Shoot Architecture’, Frontiers in Plant Science, 13, p. 889045.

Kohlen, W. et al. (2011) ‘Strigolactones are transported through the xylem and play a key role in shoot architectural response to phosphate deficiency in nonarbuscular mycorrhizal host arabidopsis’, Plant Physiology, 155(2), pp. 974–987.

Komatsu, M. et al. (2001) ‘The LAX1 and FRIZZY PANICLE 2 Genes Determine the Inflorescence Architecture of Rice by Controlling Rachis-Branch and Spikelet Development’, Developmental Biology, 231(2), pp. 364–373.

Koppolu, R. et al. (2013) ‘Six-rowed spike4 (Vrs4) controls spikelet determinacy and row-type in barley’, Proceedings of the National Academy of Sciences of the United States of America, 110(32), pp. 13198–13203.

Koppolu, R. and Schnurbusch, T. (2019) ‘Developmental pathways for shaping spike inflorescence architecture in barley and wheat’, Journal of Integrative Plant Biology, 61(3), pp. 278–295.

Kuzay, S. et al. (2019) ‘Identification of a candidate gene for a QTL for spikelet number per spike on wheat chromosome arm 7AL by high-resolution genetic mapping’, Theoretical and Applied Genetics, 132(9), pp. 2689–2705.

Leibfried, A. et al. (2005) ‘WUSCHEL controls meristem function by direct regulation of cytokinin-inducible response regulators’, Nature, 438(7071), pp. 1172–1175.

Li, Y. et al. (2021) ‘Wheat FRIZZY PANICLE activates VERNALIZATION1-A and HOMEOBOX4-A to regulate spike development in wheat’, Plant Biotechnology Journal, 19(6), pp. 1141–1154.

Li, Y. et al. (2022) ‘Functional redundancy of OsPIN1 paralogous genes in regulating plant growth and development in rice’, Plant Signaling & Behavior, 17(1), p. 2065432.

Liu, J. et al. (2017) ‘miR156-Targeted SBP-Box Transcription Factors Interact with DWARF53 to Regulate TEOSINTE BRANCHED1 and BARREN STALK1 Expression in Bread Wheat1’, Plant Physiology, 174(3), pp. 1931–1948.

Liu, P. et al. (2023) ‘Optimizing plant spatial competition can change phytohormone content and promote tillering, thereby improving wheat yield’, Frontiers in Plant Science, 14, p. 1147711.

Liu, R. et al. (2021) ‘Association of TaD14-4D, a Gene Involved in Strigolactone Signaling, with Yield Contributing Traits in Wheat’, International Journal of Molecular Sciences, 22(7), p. 3748.

Liu, Y., Liao, Y. and Liu, W. (2021) ‘High nitrogen application rate and planting density reduce wheat grain yield by reducing filling rate of inferior grain in middle spikelets’, The Crop Journal, 9(2), pp. 412–426.

Liu, Z. et al. (2020) ‘The Type-B cytokinin response regulator ARR1 inhibits shoot regeneration in an ARR12-dependent manner in Arabidopsis’, Plant Cell, 32(7), pp. 2271–2291.

Luo, L., Zhang, Y. and Xu, G. (2020) ‘How does nitrogen shape plant architecture?’, Journal of Experimental Botany, 71(15), pp. 4415–4427.

Lv, B. et al. (2014) ‘Characterization of FLOWERING LOCUS T1 (FT1) Gene in Brachypodium and Wheat’, PLoS ONE. Edited by P. Hernandez, 9(4), p. e94171.

Matthes, M.S. et al. (2022) ‘Defects in meristem maintenance, cell division, and cytokinin signaling are early responses in the boron deficient maize mutant tassel-less1’, Physiologia Plantarum, 174(2), p. e13670.

McConnaughay, K.D.M. and Bazzaz, F.A. (1991) ‘Is Physical Space a Soil Resource?’, Ecology, 72(1), pp. 94–103.

McSteen, P. and Leyser, O. (2005) ‘Shoot branching’, Annual Review of Plant Biology, 56, pp. 353–374. .

Meng, W.J. et al. (2017) ‘Type-B ARABIDOPSIS RESPONSE REGULATORs Specify the Shoot Stem Cell Niche by Dual Regulation of WUSCHEL’, The Plant Cell, 29(6), pp. 1357–1372.

Minakuchi, K. et al. (2010) ‘FINE CULM1 (FC1) works downstream of strigolactones to inhibit the outgrowth of axillary buds in rice’, Plant and Cell Physiology, 51(7), pp. 1127–1135.

Mitchell, P.L. and Sheehy, J.E. (2018) ‘Potential yield of wheat in the United Kingdom: How to reach 20 t ha−1’, Field Crops Research, 224, pp. 115–125.

Müller, D. et al. (2015) ‘Cytokinin is required for escape but not release from auxin mediated apical dominance’, Plant Journal, 82(5), pp. 874–886.

Muqaddasi, Q.H. et al. (2019) ‘TaAPO-A1, an ortholog of rice ABERRANT PANICLE ORGANIZATION 1, is associated with total spikelet number per spike in elite European hexaploid winter wheat (Triticum aestivum L.) varieties’, Scientific Reports, 9, p. 13853.

Nakagawa, M., Shimamoto, K. and Kyozuka, J. (2002) ‘Overexpression of RCN1 and RCN2, rice TERMINAL FLOWER 1/CENTRORADIALIS homologs, confers delay of phase transition and altered panicle morphology in rice’, The Plant Journal, 29(6), pp. 743–750.

Nordström, A. et al. (2004) Auxin regulation of cytokinin biosynthesis in Arabidopsis thaliana: A factor of potential importance for auxin-cytokinin-regulated development, DEVELOPMENTAL BIOLOGY, pp. 8039–8044.

Ogonowska, H. et al. (2019) ‘Specificity of expression of TaCKX family genes in developing plants of wheat and their co-operation within and among organs’, PLoS ONE, 14(4), p. e0214239.

Oscarson, P. (2000) ‘The strategy of the wheat plant in acclimating growth and grain production to nitrogen availability’, Journal of Experimental Botany, 51(352), pp. 1921–1929.

Peng, Z. et al. (2022) ‘Differential growth dynamics control aerial organ geometry’, Current Biology, p. S096098222201555X.

Pequeno, D.N.L. et al. (2021) ‘Climate impact and adaptation to heat and drought stress of regional and global wheat production’, Environmental Research Letters, 16(5), p. 054070.

Poitout, A. et al. (2018) ‘Responses to systemic nitrogen signaling in arabidopsis roots involve trans-zeatin in shoots’, Plant Cell, 30(6), pp. 1243–1257.

Poorter, H. et al. (2012) ‘Pot size matters: a meta-analysis of the effects of rooting volume on plant growth’, Functional Plant Biology, 39(11), p. 839.

Poursarebani, N. et al. (2015) ‘The genetic basis of composite spike form in barley and “miracle-wheat”’, Genetics, 201(1), pp. 155–165.

Prusinkiewicz, P. et al. (2009) ‘Control of bud activation by an auxin transport switch’, PNAS, 106(41), pp. 17431–17436.

Ramsay, L. et al. (2011) ‘INTERMEDIUM-C, a modifier of lateral spikelet fertility in barley, is an ortholog of the maize domestication gene TEOSINTE BRANCHED 1’, Nature Genetics, 43(2), pp. 169–172.

Rathore, R.S. et al. (2024) ‘Concurrent improvement of rice grain yield and abiotic stress tolerance by overexpression of cytokinin activating enzyme LONELY GUY (OsLOG)’, Plant Physiology and Biochemistry, 211, p. 108635.

Ray, D.K. et al. (2013) ‘Yield Trends Are Insufficient to Double Global Crop Production by 2050’, PLoS ONE, 8(6).

Reynolds, M. et al. (2009) ‘Raising yield potential in wheat’, Journal of Experimental Botany, 60(7), pp. 1899–1918.

Sachs, T. and Thimann, K.V. (1967) ‘The Role of Auxins and Cytokinins in the Release of Buds from Dominance’, American Journal of Botany, 54(1), pp. 136–144.

Sakuma, S. and Koppolu, R. (2023) ‘Form follows function in Triticeae inflorescences’, Breeding Science, 73(1), pp. 46–56.

Schils, R. et al. (2018) ‘Cereal yield gaps across Europe’, European Journal of Agronomy, 101, pp. 109–120.

Schultz, E. and Haughn, G. (1991) ‘LEAFY, a Homeotic Gene That Regulates Inflorescence Development in Arabidopsis.’, The Plant Cell, 3(8), pp. 771–781.

Seale, M., Bennett, T. and Leyser, O. (2017) ‘BRC1 expression regulates bud activation potential but is not necessary or sufficient for bud growth inhibition in arabidopsis’, Development (Cambridge), 144(9), pp. 1661–1673.

Shao, G. et al. (2019) ‘Tiller Bud Formation Regulators MOC1 and MOC3 Cooperatively Promote Tiller Bud Outgrowth by Activating FON1 Expression in Rice’, Molecular Plant, 12(8), pp. 1090–1102.

Shaw, L.M. et al. (2019) ‘FLOWERING LOCUS T2 regulates spike development and fertility in temperate cereals’, Journal of Experimental Botany, 70(1), pp. 193–204.

Shinohara, N., Taylor, C. and Leyser, O. (2013) ‘Strigolactone Can Promote or Inhibit Shoot Branching by Triggering Rapid Depletion of the Auxin Efflux Protein PIN1 from the Plasma Membrane’, PLoS Biology, 11(1).

Somssich, M. et al. (2016) ‘CLAVATA-WUSCHEL signaling in the shoot meristem’, Development, 143(18), pp. 3238–3248.

Song, X. et al. (2017) ‘IPA1 functions as a downstream transcription factor repressed by D53 in strigolactone signaling in rice’, Cell Research, 27(9), pp. 1128–1141.

Sorefan, K. et al. (2003) ‘MAX4 and RMS1 are orthologous dioxygenase-like genes that regulate shoot branching in Arabidopsis and pea’, Genes & Development, 17(12), pp. 1469–1474.

de Souza Campos, P.M. et al. (2019) ‘Phosphate acquisition efficiency in wheat is related to root:shoot ratio, strigolactone levels, and PHO2 regulation’, Journal of Experimental Botany, 70(20), pp. 5631–5642.

Studer, A.J., Wang, H. and Doebley, J.F. (2017) ‘Selection during maize domestication targeted a gene network controlling plant and inflorescence architecture’, Genetics, 207(2), pp. 755–765.

Sun, H. et al. (2014) ‘Strigolactones are involved in phosphate- and nitrate-deficiency-induced root development and auxin transport in rice’, Journal of Experimental Botany, 65(22), pp. 6735–6746.

Sun, J. et al. (2023) ‘Genome-edited TaTFL1-5 mutation decreases tiller and spikelet numbers in common wheat’, Frontiers in Plant Science, 14, p. 1142779.

Takei, K. et al. (2001) Nitrogen-Dependent Accumulation of Cytokinins in Root and the Transloca-tion to Leaf: Implication of Cytokinin Species that Induces Gene Expression of Maize Response Regulator, Plant Cell Physiol, pp. 85–93.

Takei, K. et al. (2004) AtIPT3 is a Key Determinant of Nitrate-Dependent Cytokinin Biosynthesis in Arabidopsis, Plant Cell Physiol, pp. 1053–1062.

Tanaka, M. et al. (2006) ‘Auxin controls local cytokinin biosynthesis in the nodal stem in apical dominance’, Plant Journal, 45(6), pp. 1028–1036.

Thimann, K. and Skoog, F. (1933) ‘STUDIES ON THE GROWTH HORMONE OF PLANTS. III. THE INHIBITING ACTION OF THE GROWTH SUBSTANCE ON BUD DEVELOPMENT’, PNAS, pp. 714–716.

Umehara, M. et al. (2008) ‘Inhibition of shoot branching by new terpenoid plant hormones’, Nature, 455(7210), pp. 195–200.

Umehara, M. et al. (2010) ‘Contribution of strigolactones to the inhibition of tiller bud outgrowth under phosphate deficiency in rice’, Plant and Cell Physiology, 51(7), pp. 1118–1126.

Waldie, T. and Leyser, O. (2018) ‘Cytokinin targets auxin transport to promote shoot branching’, Plant Physiology, 177(2), pp. 803–818.

Walker, C.H. and Bennett, T. (2018) ‘Forbidden Fruit: Dominance Relationships and the Control of Shoot Architecture’, in Annual Plant Reviews online. Wiley, pp. 217–254.

Walker, C.H., Wheeldon, C.D. and Bennett, T. (2021) ‘Integrated dominance mechanisms regulate reproductive architecture in Arabidopsis thaliana and Brassica napus’, Plant Physiology, 186(4) pp. 1985-2002.

Wang, H. et al. (2018) ‘Abscisic acid influences tillering by modulation of strigolactones in barley’, Journal of Experimental Botany, 69(16), pp. 3883–3898.

Wang, J. et al. (2018) ‘Rice nitrate transporter OsNPF7.2 positively regulates tiller number and grain yield’, Rice, 11(1).

Ware, A. et al. (2020) ‘Auxin export from proximal fruits drives arrest in temporally competent inflorescences’, Nature Plants, 6(6), pp. 699–707.

Wen, X. et al. (2020) ‘Rice dwarf and low tillering 10 (OsDLT10) regulates tiller number by monitoring auxin homeostasis’, Plant Science, 297.

Wheeldon, C.D. et al. (2021) ‘Wheat plants sense substrate volume and root density to proactively modulate shoot growth’, Plant Cell and Environment, 44(4), pp. 1202–1214.

Wheeldon, C.D. et al. (2022) ‘Environmental strigolactone drives early growth responses to neighboring plants and soil volume in pea’, Current Biology, 32(16), pp. 3593-3600.e3.

Whitewoods, C.D. et al. (2018) ‘CLAVATA Was a Genetic Novelty for the Morphological Innovation of 3D Growth in Land Plants’, Current Biology, 28(15), pp. 2365-2376.e5.

Wickson, M. and Thimann, K.V. (1958) ‘The Antagonism of Auxin and Kinetin in Apical Dominance’, Physiologia Plantarum, 11(1), pp. 62–74.

Xie, Y. et al. (2020) ‘Arabidopsis FHY3 and FAR1 integrate light and strigolactone signaling to regulate branching’, Nature Communications, 11(1).

Yeh, S.Y. et al. (2015) ‘Down-Regulation of Cytokinin Oxidase 2 Expression Increases Tiller Number and Improves Rice Yield’, Rice, 8(1), pp. 1–13.

Yoneyama, K. et al. (2022) ‘Supra-organismal regulation of strigolactone exudation and plant development in response to rhizospheric cues in rice’, Current Biology, 32(16), pp. 3601-3608.

Yoneyama, Kaori et al. (2012) ‘How do nitrogen and phosphorus deficiencies affect strigolactone production and exudation?’, Planta, 235(6), pp. 1197–1207.

Yong, J.W.H. et al. (2010) ‘Effects of root restriction on growth and associated cytokinin levels in cotton (Gossypium hirsutum)’, Functional Plant Biology, 37(10), pp. 974–984.

Youssef, H.M. et al. (2017) ‘VRS2 regulates hormone-mediated inflorescence patterning in barley’, Nature Genetics, 49(1), pp. 157–161.

Youssef, H.M. and Hansson, M. (2019) ‘Crosstalk among hormones in barley spike contributes to the yield’, Plant Cell Reports, 38(8), pp. 1013–1016.

Yuan, Y. et al. (2023) ‘Unlocking the Multifaceted Mechanisms of Bud Outgrowth: Advances in Understanding Shoot Branching’, Plants, 12(20), p. 3628.

Zalewski, W. et al. (2010) ‘Silencing of the HvCKX1 gene decreases the cytokinin oxidase/dehydrogenase level in barley and leads to higher plant productivity’, Journal of Experimental Botany, 61(6), pp. 1839–1851.

Zalewski, W. et al. (2014) ‘Expression patterns of HvCKX Genes indicate their role in growth and reproductive development of barley’, PLoS ONE, 9(12).

Zhang, B. et al. (2015) ‘Novel function of a putative MOC1 ortholog associated with spikelet number per spike in common wheat’, Scientific Reports, 5.

Zhang, J. et al. (2011) ‘Isolation and characterization of two putative cytokinin oxidase genes related to grain number per spike phenotype in wheat’, Molecular Biology Reports, 38(4), pp. 2337–2347.

Zhang, J. et al. (2022) ‘Genetic and transcriptomic dissection of an artificially induced paired spikelets mutant of wheat (Triticum aestivum L.)’, Theoretical and Applied Genetics, 135(7), pp. 2543–2554.

Zhang, K. et al. (2018) ‘AUXIN RESPONSE FACTOR3 regulates floral meristem determinacy by repressing cytokinin biosynthesis and signaling’, Plant Cell, 30(2), pp. 324–346.

Zhang, L. et al. (2012) ‘TaCKX6-D1, the ortholog of rice OsCKX2, is associated with grain weight in hexaploid wheat’, New Phytologist, 195(3), pp. 574–584.

Zhang, S.-W. et al. (2009) ‘Altered Architecture and Enhanced Drought Tolerance in Rice via the Down-Regulation of Indole-3-Acetic Acid by TLD1/OsGH3.13 Activation’, Plant Physiology, 151(4), pp. 1889–1901.

Zhang, Z. et al. (2021) ‘Spike growth affects spike fertility through the number of florets with green anthers before floret abortion in wheat’, Field Crops Research, 260, p. 108007.

Zörb, C., Ludewig, U. and Hawkesford, M.J. (2018) ‘Perspective on Wheat Yield and Quality with Reduced Nitrogen Supply’, Trends in Plant Science, 23(11), pp. 1029–1037. Available at: https://doi.org/10.1016/j.tplants.2018.08.012.

Zou, J. et al. (2006) ‘The rice HIGH-TILLERING DWARF1 encoding an ortholog of Arabidopsis MAX3 is required for negative regulation of the outgrowth of axillary buds’, Plant Journal, 48(5), pp. 687–698.

Zwirek, M., Waugh, R. and McKim, S.M. (2019) ‘Interaction between row-type genes in barley controls meristem determinacy and reveals novel routes to improved grain’, New Phytologist, 221(4), pp. 1950–1965.

Chapter 2

Materials and Methods

2.1 Plant growth conditions

2.1.1 Standard Growth conditions

All plants were grown John Innes No. 2 compost. The day/night cycle was 16h/8h of light and dark at 20^{o}C and 16 ^{o} C respectively. Plants were grown in greenhouses with a natural light source alongside LED lights with an average light intensity of ~250 µmol $m^{-2}s^{-1}$. Plants were grown in 500ml pots, except where stated in chapter 5 in which they were also grown in 100ml and 2000ml pots.

2.1.2 Hydroponics set up

Hydroponically grown cereals were grown in 500ml cylindrical pots filled with water. Each pot contained a single plant (Figure 2.01C). An air stone was attached to an AP-12 air pump (with a flow rate of 2.8 litres per minute) through a hollow rubber tube and placed under the water to allow for oxygenation of the roots (Figure 2.01A-B). Seedlings were given one week to germinate growing on perlite, after which the roots were washed and a foam collar was placed around the hypocotyl and held in place through a plastic tube in the lid of the pot, so that the roots were submerged, and the shoot emerged out of the pot (Figure 2.01C). Every 7 days ATS was replenished (section 2.1.3). Water was topped up daily and entirely removed and replenished alongside ATS every 7 days.

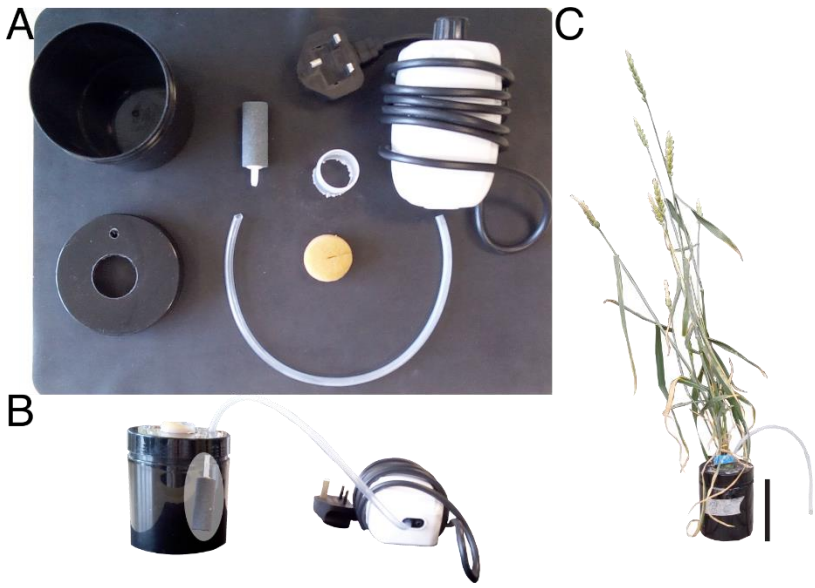

Figure 2.01: Components of the hydroponic cereal growth system.
(A) Disassembled components: 500ml cylindrical pot; removable pot lid with large hole for the plant shoot and small hole for the air tube; electric air pump, rubber tube and air stone, to provide consistent oxygen to the system; plastic collar and foam bung, to initially fit around the coleoptile and subsequently provide support to the shoot system. **(B)** Assembled components of the hydroponic system. **(C)** Hydroponic system, supporting the growth of a wheat plant.

2.1.3 ATS stock

ATS (Arabidopsis Thaliana Salts) (Wilson *et al.*, 1990) were used as a modular fertiliser which was added to the hydroponic system to provide nutrition to the plants. 7.5ml of standard ATS mix was used per 500ml pot, using the following molar concentrations:

Stock	Concentration (mM)
KNO_3	333.3
KH_2PO_4	166.7
MgSO4	133.3
$Ca(NO_3)_2$	133.3
Fe-EDTA	166.7
Micronutrients Stock solution:	
H_3BO_3	70mM
$MnCl_2$	14mM
$CuSO_4$	0.5mM
$ZnSO_4$	1mM
$NaMoO_4$	0.2mM
NaCl	10mM
CoCl	0.01mM

Table 2.01: Molar concentrations of the constituents of ATS stock used for hydroponics

2.1.4 Nitrate conditions

The different nitrate conditions established in section 4.2 modified the standard ATS mix as detailed below, replacing nitrate with chloride ions to maintain equivalent ion balance around the root system. Condition 1 is equivalent to the ‘standard’ ATS mix and is referred to as ‘High[N]’ in chapter 4. Condition 4 resulted in a significant but moderate change in development whilst condition 6 resulted in an extreme change in development, these were referred to as ‘Mid[N]’ and ‘Low[N]’ respectively.

	% concentration of 'standard'	[KNO_3] (mM)	[$Ca(NO_3)_2$] (mM)
1 (High[N])	100	333.3	133.3
2	50	166.67	66.67
3	20	66.67	26.67
4 (Mid[N])	10	33.33	13.33
5	5	16.67	6.67
6 (Low[N])	1	3.33	1.33

Table 2.02: Molar concentrations of the constituents of ATS stocks tested in developing varying nitrate conditions for hydroponics

2.2 Plant materials

Studies primarily used lines of the hexaploid spring wheat *Triticum aestivum.*

The elite spring wheat Cadenza is used as a control wheat, in studies comparing 'standard' wheat response to different treatments. Additionally, the following previously reported mutant lines were utilised:

Chapter 3 utilises the six-row barley (*Hordeum vulgare*) *vrs1* mutant and the two-row Bowman background (Zwirek, Waugh and McKim, 2019). These lines were provided by Sarah McKim, University of Dundee.

hb (highly-branched) wheat (*Triticum aestivum*), which has altered *TaTB-D1* expression in the inflorescence and tillers (Dixon *et al.*, 2018), is used for the study of paired spikelet development on wheat shoot development (Chapter 3). These lines were provided by Laura Dixon, University of Leeds.

Null-mutant *d14* barley (*Hordeum vulgare*) in the Sebastian background (Marzec *et al.*, 2016), in the study of the role of strigolactone in spikelet-tiller feedback (section 3.14) and soil volume response (section 5.6). These lines were provided by Marek Marzec, University of Silesia.

Null-mutant *d3* and *d14* and wheat (*Triticum aestivum*), in the Cadenza background, in the study of the role of strigolactone in spikelet-tiller feedback (section 3.13). These lines and a *tb1* mull-mutant in the Cadenza background were used in the investigation of the role of strigolactone in nitrate response (section 4.4) and soil volume response (section 5.5). These lines were provided by Steve Thomas, Rothamsted.

2.3 General phenotypic methods

2.3.1 Tiller number measurement

Tiller counts were taken by measuring the number of emerged, distinct shoots (tillers) on the plant. Tillers are counted as emerged, if more than 50% of the tiller is visible from the leaf that ensheathes it.

2.3.2 Ear number measurement

Ear counts are taken as a measurement of the number of healthy ears that have fully emerged at the end of plant life. Unhealthy ears are defined by being significantly smaller than the next smallest ears on the plant, producing no seed, or remaining green when other ears on the plant have completed seed filling.

2.3.3 Spikelet number measurement

Spikelet (inflorescence) counts are taken as a measurement of every fully formed spikelet along the rachis of the ear. Counts of paired spikelets included spikelets formed directly below the main spikelet at a rachis node.

2.3.4 Tiller emergence tracking

Location of tiller emergence was tracked by marking tillers with coloured string. When a new tiller emerged on a plant, the tiller would be marked with a colour unique to that tiller. The colour of this tiller was logged alongside the time of emergence and the location of emergence, allowing for the development of each tiller to be tracked with reference to ordinal tiller number and location of tiller emergence.

2.3.5 Seed number measurement

Seed counts are taken as a measurement of fully formed seeds. Seeds are discounted if their size was determined to be an outlier for the ear (greater than 2 standar deviations from mean), if the seed surface resembled unhealthy development (by being wrinkled or discoloured), or if the seed did not easily withstand pressure between the thumb and forefinger, suggesting improper grain filling or disease.

2.3.6 Seed weight measurement

Seed weight measurement was calculated by collectively weighing all healthy seeds from an ear after a minimum of one week in a drying cabinet. Single seed weight was calculated by dividing this value by the number of seeds weighed in each sample. Seeds were weighed using an Ohaus PIONEER™ Plus balance with a readability of 0.1mg.

2.3.7 Plant height measurement

Plant height was measured as the distance from the point at which the plant emerged from the growing medium to the tip of the final spikelet on the ear of the main shoot, discounting awns.

2.3.8 Shoot biomass measurement

Shoot biomass was measured by harvesting all shoot material, inclusive of tillers, ears and leaves. This material was placed in a drying cabinet for a minimum of one week to ensure all samples had been entirely an equally dried then were weighed using an Ohaus PIONEER™ Plus balance with a readability of 0.1mg.

2.3.9 Root biomass measurement

Root biomass was measured by harvesting all root material. This material was placed in a drying cabinet for a minimum of two weeks to ensure all samples had been equally dried and were subsequently weighed. Using an Ohaus PIONEER™ Plus balance with a readability of 0.1mg.

2.4 Hormone Treatment

2.4.1 6-BA treatment system

45.05g of powdered 6-Benzylaminopurine (Sigma-Aldrich, PrdocutCode - 102261972) was diluted in 20ml of ethanol then mixed with 180ml of distilled water to create 200ml of 1mM 6-BA. This stock was stored at -20°C. 100µM aliquots of 6-BA was created from this stock using serial dilutions up to one hour before treatment was conducted.

0.33ml of 100µM 6-BA was injected every 7 days into each fully emerged tiller (defined using the criteria in section 2.3.1). Injections were performed using a 0.5mm diameter needle attached to a 2ml syringe. The needle was angled at approximately 15 degrees from the tiller and inserted approximately 10mm above the predicted location of the shoot apical meristem. Control plants were injected with an equivalent dilution of ethanol in water using the same method at the same time.

Figure 2.02: Visualisation of hormone injection

2.4.2 GR24 treatment system

5.969g of powdered GR24 (Biosynth, Product Code - FG167307) was diluted in 20ml of acetone then mixed with 180ml of distilled water to create 200ml of 100µM GR24. This stock was stored at -20°C. 100nM aliquots of GR24 was created from this stock using serial dilutions up to one hour before treatment was conducted.

0.33ml of 100nM GR24 was injected every 7 days into each fully emerged tiller (defined using the criteria in 2.3.1). Injections were performed using a 0.5mm diameter needle attached to a 2ml syringe. The needle was angled at approximately 15 degrees from the tiller and inserted approximately 10mm above the predicted location of the shoot apical meristem. Control plants were injected with an equivalent dilution of ethanol in water using the same method at the same time.

2.5 Microscopy

2.5.1 Equipment

Dissections were performed on an Olympus SZ51 stereo light microscope at 2-40x magnification, lit using an Olympus KL 300 LED light source. Some dissections and imaging were performed using a Keyence VHX-7000 digital microscope.

2.5.2 Dissection of shoot apical meristem

Cereals were removed from their growing medium and the shoot system separated from the root system. Each tiller was dissected using a FEATHER® incision micro scalpel to reveal the shoot apical meristem. The stage of development was identified using the criteria outlined in (Kirby and Appleyard, 1987). The stages of development for wheat (Figure 2.01) and barley (Figure 2.02) are illustrated below.

Transition between vegetative and reproductive development in the SAM was defined by the transition between the vegetative and double ridge stage for both species, as defined in (Kirby and Appleyard, 1987), wherein floral primordia form above the leaf primordia along the apex of the SAM, creating the distinct “double ridge” appearance and indicating that the apex now can produce reproductive tissue.

Shoot apical meristems which had reached the double ridge stage or later were defined by these criteria as having initiated reproductive development.

Figure 2.03: Stages of SAM development in Wheat.
From left to right: Vegetative; Double ridge; Glume primordium; Lemma primordium; Floret primordium; Terminal spikelet. Red vertical lines are 1mm long. Identification conducted according to (Kirby and Appleyard, 1987).

Figure 2.04: Stages of SAM development in Barley.
From left to right: Vegetative; Double ridge; Triple mound; Glume primordium; Lemma primordium; Stamen primordium; Awn primordium. Red vertical lines are 1mm long. Identification conducted according to (Kirby and Appleyard, 1987).

2.5.3 Shoot apical meristem stage

Stage of development was determined and assigned a quantitative value according to the Waddington scale (Waddington, Cartwright and Wall, 1983), a quantitative measurement commonly used to measure spike development in wheat and barley using a scale of numbers from 0 (seedling emergence) to 10 (pollination). This scale allows each point in development to be assigned a quantitative value, allowing for statistical analysis and comparison not possible with phenotypic data.

2.5.4 Shoot apical meristem spikelet ridge count

Spikelet ridges were counted as all clearly defined spikelet ridges, based on the criteria outlined in (Kirby and Appleyard, 1987).

2.5.5 Identification of unemerged tiller buds

Once the shoot apical meristem of a tiller had been uncovered, leaves were peeled back using a scalpel below the emerged tiller SAM and the presence of any tiller buds, containing their own SAM were identified. Stage and spikelet number were then defined as described in sections 2.4.3-2.4.4.

2.6 Molecular methods

2.6.1 SAM sample collection

Shoot apical meristems were identified using an Olympus SZ51 stereo light microscope at 2-40x magnification and uncovered using a FEATHER® incision micro scalpel. All leaf material was removed from around the SAM, and subsequently the SAM was excised at the base and placed in a 1.5mm microcentrifuge tube which was flash frozen in liquid nitrogen where it was held until all samples had been collected, before being held in long term storage at -80°C.

For all molecular studies, 3 biological replicates (n=3) were taken for each measurement, each replicate consisting of up to 100mg of material, which was composed of main shoot SAMs from up to 20 plants, depending on stage of development, as at later sampling stages meristems had a greater mass.

2.6.2 Root sample collection

Roots were washed of growing medium. Main roots were identified by eye in the root system and the first 1cm of root tip was excised and placed in a 1.5mm microcentrifuge tube which was flash frozen in liquid nitrogen where it was held until all samples had been collected, before being held in long term storage at -80°C.

2.6.3 RNA extraction

Collected tissue was lysed using a TissueLyserLT (Qiagen) and two 3mm steel ball bearings per sample tube. Subsequently, RNA was extracted using the Qiagen RNeasy plant minikit, following the manufacturer's protocol.

2.6.4 DNAse treatment

Extracted RNA was treated with Thermo Fisher TURBO DNAse, following the manufacturer's protocol.

2.6.5 cDNA synthesis

cDNA was synthesised from RNA using the Roche Transcriptor First Strand cDNA Synthesis Kit, following the manufacturer's protocol.

2.6.6 Quantitative PCR (qPCR) analysis

qPCR was performed using Thermo SYBR green master mix, following the manufacturer's protocol.

The cDNA was diluted to 50 ng/µL and 2.5 µL was combined with 5 µL GoTaq® qPCR Master Mix (Promega) and 2.5 µL primer mix (1 µL 100 µm forward primer, 1 µL 100 µm reverse primer, 46 µL nuclease-free water), with a final reaction volume of 10 µL. Two technical replicates were used for each sample, and each reaction was also duplicated to receive primers to amplify the gene of interest and the reference gene *TraesCS5A02G015600* (Borrill, Ramirez-Gonzalez and Uauy, 2016). All primers used are listed in Table 2.3. Reaction components were pipetted into a sterile 96-well non-skirted qPCR plate, sealed with optically clear plate sealing film, and centrifuged briefly using a PCR Plate Centrifuge II (Avantor Sciences) to collect

the reaction in the bottom of the plate well. Quantitative PCR (qPCR) was performed using the CFX96 Thermal Cycler (Bio-Rad) with the following conditions:

95 °C for 5 min, 39 cycles of 95 °C for 10 s, and 60 °C for 30 s, followed by a melt starting at 65 °C for 5 s, increasing in 0.5 °C increments to 95 °C. Expression levels of the genes of interest were calculated relative to *TraesCS5A02G015600* following the $2^{-\Delta Cq}$ format (where ΔC_q = Gene of interest quantification cycle (C_q) value − *TraesCS5A02G015600* *TraesCS5A02G015600* C_q value).

2.6.7 Primer design

Wheat efp browser was used to identify transcripts of genes (*Wheat eFP Browser*) that were active in developing shoot and root meristems and are shown in the table below. Previously used primer sequences for were identified in the literature and used. Primers for *TaRRA1* and *TaRRA29* were first used in (Gahlaut *et al.*, 2014). Primers for *TaTB1, TaCKX3, TaD3* and *TaD14* were first used in (Sigalas *et al.*, 2023). The primer sequence for the actin housekeeping gene was taken from (Borrill, Ramirez-Gonzalez and Uauy, 2016).

Gene	Name	Forward primer	Reverse primer	Gene function
TaRRA1	TraesCS2A02G551100	ACAGAGGTGAGAAATCGAATCAATC	GTAGCCGTCCAATTTCTTGAAGA	Cytokinin signal perception
TaRRA29	TraesCS5A02G131600	ATCCTTGCTTTCTCCTCATAGCA	CGCCATCGGAGAAGAAAGAG	Cytokinin signal perception
TaCKX3	TraesCS1A02G159600	GGCTCATCCTCATCTATCCACTC	AGAATGCCAACCACGTACATCAC	Cytokinin degradation
TaD3	TraesCS7A02G110500	GGACTCAGGAAGCTCTTCATCC	TCTCYGGTGCTGGATAGTAGTC	Strigolactone signal perception
TaD14	TraesCS4A02G046700	CTCGCCTAGGTTCTTGAACGAC	GACATCGCCTGGAACACCTG	Strigolactone signal perception
TaTB1	TraesCS4A02G271300	GACATGCTCGGCTTCGACAAG	CAGTCATGACCTCCCTGATGG	Tiller bud outgrowth suppression
Actin	TraesCS5A02G015600	TCTAAATGTCCAGGAAGCTGTTA	CCTGTGGTGCCCAACTATT	Actin (Control)

Table 2.03: Gene transcripts used in qPCR experiments in this thesis

2.7 References

Borrill, P., Ramirez-Gonzalez, R. and Uauy, C. (2016) ‘expVIP: a Customizable RNA-seq Data Analysis and Visualization Platform1[OPEN]’, Plant Physiology, 170(4), pp. 2172–2186.

Dixon, L.E. et al. (2018) ‘TEOSINTE BRANCHED1 regulates inflorescence architecture and development in bread wheat (Triticum aestivum)’, Plant Cell, 30(3), pp. 563–581.

Gahlaut, V. et al. (2014) ‘A multi-step phosphorelay two-component system impacts on tolerance against dehydration stress in common wheat’, Functional and Integrative Genomics, 14(4), pp. 707–716.

Kirby, E.J.M. and Appleyard, M. (1987) Cereal Development Guide. Arable Unit, National Agricultural Centre.

Marzec, M. et al. (2016) ‘Identification and functional analysis of the gene involved in strigolactone signaling in Hordeum vulgare’, Physiologia Plantarum, 158(3), pp. 341–355.

Sigalas, P.P. et al. (2023) ‘Nutritional and tissue-specific regulation of cytochrome P450 CYP711A MAX1 homologues and strigolactone biosynthesis in wheat’, Journal of Experimental Botany, 74(6), pp. 1890–1910.

Waddington, S.R., Cartwright, P.M. and Wall, P.C. (1983) A Quantitative Scale of Spike Initial and Pistil Development in Barley and Wheat, Ann. Bot, pp. 119–130.

Wheat eFP Browser. Available at: https://bar.utoronto.ca/efp_wheat/cgi-bin/efpWeb.cgi (Accessed: 22 July 2024).

Wilson, A.K. et al. (1990) ‘A dominant mutation inArabidopsis confers resistance to auxin, ethylene and abscisic acid’, Molecular and General Genetics MGG, 222(2–3), pp. 377–383.

Zwirek, M., Waugh, R. and McKim, S.M. (2019) ‘Interaction between row-type genes in barley controls meristem determinacy and reveals novel routes to improved grain’, New Phytologist, 221(4), pp. 1950–1965.

Chapter 3

Spikelet-Tiller feedback in wheat and barley

3.1 Chapter Introduction & Aim

Evidence of correlative inhibition has been proposed in cereals such as wheat and barley (Bangerth, 1989; Kamal *et al.*, 2022), but currently very little species-specific work exists to test this. Furthermore, it has previously been proposed that spikelet development and tiller bud development may act as competing sinks in cereals (Alaoui, Simmons and Crookston, 1988; Gu and Marshall, 1988; Kamal *et al.*, 2022).

I hypothesised that spikelet development may act in a way that inhibits tiller development, resulting in a high spikelet, low tiller phenotype.

In this chapter, I aim to investigate the high-spikelet six-row *vrs1* barley and the paired spikelet forming *hb* wheat line, both of which also exhibit significantly reduced tillering compared with their wild-type backgrounds (described in sections 1.4.3 and 1.4.6). I aim to determine if the phenotypes of increased spikelets per rachis node and reduced tillers are distinct, unrelated traits in cereals, or if the increase in spikelet number is responsible for the decrease in tiller number via correlative inhibition.

3.2 Evidence for spikelet-tiller feedback in diverse wheat germplasm

I hypothesised that if feedback between spikelet number and tillers exists, then it might be observable as an architectural trend among different wheat landraces. I therefore analysed pre-existing data from the Bennett Lab, in which various shoot architecture parameters, including spikelets per ear and tiller number, had been collected for 93 wheat lines.

Mean spikelets per ear was compared against tiller number at 6 weeks, 9 weeks and 12 weeks after planting. The data shows a broad trend of negative correlation between spikelets/ear and tiller number, with lines which have high spikelets/ear generally producing fewer tillers (Figure 3.01). Furthermore, this trend became more pronounced with later time points, exhibiting an R^2 value of 0.11, 0.29, and 0.38 at 6, 9 and 12 weeks respectively. The correlation of these two shoot architecture parameters supports the hypothesis that a negative feedback mechanism between ear size and tillering may exist in cereals.

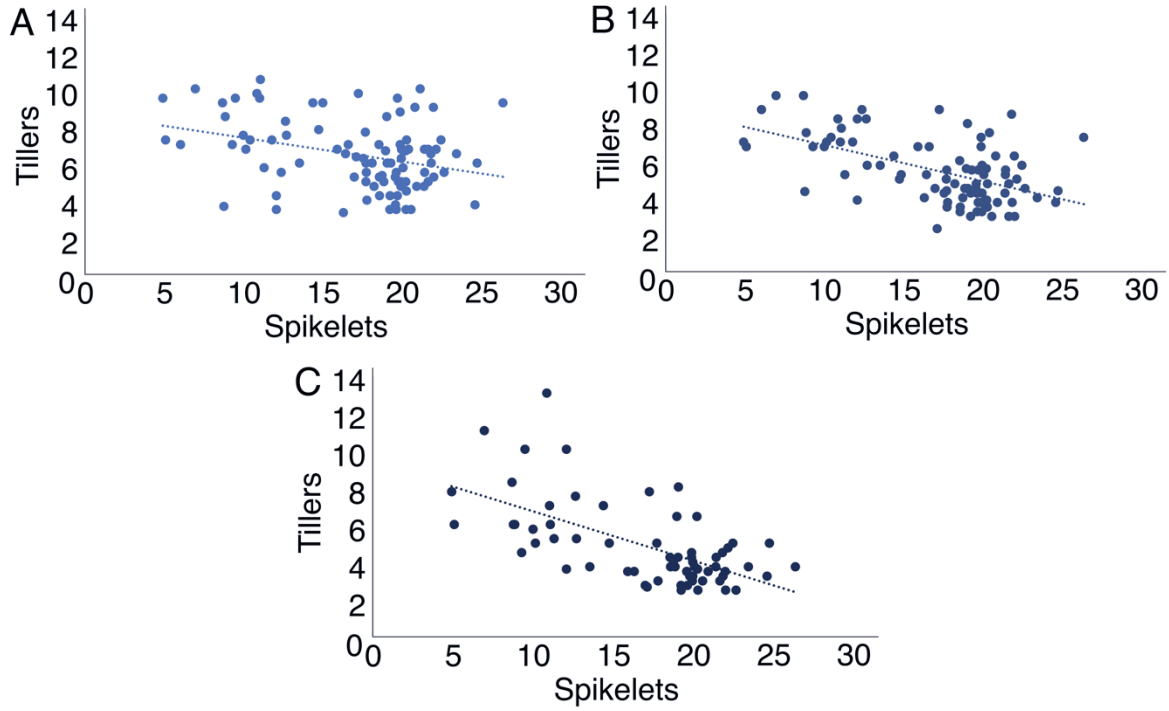

Figure 3.01: Wheat landraces exhibit some negative correlation between tiller and spikelet number that becomes stronger later in development.

(A) Scatterplot showing correlation between mean number of tillers per plant and mean number of spikelets per ear after 6 weeks of growth, with each point representing a mean for one of 93 YoGI wheat landraces (n=3-5, R^2 = 0.11). **(B)** Scatterplot showing correlation between mean number of tillers per plant and mean number of spikelets per ear after 9 weeks of growth, with each point representing a mean for one of 90 YoGI wheat landraces (n=3-5, R^2 = 0.29). **(C)** Scatterplot showing correlation between mean number of tillers per plant and mean number of spikelets per ear after 6 weeks of growth, with each point representing a mean for one of 66 YoGI wheat landraces (n=3-5, R^2 = 0.38).

3.3 Defining a timecourse for phenotypic difference in *vrs1* mutants

If developing spikelets do actively repress tillering in barley and wheat, this process is happening much earlier in development than can be observed from a change in maximum tiller number. To understand when feedback might be occurring, I conducted dissections on *vrs1* and WT at 35 days after planting, a point in

development at which tillers are still being produced and the majority of shoot apical meristems would be producing spikelets. Between planting and dissection, the emergence of each new tiller on the plant was tracked, both when it emerged, and from where it emerged on the plant.

The tracking of tiller emergence also allowed me to investigate a) if tiller development followed a predetermined pattern of emergence, b) if this pattern was affected by the number of spikelets per ear in already emerged tillers, and c) if where and when a tiller emerged impacted on the number of spikelets per ears it ultimately produced.

For reporting *when* a tiller has emerged, I will refer to ordinal tiller numbers (i.e. 2nd tiller = the second tiller to emerge, 10th tiller = tenth tiller to emerge).

For reporting *where* a tiller has emerged, I will use the nomenclature outlined in Figure 3.02 (i.e. tiller 2 = the second tiller to emerge from the main shoot, tiller 1.2.3 = the third tiller off the second tiller off the first tiller).

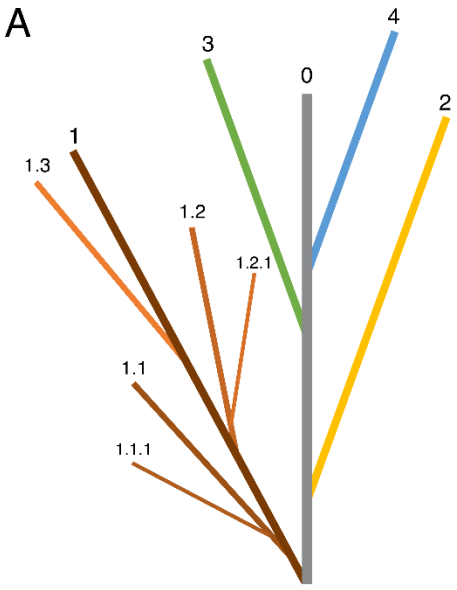

B

Tiller 0	Main Shoot
Tiller 1	First tiller off the main shoot
Tiller 2	Second tiller off the main shoot
Tiller 1.1	First tiller off Tiller 1
Tiller 1.2	Second tiller off Tiller 1
Tiller 1.1.2	Second tiller off Tiller 1

Figure 3.02: Tiller emergence in wheat and barley and the system of tracking used in this thesis.

(A) Visualisation of tiller emergence and the numbering system used in this thesis. The main shoot is labelled as tiller 0, first order tillers are labelled as x, with x representing the order of emergence from the main shoot; hence, the first tiller to emerge from 0 is tiller 1. Second order tillers are labelled as x.y, where x is equal to the first order tiller it has emerged from and y represents the order of emergence; hence the first tiller to emerge from 1 is tiller 1.1. Third order tillers are labelled as y.z, where y is equal to the second order tiller it has emerged from and z represents the order of emergence; hence the first tiller to emerge from tiller 1.1 is tiller 1.1.1. In this image and in all future figures describing this numbering system the main shoot will be represented using grey, tiller 1 and its subsequent tillers will be represented in red, tiller 2 and its subsequent tillers will be represented in yellow, tiller 3 and its subsequent tillers will be represented in green, tiller 4 and its subsequent tillers will be represented in blue. **(B)** Table explaining the tiller numbering system used.

The data showed that neither WT nor *vrs1* follow a single fixed pattern of tiller emergence. In both WT and *vrs1*, at a given ordinal position, a tiller may emerge from as many as 5 different pre-existing tillers (Figure 3.03A-C). Whilst no unanimous pattern is followed, some general rules of emergence can be observed.

Equivalent ordinal tillers in WT showed a greater variability in possible tiller location than *vrs1*, suggesting that variability is higher in higher tillering plants. *vrs1* maintained a uniform emergence pattern up to the 4th tiller (Figure 3.03A), whereas in WT uniformity ended at the 3rd tiller (Figure 3.03B). Figure 3.03C shows the mean ordinal position of each tiller position and generally shows an equal or reduced variation at a given position in *vrs1* compared to the same position in WT. For instance, tiller 1.1.1 emerges on average as the 7th ordinal tiller in *vrs1,* whereas in WT it emerges as the 11th tiller, but can emerge anywhere between the 8th and 17th tiller (Figures 3.03C).

The data also indicates that *vrs1* produces more second and third order tillers (tillers from tillers), while WT is typically seen to produce primary tillers (tillers from the main shoot) (Figure 3.03C). The average ordinal position for WT to produce tiller 3 is 4.5 (i.e. around the 4th or 5th tiller to emerge), whereas for *vrs1* the average position is 5.7, and the average position in WT and *vrs1* for tiller 4 is 7.0 and 9.6 respectively (Figures 3.03D-F). Furthermore, WT produces tiller 5 on average at position 13.0. Not a single *vrs1* plant was observed to produce this tiller (the fifth primary tiller) despite the fact that the mean number of tillers per plant at time of dissection was greater than 13. Meanwhile, most second and third order tillers were observed to emerge earlier in *vrs1*. For instance, tiller 1.2 emerged from *vrs1* and WT at an average position of 6.9 and 9.2 respectively and tiller 2.2 at an average position of 11.5 and 12.3 (Figures 3.03C). This difference in prioritisation of first order tillers in illustrated in Figure 3.03D, showing that there is no difference in when the earlier first order tillers emerge, but by tiller 3, *vrs1* is producing first order tillers at a significantly later ordinal position than WT.

These differences in tiller development between *vrs1* and WT are consistent with a model whereby emergence is influenced by the tillers already produced and the meristems developing within them. The main developmental difference between the two lines is spikelet number. I therefore hypothesise that the spikelets developing on the shoot apical meristems of the already emerged tillers are the primary cause of this developmental difference. It is very possible that a developmental feedback

effect which can reduce total tiller number would also be capable of more strongly repressing tiller development upon the main shoot as the main shoot meristem almost always produces the most spikelets in barley, thus reducing the rate at which primary order tillers develop.

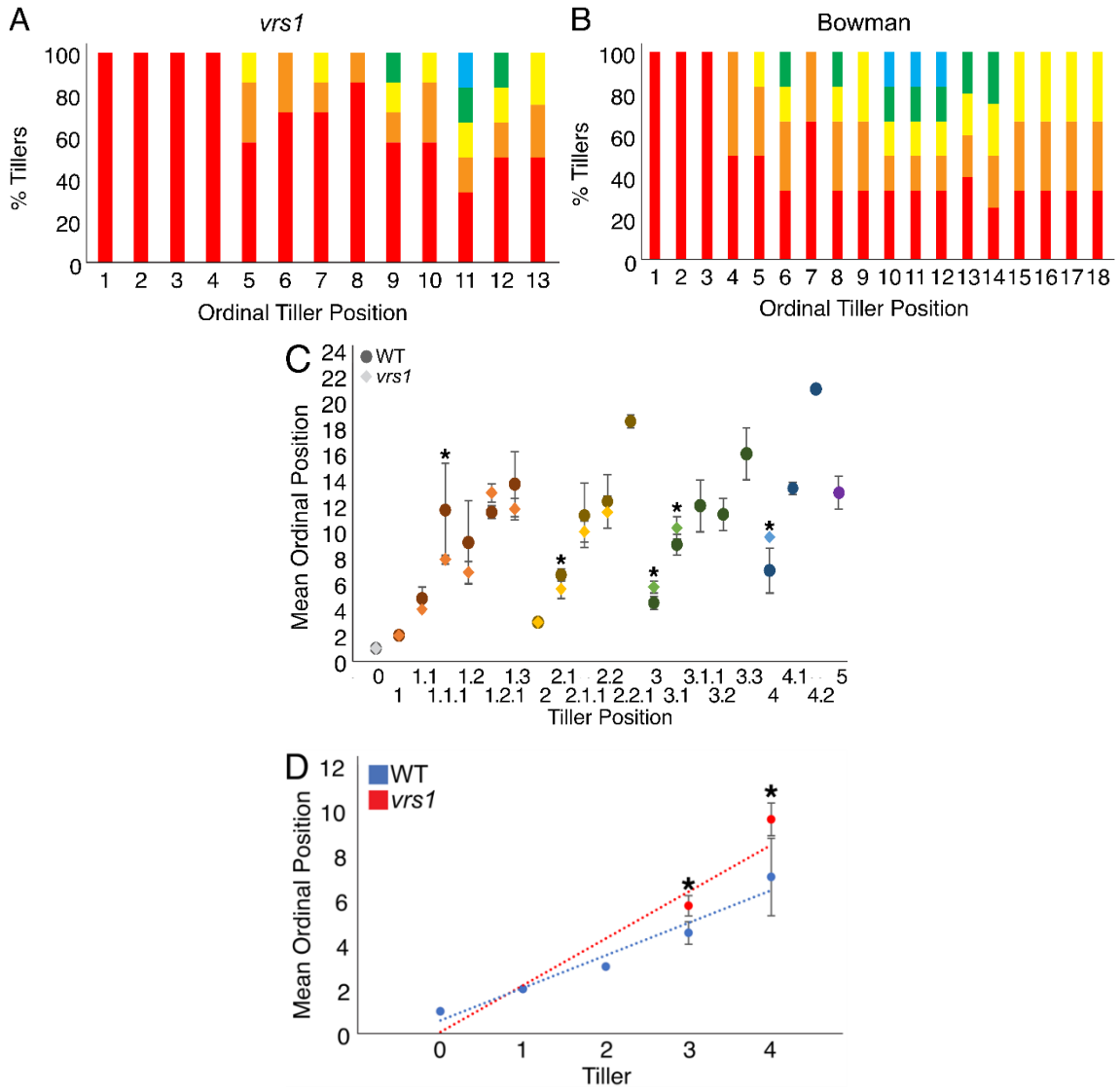

Figure 3.03: Pattern of tiller emergence in two-row and six-row barley.

(A) Bar chart of percentage distribution between different positions of emergence by ordinal tiller, for *vrs1* **(B)** Bar chart of percentage distribution between different positions of emergence by ordinal tiller, for WT (Bowman).
Measurements taken at 35 DaP. Each different position of emergence found at each ordinal location is represented in a different colour and shown as a percentage of the total number of plants which produced that tiller at that ordinal position. **(C)** Scatter plot of mean ordinal position of emergence of tillers by position of emergence on the plant, at 35 DaP. *Vrs1* is represented in light coloured diamonds; WT is represented in dark coloured circles. Error bars are 1 standard deviation from the mean. An asterisk above a point denotes statistically significant difference between lines for that tiller (two-tailed t-test, $P<0.05$, n=6-7). **(D)** Scatter plot of mean ordinal position of emergence of tillers by position of emergence on the plant, at 35 DaP; first order tillers only. *Vrs1* is represented in red; WT is represented in blue. Error bars are 1 standard deviation from the mean. An asterisk above a point denotes statistically significant difference between lines for that tiller (two-tailed t-test, $P<0.05$, n=6-7). R^2 value of WT trendlines = 0.96; R^2 value of vrs1 trendline = 0.91.

In addition to investigating tiller emergence, the developing meristems within the tillers were dissected in *vrs1* and WT, to understand spikelet development and to compare tiller and spikelet development between lines and between different tillers of the same line. The means calculated across all SAMs on the plant show that there is no difference in average rate of SAM development or spikelet ridge number (Figures 3.04A-B) between WT and *vrs1* plants. It is typical of cereals that the ears produced later in development are smaller. The data shows that both barley lines exhibit an expected gradual decline in spikelet nodes in ears initiated later in development (Figure 3.04C). The 13^{th} SAMs of *vrs1* produced significantly fewer spikelet ridges than the equivalent tillers in WT (Figure 3.04C). Trendlines plotted on Figure 3.04C indicate that the reduction in spikelet ridge productivity between

successive meristems is greater in *vrs1* than in WT. This result is consistent with feedback from early ears on spikelet production in later ears. This change in distribution between successive SAMs is also observed for rate of SAM development (Figure 3.04D). The reduction in SAM stage between successive SAMs greater in *vrs1*; the mean first shoot SAM is significantly later in development than the WT, but the mean 13th tiller SAM is significantly earlier (ultimately resulting in the equivalent means between the lines across all SAMs on the plant (Figure 3.04B)). This result also supports the hypothesis that feedback from earlier ears is delaying the development of later ears and this feedback is determined by spikelets/ear.

Differences in tiller and spikelet development between the two lines can be further elucidated by studying tillers within the context of their position within the plant, rather than their chronological emergence. The data shows that when comparing first order tillers sequentially, *vrs1* exhibits a sharper difference in rate of ageing and spikelet production between SAMs than WT (Figures 3.04E-F).

This is the pattern one would expect if early ears repress the development of later ears and tillers in barley. The main shoot represses tillering more strongly in high spikelet *vrs1,* so the plants produce fewer main shoot tillers (as shown in Figures 3.03C-D). However, the higher order tillers produce fewer spikelets, so their relative repression is weaker and therefore the plant more easily produces second order tillers. The greater number of spikelets may also explain the difference in tiller emergence pattern in *vrs1.* WT produces fewer spikelets/ear, resulting in the weaker control of the location of tiller development (Figure 3.03B), whereas the greater developmental load of the increased number of spikelets per node in *vrs1*, more tightly controls tiller emergence (Figure 3.03A).

These differences in tiller development are consistent with the presence of a system of feedback affecting tiller and meristem development, which is under the influence of early developing ears, and which is stronger in *vrs1* mutants that have more spikelets per ear.

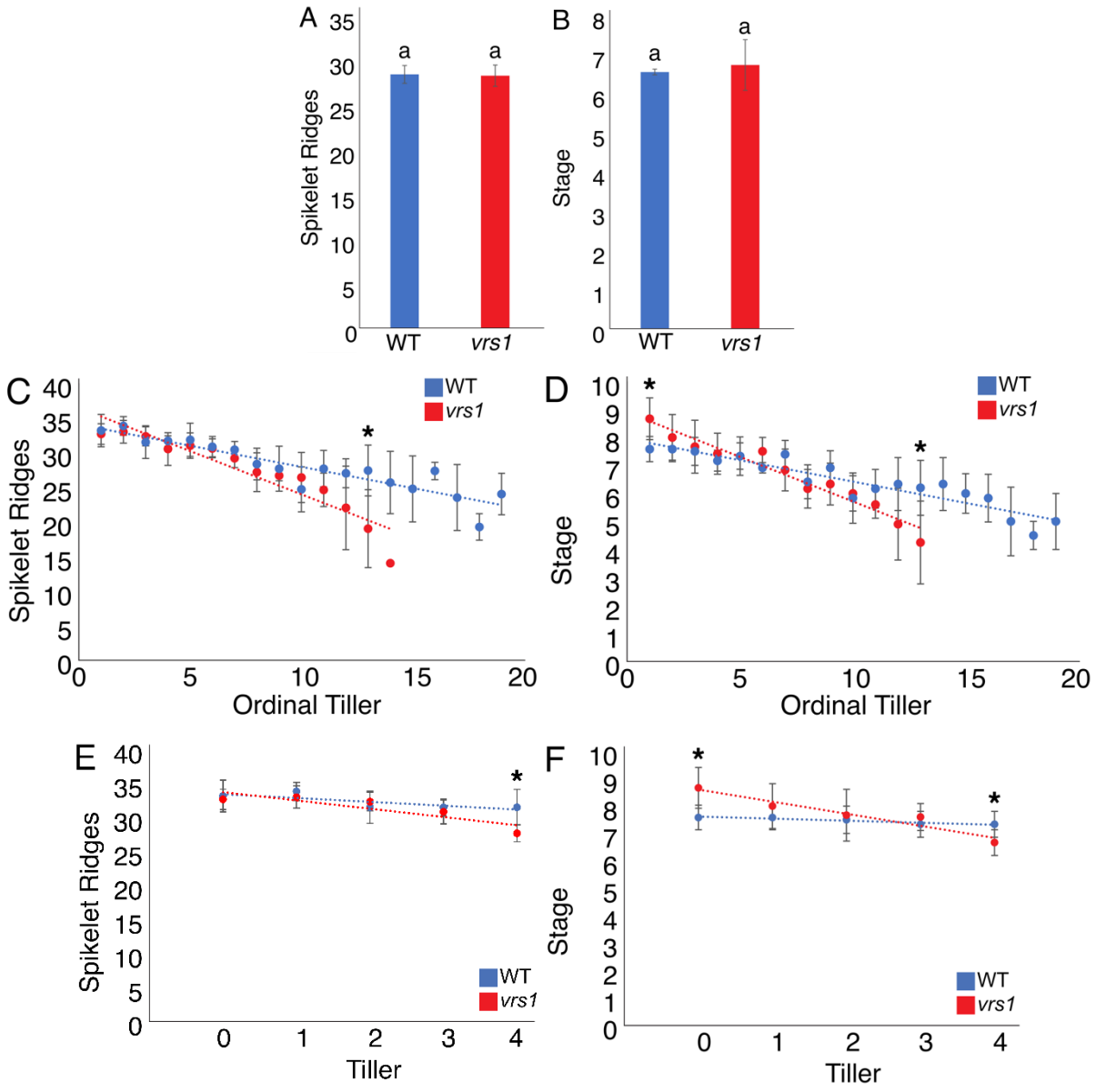

Figure 3.04: SAM development in two-row and six-row barley.

(A) Bar chart of mean number of spikelet ridges. **(B)** Bar chart of mean stage of SAM development. Measurements taken at 35 DaP. WT is represented in blue; *vrs1* is represented in red. Error bars are 1 standard deviation from the mean. Different letters above bars indicate statistically significant difference between lines (two-tailed t-test, $P<0.05$, n=6-7). **(C)** Scatter plot of mean number of spikelet ridges by ordinal tiller position. R^2 value of WT trendline = 0.83; R^2 value of *vrs1* trendline = 0.87. **(D)** Scatter plot of mean stage of SAM development by ordinal tiller position. R^2 value of WT

trendline = 0.85; R^2 value of *vrs1* trendline = 0.95. **(E)** Scatter plot of mean number of spikelet ridges by position of tiller emergence (first order tillers). R^2 value of WT trendline = 0.88; R^2 value of *vrs1* trendline = 0.92. **(F)** Scatter plot of mean sage of SAM development by position of tiller emergence (first order tillers). R^2 value of WT trendline = 0.64; R^2 value of *vrs1* trendline = 0.77. Measurements taken at 35 DaP. WT is represented in blue; *vrs1* is represented in red. Error bars are 1 standard deviation from the mean. An asterisk above a point denotes statistically significant difference between lines at that tiller (two-tailed t-test, $P<0.05$, n=6-7).

3.4 Defining a timecourse for phenotypic differences in hb mutants in wheat

As barley does not follow a fixed pattern of tiller emergence in the way the *Arabidopsis* model appears to (Schmitz and Theres, 1999; Aguilar-Martínez, Poza-Carrión and Cubas, 2007; Finlayson *et al.*, 2010), equivalent analysis on tiller emergence to those detailed and analysed in section 3.3.1 were also performed on *hb* and wild-type wheat. Order of tiller emergence was tracked in both lines and showed that, as in barley, no fixed pattern of tiller production was present (Figures 3.03A-B). As with barley, there was a strong pattern for the first few tillers, and variability increased in later tillers. The *hb* plants maintained a completely uniform pattern of emergence for longer, showing no variation until the 5th tiller to emerge, whereas in WT different tillers were emerging by the 4th tiller (Figure 3.05B). The WT plants exhibited greater variation in number of potential options. From the 5th tiller onwards four or even five different tillers could be expected to emerge, whereas in *hb* even when there was no consistent pattern of tiller production, the later tillers only varied between two different options (Figures 3.05A-B). As with barley, an increased number of already produced tillers and therefore ‘options’ for subsequent tillers should naturally result in increased variation in tiller production pattern. However, differences between the two lines in later tillers indicate this is only part of an explanation. For instance, Figure 3.05C shows that tiller 4 (the fourth primary tiller) is on average the 5th tiller to emerge in *hb* but in WT emerges on average as the 8th tiller.

However, the wheat lines do differ from barley in their tiller development in some surprising ways. In wheat, the high-spikelet/low-tiller *hb* line appears to produce mostly first order tillers. For instance, none of the *hb* plants studied produced a tiller 2.1 (Figure 3.05C). The majority of WT plants not only produced tiller 2.1 but did so either as either their 5th or 6th tiller, a tiller that was produced by many *hb* plants by the time of dissection. Furthermore, the data shows that of the four first order tillers produced in both lines, all were produced at either the same ordinal position (1 and 2 as the 2nd and 3rd tillers respectively) or were produced earlier in *hb* than in the wild type (tiller 4) (Figure 3.05D). This relationship contrasts with the one observed in barley, where the high-spikelet/low-tiller *vrs1* mutant plants appeared to more readily produce higher order tillers over additional tillers from the main shoot (Figure 3.03D). It is possible that this is primarily the result of the very small number of tillers produced by *hb* plants. It is therefore possible that the line simply does not produce enough tillers to be able to distinguish a clear relationship between first order and higher order tillers.

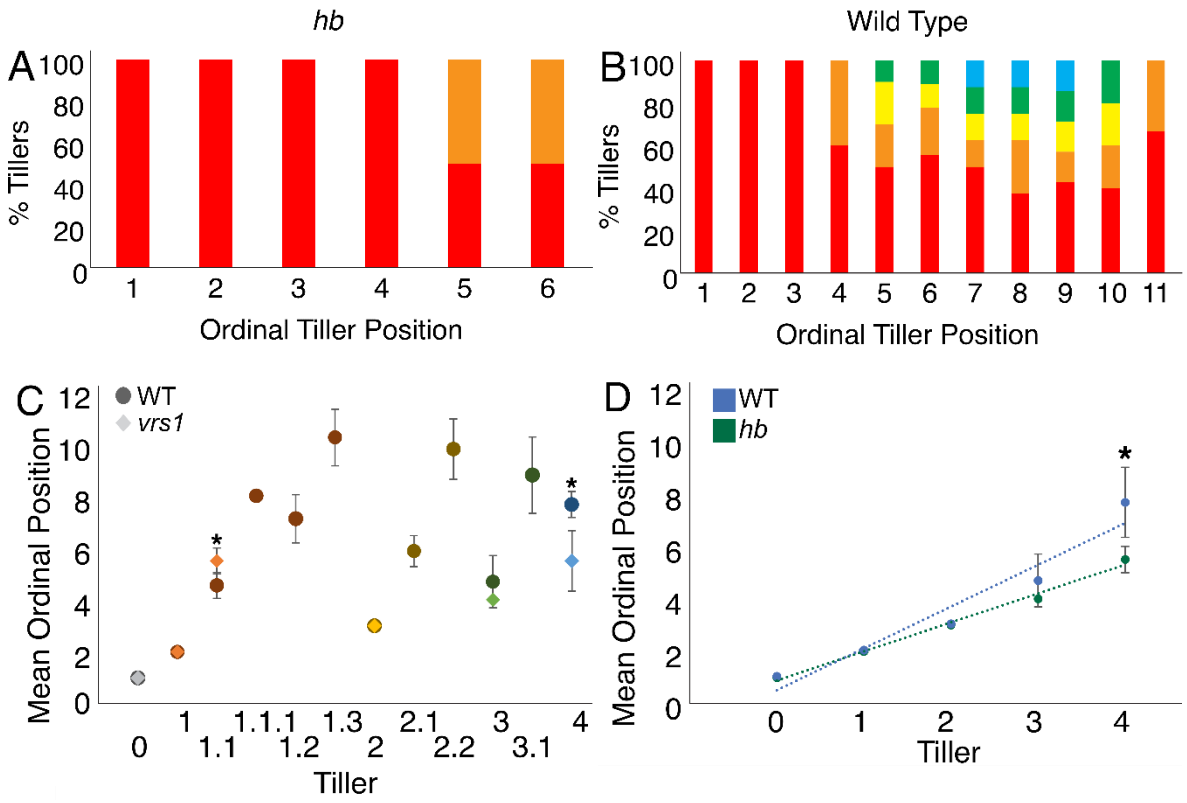

Figure 3.05: Pattern of tiller emergence in wild type and *hb* wheat.

(A) Bar chart of percentage distribution between different positions of emergence by ordinal tiller, for *hb*. **(B)** Bar chart of percentage distribution between different positions of emergence by ordinal tiller, for WT.

Measurements taken at 42 DaP, for WT. Each different position of emergence found at each ordinal location is represented in a different colour and shown as a percentage of the total number of plants which produced that tiller at that ordinal position. **(C)** Scatter plot of mean ordinal position of emergence of tillers by position of emergence on the plant. **(D)** Scatter plot of mean ordinal position of emergence of tillers by position of emergence on the plant, first order tillers only.

Measurements taken at 42 DaP. *hb* is represented in light diamonds; WT is represented in dark circles. Error bars are 1 standard deviation from the mean. An asterisk above a point denotes statistically significant difference between lines for that tiller (two-tailed t-test, $P<0.05$, $n=10$).

The data shows that the *hb* mutants produced significantly more spikelets per meristem on average and were at a significantly later stage of development (Figures 3.06A-B). As was observed in barley, both spikelet number and rate of meristem development reduced by greater margins between chronologically emerged meristems in the high spikelet *hb* line than in WT (Figure 3.06C-D). However, the difference between the two lines is more subtle than in barley; although the trendlines show different trajectories, at no individual tiller is there a significant difference in number of spikelet ridges between the lines. Furthermore, for meristem developmental rate the difference appears to be essentially identical for the tillers produced by both lines, and only appears different due to the additional tillers produced in WT, which show little difference to each other. This result was expected, given that that difference in spikelet number between the two wheat lines is smaller than that of the barley lines.

The data from wheat is not conclusive enough to make any statements on how wheat development may be affected by changes in spikelet number per ear. However, what is clear is that wheat and barley, two similar *Poaceae* species, appear to exhibit similar but not identical behaviours in the same scenario. One possible explanation for the difference is *vrs1* has a much larger difference in spikelet number/ear compared to WT, than *hb* does.

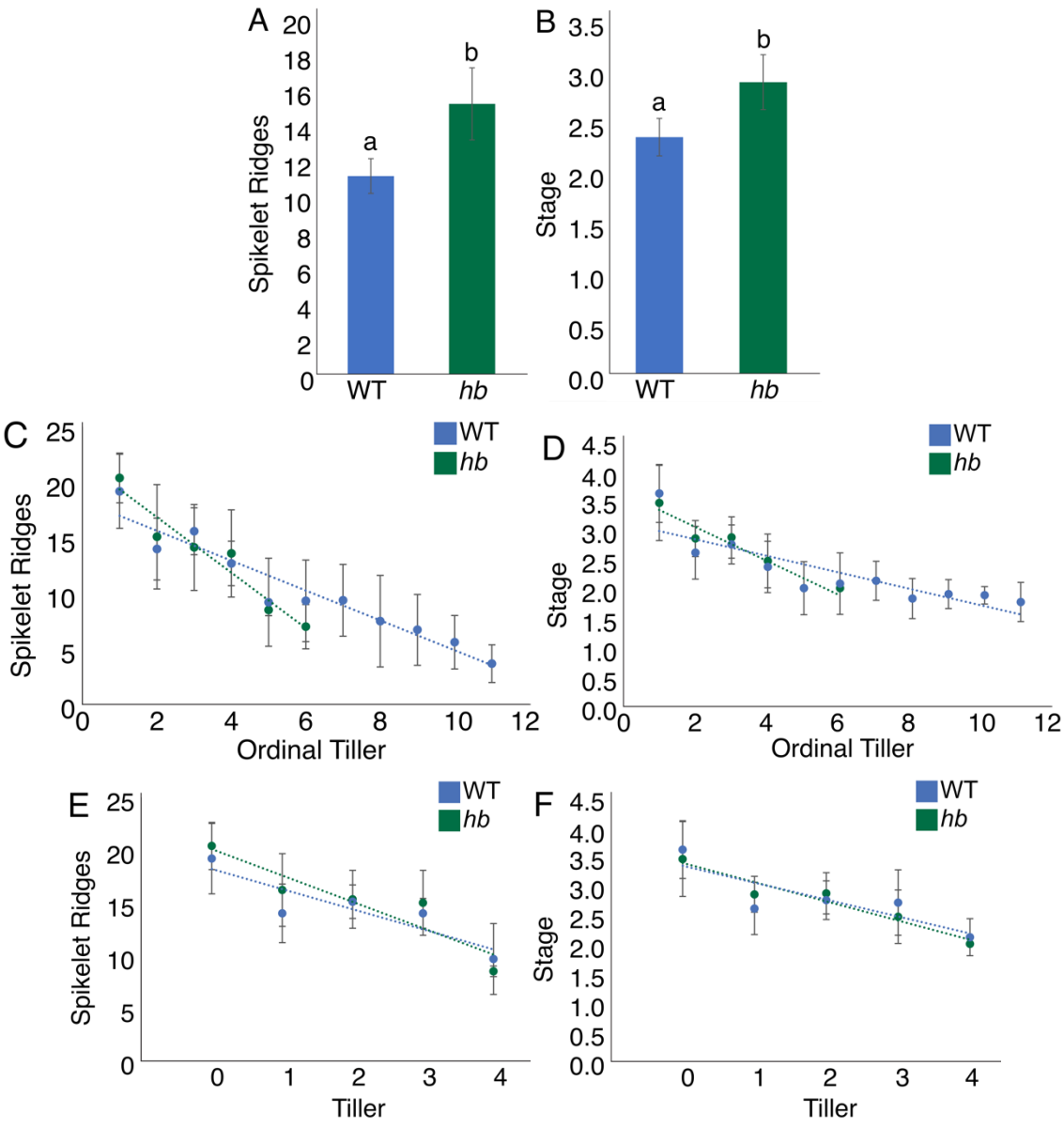

Figure 3.06: SAM development in wild type and *hb* wheat.

(A) Bar chart of mean number of spikelet ridges. **(B)** Bar chart of mean stage of SAM development.

Measurements taken at 42 DaP. WT is represented in blue; *hb* is represented in green. Error bars are 1 standard deviation from the mean. Different letters above bars indicate statistically significant difference between lines (two-tailed t-test, $P<0.05$, n=10). **(C)** Scatter plot of mean number of spikelet ridges by ordinal tiller position. R^2 value of WT trendline = 0.93; R^2 value of *hb* trendline = 0.92. **(D)** Scatter plot of mean stage of SAM

development by ordinal tiller position. R^2 value of WT trendline = 0.73; R^2 value of *hb* trendline = 0.93. **(E)** Scatter plot of mean number of spikelet ridges by position of tiller emergence (first order tillers). R^2 value of WT trendline = 0.81; R^2 value of *hb* trendline = 0.86. **(F)** Scatter plot of mean stage of SAM development by position of tiller emergence (first order tillers). R^2 value of WT trendline = 0.72; R^2 value of *hb* trendline = 0.93.

Measurements taken at 42 DaP. WT is represented in blue; *hb* is represented in green. Error bars are 1 standard deviation from the mean. An asterisk above a point denotes statistically significant difference between lines at that ordinal position (two-tailed t-test, $P<0.05$, $n=10$).

3.5 Investigation of shoot apical meristem development over time in *hb*

Recent literature has shown that regulation of meristem development and final cereal architecture are intrinsically linked. Both FT1 (Lv *et al.*, 2014) and FT2 (Shaw *et al.*, 2019) have been shown to coordinate the timing of reproductive development in wheat, and *ft1* (Brassac *et al.*, 2021) and *ft2* (Shaw *et al.*, 2019) mutants both showed an increased spikelet number. Additionally, the data presented in sections 3.3 and 3.4 indicates that several differences in shoot development between high spikelet and WT spikelet lines exist from early in development. However, these experiments only studied fully emerged tillers and the SAMs at their base. However, wheat produces SAMs within tiller buds, even if they have not grown out into an observable tiller. I hypothesised that these ‘unemerged’ SAMs might constitute a significant proportion of the plant’s shoot developmental effort, in addition to the SAMs of emerged tillers, in a way that may be pertinent to spikelet and tiller development and feedback. To better investigate this possibility, I conducted dissections of both emerged and unemerged SAMs of *hb* every 72 hours from 25 to 61 DaP. *hb* was used, so paired spikelet data could also be collected.

In addition to the expected increase in emerged tiller number throughout the course of dissections, the number of unemerged meristems per plant also increased over time (Figure 3.07A). The rate of increase is greater for tillers and therefore the

proportion of SAMs which have emerged increases over time (represented in blue in Figure 3.07A)). In fact, unemerged SAMs constitute the majority of SAMs produced by the plant, as the number of emerged SAMs never rises above 50% (Figure 3.07A).

Whilst emerged SAMs constitute a minority of SAMs on the plant, they do produce the majority of spikelet ridges; the proportion of spikelet ridges on emerged tiller SAMs was typically maintained between 60 and 80% of the total spikelet ridges on the plant (Figure 3.07B). This is the result of the further finding that the majority of unemerged SAMs are at around stage 1-2 (equating to vegetative and double ridge stage (see section 2.5.3)), meaning they have not initiated or only recently initiated reproductive development (Figure 3.07C) and have therefore produced no or few spikelet ridges. However, from 32 DaP onwards, a minority of unemerged SAMs have initiated reproductive development, such SAMs could potentially be a source of developmental inefficiency in wheat, as many of these SAMs are unlikely ever to develop into productive tillers. This potential inefficiency is further illustrated by the finding that after 32 DaP a large number of SAMs which have initiated reproductive development are not found at emerged tillers (Figure 3.07D). The ~50% of initiated but unemerged SAMs at 62 DaP are almost certainly not going to emerge into full tillers and eventually productive ears. I hypothesise that directing a portion of developmental effort towards these SAMs, reduces the productivity of the ears that do eventually develop.

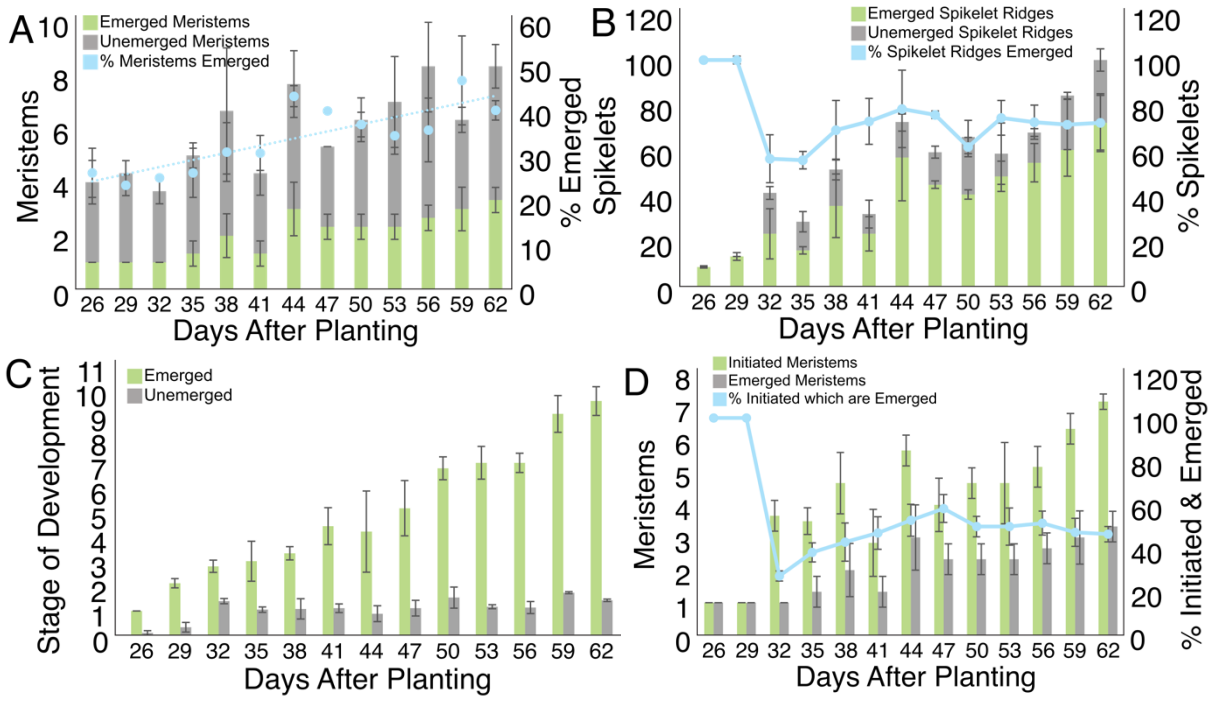

Figure 3.07: Tiller Emergence and Shoot Apical Meristem development in the *hb* wheat line.

Measurements for all figures were taken once every 3 days.

(A) Bar chart of mean number of emerged tiller SAMs per plant (green) and mean number of unemerged SAMs per plant (grey) at each timepoint (n= 3-4). Overlaid scatterplot of % of total SAMs per plant which are emerged, calculated by dividing the number of emerged meristems by total number of meristems per plant (n= 3-4), with trendline in dotted blue ($R^2 = 0.69$). Left-hand x-axis relates to the bar chart; right-hand x-axis relates to the scatterplot. **(B)** Bar chart of mean number of spikelet ridges per SAM on emerged meristems (green) and unemerged SAMs (grey) at each timepoint (n= 3-4). Overlaid line chart of % of spikelet ridges which are emerged (blue), calculated by dividing the number of emerged spikelet ridges by total number of spikelet ridges per plant (n= 3-4). Left-hand x-axis relates to the bar chart; right-hand x-axis relates to the scatterplot. **(C)** Bar chart of mean stage of development in emerged tiller SAMs (green) and unemerged SAMs (grey) at each timepoint (n= 3-4). **(D)** Bar chart of mean number of SAMs per plant which have initiated reproductive development (green) and mean number of emerged tiller shoot apical meristems per

plant (grey) at each timepoint (n= 3-4). Overlaid line chart of % of initiated meristems which are also emerged (blue), calculated by dividing the number of emerged and initiated meristems by total number of initiated meristems per plant (n= 3-4). Left-hand x-axis relates to the bar chart; right-hand x-axis relates to the scatterplot.

The development of paired spikelets is very difficult to accurately determine early in meristem development. Therefore, spikelet node counts were taken for all time points, but total spikelet counts (including paired spikelets) were only taken at 62 DaP. The data shows that the frequency of supernumerary spikelets gradually decreases with later emerging meristems (Figure 3.08A). As a result of this, a majority (~60%) of all paired spikelets on a given plant at the end of its development are on the main shoot meristem (Figure 3.08B). This pattern of development contributes further to the proposed inhibitory effect that spikelets may have: in successive SAMs paired spikelet development is more strongly repressed, potentially as a result of an increased developmental load of the increased number of spikelets developing on emerged SAMs.

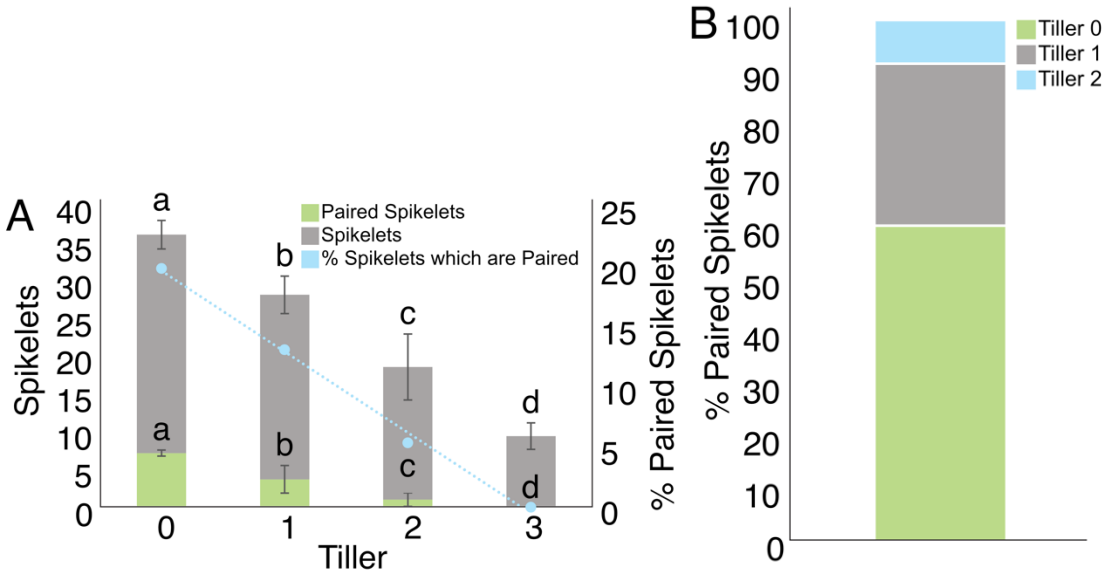

Figure 3.08: Paired spikelet development in *hb* wheat line.

(A) Bar chart of mean number of paired spikelets per shoot apical meristem (n= 3-4) and mean number of regular spikelets per shoot apical meristem (n= 3-4), ordered by position of emergence, at 62 DaP. Overlayed scatter plot of % of spikelets which are paired, calculated by dividing total number of spikelets per meristem by number of paired spikelets at each tiller position (n= 3-4), with trendline in dotted blue. Left-hand x-axis relates to the bar chart; right-hand x-axis relates to the scatterplot. **(B)** Bar chart showing percentage distribution of paired spikelets per plant by position of emergence of the tiller on which they are found, at 62 DaP.

These experiments support the hypothesis that unemerged SAM and spikelet development constitutes a significant portion of shoot development. To better explore the effect of spikelets/ear on SAM development a timecourse of dissections were performed on the background WT wheat, at 26, 38 and 47 DaP (when the meristems would be approximately at the start middle and end of reproductive development) and compared to determine differences in development from *hb*.

As previously established, *hb* plants make significantly fewer tillers than WT (Figure 3.09A). However, differences in the number of unemerged SAMs (Figure 3.09B) result in the two lines producing an equivalent number of total SAMs at every time

point (Figure 3.09C). This suggests that the increased spikelet number of *hb* may cause the observed reduced tiller phenotype specifically by repressing tiller bud outgrowth. This finding aligns with recent literature that suggests that *TB1* (which is primarily known for regulating tiller bud outgrowth), may also be partly responsible for regulating paired spikelet development (Boden *et al.*, 2015; Dixon *et al.*, 2018). The significantly increased expression levels of *TaTB1-D1* in the *hb* plants could cause the observed reduction in tiller bud outgrowth, acting as a central coordinator of increased spikelet number and reduced emerged tiller number.

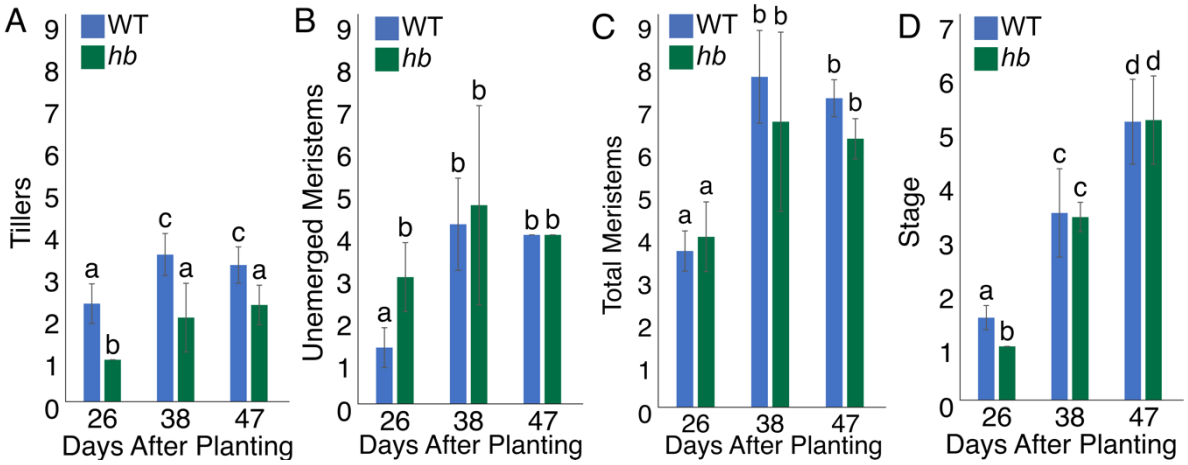

Figure 3.09: Tiller emergence in high and WT spikelet wheat lines.

(A) Bar chart of mean number of emerged tillers per plant **(B)** Bar chart of mean number of unemerged SAMs per plant **(C)** Bar chart of mean total number of SAMs per plant **(D)** Bar chart of mean stage of SAM development.

Measurements taken at 26, 38 and 47 DaP. WT is represented in blue and *hb* is represented in green. Error bars are 1 standard deviation from the mean. Different letters above bars indicates statistically significant difference between lines (two-tailed t-test, $P<0.05$, n=3-5).

3.6 The effect of meristem ablation on shoot architecture in vrs1

The experimental results outlined in section 3.2 and 3.3 establish where and when the differences in tiller development occur between high and WT spikelet lines of wheat and barley. I now wanted to test the hypothesis that the difference in

spikelets/ear was directly responsible for these developmental differences. If true, I predicted that if I were to remove a quantity of spikelets from the plant, then an increase in tiller production would be observed, proportional to the number of spikelets removed.

A series of experiments were therefore carried out, involving the ablation of developing shoot apical meristems and studying the response in remaining shoot apical meristems and the effect on subsequent tiller development. Herein, the term ‘ablation’ is used to describe the excision of the shoot apical meristem, causing minimal damage to the remaining shoot system.

Initially, ablation was performed on the SAM of the main shoot of WT and *vrs1* barley at 28 DaP, a point in development at which the main shoot meristem was in a stage of reproductive development and actively producing spikelets. The main shoot meristem typically produces the most spikelets of any ear on the plant (as shown in Figure 3.06C). I therefore expected the removal of these developing spikelets to result in the reduction of the hypothesised spikelet-tiller feedback effect and result in a significant increase in tillers.

The data shows that a significant difference in tiller number was observed between the ablated and control plants of each line after one week (Figure 3.10A). This difference was maintained until week 10, when all plants reached their maximum tiller number, an avergae of 15.2 and 17.2 tillers for control and ablated WT and 11.2 and 14.1 tillers for *vrs1*. This behaviour is indicative of apical dominance, suggesting that the presence of the developing SAM represses tiller production in barley.

However, the high spikelet *vrs1* plants showed a stronger tillering response to ablation than the WT plants, supporting the hypothesis that there is additionally a feedback effect that is specifically the result of spikelet number. At the point of maximum tiller number, the ablated plants of both lines had produced significantly more tillers than the control plants, but while the ablation caused an average of 13% increase in tillering in WT, the same ablation resulted in an effect twice the size (26% increase) on tillering in *vrs1*. In fact, the profile of tiller production in ablated *vrs1* is remarkably similar to control WT. At no point is there a statistically significant

difference (by two tailed t-test, P<0.05) in tiller number between control WT and ablated *vrs1* (Figure 3.10A). This result implies not only that the developing main shoot meristem has a repressive effect on tiller production but that the effect is stronger from a SAM producing a greater number of spikelets.

Following maximum tiller number, the most productive tillers survive, from which ears emerge resulting in an equivalent final tiller and ear number between the two conditions for each line (Figure 3.10B). The ablated, higher tillering plants therefore had a lower tiller survival rate than the control plants. It is possible that similar feedback mechanisms influence tiller senescence, as well as tiller production. The greater total number of developing tillers on the ablated plants could possibly have combined to create a stronger 'tiller senescence' signal than that created by the sum of the meristems in the control plants. The result being that both conditions eventually reached the same end point, regarding tillers, simply by different pathways. This feedback system would make sense in the cereals, as a mechanism of tightly controlling tiller development to reliably produce the optimum number of productive ears.

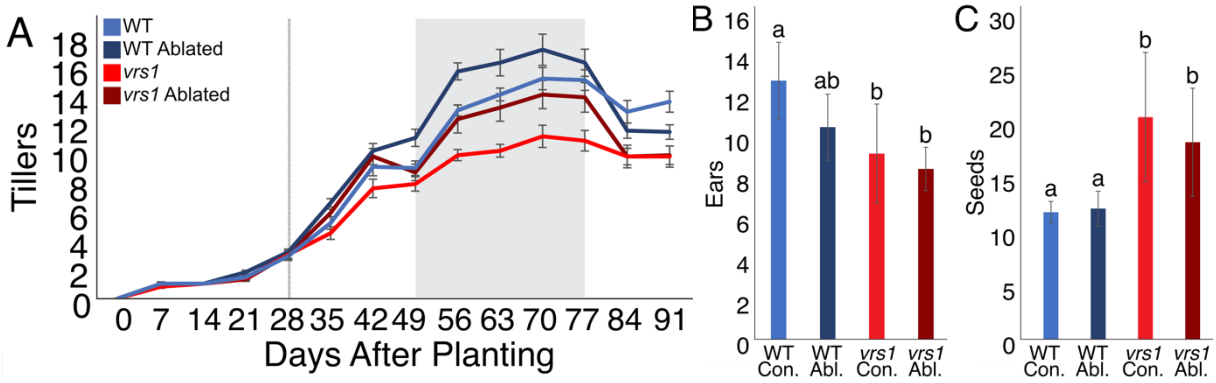

Figure 3.10: The effect of ablation of the main shoot apical meristem on the shoot architecture of two-row and six-row barley.

(A) Line chart of mean tiller number per plant over time. The point of ablation is represented by the grey vertical line at 28 DaP. From 49 to 77 DaP (shown in grey) *vrs1* mean tiller number was significantly less than *vrs1* ablated and WT, both of which were not different from each other, but produced significantly fewer tillers than WT ablated.

(ANOVA, P<0.05, n=10). **(B)** Bar chart of mean final ear number per plant. **(C)** Bar chart of mean number of seeds per ear.
WT is represented in blue and *vrs1* is represented in red. Controls are represented in the paler shade and ablated plants are represented in the darker shade. Different letters above bars indicates statistically significant difference between conditions (ANOVA, P<0.05, n=10).

To clarify the effect of the developmental feedback of spikelet number distinct from feedback from the entire SAM, I conducted further ablation experiments to test how low spikelet WT and high spikelet lines would develop if they were both set to an equal number of tillers. I hypothesised that if later emerging tillers were removed from WT plants so that they had the same number as *vrs1* at the beginning of reproductive development, the WT plants would still ultimately produce a greater number of tillers, as the reduced number of spikelets would allow for greater tiller production than in *vrs1*.

Tiller development and final architecture were measured to compare how the development of WT plants ablated in this manner compared to un-ablated control plants of WT and *vrs1*. This experiment was intended to confirm that the change in development was solely the result of spikelet number and was not the result of difference in number of tillers, which themselves could repress tiller production.

At 49 DaP ablated WT plants had produced significantly more tillers than the *vrs1* plants (as well un-ablated control WT) (Figure 3.11A) supporting the proposed relationship in which the increase in tillering that results from meristem ablation is proportional to the number of spikelets on the ablated meristem or meristems. From the same point in development, with an equal number of tillers but an unequal rate of spikelet production, WT produced more tillers than the high spikelet *vrs1* plants. Meristems with a smaller number of developing spikelets appear to repress tillering to a weaker degree, thus resulting in a larger final tiller number.

To confirm the result, final ear and spikelet number were measured. The data shows that these parameters didn’t differ significantly between the ablated and control WT

(Figure 3.11B-C), allowing me to conclude that standard development was not significantly disrupted by the ablation and any effects seen are the result of the reduction in developing spikelets.

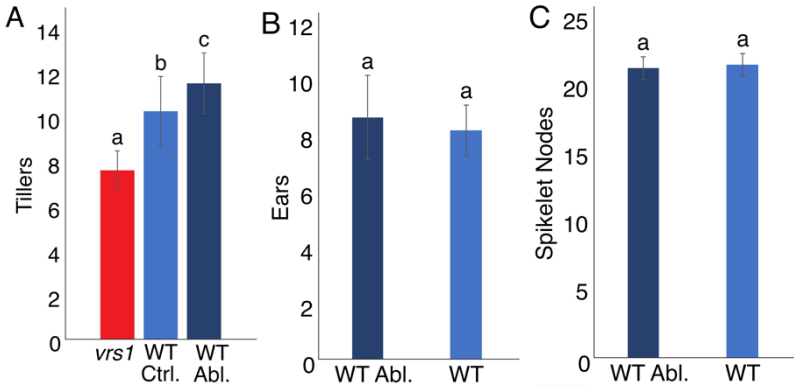

Figure 3.11: The effect of ablation of shoot apical meristems in WT and *vrs1* to create two-row and six-row plants with equal shoot apical meristem number.

(A) Bar chart of maximum mean tiller number per plant (taken at 49 DaP) in *vrs1*, WT and ablated WT (shoot apical meristems ablated at 28 DaP so that both lines had an equal number of shoot apical meristems). *vrs1* is represented in red, WT in light blue, ablated WT in dark blue. Different letters above bars indicates statistically significant difference between conditions (ANOVA, $P<0.05$, n=8-10). **(B)** Bar chart of final ear number per plant in control WT and ablated WT (shoot apical meristems ablated at 28 DaP so that both lines had an equal number of shoot apical meristems). Control WT is represented in light blue, ablated WT in dark blue. Different letters above bars indicates statistically significant difference between conditions (two-tailed t-test, $P<0.05$, n=8-10). **(C)** Bar chart of spikelet nodes per ear in control WT and ablated WT (shoot apical meristems ablated at 28 DaP so that both lines had an equal number of shoot apical meristems). Control WT is represented in light blue, ablated WT in dark blue. Different letters above bars indicates statistically significant difference between conditions (two-tailed t-test, $P<0.05$, n=8-10).

3.7 Ablation of the main shoot meristem in *hb* mutants

Subsequent ablation experiments were conducted in the *hb* and WT wheat lines. These experiments were intended to confirm if the observed feedback effect was also present in wheat and to determine if there was any difference in the way the feedback affected development in the two similar but distinct cereal species. I hypothesised that, as in barley, an increase in tillering would be observed, proportional to the quantity of spikelets ablated.

Ablation was performed on the main shoot SAM (as in barley), and additionally on the second tiller SAM, or on every SAM, except that of the main shoot. These experiments were intended to identify if the effect of ablation on tillering is proportional to spikelet number, regardless of how the spikelets are distributed.

In both lines, maximum tiller number increased significantly compared with the unablated controls (Figure 3.12A). Additionally, in *hb* the proportional increase in tillering was greater than the increase in the WT (Figure 3.12B). Ablation of the second shoot meristem resulted in a significant increase in tillering compared to the control plants, but an increase that was slightly smaller than the one caused by the ablation of the main shoot meristem (Figure 3.12). Furthermore, in both wheat lines, the ablation of multiple SAMs resulted in an increase in tillering greater than the increase that resulted from the ablation of either single SAM.

In all three ablation experiments, the increase in the *hb* plants was greater than that of the wild type (Figure 3.12), supporting the hypothesis that a tiller repressing feedback exists in wheat, the strength of which is determined by spikelets/ear. Not only does the removal of a developing meristem increase tiller production, but the removal of more spikelets, increases tiller production by a greater amount, and the total effect is the result of proportional contributions from all developing SAMs on the plant.

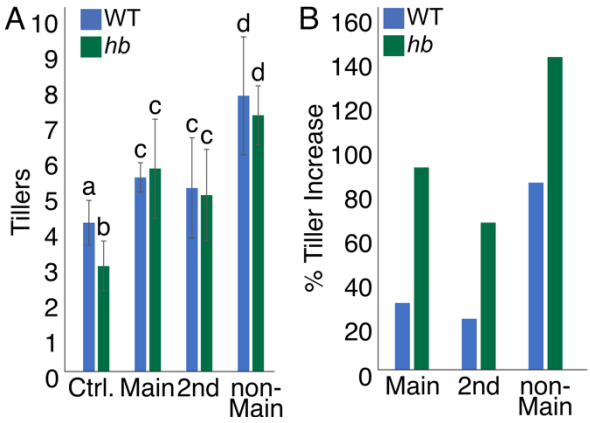

Figure 3.12: The effect of ablation of different shoot apical meristems on the shoot architecture of WT and *hb* wheat lines.

(A) Bar chart of maximum mean tiller number per plant (taken at 56 DaP). WT is represented in blue, *hb* is represented in green. Different letters above bars indicates statistically significant difference between lines (ANOVA, $P<0.05$, n=9-10). **(B)** Bar chart of the % increase in maximum tiller number from control plants as a result of ablation of the main shoot apical meristem, the shoot apical meristem of the second tiller produced, or all shoot apical meristems besides that of the main shoot. WT is represented in blue and *hb* is represented in green.

3.8 Ablation of post-reproductive development meristems in wheat and barley

The observed feedback effect of spikelets on tiller is likely the result of both structures competing for the plant's total developmental effort. I hypothesised that the repressive effect on tillering was specifically the result of actively developing spikelets on the SAM, as reproductive development is when spikelet meristems develop, after which spikelet number is set. I therefore predicted that fully developed spikelets would have no, or a greatly reduced developmental effect. Ablations were therefore conducted on SAMs that had completed reproductive development, but when the plants were still producing tillers.

The data shows that in both barley and wheat, no significant difference in maximum tiller number was observed between the ablated plants and control plants for both

the high spikelet lines and the WT spikelet lines (Figure 3.13). This is in contrast to the increases in tillering seen when ablation is performed on developing shoot meristems. This data supports the hypothesis that it is not simply the presence of spikelets that represses tillering, but tillering is specifically repressed proportional to the number of developing spikelets.

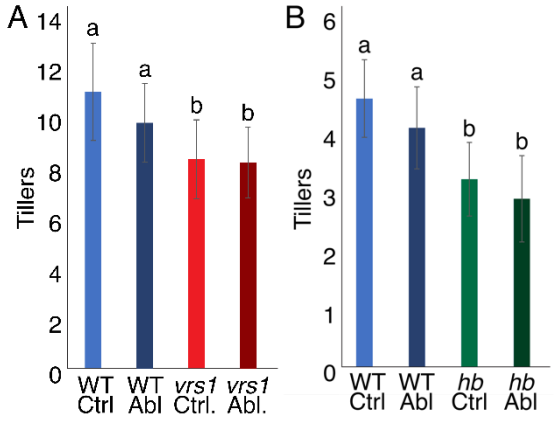

Figure 3.13: The effect of ablation of the main shoot apical meristem in wheat and barley, when ablation occurs after reproductive meristem development.

(A) Bar chart of maximum mean tiller number per plant (taken at 42 DaP) in WT and *vrs1;* WT is represented in blue, *vrs1* is represented in red. Different letters above bars indicates statistically significant difference between lines (ANOVA, P<0.05, n=8-10). **(B)** Bar chart of maximum mean tiller number per plant (taken at 49 DaP) in WT and *hb;* WT is represented in blue, *hb* is represented in green. Different letters above bars indicates statistically significant difference between lines (ANOVA, P<0.05, n=8-10).

3.9 The effect of exogenous cytokinin treatment on wheat shoot architecture

The work presented thus far implies the presence of a feedback effect between spikelets developing on reproductive shoot apical meristems against the production of new tillers. Additionally, this effect appears to be proportional to spikelet number.

I hypothesise that this feedback between the development of two different shoot structures is coordinated by long-distance, molecular signals. Many known phytohormones exist that fit this criteria, but I hypothesise that cytokinin is the most

probable candidate. A number of studies exist confirming cytokinin as a regulator of inflorescence development, tiller development and spikelet development in wheat and barley, which are fully discussed in section 1.4.7 (G. Li *et al.*, 2021; J. Sun *et al.*, 2023; Wang, Chen and Wang, 2023). Furthermore, cytokinin has been implicated in the CLAVATA-WUSHEL pathway in *Arabidopsis*, maize and rice, which is a major regulator of meristem fate determinacy and developmental timing (Somssich *et al.*, 2016; Liu *et al.*, 2020; Cammarata *et al.*, 2022; Matthes *et al.*, 2022). Together, these indicate that cytokinin has the potential to regulate spikelet-tiller feedback in cereals.

To investigate the role of cytokinin in spikelet-tiller feedback, I developed a method of increasing cytokinin levels within the shoot system. The system needed to be minimally invasive, so that any disruption to development could be attributed solely to the hormonal change. I trialled multiple treatments, varying 6-BA concentration and frequency of treatment. I measured their success by their increase on tillering, an established effect of cytokinin in wheat. The synthetic cytokinin 6-Benzylaminopurine (6-BA) was injected into every emerged tiller on the plant once per week. Initial troubleshooting found that conducting this treatment with 0.33ml of 100µM 6-BA elicited the greatest increase in tillering and height (Figures 3.14A-B), both of which are expected effects of cytokinin on wheat shoot development, based on current literature (Shoaib *et al.*, 2020; J. Sun *et al.*, 2023). Having achieved these expected effects, the exogenous 6-BA treatment could now be used to identify novel developmental effects. Full details of the method carried out can be found in chapter 2.4.1.

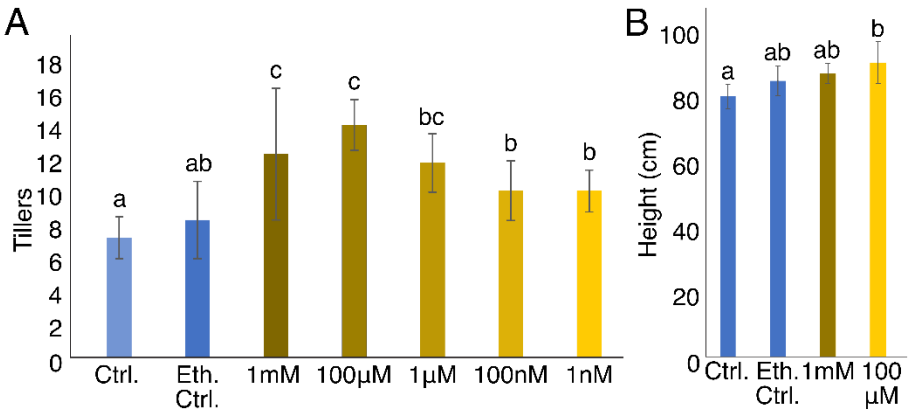

Figure 3.14: The effect of synthetic cytokinin 6-BA treatments of different concentrations on wheat shoot architecture development.

(A) Bar chart of mean maximum tiller number per plant (taken at 42 DaP). The two controls (no treatment and treatment of ethanol only) are represented in blue, and 6-BA treated conditions are represented in shades of yellow, treatments of higher concentrations are shown in darker shades. Different letters above bars indicates statistically significant difference between conditions (ANOVA, $P<0.05$, n=6-8). **(B)** Bar chart of mean plant height (cm) at the end of plant life. Height was measured from the point where the shoot emerged from the soil to the tip of the terminal spikelet of the main shoot ear. The two controls (no treatment and treatment of ethanol only) are represented in blue, the 1mM 6-BA treatment is represented in dark yellow, the 100µM 6-BA treatment is represented in yellow. Different letters above bars indicates statistically significant difference between conditions (ANOVA, $P<0.05$, n=6-8).

The established hormonal treatment system was performed on the elite wheat line Cadenza. SAMs of these plants were dissected to determine rate of development, spikelet production and tiller production. I hypothesised that, given that cytokinin can act as a long-distance signal and elicit developmental changes in the shoot, it might be used by the plant to coordinate tiller and spikelet development.

The data shows that not only did emerged tiller number increase significantly, but the number of unemerged meristems also increased as a result of the 6-BA treatment from a mean of 7.7 to 16.0 (Figures 3.15A-B). The increase of both was

proportionally similar, as the 6-BA treatment did not significantly affect the ratio of unemerged to emerged SAMs (Figure 3.15D). This increase strongly implies that the increased tillering effect is the result of cytokinin increasing both tiller bud formation and outgrowth in wheat. Cytokinin has previously been shown to regulate tiller bud outgrowth in wheat (via regulation of *TB1*), but its involvement in bud formation has only been postulated in *Arabidopsis* and rice (Lu *et al.*, 2015; Yang *et al.*, 2023).

At the time of dissection, SAMs appeared to be early in reproductive development, and a small but significant decrease in mean developmental stage was observed in the emerged meristems of the 6-BA treated plants (Figure 3.15F). The treated plants also had significantly fewer spikelet ridges per ear (Figure 3.15E). It thus appears that cytokinin slows both meristem development and the rate of spikelet production. It is possible that this delay in spikelet production could influence the observed increase in tiller development and suggests that cytokinin is involved in balancing development of spikelets and tillers in wheat, and that an increase in the amount of available cytokinin in the developing shoot system pushes the system to favour a greater number of less productive meristems.

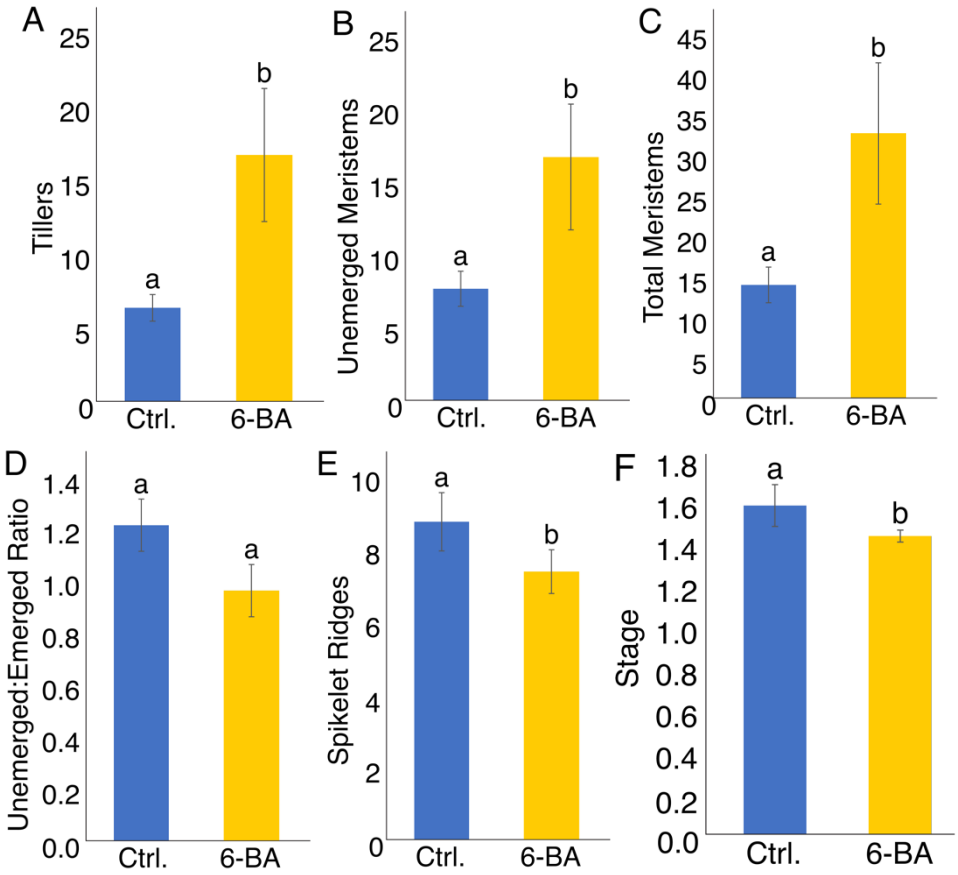

Figure 3.15: The effect of treatment of 100μM synthetic cytokinin 6-BA on wheat shoot apical meristem development.

(A) Bar chart of mean maximum tiller number per plant **(B)** Bar chart of mean number of unemerged shoot apical meristems per plant **(C)** Bar chart of mean total number of SAMs per plant, calculated as the sum of emerged tillers and unemerged meristems **(D)** Bar chart of mean ratio of unemerged to emerged meristems per plant, calculating by dividin g the number of unemerged shoot apical meristems by the number of emerged tiller meristems **(E)** Bar chart of mean number of spikelet ridges per SAM **(F)** Bar chart of mean SAM stage of development per plant.

Measurements taken at 49 DaP. Ethanol injected control is represented in blue, plants treated with 0.33ml of 100μM 6-BA once per week are represented in yellow. Different letters above bars indicates statistically significant difference between conditions (two-tailed t-test, $P<0.05$, $n=4$).

The data shows that following the end of the treatment, the plants appear to have mostly closed the developmental gap identified during the treatment (Figures 3.16A-B), so that no significant difference is seen between the control and 6-BA treated plants regarding ear or spikelet number.

The largest difference between the two lines is the frequency of paired spikelet formation. The data shows that the 6-BA treatment of Cadenza (an elite wheat variety which typically produces few supernumerary spikelets) has resulted in an 8-fold increase in paired spikelet production (Figure 3.16C). This strongly implicates a role for cytokinin in controlling the formation of an increased number of spikelets per node and indicates the validity of investigating the activity of cytokinin in high and WT spikelet lines.

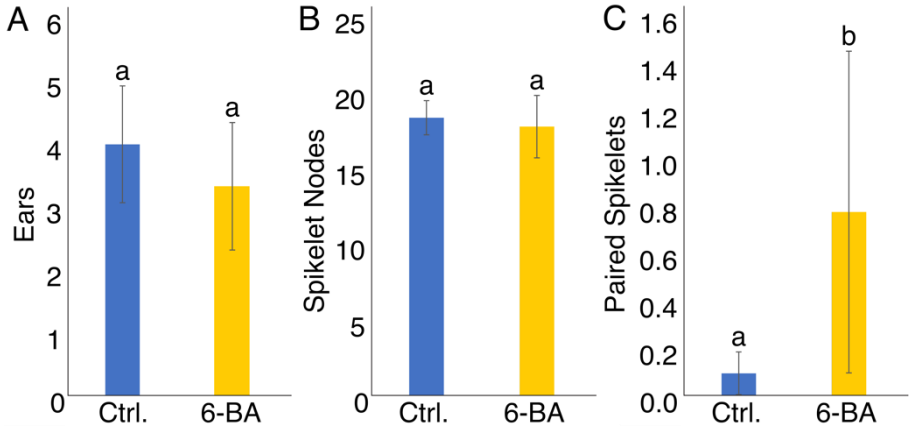

Figure 3.16: The effect of treatment of 100μM synthetic cytokinin 6-BA on wheat shoot architecture.

(A) Bar chart of mean number of ears per plant **(B)** Bar chart of mean number of spikelet nodes per ear **(C)** Bar chart of mean number of paired spikelets per ear.
Measurements taken at end of plant life. Ethanol injected control is represented in blue, plants treated with 0.33ml of 100μM 6-BA once per week are represented in yellow. Different letters above bars indicates statistically significant difference between conditions (two-tailed t-test, $P<0.05$, $n=15$).

I hypothesised that the effect of cytokinin on shoot development and spikelet-tiller coordination might become stronger, the longer the plant was exposed to increased

cytokinin levels. To further understand the role of cytokinin might influence spikelet-tiller feedback, I therefore conducted a series of experiments in which Cadenza was treated with 6-BA for different periods of time. Three different treatments were carried out, all of which began 21 DaP but ended after 2, 4 and 6 weeks respectively (hence referred to as treatments END1, END2, and END3 respectively). Preliminary dissections determined that at 35 DaP, the SAMs would be in either vegetative or early reproductive development, and there would be relatively few spikelets present (as confirmed in Figure 3.18A). At 49 DaP all emerged tiller SAMs would be in reproductive development, and in the process of spikelet production (as confirmed in Figure 3.19A). At 63 DaP they would all have ended reproductive development, and spikelets would no longer be actively produced. SAM dissections were conducted at 36 and 49 DaP and final architecture measurements were taken.

As has been established (Figures 3.14 and 3.15), exogenous cytokinin treatment increased tillering compared to the control plants. However, the data indicates that while even the shorter treatment of END1 resulted in an increase in tillering, a longer course of 6-BA treatment resulted in a further increase in tillering (Figure 3.18). Once maximum tiller number is reached, there is no significant difference between the END2 and END3 plants. There are two likely explanations for this observation. The first is that between the end points of these two conditions (49 and 63 DaP), the feedback from existing structures (including spikelets) prevents the formation of new tillers and therefore the additional 6-BA given to END3 plants can no longer influence the process. In END2, END3 and control plants, maximum tiller number was reached at 56 DaP (Figure 3.17A). However, given the delay to the rate of SAM development (Figure 3.19A), it could be expected that the SAMs of these plants are still at an earlier stage of development and 6-BA may prolong the timeframe of tiller production. Therefore, a second possibility should be considered, that the fixed amount of additional 6-BA allows a new, higher tiller number to be produced, but once this number is reached, the feedback is also increased and therefore prolonging the treatment has no effect. A greater amount of 6-BA might then be expected to increase tillering further, however the observations from troubleshooting exogenous cytokinin treatment (Figure 3.14A) do not show this.

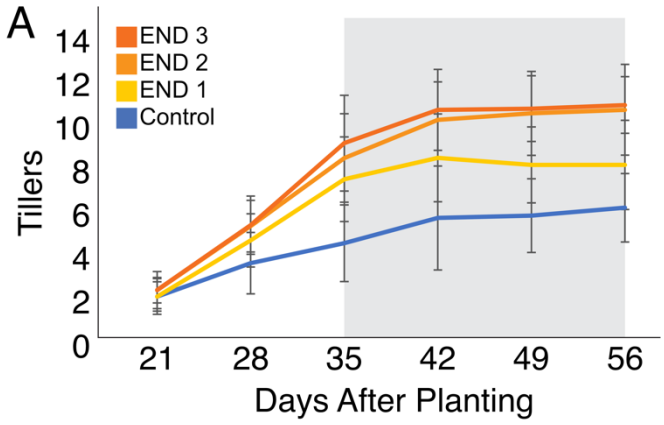

Figure 3.17: The effect of treatments of 100µM synthetic cytokinin 6-BA for different periods of time on wheat shoot architecture.

For all 6-BA treated plants, treatment began at 21 DaP. In the END 1 condition, treatment ended after 2 weeks; in the END 2 condition, treatment ended after 4 weeks; in the END 3 condition, treatment ended after 6 weeks.

(A) Line chart of mean number of tillers per plant plotted against DaP. Ethanol injected control is represented in blue, END 1, END 2 and END 3 plants treated with 0.33ml of 100µM 6-BA once per week are represented in yellow, orange and red respectively. Grey background indicates statistically significant difference between Control, END 1 and the END 2 and END 3 treatments (ANOVA, $P<0.05$, $n=12$-16).

At 35 DaP, there is no significant difference in the stage of development between the control and END 1 condition plants (Figures 3.18). But eventually, by 49 DaP the END 1 plants are shown to be significantly earlier in development than the control (Figures 3.19A). Furthermore, the END 2 plants at the 49 DaP are significantly earlier in development than the control and END 1 plants. Earlier reported data showing a delay in SAM development in 6-BA treated wheat (Figure 3.15F) alongside this evidence that a longer exposure to elevated 6-BA concentration elicits a stronger delay in SAM development, leads me to hypothesise that cytokinin functions as a developmental brake in the wheat SAM.

The lack of difference in SAM stage of development between control and 6-BA treated wheat at 35 DaP (Figures 3.18A-B) is likely the result of the SAMs still

primarily being in a stage of vegetative development. This indicates that the difference in SAM development brought about by cytokinin does not occur until after initiation of reproductive development and leads me to hypothesise that the eventually observed difference in stage of SAM development (Figure 3.19A) results from a reduction in rate of SAM reproductive development, and not from a delay in the initiation of reproductive development.

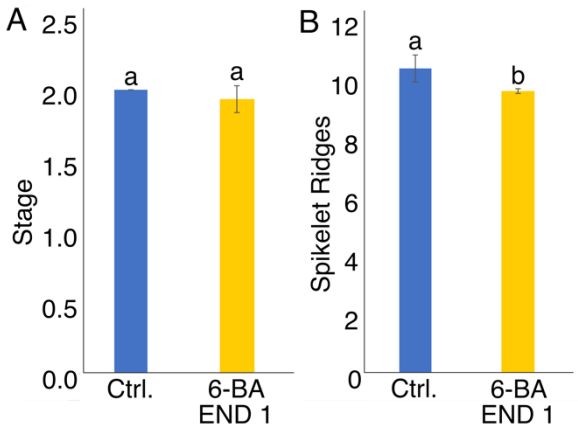

Figure 3.18: The effect of treatments of 100µM synthetic cytokinin 6-BA for different periods of time on wheat shoot apical meristem development - 35 DaP.

(A) Bar chart of mean shoot apical meristem stage of development per plant **(B)** Bar chart of mean spikelet ridges per meristem.

For all 6-BA treated plants, treatment began 21 DaP. In the END 1 condition, treatment ended after 2 weeks, at 35 DaP**.** Measurements taken at 35 DaP. Ethanol injected control is represented in blue, plants treated with 0.33ml of 100µM 6-BA once per week are represented in yellow. Different letters above bars indicates statistically significant difference between conditions (two-tailed t-test, $P<0.05$, n=3-4).

The effect of cytokinin on spikelet development is unclear. The dissections at both time points appear to show a small decrease in spikelet ridge number as a result of the 6-BA treatment but is found to be statistically insignificant (Figure 3.19B). Though this might ultimately suggest that cytokinin maintains a higher rate of spikelet production, as the three conditions are found to have made equivalent

number of spikelet ridges, whilst being at significantly different stages of development (Figure 3.19A).

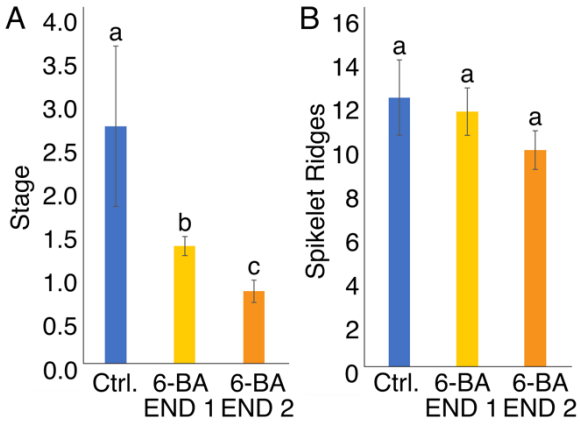

Figure 3.19: The effect of treatments of 100µM synthetic cytokinin 6-BA for different periods of time on wheat shoot apical meristem development - 49 DaP.

(A) Bar chart of mean shoot apical meristem stage of development per plant **(B)** Bar chart of mean spikelet ridges per meristem.

For all 6-BA treated plants, treatment began 21 DaP. In the END 1 condition, treatment ended after 2 weeks, at 35 DaP; in the END 2 condition, treatment ended after 4 weeks, at 49 DaP. Measurements taken at 49 DaP. Ethanol injected control is represented in blue, plants treated with 0.33ml of 100µM 6-BA once per week are represented in yellow (END 1) and orange (END 2). Different letters above bars indicates statistically significant difference between conditions (two-tailed t-test, $P<0.05$, n=3-4).

As previously reported (Figure 3.16), no significant difference in spikelet nodes per ear is seen in the final architecture. However, a clear gradient of paired spikelet production can be observed, with longer treatments resulting in significantly more paired spikelets (Figure 3.20B). This suggests that while cytokinin does not appear to play a role in determining spikelets nodes per ear number, it is reasonable to hypothesise that it influences the number of spikelets that develop from each node.

This activity, combined with the established role in tiller development, makes cytokinin a strong candidate for a coordinating molecule in the observed feedback

effect between spikelet and tiller development. It appears that cytokinin can somewhat overcome spikelet-tiller feedback, allowing for development of a higher number of tillers with a greater total number of spikelets.

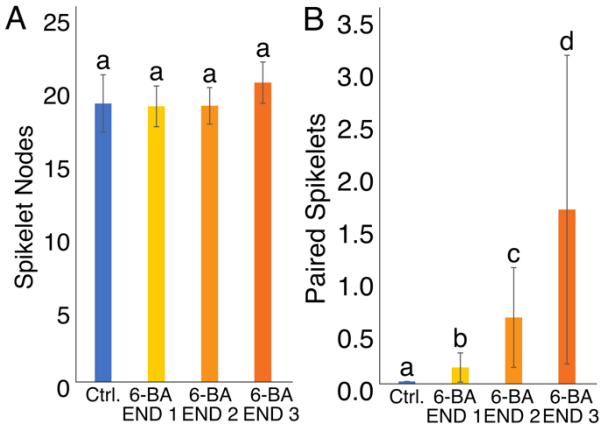

Figure 3.20: The effect of treatments of 100µM synthetic cytokinin 6-BA for different periods of time on mature wheat shoot architecture.

(A) Bar chart of mean number of spikelet nodes per ear **(B)** Bar chart of mean number of paired spikelets per ear

For all 6-BA treated plants, treatment began 21 DaP. In the END 1 condition, treatment ended after 2 weeks, at 35 DaP; in the END 2 condition, treatment ended after 4 weeks, at 49 DaP; in the END 3 condition, treatment ended after 6 weeks, at 63 DaP**.** Measurements taken at end of plant life. Ethanol injected control is represented in blue, plants treated with 0.33ml of 100µM 6-BA once per week are represented in yellow (END 1), orange (END 2) and red (END 3). Different letters above bars indicates statistically significant difference between conditions (ANOVA, $P<0.05$, n=11-14).

3.10 Effect of an exogenous cytokinin treatment timecourse on wheat shoot development

In the above 6-BA treatment experiments, the 6-BA treated plants often produce an equivalent final number of spikelet nodes at their final architecture (Figure 3.18B and 3.20A). However, a small but significant reduction in spikelet ridges can be seen mid-reproductive development (Figures 3.15E and 3.18B). Furthermore, in section 3.6 I established that the repressive feedback of spikelets on tiller development was specifically caused by actively developing spikelets, not by fully developed spikelets.

I thus hypothesised that this reduction in spikelet ridges during development may contribute to the increase in tillering seen in the 6-BA treated plants in a manner distinct from cytokinin's already known ability to increase tillering (J. Sun *et al.*, 2023; Yuan *et al.*, 2023).

I further hypothesised that if this were the case, then the reduction in spikelet ridges would precede the increase in tiller development. Therefore, I conducted a course of regular dissections on control and 6-BA treated wheat. The cytokinin treatment was applied to the YoGI 028 wheat landrace, which develops significantly quicker than the Cadenza line used in the previous 6-BA treatment experiments. The shorter total length of development therefore made it feasible to conduct dissections every 48 hours across the entirety of development.

The dissections showed that a significant difference in tillering between the treated and control plants can be observed from 28 DaP, and 14 days after beginning of treatment (Figure 3.21A). However, a significant reduction in spikelet ridges/ear is observed as early as 22 DaP, or 8 days after beginning of treatment (Figure 3.21B). These findings align with the hypothesis that a reduction in spikelet ridges precedes the increase in tillering. In combination with the data from previous sections that the number of developing spikelet ridges/ear proportionally represses tillering, this suggests that the increased tillering in 6-BA treated plants may be partially the result of a reduction in spikelet ridges. However, another possible explanation is that the reduction in spikelet ridges is a result of delayed meristem development (Figures 3.21C-D) being an effect that precedes the change in tillering.

Data collected from this experiment further supports two hypotheses: Firstly, in both control and treated wheat, the mean stage of development for unemerged SAMs is greatly delayed in comparison to emerged tillers on the same plant (Figure 3.21C-D); secondly, cytokinin is again shown to reduce the rate of development in the SAMs of emerged tillers, compared with control plants (Figure 3.21C-D).

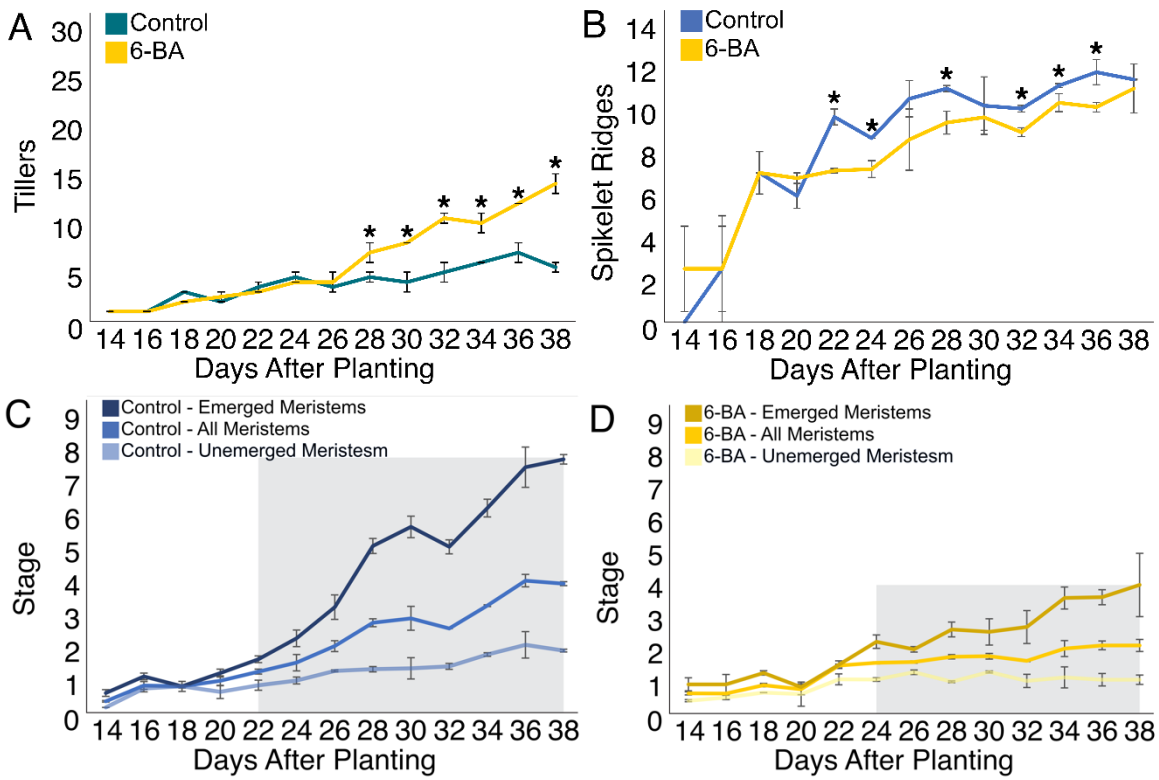

Figure 3.21: The effect of 100µM synthetic cytokinin 6-BA treatment on wheat spikelet production and shoot apical meristem rate of development over time.

For all 6-BA treated plants, treatment began 14 DaP and was maintained throughout the experiment**.**

(A) Line chart of mean number of emerged tillers per plant **(B)** Line chart of mean number of spikelet ridges per meristem.

Measurements were taken every 48 hours. Ethanol injected control is represented in blue, plants treated with 0.33ml of 100µM 6-BA once per week are represented in yellow. An asterisk above bars indicates statistically significant difference between conditions at that time point (two-tailed t-test, $P<0.05$, $n=3$).

(C) Line chart of mean shoot apical meristem stage of development in ethanol control plants **(D)** Line chart of mean shoot apical meristem stage of development in plants treated with 0.33ml of100µM 6-BA once per week.

Significant difference between emerged and unemerged stage is represented in grey (two-tailed t-test, $P<0.05$, $n=3$).

3.11 The effect of exogenous cytokinin treatment on *hb* shoot development

The results discussed in sections 3.9 and 3.10 have detailed the effects of cytokinin on wheat SAM development and shoot architecture. Previous studies have hypothesised that correlative inhibition may be achieved as a result of source-sink relationships between plant organs (Domagalska and Leyser, 2011; Abbai *et al.*, 2024). If cytokinin coordinates the observed feedback, then the high spikelet ears of *hb* might be acting as a stronger cytokinin sink than the developing ears of WT, resulting in a smaller amount of available cytokinin in the shoot system and reduced tillering. I therefore hypothesised that an equivalent exogenous 6-BA treatment would result in a proportionally greater increase in tillering, as the *hb* shoot would have less available cytokinin than the WT. 6-BA treatments were therefore conducted on *hb* and WT plants following the previously used protocol (section 2.4.1). After 4 weeks of treatment, tillering, spikelet number and stage of development were compared between lines to determine if the two lines were differently affected by the same treatment.

The data shows that, as expected, maximum tiller number increased after 4 weeks of exogenous cytokinin treatment in both lines (Figure 3.22A). However, tillering increased by a greater extent *hb* treated plants, than in the WT control line (Figure 3.22B). It is possible that the typically lower tillering plants have more opportunity to increase tiller number, before reaching some other limit on tiller production. The amount of cytokinin added to the shoot system by the introduction of exogenous 6-BA may set a new maximum tiller number in both lines, which the WT wheat line was already closer to. In both lines, the increase in cytokinin results in a delayed rate of SAM development (Figure 3.22C). The effect is again proportionally stronger in *hb (*Figure 3.22D), though the difference (between 11% for WT and 15% for *hb*) is negligible compared to the difference seen in tillering (Figure 3.22B),

The data suggests that at 49 DaP, the treatment has had no effect on spikelet ridge number in WT, but has in *hb*, though this difference is small (Figures 3.22E-F), and the % change is of the same magnitude as seen for the delay in SAM development (Figure 3.22D). Therefore, it is likely this is only the result of the delayed SAM

development; this is further supported by Figure 3.23A, which shows that there is no difference in spikelets per ear in the final architecture. The greater sensitivity to 6-BA treatment in *hb* supports the hypothesis that in *hb* a greater quantity of endogenous cytokinin is used in upregulating paired spikelet development, resulting in reduced quantity available in the shoot and tiller unemerged tiller buds to encourage tiller bud outgrowth than in the WT, and that the exogenous treatment is proportionally larger in this system and has a greater effect on development.

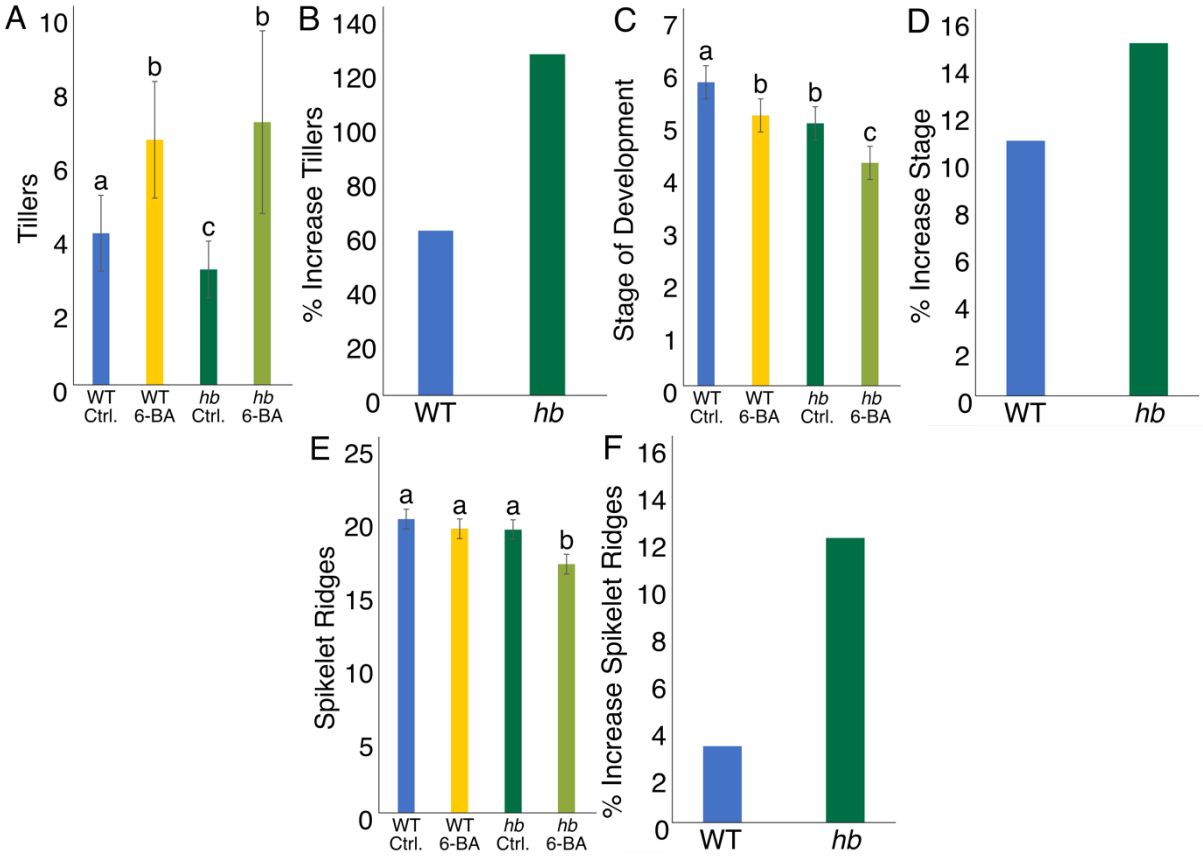

Figure 3.22: The effect of 100µM synthetic cytokinin 6-BA treatment on SAM Development in high and WT spikelet wheat lines.

For all 6-BA treated plants, treatment began 21 DaP and was maintained until 49 DaP**. (A)** Bar chart of mean number of tillers per plant **(B)** Bar chart of the percentage increase in number of tillers per plant as a result of 6-BA treatment **(C)** Bar chart of mean SAM stage of development **(D)** Bar chart of the percentage increase in SAM stage of development as a result of 6-BA treatment **(E)** Bar chart of mean number of spikelet ridges per SAM **(F)** Bar chart of the percentage increase in mean number of spikelet ridges per SAM as a result of 6-BA treatment.

Measurements taken at 49 DaP. Ethanol injected control is represented in blue (WT) and dark green *(hb*) and plants treated with 0.33ml of 100µM once per week are represented in yellow (WT) and light green (*hb*). Different letters above bars indicates statistically significant difference between conditions (ANOVA, $P<0.05$, n=3-4).

In all lines the number of spikelet nodes per ear was equivalent (Figure 3.23A), but the cytokinin treated plants produced significantly more paired spikelets (Figure 3.23B). Whilst this effect was seen previously in other wheat lines, this experiment grants the additional insight that the *hb* line, which already exhibited this developmental phenotype, frequency of paired spikelet formation can be increased further, but by a smaller extent than the WT plants.

The number of paired spikelets became equivalent between the two lines when exposed to the same quantity of cytokinin. Just as the WT tillering *hb* plants increased tillering by a greater extent, to become similar to WT (Figure 3.22A), the lower spikelet producing WT plants have increased paired spikelet production by a greater extent, to become similar to *hb*. This result implicates cytokinin in the regulation of spikelet and tiller development in an interdependent and dosage dependent manner.

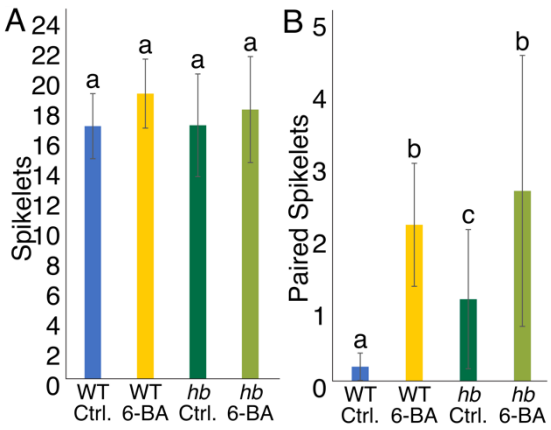

Figure 3.23: The effect of 100µM synthetic cytokinin 6-BA treatment on shoot architecture in high and WT spikelet wheat lines.

(A) Bar chart of mean number of spikelets per ear **(B)** Bar chart of mean number of paired spikelets per ear.

For all 6-BA treated plants, treatment began 21 DaP and was maintained until 49 DaP**.** Measurements taken at end of plant life. Ethanol injected control is represented in blue (WT) and dark green *(hb*) and plants treated with 0.33ml of 100µM once per week are represented in yellow (WT) and light green (*hb*). Different letters above bars indicates statistically significant difference between conditions (ANOVA, P<0.05, n=3-4).

3.12 The effect of exogenous cytokinin treatment on *vrs1* shoot development

Given the similarities in development between wheat and barley, I hypothesised that 6-BA treatment of *vrs1* and WT barley would produce similar results to those reported for tiller development, spikelet development, and rate of reproductive development in wheat, reported in section 3.11.

After troubleshooting to optimise the 6-BA treatment protocol for barley, standard 6-BA treatments (section 2.4.1) were performed on both the two-row WT and the six-row *vrs1* mutant for four weeks. As with the wheat experiments, weekly tiller data, final architecture measurements and shoot apical meristem dissections were used to develop an understanding of the effect of cytokinin on barley shoot development and how this effect differed in high and WT spikelet lines.

49 DaP the plants had reached maximum tiller number. At this point the data shows that the cytokinin treated plants had produced significantly more tillers than the control plants of both lines (Figure 3.24A). Furthermore, the increase in tillering in the WT plants was proportionally greater than the increase in *vrs1*, increasing tiller number by 64% and 34% respectively (Figure 3.24B). This result was unexpected and is opposite to what was observed in wheat (Figure 3.22B). It is possible that the difference is the result of the two species utilising cytokinin in different ways to coordinate aspects of tiller development. However, the most probable explanation is that the difference results from the different methods by which *vrs1* increased spikelet number over the WT (increased lateral spikelet fertility), compared to *hb* (increased paired spikelet development).

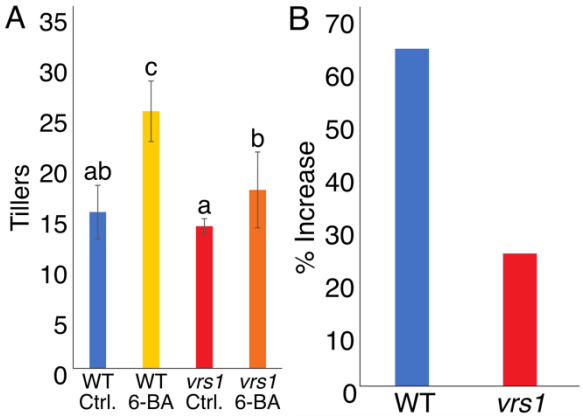

Figure 3.24: The effect of 100µM synthetic cytokinin 6-BA treatment on barley tiller development.

For all 6-BA treated plants, treatment began 21 DaP and was maintained until 49 DaP**.** **(A)** Bar chart of mean number of tillers per plant (taken at 49 DaP). Ethanol injected control is represented in blue (WT) and red (*vrs1*) and plants treated with 0.33ml of 100µM once per week are represented in yellow (WT) and orange (*vrs1*). Different letters above bars indicates statistically significant difference between conditions (ANOVA, $P<0.05$, $n=5$). **(B)** Bar chart of the percentage increase in maximum number of tillers per plant as a result of 6-BA treatment (taken at 49 DaP). Percentage increase in WT is represented in blue and in *vrs1* is represented in red.

Subsequently, SAMs were dissected to determine any further effect on development in addition to the expected increase in tillering. The SAMs of the cytokinin treatment plants of both lines were at an earlier stage of development than the control plants (Figure 3.25A). These results support the theory that cytokinin delays SAM development in cereals.

In contrast to wheat (Figure 3.21), the unemerged shoot meristem in barley could often be found to have initiated reproductive development (Figure 3.25B) and at 49 DaP it had even reached, on average, as far as the glume primordium stage (Figures 3.25B). This phenotype could point to a use for cytokinin in encouraging a more productive shoot architecture, by producing fewer ‘wasted’ spikelets on meristems that will not result in productive ears. Importantly, these are meristems that have not been directly treated with 6-BA, as the treatment system developed in section 3.9 and used for all subsequent experiments only involves the injection of emerged tillers. This result therefore provides further evidence that cytokinin treatment is effective in affecting the development of the entire shoot system. Furthermore, this result supports the hypothesis that cytokinin acts to balance development between tillers and spikelets simultaneously. It is possible that the unemerged meristems are responding as expected, as a drop in spikelet node number is typically expected, given the meristems are at an earlier stage of development (Figure 3.25B). Whereas the emerged meristems have produced an equal number of spikelets by an earlier stage in development. This implies that an increased quantity of cytokinin, whilst slowing development, actually results in an increased rate of spikelet production, proportional to stage of meristem development.

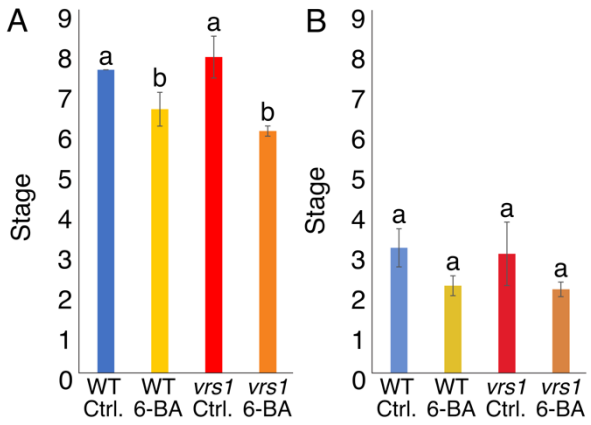

Figure 3.25: The effect of 100µM synthetic cytokinin 6-BA treatment on barley shoot apical meristem rate of development

(A) Bar chart of mean stage of development of emerged tiller SAMs **(B)** Bar chart of mean stage of development of unemerged SAMs.

For all 6-BA treated plants, treatment began 21 DaP and was maintained until 49 DaP**.** Measurements taken at 49 DaP. Ethanol injected control is represented in blue (WT) and red (*vrs1*) and plants treated with 0.33ml of 100µM once per week are represented in yellow (WT) and orange (*vrs1*). Different letters above bars indicates statistically significant difference between conditions (ANOVA, $P<0.05$, $n=5$).

3.13 The role of strigolactone in regulating wheat shoot development

The experimental data presented and discussed in this chapter establishes that a system of proportional feedback between spikelet development and tiller development exists and establishes cytokinin as a phytohormone that is partially responsible for such an effect. However, many developmental processes in plants are coordinated by more than one phytohormone, and I therefore investigated further phytohormones for their potential role in this feedback. I hypothesised that strigolactone was another reasonable candidate for coordinating the observed feedback. It has previously been reported to influence shoot architecture in a number of plant species and has been specifically shown to be a regulator of tillering and inflorescence development in wheat and barley (discussed in section 1.4.8) (Bai *et al.*, 2024). Also encouraging, is the proposed involvement of strigolactone in apical

dominance (Domagalska and Leyser, 2011; Khuvung, Silva Gutierrez and Reinhardt, 2022).

Two mutant wheat lines were acquired, with disruptions to genes which encode proteins involved in the canonical strigolactone signalling pathway. *D3* and *D14* null mutants were utilised, both of which are essential for the perception of strigolactone signal. The *d3* and *d14* mutant lines were grown alongside the wild-type background line to study and compare the effects of these mutations on shoot architecture.

An expected increase in maximum tiller number was observed (Figure 3.26A) which additionally resulted in a significant increase in ear number in the two mutant lines (Figure 3.26B). Also observed was a reduction in plant height in the mutants (Figure 3.26H), which, alongside an increase in tillering, is a phenotype indicative of reduced strigolactone activity and confirms the plants as the reported strigolactone mutants.

In contrast to the increase in tiller number, the two strigolactone mutants both produced significantly fewer spikelets per ear than the wild type (Figure 3.26C). However, both mutant lines produced significantly more spikelets across all meristems than the wild type (Figure 3.26D), but a smaller proportion of spikelets in the mutant plants were fertile and produced seed (Figure 3.26E). Overall, the seed mass produced by the strigolactone mutants was therefore significantly reduced compared to wild-type (Figure 3.26F). Despite these very different shoot architectures, the final dry shoot biomass between the wild type and strigolactone mutants was the same (Figure 3.26G).

The reduced spikelet/increased tiller phenotype supports strigolactone as a possible candidate for the proposed phytohormone-mediated feedback between spikelet and tiller development. However, investigation is required to determine if the influence exerted by strigolactone on tiller development and spikelet development are interdependent phenomena. The absence of strigolactone signalling had no significant effect on the production of supernumerary spikelets (Figure 3.26C). It may therefore play a distinct role to cytokinin in regulating such developmental feedback, instead of relating to spikelets per node it may be more strongly influence spikelet ridge development and final rachis node number.

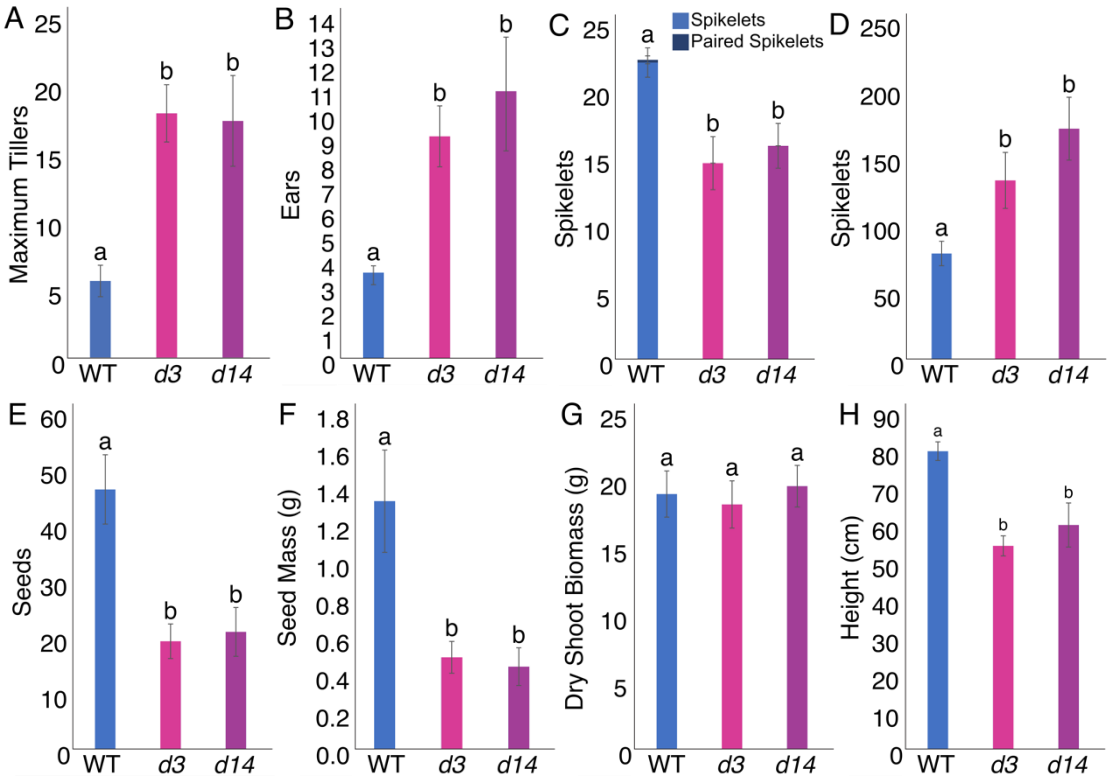

Figure 3.26: The effect of disruption of the D3 and D14 strigolactone perception proteins on wheat shoot architecture.

(A) Bar chart of mean maximum number of tillers per plant **(B)** Bar chart of mean number of ears per plant **(C)** Bar chart of mean number of regular spikelets and paired spikelets per ear **(D)** Bar chart of mean number of spikelets per plant **(E)** Bar chart of mean number of seeds per ear **(F)** Bar chart of mean seed mass **(G)** Bar chart of mean dry shoot biomass **(H)** Bar chart of mean plant height.

Measurements taken at end of plant life (measured from the point at which the main shoot emerged from the soil to the tip of the terminal spikelet on the ear of the main shoot ear). The wild-type background is represented in blue, the *d3* mutant is represented in pink and the *d14* mutant is represented in purple. Different letters above bars indicates statistically significant difference between conditions (ANOVA, $P<0.05$, n=8-10).

I hypothesised that strigolactone might regulate aspects of wheat development, including tillering, rate of spikelet development, and SAM development. I began

testing this by conducting weekly dissections of WT, *d3* and *d14* plants every week from 21 to 63 DaP, measuring tiller and unemerged tiller bud number, mean stage of development and spikelet ridge number. These were intended to pinpoint when differences in tillering and spikelet number occurred between WT and SL mutants. Unlike cytokinin, there is currently no literature to suggest that strigolactone might regulate rate of meristem development. I therefore hypothesised that, unlike cytokinin, strigolactone might achieve a difference in spikelet number without affecting rate of SAM development.

The *d3* and *d14* wheat lines produce significantly more tillers compared with the wild type (Figure 3.27A) but also significantly more unemerged meristems (Figure 3.27B) at approximately equal rates, resulting in an unchanged final ratio between the two (Figure 3.27C). This result implicates strigolactone in regulating tiller bud outgrowth in wheat as has previously been reported in *Arabidopsis* (section 1.3) but does not implicate it in coordinating the balance between tiller bud production and outgrowth, as the increase in unemerged SAMs is most likely a result of the increased number of tillers on which they can develop.

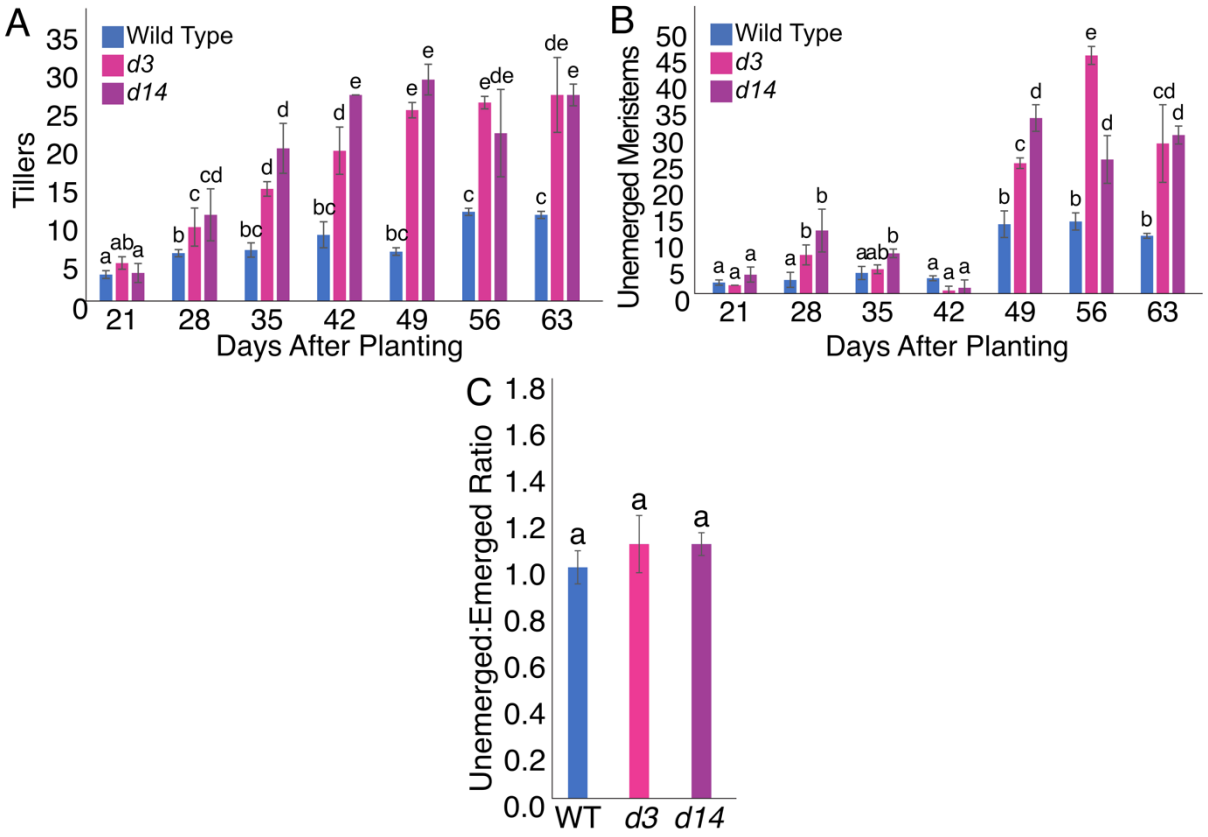

Figure 3.27: Tiller development and emergence in wheat strigolactone signalling mutants.

(A) Bar chart of mean number of emerged tillers per plant **(B)** Bar chart of mean number of unemerged SAMs per plant **(C)** Bar chart of mean ratio of unemerged to emerged SAMs per plant at 63 DaP.

Measurements were taken every 7 days between 21 and 63 DaP, calculated by dividing unemerged SAMs by emerged tillers per plant. The wild type background line is represented in blue; the *d3* mutant is represented in pink and the *d14* mutant is represented in purple. Error bars are 1 standard deviation from the mean. Different letters above bars indicate statistically significant difference between lines at that time point (ANOVA, $P<0.05$, $n=3$-5).

The data indicates that the meristems within fully emerged tillers have mostly initiated reproductive development and through the course of dissections can be seen to progress through it until they reach the Terminal Spikelet stage (Figure

3.28A). A significant difference in mean meristem stage is evident from as early as 21 DaP (Figure 3.28A). At this point there is no observable difference in tillering between the wild type and strigolactone mutant plants, (Figure 3.28A), a typical indicator of reduced strigolactone signalling. From here, the difference in stage grows wider and by the end of the measurements at 63 DaP, the *d3* and *d14* meristems are significantly earlier in development than the wild type.

However, in both WT and mutant lines, unemerged meristems are almost universally held in the vegetative stage of development (Figure 3.28B). Interestingly, this suggests that strigolactone acts as an accelerator of SAM development but is not responsible for maintaining unemerged SAMs at an early stage in development, compared with emerged tiller SAMs.

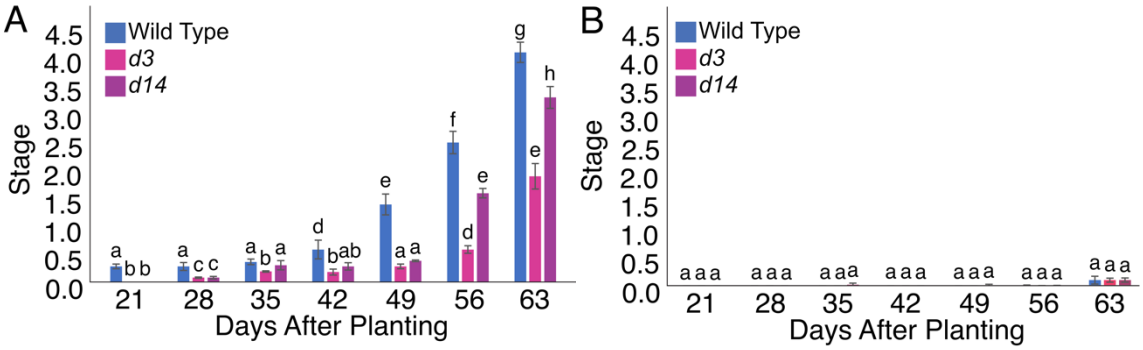

Figure 3.28: Rate of SAM development in wheat strigolactone signalling mutants.

(A) Bar chart of mean stage of SAM development for emerged tiller SAMs **(B)** Bar chart of mean stage of SAM development for unemerged SAMs.
Measurements were taken every 7 days between 21 and 63 DaP. The wild-type background line is represented in blue; the *d3* mutant is represented in pink and the *d14* mutant is represented in purple. Error bars are 1 standard deviation from the mean. Different letters above bars indicate statistically significant difference between lines at that time point (ANOVA, $P<0.05$, n=3-5).

Until 35 DaP there is no difference in the number of spikelet ridges per meristem between the lines (Figure 3.29A-B). However, from 42 DaP onwards a clear difference in rate of spikelet production becomes apparent. This difference in

spikelet ridge number per meristem is maintained for the remainder of development, resulting in the reported decrease in final spikelet number (Figure 3.26C).

Spikelet production and tiller production are partly the result of the time spent in the stages of reproductive development. It is possible that in addition to current models, in which strigolactone influences tiller and spikelet number directly, modulation of rate of meristem development acts as an additional method through which strigolactone influences the number of tillers and spikelets that are produced. In section 3.5, data was presented that indicated that an increase in cytokinin resulted in increased tiller number and decreased rate of meristem development. This phenotype closely resembles the one now reported from these strigolactone mutants, implying an opposite effect for strigolactone. Strigolactone and cytokinin act as long-distance signals for information regarding resource availability, current literature supports the idea that these signals associate resource availability with shoot development by modulating tiller bud outgrowth (Gomez-Roldan *et al.*, 2008; Umehara *et al.*, 2008). Rate of meristem development could be an additional process on which these signals are integrated to bring about a proportional response in shoot architecture development. The two phytohormones potentially work in concert to regulate spikelet development by controlling the progression of the meristem through certain developmental stages, strigolactone acting as an accelerator, cytokinin as a brake.

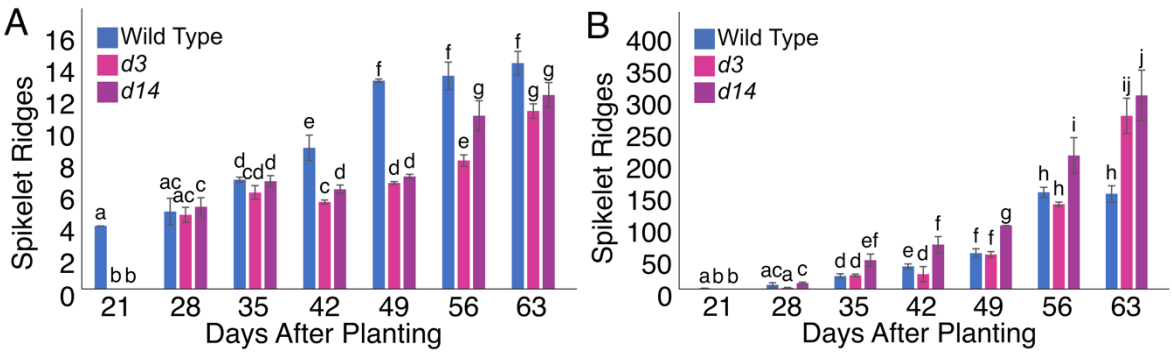

Figure 3.29: Spikelet development in wheat strigolactone signalling mutants.

(A) Bar chart of mean number of spikelet ridges per SAM **B)** Bar chart of mean number of spikelet ridges per plant.

Measurements were taken every 7 days between 21 and 63 DaP. The wild type background line is represented in blue; the *d3* mutant is represented in pink and the *d14* mutant is represented in purple. Error bars are 1 standard deviation from the mean. Different letters above bars indicate statistically significant difference between lines at that time point (ANOVA, P<0.05, n=3-5).

3.14 The role of strigolactone in regulating barley shoot development

In addition to the two mutant wheat lines investigated in section 3.13, a *D14* null mutant barley line was also acquired and the development of its reproductive architecture was studied and compared to the wild type 'Sebastian' background. Although wheat and barley are relatively similar species, cytokinin experiments conducted in this chapter have often produced different results in the different species (Figure 3.22B vs Figure 3.24B). I thus hypothesised that shoot development of the *d14* barley mutant might be affected differently to the orthologous wheat mutant and reveal how and when these differences arise.

The WT background line and the *d14* mutant line were grown and their final shoot architecture was measured. The effect of the *d14* mutation in barley was found to be very similar to the mutation of the orthologous *d14* gene in wheat. As would be expected in a plant with reduced strigolactone perception, tiller number (Figure 3.30) and final ear number (Figure 3.31A) was increased compared with the wild type

(Figure 3.26). Furthermore, as was reported in wheat, the number of spikelets per ear was reduced in the mutant line (Figure 3.31B), but to a smaller degree than the increase in tillering, causing the mutant plants to produce more spikelets across the entire plant (Figure 3.31C). Also similar to wheat was that the *d14* plants produced fewer and smaller seeds than the wild type (Figures 3.31D-H). However, whereas in wheat the effect on seed development resulted in the mutant producing a greatly reduced total seed mass, in *d14* barley the reduction in seed mass is proportional to the increase in total spikelets, resulting in the mutant and wild type lines producing a similar total seed mass (Figure 3.31G). This result draws attention to the fact that, whilst the change in shoot architecture development in wheat and barley *d14* mutants is qualitatively similar the same (increased tillering, decreased spikelets), the magnitude of the changes is not necessarily the same. The maximum tiller number in wheat *d14* mutants was 207% of WT, compared to 147% in barley, while the decrease in spikelet number was 29% in wheat and 13% in barley. Wheat and barley are similar, but not identical species, therefore a qualitatively similar, but quantitatively different response in the *d14* mutants still suggests a similarity in the role of strigolactone.

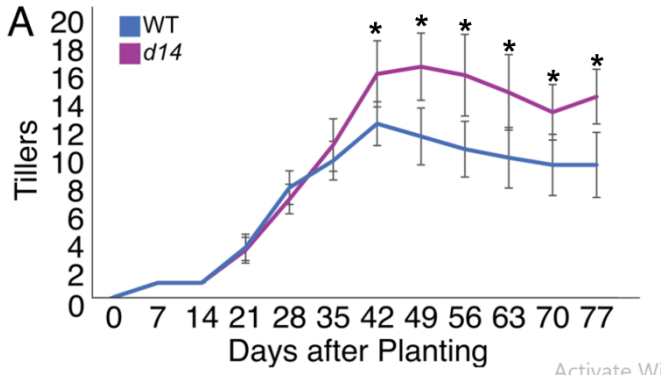

Figure 3.30: The effect of disruption of the D14 strigolactone perception protein on barley shoot architecture.

(A) Line chart of mean number of tillers per plant plotted against time (measurements taken every 7 days). The wild type background is represented in blue, the *d14* mutant is represented in purple. An asterisk above a time point indicates a statistically

significant difference between the two lines at that point (two-tailed t-test, P<0.05, n=8-10).

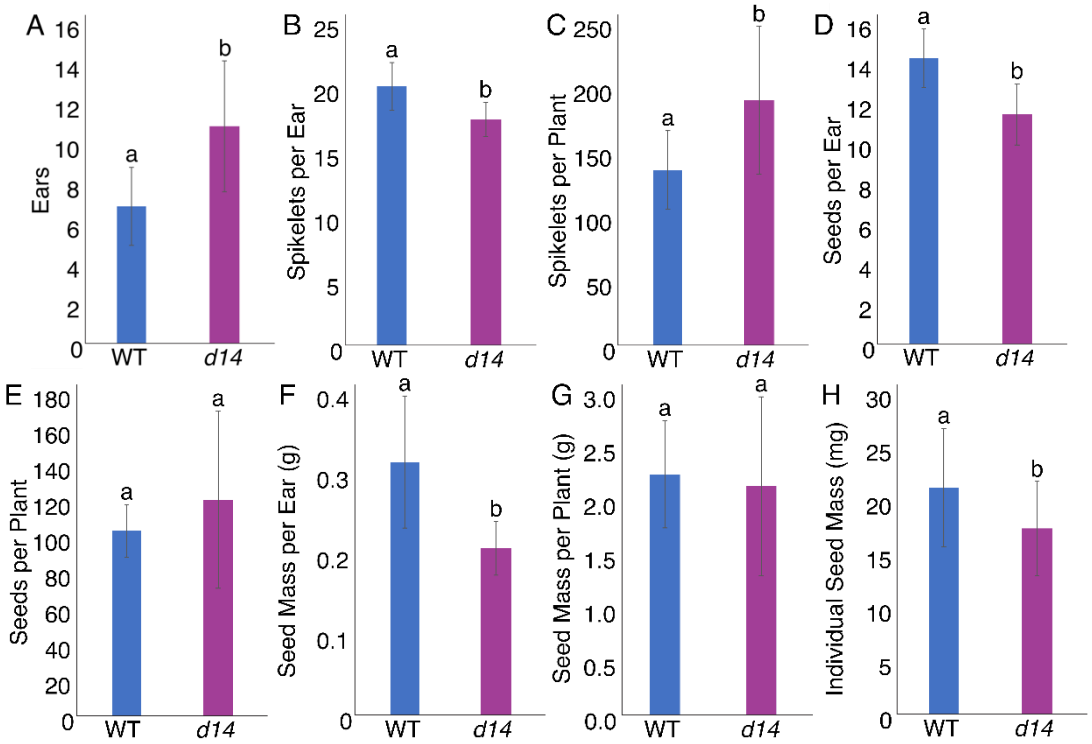

Figure 3.31: The effect of disruption of the D14 strigolactone perception protein on barley shoot architecture.

(A) Bar chart of mean number of ears per plant **(B)** Bar chart of mean number of spikelets per ear **(C)** Bar chart of mean number of spikelets per plant **(D)** Bar chart of mean number of seeds per ear **(E)** Bar chart of mean number of seeds per plant **(F)** Bar chart of mean mass per seed (mg) **(G)** Bar chart of mean seed mass per ear (g) **(H)** Bar chart of mean seed mass per plant (g).

Measurements were taken at end of plant life. The wild type background is represented in blue, the *d14* mutant is represented in purple. Different letters above bars indicates statistically significant difference between lines (two-tailed t-test, P<0.05, n=10-11).

Given that unemerged SAM number increased proportional to tillering in wheat WT and *d14,* I hypothesised that a timecourse of dissections would show the same result in barley. As was observed in the final architecture, the effect of *d14* mutation in

barley produced qualitatively similar results to those in wheat, though often the effects differed in magnitude. In addition to the tillering increase (Figure 3.32A), the mutants did increase the number of unemerged meristems compared to the wild type (Figure 3.32B). However, this increase was relatively small, and unlike wheat, by 56 DaP, there was a significant increase in the proportion of meristems that had produced observable tillers in the mutants (Figure 3.32D).

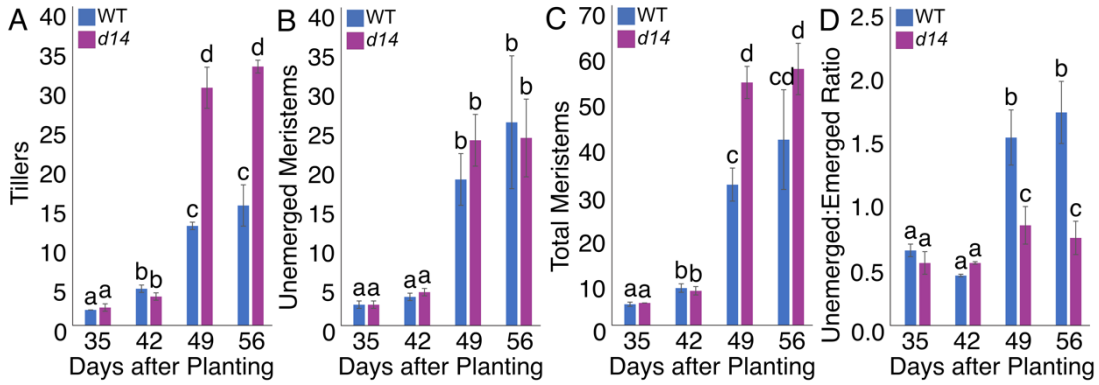

Figure 3.32: The effect of disruption of the D14 strigolactone perception protein on barley tiller emergence.

(A) Bar chart of mean number of emerged tillers per plant **(B)** Bar chart of mean number of unemerged SAMs per plant **(C)** Bar chart of mean total number of shoot apical meristems per plant (calculated as the sum of emerged tiller meristems and unemerged shoot apical meristems) **(D)** Bar chart of mean ratio of unemerged:emerged meristems (calculated by dividing number of unemerged shoot apical meristems per plant by emerged tiller meristems).

Measurements were taken every 7 days between 35 and 56 DaP. The wild-type background is represented in blue, the *d14* mutant is represented in purple. Different letters above bars indicates statistically significant difference between lines and time points (two-tailed t-test, $P<0.05$, $n=3$).

As was observed in wheat, the *d14* barley tiller meristems exhibited a reduced rate of SAM development and spikelet ridge number (Figures 3.33A and 3.33C). Additionally, whereas in wheat virtually all unemerged meristems were vegetative (as has been observed in other experiments, (Figures 3.07C and 3.22C-D), barley

unemerged meristems often have initiated reproductive development, especially from 49 DaP (Figure 3.33B). The mean stage of unemerged SAMs in barley appear to be consistently further in development than wheat at the same point in time (Figure 3.34).

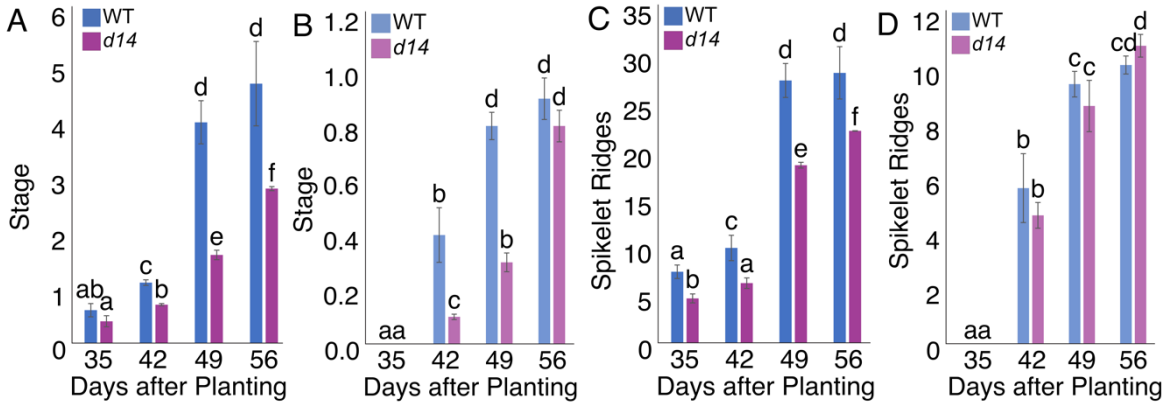

Figure 3.33: The effect of disruption of the D14 strigolactone perception protein on barley shoot apical meristem development.

(A) Bar chart of mean SAM stage of development of emerged tiller SAMs **(B)** Bar chart of mean SAM stage of development of unemerged SAMs **(C)** Bar chart of mean spikelet ridges per SAM of emerged tiller meristems **(D)** Bar chart of mean spikelet ridges per SAM of unemerged SAMs.

Measurements were taken every 7 days between 35 and 56 DaP. The wild-type background is represented in blue, the *d14* mutant is represented in purple. Different letters above bars indicates statistically significant difference between lines and time points (two-tailed t-test, $P<0.05$, n=3).

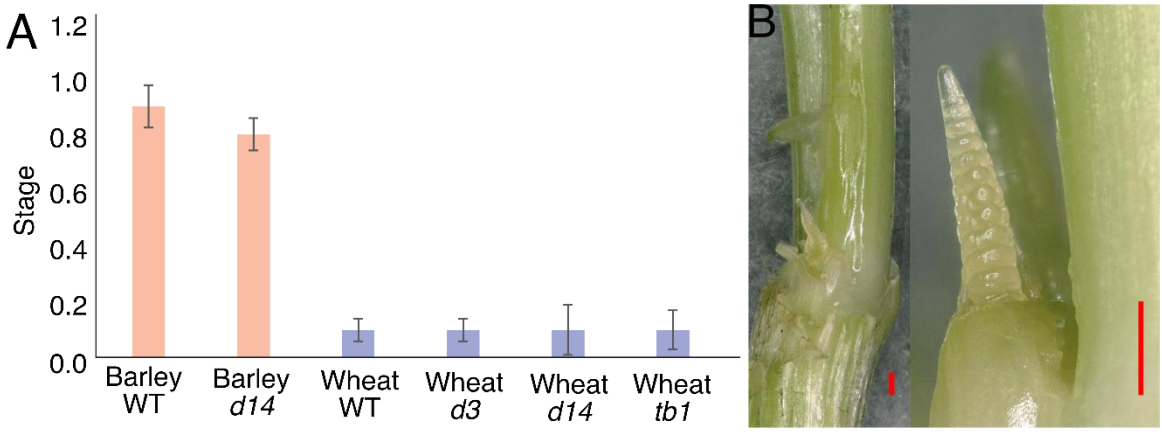

Figure 3.34: Comparison of rate of development of unemerged shoot apical meristems in barley and wheat

(A) Bar chart of mean stage of development of unemerged shoot apical meristems, at 56 DaP. Lines of barley are represented in pink, lines of wheat are represented in pale blue. Different letters above bars indicates statistically significant difference between conditions (two-tailed t-test, $P<0.05$, $n=3$). **(B)** Images of an unemerged barley SAM, which has initiated reproductive development. Red lines are 500µm.

3.15 The effect of exogenous strigolactone treatment on *hb* wheat

The results presented in sections 3.13 and 3.14 describe significant changes in shoot apical meristem development and final shoot architecture, resulting from a lack of strigolactone perception within the plant. To complement these results, I wanted to study the effect of increased perception of strigolactone. I hypothesised that an increase in shoot strigolactone levels would have the opposite effect, increasing rate of SAM development, decreasing tiller number and increasing spikelet number. I also hypothesised that the lack of difference between WT and *d14* unemerged SAM rate of development, may be the result of the unemerged SAMs of WT plants already being very early in development, so little further reduction could be enacted. Therefore, an increase in strigolactone may have a more noticeable effect, particularly in wheat. Additionally, these treatments would allow me to study the effect of changes in strigolactone not only in a mutant line, but in the *hb* and *vrs1* lines of wheat and barley. As discussed in section 3.9, spikelet-

tiller feedback in cereals may result from developing spikelets acting as a hormonal sink and thus a greater number acting as a stronger sink, resulting in a reduced quantity available to affect tillering. I hypothesised that these lines would be more sensitive than their WT background.

To achieve this increase, the exogenous hormone treatment system developed in section 3.5.1 was modified, to allow for the injection of the synthetic strigolactone GR24. An initial experiment trialled injections of 10µM and 100nM (Figure 3.35). Both treatments resulted in a significant decrease in tiller number, compared to the control. Such a result would be expected to result from an increase in strigolactone perception, as strigolactone is known to repress tillering (Yuan *et al.*, 2023). However, there was no difference in tiller production between the two treatment concentrations. Therefore, a 100nM concentration of GR24 was used in future experiments, which is fully described in section 2.4.2.

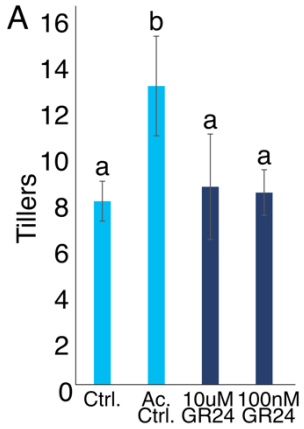

Figure 3.35: The effect of different concentrations of synthetic strigolactone GR24 tiller development in wheat.

(A) Bar chart of mean number of tillers, at 35 DaP. The control plants are represented in pale blue, the GR24 treated plants are represented in dark blue. Each treated plant was injected once per week with 0.33ml of GR24 of different concentrations. Different letters above bars indicates statistically significant difference between conditions (ANOVA, $P<0.05$, $n=8$).

The established treatment was applied to both *hb* and WT wheat. In both lines the strigolactone treatment resulted in a significant reduction in tiller number (Figure 3.36A). In fact, the strigolactone treated WT plants produced an equivalent number of tillers to the control *hb* plants. This data shows the known ability of strigolactones to inhibit tillering, but interestingly *hb* is more sensitive to the strigolactone treatment than the WT (Figure 3.36B-C). However, from this data alone it is not possible to conclude that the difference is a direct result of increased spikelet number, rather than simply the *hb* plants having fewer tillers to lose.

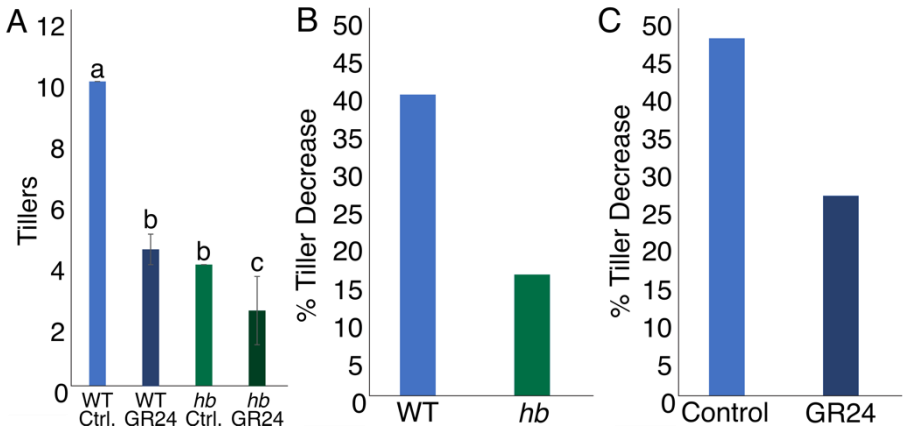

Figure 3.36: The effect of 100nM synthetic strigolactone GR24 treatment on wheat tiller development.

All GR24 treated plants were injected with 0.33ml of 100nM once per week beginning 21 DaP until 35 DaP.

(A) Bar chart of mean tiller number per plant (taken at 35 DaP). The WT line is represented in blue, the *hb* mutant in green, controls of both lines in the paler shade and GR24 treated plants represented in the darker shade. Different letters above bars indicates statistically significant difference between conditions (ANOVA, $P<0.05$, n=7-10). **(B)** Bar chart of the percentage decrease in tiller number (taken at 35 DaP) caused by GR24 treatment. The effect on the WT line of wheat is represented in blue, the effect on the *hb* mutant line is represented in green. **(C)** Bar chart of the percentage decrease in tiller number (taken at 35 DaP) observed between the WT background line and the *hb* mutant line. The difference between lines observed in control plants is represented

in light blue, the difference between the GR24 treated plants of both lines is represented in dark blue.

Further experiments using the same treatments were conducted, in which the developing SAMs were dissected. This data confirms the effect on tillering (Figure 3.37A), matching the data previously presented (Figure 3.36A). Unsurprisingly, the data also shows a similar effect on the number of unemerged shoot apical meristems (Figure 3.37B), resulting in the total number of meristems per plant similarly being reduced by the GR24 treatment in both lines. Subsequently, the similarity of these results means there is no statistically significant difference in the ratio of unemerged to emerged meristems in any of the conditions (Figure 3.37D). The increase in strigolactone results in a statistically significant acceleration in the rate of meristem development (Figure 3.37E). This result is the opposite of the effect seen in the strigolactone mutant lines and observed from cytokinin treatment, further supporting the hypothesis that cytokinin and strigolactone have opposing effects on regulating the rate of SAM development in wheat. Curiously, spikelet node number is significantly increased by strigolactone treatment in in WT, but not in *hb* (Figure 3.37F).

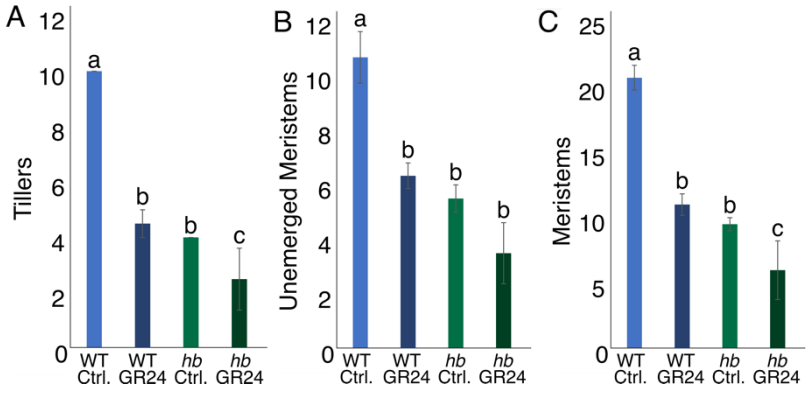

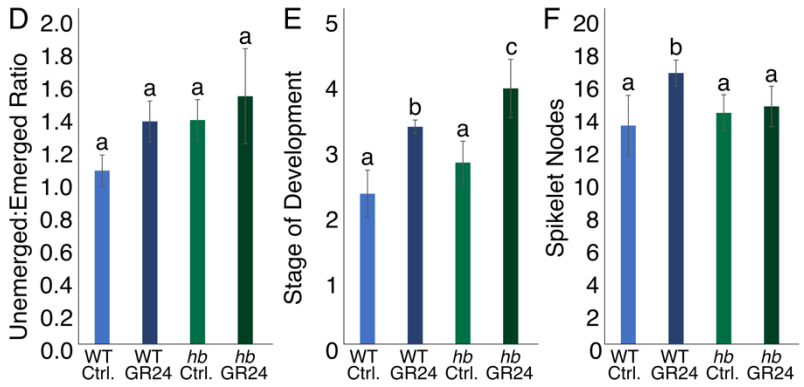

Figure 3.37: The effect of 100nM synthetic strigolactone GR24 treatment on wheat tiller emergence and shoot apical meristem development.

(A) Bar chart of mean number of emerged tiller meristems per plant **(B)** Bar chart of mean number of unemerged shoot apical meristems per plant **(C)** Bar chart of mean total number of shoot apical meristems per plant **(D)** Bar chart of mean ratio of unemerged:emerged meristems per plant **(E)** Bar chart of mean shoot apical meristem stage of development **(F)** Bar chart of mean number of spikelet ridges per SAM.
All GR24 treated plants were injected with 0.33ml of 100nM once per week beginning 21 DaP until 35 DaP. Measurements were taken at 35 DaP. The WT line is represented in blue, the *hb* mutant in green, controls of both lines in the paler shade and GR24 treated plants represented in the darker shade. Different letters above bars indicates statistically significant difference between conditions (two-tailed t-test, $P<0.05$, $n=3$).

3.16 The effect of exogenous strigolactone treatment on *vrs1* and WT barley lines

To complement the data presented in section 3.15, equivalent experiments were conducted in the two-row barley line WT and the six-row *vrs1* mutant. I hypothesised that barley would respond in a similar manner as wheat, with the WT being approximately as sensitive to GR24 treatment than the high spikelet line.

The strigolactone treatment results in significantly reduced tiller number in both barley lines (Figure 3.38A) and resulted in control *vrs1* and strigolactone treated WT to having the same number of tillers. Unlike wheat, the response of WT and *vrs1*

lines to SL treatment is similar (Figure 3.38B-C). Both WT and *vrs1* decrease tillering by a similar amount (16% and 20% respectively) and the GR24 injection had no effect on the difference in tillering between the two lines, in both conditions *vrs1* produces 20% fewer tillers than WT (Figure 3.38B-C). This further suggests that the reduced response in *hb* resulted from the untreated *hb* already having so few tillers.

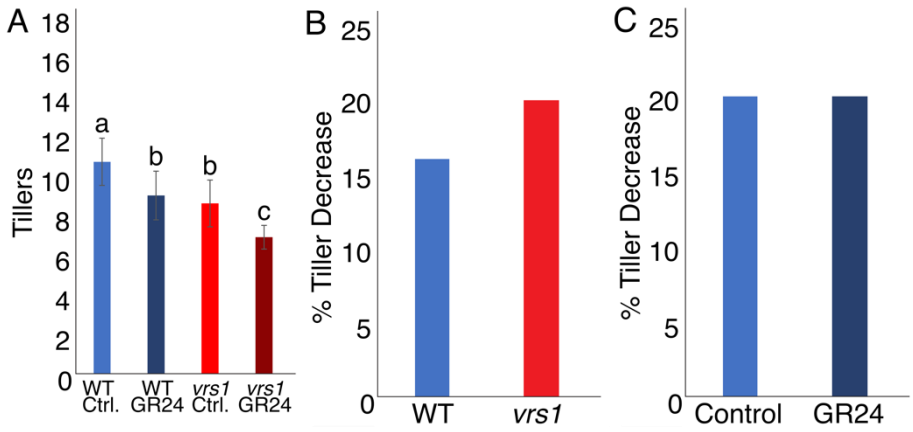

Figure 3.38: The effect of 100nM synthetic strigolactone GR24 treatment on barley tiller development.

All GR24 treated plants were injected with 0.33ml of 100nM once per week beginning 21 DaP until 35 DaP.

(A) Bar chart of mean tiller number per plant (taken at 35 DaP). The WT line is represented in blue, the *vrs1* mutant in red, controls of both lines in the paler shade and GR24 treated plants represented in the darker shade. Different letters above bars indicates statistically significant difference between conditions (ANOVA, $P<0.05$, n=6-10). **(B)** Bar chart of the percentage decrease in tiller number (taken at 35 DaP) caused by GR24 treatment. The effect on the WT line of wheat is represented in blue, the effect on the *vrs1* mutant line is represented in red. **(C)** Bar chart of the percentage decrease in tiller number (taken at 35 DaP) observed between the WT background line and the *vrs1* mutant line. The difference between lines observed in control plants is represented in light blue, the difference between GR24 treated plants of both lines is represented in dark blue.

Further experiments were conducted, in which the plants were dissected at 35 DaP, comparable to data previously presented (Figures 3.38). These experiments were intended to determine how an increase in strigolactone specifically affected shoot apical meristem development in barley, and if this effect differed between WT and *vrs1*, or if it differed from that observed in wheat. Dissections of the *d14* barley line, showed that the SAMs of the strigolactone insensitive mutant were significantly delayed compared with the WT (Figure 3.33A). I therefore hypothesised that strigolactone would act as an accelerator of SAM development and the GR24 treatment would significantly increase rate of SAM development, as was observed in wheat (Figure 3.37E).

No significant difference in spikelet initiation was observed between control and GR24 treated plants (Figure 3.39B). However, the data does show a significant acceleration in rate of meristem development in *vrs1* plants (Figure 3.39A), the increase in WT was not found to be statistically significant. Overall, these results are less clear than those found for wheat in section 3.15. Strigolactone appears to have broadly similar developmental roles in the two species, but the specific behaviour may differ, resulting in the similar but weaker response in barley compared with wheat.

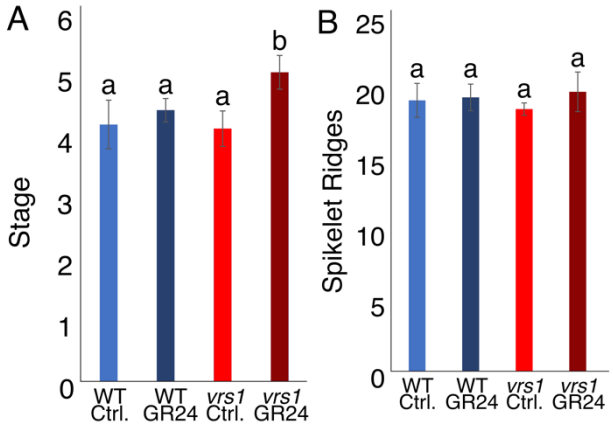

Figure 3.39: The effect of 10nM synthetic strigolactone GR24 treatment on barley tiller emergence and shoot apical meristem development.

(A) Bar chart of mean SAM stage of development **(B)** Bar chart of mean number of spikelet ridges per SAM.

All GR24 treated plants were injected with 0.33ml of 100nM once per week beginning 21 DaP until 35 DaP. Measurements taken at 35 DaP. The WT line is represented in blue, the *vrs1* mutant in red, controls of both lines in the paler shade and GR24 treated plants represented in the darker shade. Different letters above bars indicates statistically significant difference between conditions (two-tailed t-test, $P<0.05$, $n=3$).

3.17 Discussion

3.17.1 Spikelet-tiller feedback exists in wheat and barley

A guiding hypothesis of this chapter was that a previously unreported form of correlative inhibition exists between spikelets and tillers in cereals. Lines of barley and wheat with a high-spikelet/low-tiller phenotype were studied to determine if the increased spikelet number was responsible for the reduction in tillering.

Dissections initially suggested that the SAMs of *vrs1* and WT barley produced the same number of spikelet nodes and developed at the same rate (Figures 3.04A-B). However, when these measurements were studied at the level of individual tillers, rather than as a mean of the entire plant, a significant difference in the distribution of reproductive effort was observed, in which the high spikelet line exhibited a significantly greater reduction in stage of development and spikelet production between successively-initiated meristems (Figures 3.04C-D). This pattern suggests that there may be a proportional correlative inhibition effect from existing spikelets on SAM development, in which spikelets on already-developing reproductive meristems repress activation of new meristems, and a greater number of spikelets thus has a stronger effect. The same effect was seen in *hb* wheat, though the difference from the WT was less extreme than in barley (Figure 3.06). This further

supports the theory, as the difference in spikelet number per ear between *hb* and its wild-type was less than that for *vrs1* relative to its wild-type.

In sections 3.6-3.8 I showed that the ablation of developing meristems resulted in an increase in tillering proportional to the number of spikelets removed (Figure 3.10). In both barley and wheat meristem ablation had a greater effect on tillering in the high spikelet line than the wild-type (Figures 3.10A and 3.12) and the removal of earlier meristems with more spikelets on the same plant had a greater effect than the ablation of smaller, later meristems (Figure 3.12). Furthermore, ablation of fully formed spikelets had no effect on tillering (Figure 3.13). Taken together these data support the hypothesis that actively developing spikelets repress tiller development.

3.17.2 Cytokinin influences spikelet-tiller feedback in wheat and barley

Cytokinin is known to upregulate tiller bud outgrowth and spike development in cereals (J. Sun *et al.*, 2023) and has been proposed as essential for the maintenance of normal spikelet development in barley and wheat (Youssef and Hansson, 2019; Wang, Chen and Wang, 2023). Therefore, one hypothesised mechanism for spikelet-tiller feedback is the competition between spikelets and tillers for a finite quantity of cytokinin.

My investigations into cytokinin showed that exogenous cytokinin treatment (section 2.4.1) results in a significant increase in tillering, in addition to an increased or equivalent number of spikelets (Figures 3.15, 3.16 & 3.22). Such a result is consistent with the earlier ablation experiments, which achieved the same result, by decreasing meristem number. This suggests that cytokinin might be involved in coordinating the observed repression of tillering. Additionally, *hb* wheat was found to be more sensitive to cytokinin treatment than the wild type. It is possible that this is the result of developing spikelets acting as a cytokinin sink, resulting in reduced availability of cytokinin in the *hb* shoot system, leading to reduced tillering. The involvement of cytokinin in tiller and spikelet development (Mrízová *et al.*, 2013; Youssef and Hansson, 2019; Chen *et al.*, 2020) means that if a finite quantity of

endogenous cytokinin must be shared between the two, the increase in spikelet number would result in a decrease in tiller number. This would align with recently reported data in *Arabidopsis* that the suggests that the development of new inflorescences results in a progressive dilution of available cytokinin in the shoot system (Walker *et al.*, 2023). I hypothesise that a similar process could be occurring in cereals. Further supporting this is the recent proposal that an altered sink-source relationship results in feedback between spikelets and grain in miracle wheat (Abbai *et al.*, 2024), a line of wheat in which secondary spikes develop in place of spikelets, resulting in increased spikelet number per ear and reduced tillering (Poursarebani *et al.*, 2015).

An increased production of paired spikelets is one of the clearest developmental observations from the exogenous cytokinin treatment of wheat (Figure 3.28B). This result is especially relevant, as it mimics the phenotype of the *hb* mutant line regarding spikelet production, but also exhibits increased tiller production (Figure 3.25). The creation of a *hb* resembling spikelet phenotype without the compensatory reduction in tillering further supports the hypothesis that cytokinin is involved in regulating spikelet-tiller feedback.

It is likely that multiple hormones are involved in the coordination of spikelet-tiller feedback, however the results presented here do not support the hypothesis that strigolactone is one of them, despite its known ability to regulate tillering and spike development. Another possibility is that the developing spikelets are acting as an auxin source. In a canalization model, branch development is related to each branch's ability to act as an auxin exporting 'source' (Bennett, Hines and Leyser, 2014). More, or stronger sources, weaken the stem's function as an auxin 'sink', making auxin export from future buds more difficult, thus repressing new bud outgrowth (i.e. apical dominance). Perhaps an increased number of developing spikelets on the tiller meristem increases the tillers source strength, resulting in the observed reduction in tiller development (Muller and Leyser, 2011; Bennett, Hines and Leyser, 2014). The increased concentration of auxin in the shoot could also repress tillering via auxin's repression of cytokinin biosynthesis (Tanaka *et al.*, 2006).

3.17.3 Cytokinin promotes paired spikelet formation

Wheat typically produces a single spikelet per rachis node. However, additional ‘supernumerary’ spikelets may also develop at a node. One such example is ‘paired spikelets’, in which a second spikelet develops at the same node, directly below the main spikelet. This phenotype may be a route to increasing wheat yield, as an increased number of spikelets would theoretically allow an increased number of grains to develop.

In the process of investigating spikelet and tiller development, it became clear that shoot cytokinin concentration directly correlated with the frequency of paired spikelet formation.

In section 3.9 I treated several wheat lines with cytokinin. This exogenous increase in cytokinin in the developing shoot system, resulted in a significant increase in paired spikelets per ear against control plants of the same line. This effect was first seen in the elite line Cadenza (Figure 3.16C), which typically does not produce paired spikelets. The exogenous cytokinin treatment resulted in a small amount of paired spikelet formation, resulting in a mean of 0.8 paired spikelets per ear (Figure 3.16C). Extended cytokinin treatments resulted in higher levels of paired spikelet formation to 1.7 per ear (Figure 3.20B), indicating that paired spikelet formation is proportional to the amount of cytokinin within the shoot system or developing meristem.

Very little is currently known about the mechanisms that regulate paired spikelet formation, but what we do know, could be explained by these findings. Recently, a transcription factor called *WPS1* was proposed to repress paired spikelet formation, as the *wps1* mutant was found to produce paired spikelets (Zhang *et al.*, 2022). Further investigation of *WPS1* found that among its downstream targets, were included several Type-B RRAs and a putative LOG gene, which were downregulated by functional WPS1 (Zhang *et al.*, 2022). Type-B RRAs activate transcription in response to perception of cytokinin (Müller B and Sheen J, 2007) and LOGs are essential cytokinin biosynthesis enzymes (Chen *et al.*, 2022), thus their downregulation would result in decreased cytokinin concentration and perception.

The analysis of WPS1 function therefore supports the hypothesis that cytokinin is used by wheat to coordinate paired spikelet development.

Currently, *WPS1* is the only gene identified to regulate paired spikelet formation, that is not a previously identified flowering development gene. *Photoperiod-1 (Ppd-1)* is a pseudo-response regulator gene (PRR). PRRs often act as circadian clock regulators and *Ppd-1* is primarily understood as an integrator of day length into shoot development (Nakamichi *et al.*, 2005; Beales *et al.*, 2007; Shaw, Turner and Laurie, 2012; Shaw *et al.*, 2013). *FLOWERING LOCUS T1 (FT1)* is established as a central coordinator of flowering time in wheat (Nitcher *et al.*, 2013; Lv *et al.*, 2014). It regulates inflorescence development in response to other developmental regulators including *PPD-1* and *Teosinte Branched 1 (TB1)* (Boden *et al.*, 2015). Some alleles of *PPD-1* and *TB1* were shown to have weaker interactions with *FT1,* a result of which was increased paired spikelet development (Boden *et al.*, 2015; Dixon *et al.*, 2018). Cytokinin has already been shown to repress *TB1* (see section 1.3) (Rameau *et al.*, 2015), and this represents a possible mechanism by which the hormone may influence paired spikelet formation. *PPD-1* also acts as an upstream regulator of transcription factors *PDB1* in wheat (Gauley *et al.*, 2024) and *ALOG1* in barley (Jiang *et al.*, 2024), which affect spikelet termination and spikelet branching respectively (Errum *et al.*, 2023; Gauley *et al.*, 2024). *PPD-1* therefore appears to be an important regulator of several aspects of spikelet development in cereals and. I hypothesise that it could achieve these results by interacting with cytokinin or cytokinin signalling genes.

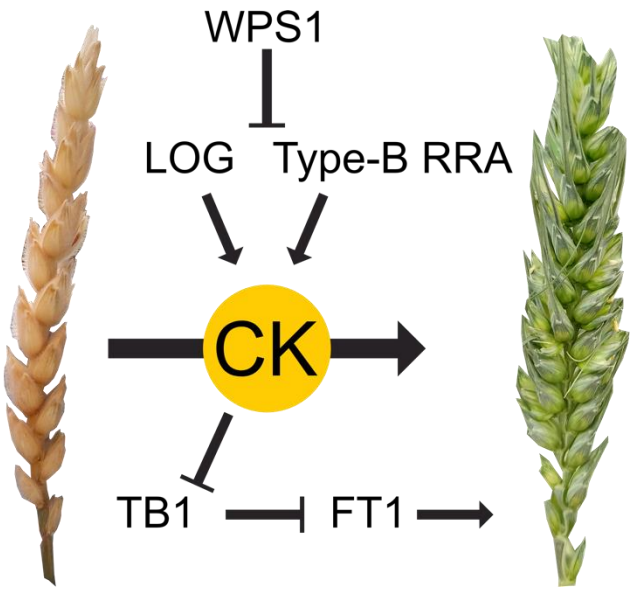

Figure 3.40: Possible mechanisms of cytokinin affecting paired spikelet formation.

The paired spikelets that formed on cytokinin treated plants still only represent a small percentage of the total number of nodes that could produce paired spikelets. Part of the cause of this, is that paired spikelet development does not appear to be evenly distributed between ears. In the naturally paired spikelet forming line *hb*, paired spikelets per ear greatly decreases between successive ears (Figure 3.08). The ear of the main shoot produces paired spikelets at almost a quarter of all nodes, but percentage of nodes with paired spikelets then decreases sharply in the next two ears to emerge and as early as the fourth ear, no paired spikelets are found (Figure 3.08A). This results in more than 60% of all paired spikelets on the plants being found on the main shoot ear (Figure 3.08B). Similarly, most of the new paired spikelets that developed as a result of cytokinin treatment were found on the earliest few ears, whilst the later ears would have none, hence the large standard deviations for mean spikelets per ear for these plants (Figure 3.16C and Figure 3.20B).

Therefore, I hypothesise that increased cytokinin levels specifically in the spikelet meristems during reproductive development, could be the cause of the paired spikelet phenotype in *hb* wheat. The cytokinin treatment system used here introduced exogenous cytokinin weekly into fully emerged tillers. Future work, in

which endogenous cytokinin levels are increased in the SAM more consistently throughout development, might result in still further increases in paired spikelet formation, both by causing a greater increase in shoot cytokinin concentration than the exogenous treatments, and by allowing the increase to occur in all meristems throughout their entire development, rather than the meristems of earlier emerging meristems receiving a longer treatment. Increasing shoot cytokinin levels has already been proposed as a method of increasing cereal yield (Chen *et al.*, 2020; Rathore *et al.*, 2024). Increased spikelet and grain number via increased paired spikelet formation may form an aspect of this approach to yield improvements. However homeostatic pushback against abnormally high endogenous cytokinin concentrations is likely to occur. The function of Type-A RRAs is to compete with functional Type-B RRAs to prevent excessively strong signals. Cytokinin concentration can also be reduced by other hormones, such as auxin and strigolactone which both upregulate cytokinin degrading *CKXs,* a process which is upregulated by increased cytokinin, thus creating a negative feedback loop (Gao *et al.*, 2014; Ogonowska *et al.*, 2019). Therefore, a nuanced understanding of hormonal signalling will be required to achieve spikelet dependent yield increases. However, exogenous cytokinin treatments of *hb* resulted in significant increase in paired spikelet number (Figure 3.23B), encouraging the theory that even in lines or conditions already producing paired spikelets, frequency can be increased further by additional cytokinin.

3.17.4 Cytokinin and strigolactone regulate rate of shoot meristem development

In my investigations into the potential effect of cytokinin and strigolactone on spikelet-tiller feedback multiple experiments were conducted in which stage of development was measured for shoot meristems.

The data from these experiments leads me to hypothesise that cytokinin and strigolactone directly influence the rate of meristem development. An increase of exogenous cytokinin in the meristems resulted in a delay in mean stage of development (Figures 3.19, 3.21 and 3.25). Conversely, increase in exogenous

strigolactone resulted in an acceleration in development (Figure 3.37E) and meristems in strigolactone signalling mutants were found to be significantly earlier in development (Figure 3.28 and 3.33).

Cytokinin has previously been implicated in regulating the rate of inflorescence development. Levels of endogenous cytokinin have been shown to vary in the meristem, depending on the stage of development (Youssef and Hansson, 2019). Exogenous cytokinin treatment of *Arabidopsis* was shown to delay the arrest of inflorescence development (Walker *et al.*, 2023). However, the data in wheat suggests cytokinin treatment causes a delay in earlier stages of reproductive development. It is reasonable to hypothesise that the two species differ somewhat, but the action of cytokinin levels preventing progression in development is widespread amongst plants.

Additionally, cytokinin is implicated in regulating meristem development via the *CLAVATA-WUSCHEL* pathway. This pathway determines meristem growth and determinacy, though there is little wheat-specific knowledge. In *Arabidopsis*, cytokinins have been shown to work antagonistically with *CLV1* and *WUS,* which repress cytokinin signalling by competing with type-A RRAs (Leibfried *et al.*, 2005; Cammarata *et al.*, 2022).

Although strigolactone has been implicated in spike development (Bai *et al.*, 2024), there is currently very little literature to suggest a genetic pathway for how it might interact with meristem developmental rate or determinacy. Therefore, these findings encourage further investigation into both cytokinin and strigolactone in cereal meristem development. Further investigation into endogenous levels and expression of related signalling genes at different stages of development may elucidate a more precise method of utilising these hormones to control meristem development and optimise shoot architecture for yield.

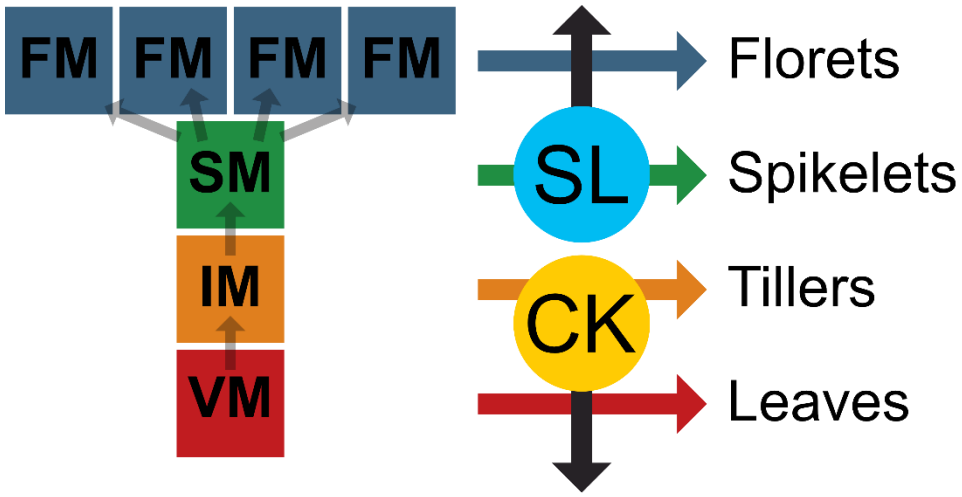

Figure 3.41: Strigolactone acts to accelerate meristem development and cytokinin acts to delay meristem development in wheat and barley, modulating shoot architecture.

3.17.5 Future work and concluding remarks

The work presented in this chapter aimed to investigate the negative feedback between spikelet and tiller development in wheat and barley. In conducting these investigations, data was presented that supports the existence of such a feedback. However, increased spikelet number appears to have other developmental effects in addition to reduced tillering. High spikelet lines are also commonly reported to exhibit reduced spikelet node number and grain weight (Dixon *et al.*, 2018, 2022; Zwirek, Waugh and McKim, 2019). These effects may also result from a correlative inhibition, the strength of which is proportional to the number of spikelets developing on the inflorescence and similar work investigating this possibility would be valuable in assessing the trade-offs of high spikelet lines, and how these can be mitigated in the development of high yielding cereal ideotypes (Wang, Smith and Li, 2018).

Further study of endogenous hormone levels and comparison of these between high and low spikelet lines would further support or disprove the hypothesised feedback. Mass spectrometry could be used to investigate differences in the quantity and forms of hormones between high and low spikelet meristems. RNA-seq could be useful in developing a more detailed understanding of the differences in transcriptome of high and low spikelet meristems. Such data could identify changes in known hormonal

signalling genes and known spikelet development genes as well as identifying genes with large transcriptional variation between lines, suggesting previously uninvestigated genes responsible for the observed phenomenon.

Recently developed fluorescent reporter lines for cytokinin allow for microscopy studies of cytokinin levels and location within the SAM (Liu and Müller, 2017; Kirschner *et al.*, 2018; Zhang *et al.*, 2020). Such lines could be used to study differences within high and low spikelet SAMs and could further be used to image the real-time effect of meristem ablation, to determine if meristem ablation resulted in increased cytokinin availability in other SAMs.

Finally, the effects of cytokinin and strigolactone on rate of SAM development identified here could be highly relevant for our understanding of meristem development, flowering time, and ultimately yield. Therefore, further detail into how these effects are enacted and if they are distinct from previously proposed effects on bud outgrowth could prove valuable. More fine detail dissections of mutant, or hormone treated plants should provide useful information on precisely where and when the rate of development is affected; are all meristems and all stages of development affected equally? Or are different meristems or stages of development more strongly delayed or accelerated by cytokinin and strigolactone? The potential application of these findings to yield means that related cereals, such as rice and maize should also be investigated, to determine if these hormones similarly regulate rate of inflorescence development and how this impacts their yield.

3.18 References

Abbai, R. et al. (2024) ‘Grain yield trade-offs in spike-branching wheat can be mitigated by elite alleles affecting sink capacity and post-anthesis source activity’, Journal of Experimental Botany. 75(1), pp. 88–102.

Aguilar-Martínez, J.A., Poza-Carrión, C. and Cubas, P. (2007) ‘Arabidopsis BRANCHED1 Acts as an Integrator of Branching Signals within Axillary Buds’, The Plant Cell, 19(2), pp. 458–472.

Alaoui, A.C.E., Simmons, S.R. and Crookston, R.K. (1988) ‘Effects of Tiller Removal on Spring Barley’, Crop Science, 28(2), pp. 305–307. .

Bai, J. et al. (2024) ‘Strigolactone and abscisic acid synthesis and signaling pathways are enhanced in the wheat oligo-tillering mutant ot1’, Molecular Breeding : New Strategies in Plant Improvement, 44(2), p. 12.

Bangerth, F. (1989) ‘Dominance among fruits/sinks and the search for a correlative signal’, Physiologia Plantarum, 76(4), pp. 608–614.

Beales, J. et al. (2007) ‘A Pseudo-Response Regulator is misexpressed in the photoperiod insensitive Ppd-D1a mutant of wheat (Triticum aestivum L.)’, Theoretical and Applied Genetics, 115(5), pp. 721–733.

Bennett, T., Hines, G. and Leyser, O. (2014) ‘Canalization: What the flux?’, Trends in Genetics, 30(2), pp. 41–48.

Boden, S.A. et al. (2015) ‘Ppd-1 is a key regulator of inflorescence architecture and paired spikelet development in wheat’, Nature Plants, 1.

Brassac, J. et al. (2021) ‘Linkage mapping identifies a non-synonymous mutation in FLOWERING LOCUS T (FT-B1) increasing spikelet number per spike’, Scientific Reports, 11(1), p. 1585.

Cammarata, J. et al. (2022) ‘Cytokinin–CLAVATA cross-talk is an ancient mechanism regulating shoot meristem homeostasis in land plants’, Proceedings of

the National Academy of Sciences of the United States of America, 119(14), p. e2116860119.

Chen, L. et al. (2020) ‘Cytokinin dehydrogenase: a genetic target for yield improvement in wheat’, Plant Biotechnology Journal, 18(3), pp. 614–630.

Chen, L. et al. (2022) ‘The LONELY GUY gene family: from mosses to wheat, the key to the formation of active cytokinins in plants’, Plant Biotechnology Journal, 20(4), pp. 625–645.

Dixon, L.E. et al. (2018) ‘TEOSINTE BRANCHED1 regulates inflorescence architecture and development in bread wheat (Triticum aestivum)’, Plant Cell, 30(3), pp. 563–581.

Dixon, L.E. et al. (2022) MicroRNA-resistant alleles of HOMEOBOX DOMAIN-2 modify inflorescence branching and increase grain protein content of wheat, Sci. Adv, p. 5907.

Domagalska, M.A. and Leyser, O. (2011) ‘Signal integration in the control of shoot branching’, Nature Reviews Molecular Cell Biology, 12(4), pp. 211–221.

Errum, A. et al. (2023) ‘CRISPR/Cas9 editing of wheat Ppd-1 gene homoeologs alters spike architecture and grain morphometric traits’, Functional & Integrative Genomics, 23(1), p. 66.

Finlayson, S.A. et al. (2010) ‘Phytochrome Regulation of Branching in Arabidopsis’, Plant Physiology, 152(4), pp. 1914–1927.

Gao, S. et al. (2014) ‘CYTOKININ OXIDASE/DEHYDROGENASE4 Integrates Cytokinin and Auxin Signaling to Control Rice Crown Root Formation1[W][OPEN]’, Plant Physiology, 165(3), pp. 1035–1046.

Gauley, A. et al. (2024) ‘Photoperiod-1 regulates the wheat inflorescence transcriptome to influence spikelet architecture and flowering time’, Current Biology, 34(11), pp. 2330-2343.e4.

Gomez-Roldan, V. et al. (2008) ‘Strigolactone inhibition of shoot branching’, Nature, 455(7210), pp. 189–194.

Gu, J. and Marshall, C. (1988) ‘The effect of tiller removal and tiller defoliation on competition between the main shoot and tillers of spring barley’, Annals of Applied Biology, 112(3), pp. 597–608.

Jiang, G. et al. (2024) ‘Non-cell-autonomous signaling associated with barley ALOG1 specifies spikelet meristem determinacy’, Current Biology, 34(11), pp. 2344-2358.e5.

Kamal, R. et al. (2022) ‘Spikelet abortion in six-rowed barley is mainly influenced by final spikelet number, with potential spikelet number acting as a suppressor trait’, Journal of Experimental Botany. Edited by Z. Wilson, 73(7), pp. 2005–2020.

Khuvung, K., Silva Gutierrez, F.A.O. and Reinhardt, D. (2022) ‘How Strigolactone Shapes Shoot Architecture’, Frontiers in Plant Science, 13, p. 889045.

Kirschner, G.K. et al. (2018) ‘Fluorescent reporter lines for auxin and cytokinin signalling in barley (Hordeum vulgare)’, PLoS ONE, 13(4), p. e0196086.

Leibfried, A. et al. (2005) ‘WUSCHEL controls meristem function by direct regulation of cytokinin-inducible response regulators’, Nature, 438(7071), pp. 1172–1175.

Li, G. et al. (2021) ‘MADS1 maintains barley spike morphology at high ambient temperatures’, Nature Plants, 7(8), pp. 1093–1107.

Liu, J. and Müller, B. (2017) ‘Imaging TCSn::GFP, a Synthetic Cytokinin Reporter, in Arabidopsis thaliana’, in J. Kleine-Vehn and M. Sauer (eds) Plant Hormones: Methods and Protocols. New York, NY: Springer, pp. 81–90.

Liu, Z. et al. (2020) ‘The Type-B cytokinin response regulator ARR1 inhibits shoot regeneration in an ARR12-dependent manner in Arabidopsis’, Plant Cell, 32(7), pp. 2271–2291.

Lu, Z. et al. (2015) ‘MONOCULM 3, an ortholog of WUSCHEL in rice, is required for tiller bud formation’, Journal of Genetics and Genomics = Yi Chuan Xue Bao, 42(2), pp. 71–78.

Lv, B. et al. (2014) ‘Characterization of FLOWERING LOCUS T1 (FT1) Gene in Brachypodium and Wheat’, PLoS ONE. Edited by P. Hernandez, 9(4), p. e94171.

Matthes, M.S. et al. (2022) ‘Defects in meristem maintenance, cell division, and cytokinin signaling are early responses in the boron deficient maize mutant tassel-less1’, Physiologia Plantarum, 174(2), p. e13670.

Mrízová, K. et al. (2013) ‘Overexpression of Cytokinin Dehydrogenase Genes in Barley (Hordeum vulgare cv. Golden Promise) Fundamentally Affects Morphology and Fertility’, PLoS ONE, 8(11), p. e79029.

Müller B and Sheen J (2007) ‘Arabidopsis Cytokinin Signaling Pathway’, Science 5847(318) pp.68-69.

Muller, D. and Leyser, O. (2011) ‘Auxin, cytokinin and the control of shoot branching’, Annals of Botany, 107(7), pp. 1203–1212.

Nakamichi, N. et al. (2005) ‘The Arabidopsis Pseudo-response Regulators, PRR5 and PRR7, Coordinately Play Essential Roles for Circadian Clock Function’, Plant and Cell Physiology, 46(4), pp. 609–619.

Nitcher, R. et al. (2013) ‘Increased copy number at the HvFT1 locus is associated with accelerated flowering time in barley’, Molecular Genetics and Genomics, 288(5), pp. 261–275.

Ogonowska, H. et al. (2019) ‘Specificity of expression of TaCKX family genes in developing plants of wheat and their co-operation within and among organs’, PLoS ONE, 14(4), p. e0214239.

Poursarebani, N. et al. (2015) ‘The genetic basis of composite spike form in barley and “miracle-wheat”’, Genetics, 201(1), pp. 155–165.

Rameau, C. et al. (2015) ‘Multiple pathways regulate shoot branching’, Frontiers in Plant Science, 5, p. 741.

Rathore, R.S. et al. (2024) ‘Concurrent improvement of rice grain yield and abiotic stress tolerance by overexpression of cytokinin activating enzyme LONELY GUY (OsLOG)’, Plant Physiology and Biochemistry, 211, p. 108635.

Schmitz, G. and Theres, K. (1999) ‘Genetic control of branching in Arabidopsis and tomato’, Current Opinion in Plant Biology, 2(1), pp. 51–55.

Shaw, L.M. et al. (2013) ‘Mutant Alleles of Photoperiod-1 in Wheat (Triticum aestivum L.) That Confer a Late Flowering Phenotype in Long Days’, PLOS ONE, 8(11), p. e79459.

Shaw, L.M. et al. (2019) ‘FLOWERING LOCUS T2 regulates spike development and fertility in temperate cereals’, Journal of Experimental Botany, 70(1), pp. 193–204.

Shaw, L.M., Turner, A.S. and Laurie, D.A. (2012) ‘The impact of photoperiod insensitive Ppd-1a mutations on the photoperiod pathway across the three genomes of hexaploid wheat (Triticum aestivum)’, The Plant Journal, 71(1), pp. 71–84.

Shoaib, M. et al. (2020) ‘TaCKX gene family, at large, is associated with thousand-grain weight and plant height in common wheat’, Theoretical and Applied Genetics, 133(11), pp. 3151–3163.

Somssich, M. et al. (2016) ‘CLAVATA-WUSCHEL signaling in the shoot meristem’, Development, 143(18), pp. 3238–3248.

Sun, J. et al. (2023) ‘Genome-edited TaTFL1-5 mutation decreases tiller and spikelet numbers in common wheat’, Frontiers in Plant Science, 14, p. 1142779.

Tanaka, M. et al. (2006) ‘Auxin controls local cytokinin biosynthesis in the nodal stem in apical dominance’, Plant Journal, 45(6), pp. 1028–1036.

Umehara, M. et al. (2008) ‘Inhibition of shoot branching by new terpenoid plant hormones’, Nature, 455(7210), pp. 195–200.

Walker, C.H. et al. (2022) ‘Cytokinin signaling regulates two-stage inflorescence arrest in Arabidopsis’, Plant Physiology, 191(1), pp. 479–495.

Walker, C.H. et al. (2023) ‘Cytokinin signaling regulates two-stage inflorescence arrest in Arabidopsis’, Plant Physiology, 191(1), pp. 479–495.

Wang, B., Smith, S.M. and Li, J. (2018) ‘Genetic Regulation of Shoot Architecture’. Available at: https://doi.org/10.1146/annurev-arplant-042817.

Wang, W., Chen, W. and Wang, J. (2023) ‘FRIZZLE PANICLE (FZP) regulates rice spikelets development through modulating cytokinin metabolism’, BMC Plant Biology, 23(1), p. 650.

Yang, Q. et al. (2023) ‘KNOX Genes Were Involved in Regulating Axillary Bud Formation of Chrysanthemum × morifolium’, International Journal of Molecular Sciences, 24(8), p. 7081.

Youssef, H.M. and Hansson, M. (2019) ‘Crosstalk among hormones in barley spike contributes to the yield’, Plant Cell Reports, 38(8), pp. 1013–1016.

Yuan, Y. et al. (2023) ‘Unlocking the Multifaceted Mechanisms of Bud Outgrowth: Advances in Understanding Shoot Branching’, Plants, 12(20), p. 3628.

Zhang, J. et al. (2022) ‘Genetic and transcriptomic dissection of an artificially induced paired spikelets mutant of wheat (Triticum aestivum L.)’, Theoretical and Applied Genetics, 135(7), pp. 2543–2554. .

Zhang, M. et al. (2020) ‘A fluorescence-based high-throughput screening method for cytokinin translocation mutants’, Plant Methods, 16, p. 134.

Zwirek, M., Waugh, R. and McKim, S.M. (2019) ‘Interaction between row-type genes in barley controls meristem determinacy and reveals novel routes to improved grain’, New Phytologist, 221(4), pp. 1950–1965.

Chapter 4

Coordination of reproductive shoot architecture in cereals with nitrate availability

4.1 Chapter Aim

Nitrogen is an essential element in plant development and nitrate is one of the main forms through which plants procure it (Andrews, Raven and Lea, 2013). Therefore, variations in nitrate availability significantly affect plant reproductive effort and increased nitrate requirement is a principal driver of industrial fertiliser production and use. It is well documented that Arabidopsis oordinates perceived nitrate availability by altering cytokinin concentration in the shoot to influence branching (Takei *et al.*, 2004; Müller *et al.*, 2015). Less well understood is the possibility that nitrogen availability may also be communicated to the shoot by strigolactone levels (in addition to its more established role communicating phosphate availability) (de Jong, Ongaro and Ljung, 2014). Recent work in rice has established the potential for both strigolactone to coordinate shoot developmental response to nitrate in rice, suggesting the broadly conserved signalling pathways are likely to deviate between the *Poaceae* and the Arabidopsis model (Xu *et al.*, 2015; H. Sun *et al.*, 2023).

In this chapter, I aim to examine the shoot developmental response of bread wheat (*Triticum* aestivum) to nitrate availability, with particular focus on tiller and SAM development. I then work to identify hormonal candidates which might coordinate nitrate availability with the observed developmental effects on wheat reproductive architecture.

4.2 Optimising a hydroponic system under different nitrate concentrations

To study the way wheat shoot architecture development responds to nitrate availability, I needed to establish a method for treatments of varying nitrate availability. I aimed to establish clear, quantitative nitrate treatments that could be utilised in all future experiments, to allow for a greater level of comparison between experiments. Using a pre-established hydroponic system (detailed in section 2.1.2) as a starting point, the concentration of nitrates was varied, and the development of tillers was measured weekly to determine how shoot development varied between treatments. Treatments 1 to 6 were created containing decreasing concentrations of KNO_3 and $Ca(NO_3)_2$ (molar concentrations can be found in section 2.1.4). The

emergence of tillers over time was tracked in each of the nitrate treatments (Figure 4.01A). 21 days after planting there was no difference in tiller development between any of the treatments. However, by 42 DaP plants in the different treatments produced statistically significant different tiller numbers from each other. For future experimental work, I decided that it would be useful to establish three nitrate treatments; high, medium and low nitrate availability. The low treatment to be used when extreme limitation was needed, while the medium treatment would be used when a more modest reduction in nitrate was desired (e.g. when a significant change in development was needed, without causing extreme stress responses in the plant). The high treatment would act essentially as a control, the results of which could be compared against the changes in development observed under the two nitrate restriction treatments. At 42 DaP, Treatment 1 had produced significantly more tillers than all other treatments and therefore I selected this as high nitrate treatment. At the same time point, Treatments 2, 3 and 4 had produced an equivalent number of tillers and significantly more than Treatments 5 and 6. I therefore selected Treatments 4 and 6 as Mid[N] and Low[N] treatments respectively. Maximum tiller number is compared between the three treatments which will henceforth be referred to as ‘High[N]’, ‘Mid[N]’ and Low[N] respectively (Figure 4.01C). The relative decrease in tillers between High[N] and Mid[N] is almost identical as the decrease from Mid[N] to Low[N] (Figure 4.01D), showing that the plants respond to the same proportional decrease in nitrate availability by approximately halving their 42 DaP tiller number.

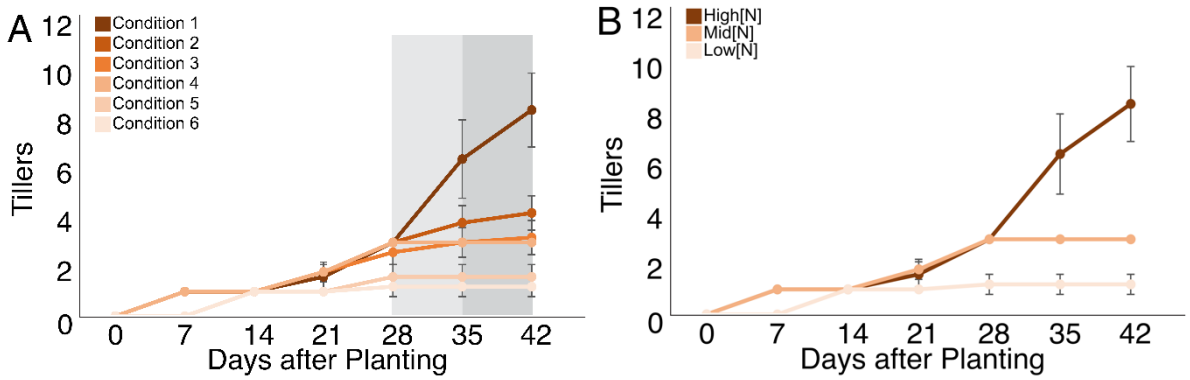

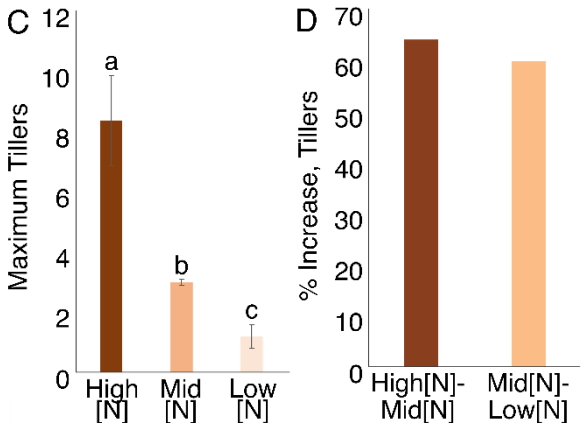

Figure 4.01 The effect of nitrate restriction on tiller development in wheat

(A) Line chart of mean tiller number per plant over time. Light grey square represents time points at which there is significant difference between treatments 1-4 and 5-6; dark grey square represents time points at which there is a significant difference between treatment 1, treatments 2-4 and treatments 5-6. **(B)** Line chart of mean tiller number per plant over time, showing only Treatments 1, Treatment 4 and Treatment 7, which are henceforth renamed as High[N], Mid[N] and Low[N].

Treatments are represented in shades of brown, treatments containing a smaller quantity of nitrate are represented in paler shades. Error bars are 1 standard deviation for the mean. Different letters above a time point indicates statistically significant difference between treatments at that time point, with the lowest letter corresponding to the lowest value and the highest letter corresponding to the highest value (ANOVA, $P<0.05$, $n=5$). **(C)** Bar chart of mean number of tillers per plant (taken at 49 DaP). High[N] is represented in dark brown, Mid[N] is represented in brown, Low[N] is represented in pale brown. **(D)** Bar chart of % increase in maximum tillers per plant between nitrate treatments (taken at 49 DaP). High[N] increase over Mid[N] is represented in dark brown; Mid[N] increase over Low[N] is represented in light brown.

4.3 Studying wheat shoot development under nitrate restriction

In rice, nitrogen fertilisation has been shown to affect transition from vegetative to reproductive development and affect inflorescence structure (Luo, Zhang and Xu, 2020). I therefore hypothesised that nitrate restriction might alter SAM development in wheat, resulting in overall changes to the rate of SAM development as well as the

location and timing of SAM production. To develop an understanding of how nitrate limitation affects SAM development in wheat, YoGI 028 wheat was grown in the High[N] and Low[N] treatments. This line progresses through reproductive development at a particularly high rate, allowing for regular dissections across the entirety of development. From 15 DaP to 35 DaP, these plants were dissected every 5 days, to determine the rate of development of the SAM, the rate of spikelet ridge production and the number of spikelet ridges standardised for the rate of development.

By 25 DaP, the Low[N] plants were significantly further in SAM development compared with the plants with High[N] and this difference was maintained for the rest of the experiment (Figure 4.02A). This suggests that the perception of nitrate restriction in wheat not only reduces the quantity of certain structures such as tillers (Figure 4.01) but also affects the way in which the SAM develops, by causing a significant acceleration in development.

At 25 DaP spikelet ridge number in Low[N] plants stagnated, whilst in the High[N] treatment spikelet ridges per meristem continue to increase for the rest of the experiment (Figure 4.02B). Thus in response to nitrate restriction, wheat plants appear to accelerate SAM development. The result of this shift in development, is that by 35 DaP the High[N] plants have produced more than 5 times as many spikelet ridges as the Low[N] plants (Figure 4.02C). From these data a value of spikelets relative to stage of development was calculated, which shows that the High[N] plants produce more spikelets relative to their earlier stage of development; the SAMs of High[N] plants are not only developing slower but producing more in the same amount of time (Figure 4.02D).

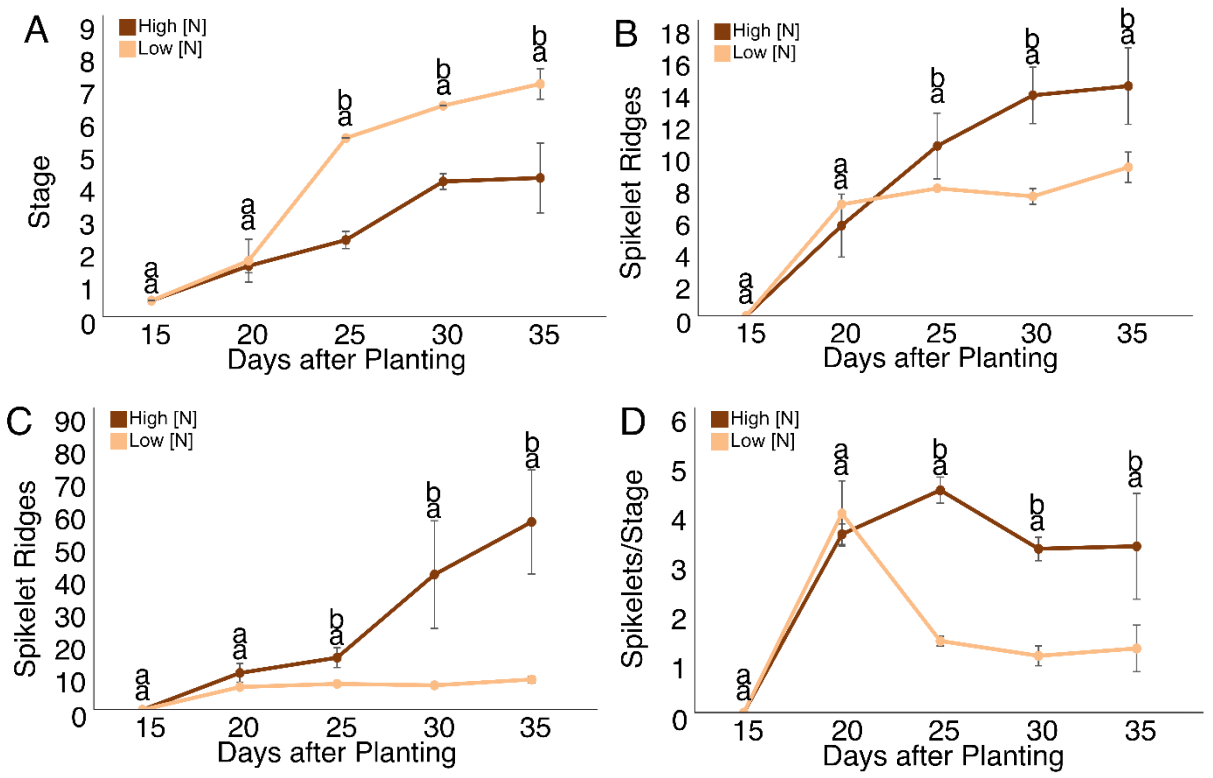

Figure 4.02: The effect of High and Low concentrations of Nitrate on tiller emergence in wheat.

Detailed quantities of constituents for all treatments can be found in chapter 2.1.4. Low[N] has 1% the quantity of nitrate that is in High[N].

(A) Line chart of mean stage of development **(B)** Line chart of mean number of spikelet ridges per SAM **(C)** Line chart of mean number of spikelet ridges per plant **(D)** Line chart of mean number of spikelet ridges per stage (calculated by dividing number of spikelet ridges by stage of development).

Dissections occurred once every 5 days, between 15 and 35 DaP. High[N] is represented in dark brown, Low[N] is represented in light brown. Error bars are 1 standard deviation for the mean. Different letters above a time point indicates statistically significant difference between treatments at that time point, with the lowest letter corresponding to the lowest value and the highest letter corresponding to the highest value (two-tailed t-test, $P<0.05$, $n=3$).

The data presented establishes clear differences in SAM development in response to nitrate availability. However, because the YoGI 028 line being used in the experiments was selected because of the fast rate of SAM development, I wanted to confirm that similar results could be seen in an elite wheat line. I therefore grew the elite wheat line Cadenza under the High[N] and Mid[N] treatments and dissected at 35 DaP to determine if the changes I had observed would remain under a more moderate difference in nitrate availability and in a line of slower SAM development.

The data shows that the Cadenza plants do respond to nitrate limitation in the same way as the YoGI 028 line (Figures 4.03A-C). There is a significant difference in maximum tiller number between the two treatments, while the dissections at 35 DaP showed that the nitrate restricted plants were significantly further ahead in SAM development and had produced significantly fewer spikelet ridges per meristem and per plant then the High[N] plants.

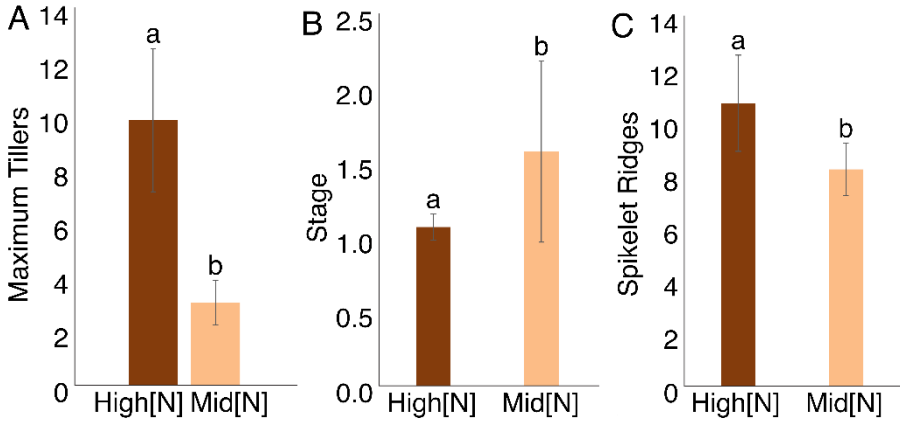

Figure 4.03: The effect of High and Mid concentrations of nitrate on tiller and shoot apical meristem development.

(A) Bar chart of mean number of tillers per plant **(B)** Bar chart of mean stage of development per SAM **(C)** Bar chart of mean number of spikelet ridges per SAM Measurements taken at 35 DaP. High[N] plants are represented in dark brown, Mid[N] plants are in light brown. Error bars are 1 standard deviation from the mean. Different letters above bars indicate statistically significant difference between treatments (two-tailed t-test, $P<0.05$, n=10-13).

In addition to the SAM dissection experiments used to study SAM development, tiller emergence was tracked (using the system established in section 3.3). This was conducted to determine where changes in tiller development occur between the two treatments, and specifically which tillers are not being produced when nitrate availability is reduced.

This data shows that all Mid[N] tillers (an average of 3.1 per plant, but could reach 4 tillers, as shown in Figure 4.03A) are first order tillers, emerging from the main shoot (Figure 4.04A). Whilst the High[N] plants produce many higher order tillers (Figure 4.04A), these are developed later, so that the first-order tillers 0-3 in both lines are produced sequentially as tiller 1-4 (Figure 4.04B). It appears then, that in reducing tiller number in response to nitrate restriction, the wheat plant prioritises the typically more productive main shoot tillers and focuses remaining developmental effort on reaching the end of development, instead of producing more tillers.

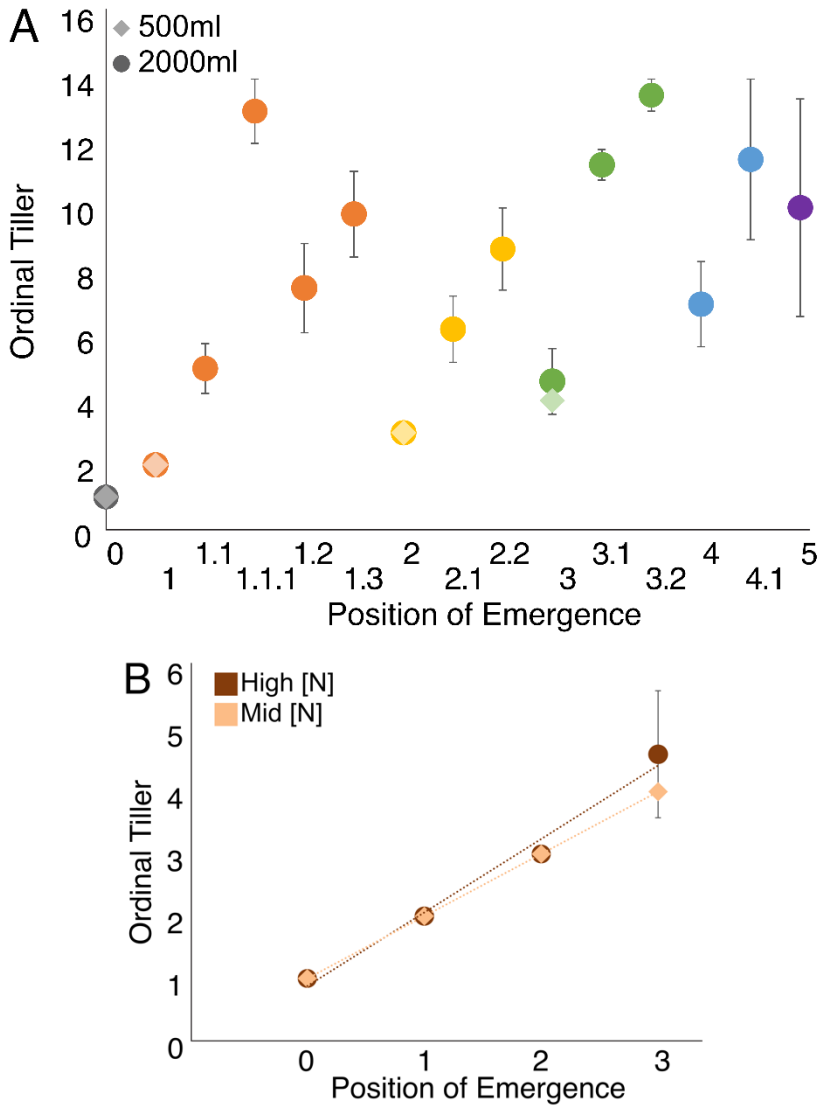

Figure 4.04: The effect of High and Mid concentrations of nitrate on position of tiller emergence.

(A) Scatterplot of mean ordinal position of emergence for each tiller at 35 DaP. High[N] is represented in the darker shade, Mid[N] in the lighter shade. Error bars are 1 standard deviation from the mean. No statistically significant difference was found between the two treatments (two-tailed t-test, $P<0.05$, n=10-13). **(B)** Scatterplot of mean ordinal position of emergence for each tiller at 35 DaP, for first order tillers only. High[N] is represented in the dark brown circles, Mid[N] in the light brown diamonds. Error bars are 1 standard deviation from the mean. No statistically significant difference was found between the two treatments (two-tailed t-test, $P<0.05$, n=10-13).

However, this acceleration of development was only observed in the main shoot meristem. Average stage of development for individual SAMs was measured and categorised by position of emergence (Figure 4.05). There is a far greater difference in development between successively emerging SAMs in the Mid[N] treatment than the High[N] treatment (Figure 4.05A). Not only do the nitrate restricted plants restrict their development to a small number of tillers, but even among the tillers they do produce, a greater extent of their developmental effort is focused on the main shoot meristem.

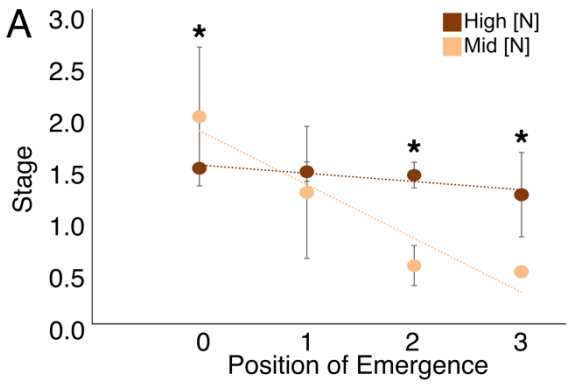

Figure 4.05: The effect of High and Mid concentrations of nitrate on the rate of SAM development in wheat.

(A) Scatterplot of mean stage of development of each tiller by position of tiller emergence.

Measurements taken at 35 DaP. High[N] is represented in the darker shade, Mid[N] in the lighter shade. Error bars are 1 standard deviation from the mean. An asterisk above bars indicates statistically significant difference between treatments for that tiller (two-tailed t-test, $P<0.05$, n=10-13).

Development of spikelet ridges follows a similar pattern to the one described above for developmental rate (Figure 4.06A). Again, the difference in productivity between tillers is greater in the Mid[N] plants. The data shows that the main shoot meristem produces a statistically equivalent number of spikelet ridges to High[N], despite the 10-fold reduction in nitrate. However, the following SAMs produce significantly fewer spikelet ridges in the Mid[N] treatment and the difference between the two

treatments grows larger with each successive SAM. Although plants in the two treatments produce an equivalent number of spikelet ridges on their main shoot SAM, these constitute 20% of the total spikelet production in High[N] plants, but almost 60% in Mid[N] (Figure 4.06B) One can conclude from this that Mid[N] wheat distributes a proportionally greater amount of its developmental effort to the main shoot.

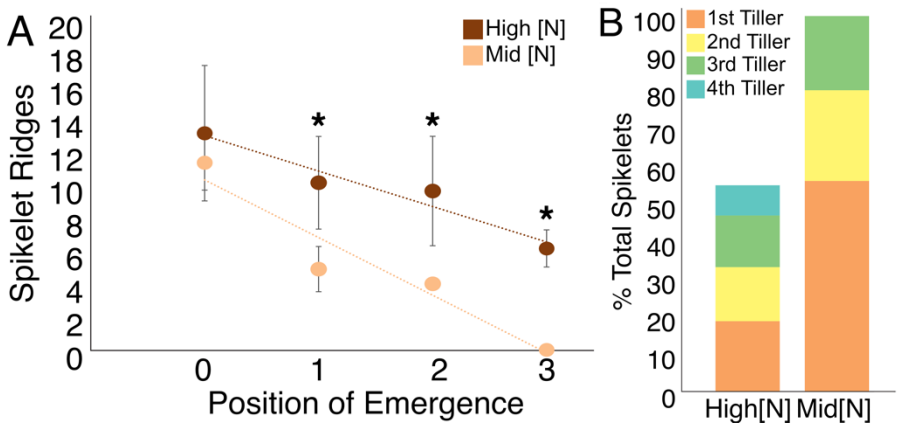

Figure 4.06: The effect of High and Mid concentrations of nitrate on the rate of spikelet development in wheat.

(A) Scatterplot of mean number of spikelet ridges of each tiller by position of tiller emergence.

Measurements taken at 35 DaP. High[N] is represented in the darker shade, Mid[N] in the lighter shade. Error bars are 1 standard deviation from the mean. An asterisk above bars indicates statistically significant difference between treatments for that tiller (two-tailed t-test, $P<0.05$, n=10-13). **(B)** Bar chart of mean % of spikelet ridges that are found on each ordinal tiller at 35 DaP. 1st tiller SAM is represented in orange, 2nd tiller SAM is represented in yellow, 3rd tiller SAM is represented in green, 4th tiller SAM is represented in blue.

4.4 Studying the effect of strigolactone insensitivity on wheat shoot developmental response to nitrate restriction

The results presented in section 4.2-4.3 detail the specific response of wheat shoot development to differences in nitrate availability, showing that nitrate restriction

results in a reduction in tillering, an acceleration of reproductive development, a reduction in rate of spikelet production and a redistribution of reproductive effort to highly prioritise the main shoot meristem. The remaining sections of this chapter will focus on investigating potential phytohormones, whose molecular activity may engender the observed phenotypes.

Strigolactone is well documented in its role in nitrate sensing in the root system and its influence on shoot development (Bennett *et al.*, 2016; Waters *et al.*, 2017). As a secondary function, strigolactone has been proposed to communicate nitrate availability in the root to the developing shoot (de Jong, Ongaro and Ljung, 2014; H. Sun *et al.*, 2023).

I thus hypothesised that strigolactone may coordinate shoot architecture development with perceived nitrate availability in wheat. I predicted that growing strigolactone mutants in nitrate restricted treatments would show aspects of shoot development that were coordinated by strigolactone.

To understand the potential role of strigolactone in wheat shoot developmental response to nitrate availability, wild type and *d3* and *d14* strigolactone perception mutants (whose phenotypes under standard growing treatments are detailed in section 3.13) were grown High[N] and Mid[N] treatments. Additionally, a *tb1* mutant line was also grown to study how the developmental response in the strigolactone mutants would differ from a high tiller line. From planting to 42 DaP tiller number was tracked every week and compared between time points, nitrate treatments and lines.

In the High[N] treatment, the three mutant lines showed a significantly increased tiller number over the wild type at 35 DaP (Figure 4.07A). At 42 DaP, there is still no difference in tiller number between the three mutant lines. However, a different trend is observed under Mid[N] treatments (Figure 4.07B). Here, the first significant difference in tiller number occurs 14 days earlier than in the High[N] treatments. At 21 DaP the *d3* and *d14* mutants have produced significantly more tillers than the wild type and by 28 DaP significantly more than *tb1* (Figure 4.07B). Unlike in the High[N] treatment, by 42 DaP *tb1* produces a statistically equivalent number of tillers to the wild type.

The tiller number at 42 DaP for each line was compared between the two treatments (Figure 4.07C). This data shows that, whilst every line produces significantly fewer tillers in the nitrate restricted treatments, the reduction is smaller in the strigolactone signalling mutants (Figure 4.07D). These results indicate that strigolactone signalling mutants are much less sensitive to nitrate level than wild type and the *tb1* tillering mutant

The wild type and *tb1* lines show a proportionally similar difference in tillering between the two nitrate treatments of 162% and 237%, while the two strigolactone signalling mutants show differences of only 41% and 68% (Figure 4.07D). Finally, the proportional increase in tiller number over wild type in the three mutant lines illustrates that in nitrate restricted treatments *tb1* reduced its tillering increase over the wild type in the Mid[N] treatment, whereas in *d3* and *d14* the proportional difference in tiller number is far greater (Figure 4.07E). Taken together these results provide strong support for the hypothesis that functional strigolactone signalling is used by wheat to coordinate tiller development with perceived nitrate availability.

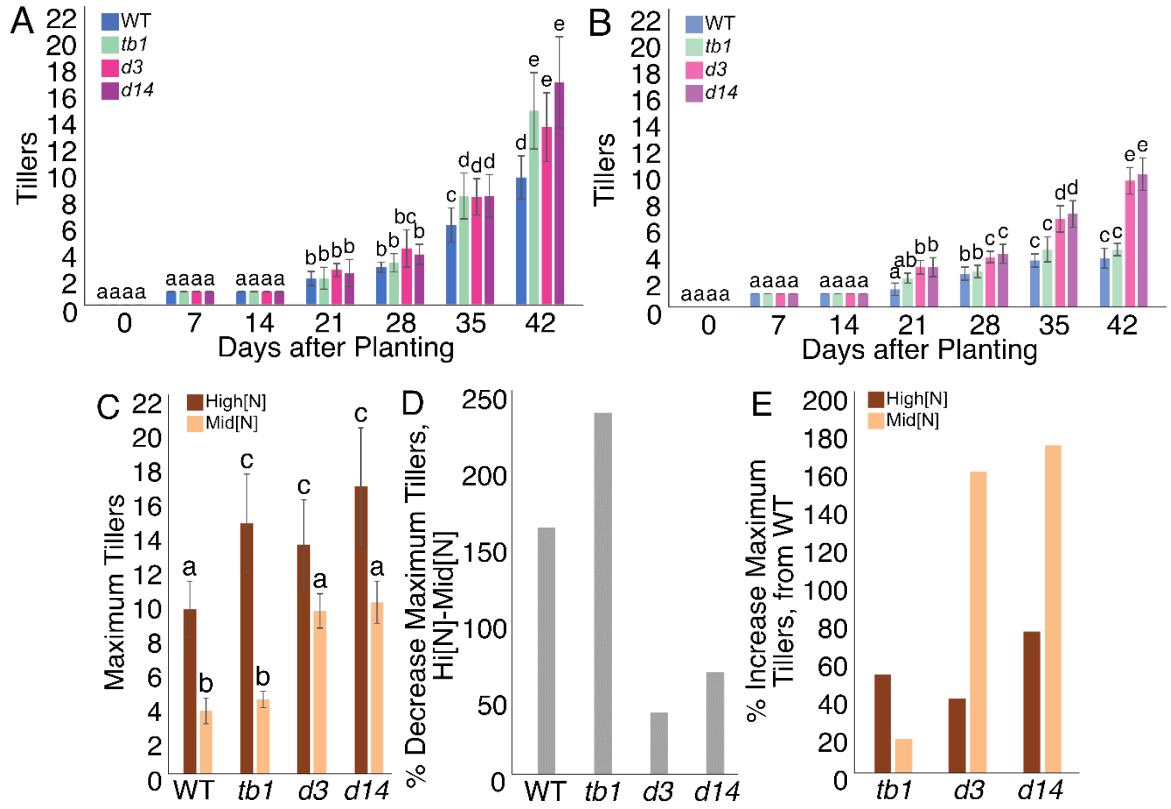

Figure 4.07: The effect of nitrate restriction on tiller development in d3 and d14 wheat mutants.

(A) Bar chart of mean number of tillers per plant, plotted against DaP, in High[N] treatments. **(B)** Bar chart of mean number of tillers per plant, logged against DaP, in Mid[N] treatments. The wild type background is represented in blue, the *tb1* mutant is represented in green, the *d3* mutant is represented in pink and the *d14* mutant is represented in purple. Error bars are 1 standard deviation from the mean. Different letters above bars indicates statistically significant difference between lines (ANOVA, $P<0.05$, n=6-8). **(C)** Bar chart of mean maximum number of tillers per plant. Plants of all lines in the High[N] treatment are represented in dark brown and Mid[N] in light brown. Error bars are 1 standard deviation from the mean. Different letters above bars indicates statistically significant difference between lines (ANOVA, $P<0.05$, n=6-8). **(D)** Bar chart of percentage increase in maximum tillers per plant between the Mid[N] and High[N] treatment. **(E)** Bar chart of percentage increase in maximum tillers per plant between the wild type background and mutant lines. Plants of all lines in the High[N] treatment are represented in dark brown and Mid[N] in light brown.

At 42 DaP plants of all lines in both treatments were harvested and total biomass of the shoot system and the root system was measured. There was no statistically significant difference in shoot biomass between the mutants and the wild type in the High[N] treatment (Figure 4.08A). Similarly, there is also no difference between the mutants and wild type for root biomass at this treatment (Figure 4.08B). There was also no difference in root biomass at the Mid[N] treatment (Figure 4.08B). In fact, the only difference observed is that under the Mid[N] treatment the *d3* mutant (but not the *d14* mutant) exhibits a small but significant increase in shoot biomass over the wild type. The lack of difference seen in shoot biomass indicates that, whilst tillering in these plants can be as much as 160% greater than the wild type (Figure 4.07E), this is a result of a change in the distribution of development of the shoot system. Rather than a total increase in biomass production, the same or similar amount of biomass is distributed in a different pattern.

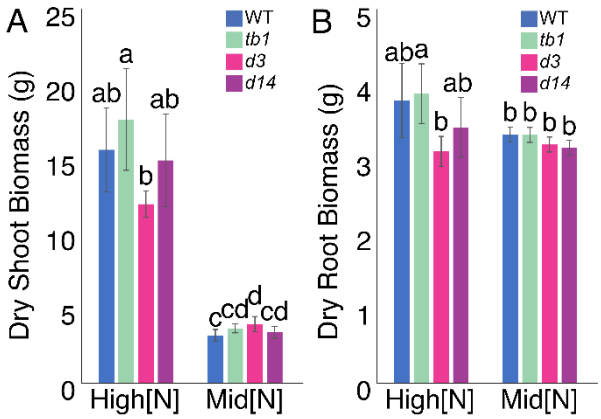

Figure 4.08: The effect of nitrate restriction on biomass development in d3 and d14 wheat mutants.

(A) Bar chart of mean dry shoot biomass (g) per plant. **(B)** Bar chart of mean dry root biomass (g) per plant.

Measurement taken at end of plant life. The wild type background is represented in blue, the *tb1* mutant is represented in green, the *d3* mutant is represented in pink and the *d14* mutant is represented in purple. Error bars are 1 standard deviation from the mean. Different letters above bars indicates statistically significant difference between lines (ANOVA, $P<0.05$, n=6-8).

I performed further experiments, in which the same lines and treatments were used, and in which the developing shoot apical meristems were dissected to determine how SAM developmental response to nitrate availability might also be affected by strigolactone signalling.

Firstly, this data confirms the previous observation that in wild type wheat, nitrate restriction results in a significant acceleration in SAM development (Figure 4.09A). The same relationship is observed in the *tb1* tillering mutant. However, whilst in the High[N] treatment all four lines are at the same point in development at the point of dissection, the *d3* and *d14* mutants respond to nitrate restriction not with an increased rate of SAM development, but with a significant decrease (Figure 4.09A). Data presented in section 3.13-3.15 supported the theory that strigolactone functions as a developmental accelerator in wheat. I therefore hypothesise that

strigolactone signalling is required to coordinate proper rate of SAM development with nitrate availability. The wild type may respond to a reduction in nitrate availability by increased levels of strigolactone in the shoot system, which subsequently reduces tillering and accelerates SAM development. This hypothesis correlates with not only the experimental data presented here but reports in the literature on how wheat responds to phosphate restriction (de Souza Campos *et al.*, 2019).

Wild type plants increase spikelet ridge number in nitrate restricted treatments, while *d3* and *d14* plants significantly reduce it. An increase in spikelet number in response to reduced nutrition may initially appear to be counterintuitive. However, Figure 4.09D suggests that this is simply the result of the wild type Mid[N] SAMs being later in development; when standardised for stage of development, all four lines show a significant decrease in spikelet production. A similar pattern for total number of spikelets per plant was observed (Figure 4.09C); despite the high number of tillers maintained in the strigolactone signalling mutants, the significant reduction in spikelet production is so great that these lines still reduce total spikelet productivity under nitrate restriction more strongly than the wild type. This result indicates the advantage of the wild-type nitrate response. As identified in section 4.3, wheat responds to nitrate restriction by prioritising high level of productivity in a small number of tillers. It appears that this approach ultimately results in a greater number of spikelets per plant (and thus potentially increased grain number) than producing more tillers with reduced spikelet productivity (Figure 4.09C-D).

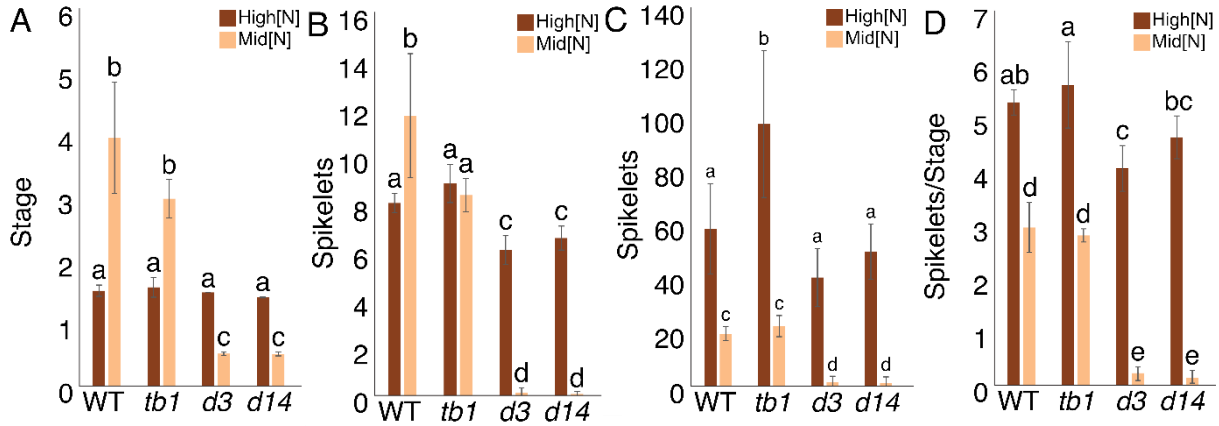

Figure 4.09: The effect of nitrate restriction on SAM development in d3 and d14 wheat mutants.

(A) Bar chart of mean stage of development per SAM. **(B)** Bar chart of mean spikelet ridges per SAM. **(C)** Bar chart of mean spikelet ridges per plant. **(D)** Bar chart of mean spikelet ridges per stage.

Measurements taken at 42 DaP, calculated by dividing mean number of spikelet ridges by mean stage of development. High[N] is represented in dark brown and Mid[N] is represented in light brown. Error bars are 1 standard deviation from the mean. Different letters above bars indicates statistically significant difference between lines and treatments (ANOVA, $P<0.05$, $n=6$-8).

The two strigolactone signalling mutants produce significantly more vegetative meristems in both treatments and all four lines shows a significant reduction in vegetative SAMs in the nitrate restricted treatment (Figure 4.10A). Meanwhile, nitrate restriction results in *d3* and *d14* producing significantly fewer SAMs which have initiated reproductive development than the wild type, whereas there is no difference at the High[N] treatment (Figure 4.10B). Also shown is that in the wild type and *tb1* lines, the ratio between vegetative and initiated SAMs remains equivalent between the two nitrate treatments (Figure 4.10C), despite the changes in tiller number and SAM stage (Figure 4.07C and Figure 4.09A). Strigolactone signalling mutants show a significant increase in the proportion of vegetative SAMs in the High[N] treatment and furthermore, shows a large increase in this ratio as a result of nitrate restriction. This adds to the hypothesis that strigolactone functions as a developmental accelerator in the wheat shoot system and implies an even more specific role, in regulating the initiation of reproductive development.

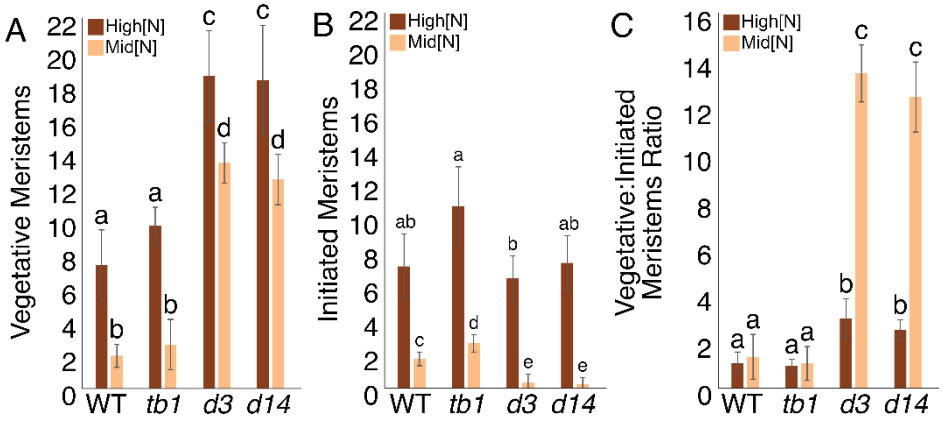

Figure 4.10: The effect of nitrate restriction on initiation of SAM reproductive development in d3 and d14 wheat mutants.

(A) Bar chart of mean number of vegetative meristems. **(B)** Bar chart of mean number of meristems which have initiated reproductive development. **(C)** Bar chart of mean ratio of vegetative meristems to initiated meristems.

Measurements taken at 42 DaP, calculated by dividing number of vegetative meristems per plant by number of initiated meristems. High[N] is represented in dark brown and Mid[N] is represented in light brown. Error bars are 1 standard deviation from the mean. Different letters above bars indicates statistically significant difference between lines and treatments (ANOVA, $P<0.05$, n=6-8).

In addition to calculating mean values of stage of development, spikelet ridges per meristem across all tillers on the plant (Figures 4.09A-B) the emergence of tillers was tracked (following the system described in section 3.3), to allow for changes in the distribution of reproductive effort between tillers to be studied. In section 4.3 I presented data that showed that nitrate restriction affects the difference in development between successive SAMs. As I had now shown that strigolactone relates nitrate availability to shoot development, I hypothesised that a lack of strigolactone might also result in a more consistent development between SAMs.

In the High[N] treatment there is no significant difference at any tiller (Figure 4.11A), which aligns with the finding reported in Figure 4.09A. The data also shows that in the Mid[N] treatment the wild type and *tb1* plants decrease in stage of development

between successive tillers, as expected (Figure 4.11B). However, the *d3* and *d14* plants show no difference between successive tillers, with all SAMs in an early stage of development (Figure 4.09A). This data correlates with the previous finding that wheat responds to nitrate restriction by focusing its development on accelerating the development of a small number of SAMs (Figure 4.02A). The data shows that this response is coordinated by strigolactone signalling and in an absence of strigolactone signalling, wheat fails to focus development into the main SAM. However, simultaneously, all SAMs are in a much earlier stage of development. The same pattern can be seen for spikelet ridge development (Figures 4.11C-D).

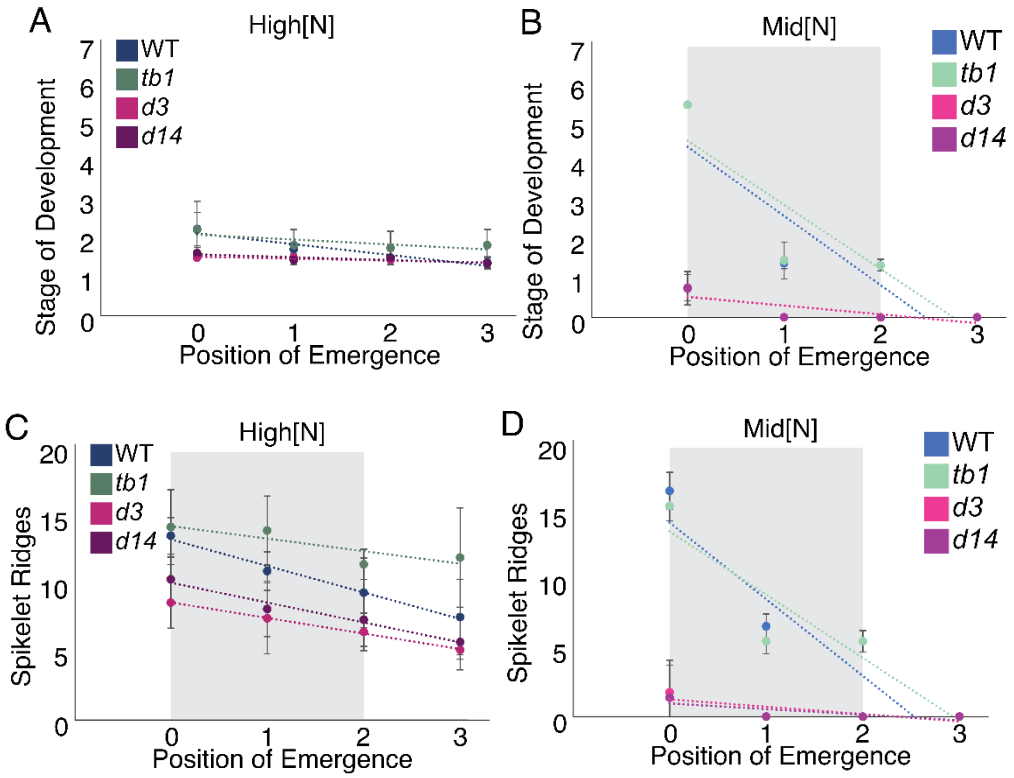

Figure 4.11: The effect of nitrate restriction on SAM development in d3 and d14 wheat mutants, by position of tiller emergence.

(A) Scatterplot of mean stage of development by tiller, High[N] treatment. R^2 Values: WT = 0.73; *tb1* = 0.58; *d3* = 0.83; *d14* = 0.91. There is no significant difference between lines at any tiller (ANOVA, P<0.05, n=6-8). **(B)** Scatterplot of mean stage of

development by tiller, Mid[N] treatment. R^2 Values: WT = 0.79; *tb1* = 0.82; *d3* = 0.6; *d14* = 0.6. Grey square represents significant difference between WT and *d3* and *d14* at that tiller (ANOVA, P<0.05, n=6-8). **(C)** Scatterplot of mean spikelet ridges per SAM by tiller, High[N] treatment. R^2 Values: WT = 0.99; *tb1* = 0.74; *d3* = 0.99; *d14* = 0.97. Grey square represents significant difference between WT and *d3* and *d14* at that tiller (ANOVA, P<0.05, n=6-8). **(D)** Scatterplot of mean spikelet ridges per SAM by tiller, Mid[N] treatment. R^2 Values: WT = 0.86; *tb1* = 0.86; *d3* = 0.6; *d14* = 0.6. Grey square represents significant difference between WT and *d3* and *d14* at that tiller (ANOVA, P<0.05, n=6-8).

Measurements taken at 42 DaP. The wild type background is represented in blue, the *tb1* mutant is represented in green, the *d3* mutant is represented in pink and the *d14* mutant is represented in purple. Error bars are 1 standard deviation from the mean.

4.5 Measuring the effect of nitrate restriction on the relative expression of strigolactone signalling genes in wheat

The experiments presented in this section indicate a requirement for functional strigolactone signalling to coordinate nitrate availability with shoot development in wheat. To further test this theory, I examined changes in expression of canonical strigolactone signalling genes in High[N] and Low[N] nitrate treatments. If nitrate availability does enact shoot developmental changes through strigolactone, it can do this either by increasing strigolactone concentration (by upregulating biosynthesis or transporter genes) or strigolactone sensitivity (by upregulating strigolactone perception genes). For instance, nitrogen fertilisation in rice was recently shown to enact tillering increase through expression of *Os1900*, a *MAX1* strigolactone synthesis gene and in wheat (Cui *et al.*, 2023). I therefore hypothesised that wheat would respond to nitrate restriction with altered expression of strigolactone signalling genes. The elite wheat line Cadenza was grown in both treatments and at 42 DaP, reproductive SAMs were excised from the main shoot of the plants. RNA was extracted from the collected SAMs, transcribed into cDNA and relative levels quantified via quantitative PCR (qPCR). qPCR was performed on the strigolactone perception genes *D3* and *D14* and tillering regulator TB1, which is

known to be positively regulated in the presence of strigolactone (Yuan *et al.*, 2023; Bai *et al.*, 2024). Wheat efp browser was used to identify transcripts of these genes that were specifically highly expressed in the reproductive SAM (*Wheat eFP Browser*).

The data shows that relative expression of *D3*, *D14* and *TB1* in the wheat SAM are all significantly higher under nitrate restricted treatments (Figure 4.12). The result in *TB1* is expected and aligns with our understanding of TB1 as a repressor of tiller bud outgrowth (Dixon *et al.*, 2018).

The increased expression of the *D3* and *D14* genes suggests an increased sensitivity to strigolactone in the SAM under Low[N] treatments. Perhaps the observed reduction in tillering and accelerated SAM associated with the Low[N] treatment results from increased levels of strigolactone sensing D3 and D14, and thus a shoot system with increased sensitivity to the effects of strigolactone. These findings further support the hypothesis that strigolactone is used in wheat to coordinate shoot developmental response with nitrate availability. Under nitrate restricted treatments wheat may increase strigolactone perception in the shoot system, to bring about an appropriate developmental response, which includes a reduction in tiller number (Dixon *et al.*, 2018) and an acceleration in SAM development (section 3.13-3.16), which ultimately increases plant fitness.

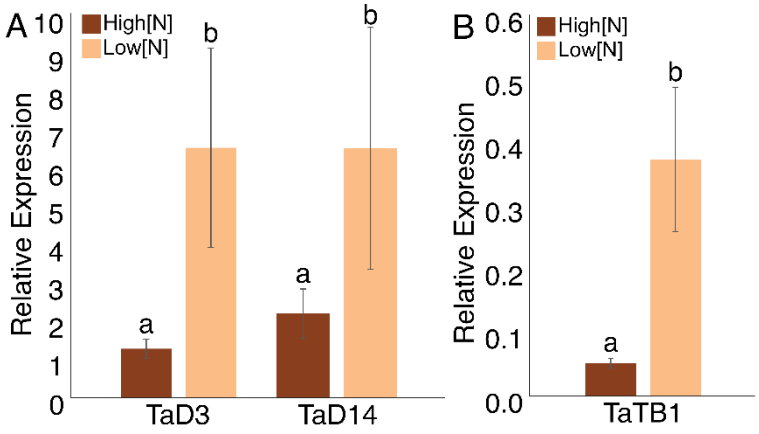

Figure 4.12: Relative expression of canonical strigolactone signalling genes in the shoot apical meristem of elite wheat Cadenza, under nitrate restricted treatments

(A) Bar chart showing the relative gene expression of TaD3 and TaD14. **(B)** Bar chart showing the relative gene expression of TaTB1.

Samples were collected from the shoot apical meristem of the main shoot of Cadenza, 42 DaP. Plants grown under High[N] treatments are shown in dark brown, plants grown under Low[N] treatments are shown in light brown. Error bars represent 1 standard deviation. Letters above bars represent statistical significance between treatments for that gene (n=3). Relative expression was normalised against a control actin housekeeping gene TraesCS5A02G015600 (Borrill et. al., 2016).

4.6 The effect of exogenous strigolactone treatment on nitrate restricted wheat

The results presented and discussed in section 4.4 appear to support the hypothesis that the phytohormone strigolactone coordinates wheat shoot developmental response to nitrate availability. To further test this hypothesis, I conducted experiments in which exogenous strigolactone was introduced to the wheat shoot system, to study the effects of increased levels of strigolactone, in contrast to the effects of decreased strigolactone perception in the *d3* and *d14* mutant lines used in the previous section. These experiments utilise the system of exogenous strigolactone treatment developed in section 3.6.3, which entails a weekly injection of 0.33ml of 100nM of the synthetic strigolactone GR24 into each emerged tiller, resulting in a significantly reduced tiller number compared to control plants injected with an equivalent dilution of acetone in water.

Wheat growing in High[N] and Mid[N] treatments was treated with GR24, to determine if an increase in strigolactone in the shoot system would elicit different responses in nitrate restricted treatments, compared with nitrate abundant treatments. At 35 DaP, following two weeks of GR24 treatment, tiller number was recorded for all treatments. In both nitrate treatments, the GR24 treatment results in a significantly reduced number of tillers (Figure 4.13A). However, the reduction in

tillering is much smaller in the Mid[N] treatment than in the High[N] treatment (Figure 4.13B). This is likely the result of the control Mid[N] treatment plants already producing a small number of tillers. If this response to nitrate restriction was being coordinated by an increase in shoot strigolactone levels, then the additional strigolactone introduced by the GR24 treatment would have a proportionally reduced effect, as is observed here. However, it is also possible that the already reduced tiller number of Mid[N] plants means there is less room for tillering to reduce further.

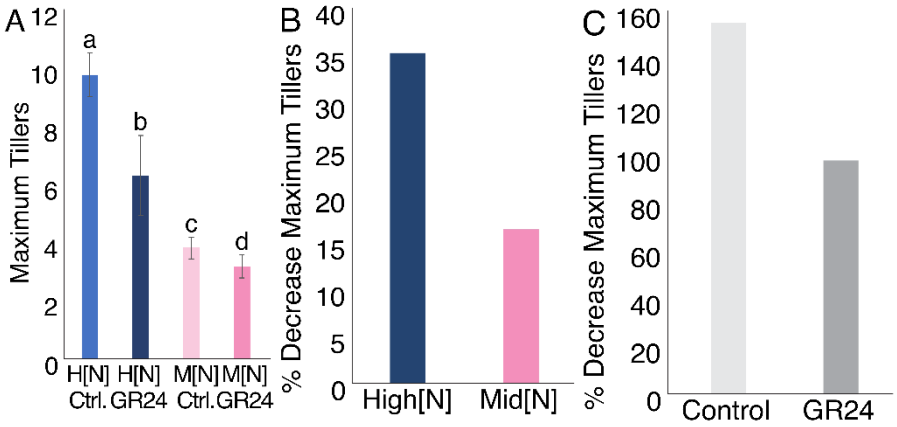

Figure 4.13: The effect of strigolactone treatment on wheat tiller development under nitrate restricted treatments.

All GR24 treated plants were injected with 0.33ml of 100nM once per week beginning 21 DaP until 35 DaP.

(A) Bar chart of mean number of tillers per plant, taken at 35 DaP. High[N] plants are represented in blue, Mid[N] plants are represented in pink, GR24 treated plants in each treatment are represented in a darker shade and the control plants in a lighter shade. Error bars are 1 standard deviation from the mean. Different letters above bars indicates statistically significant difference between treatments (ANOVA, $P<0.05$, n=5-6). **(B)** Bar chart of % decrease in maximum tiller number caused by the GR24 treatment on plants growing in High[N] and Mid[N] treatments. High[N] is represented in dark blue, Mid[N] is represented in pink. **(C)** Bar chart of % decrease in maximum tiller number caused by nitrate restriction of the Mid[N] treatment compared to the High[N] treatment in control and GR24 treated plants. Control plants are represented in light grey, GR24 treated plants are represented in dark grey.

Dissections were conducted on each tiller, to determine rate of SAM development and production of spikelet ridges and compare how these parameters were affected by the GR24 treatment in High[N] and Mid[N] treatments. Tiller emergence tracking also allowed these measurements to be compared between tillers.

No significant difference in stage of development is seen between any of the treatments (Figure 4.14A). This result does not align with the other data I have reported, wherein rate of SAM development is significantly increased both by nitrate restriction (Figure 4.02) and GR24 treatment (Figure 3.48, Chapter 3.6). It is possible that the lack of difference results from the plants having reached the end of reproductive development, and that the strigolactone only affects time taken to complete reproductive development but does not affect further SAM and ear development in the same way. I have earlier hypothesised that strigolactone functions as an accelerator of SAM development (Section 3.13-3.15). This may explain why the differences in nitrate availability and GR24 treatment have affected other aspects of shoot architecture development in these experiments, but not stage of SAM development.

The data does show a significant reduction in spikelet ridges per meristem (as previously reported in Figure 4.02), but that the GR24 treatment has no effect on either nitrate treatment (Figure 4.14B). These measurements would essentially equate to final spikelet number, given all four treatments have reached terminal spikelet. This data therefore suggests that strigolactone has relatively little direct impact on spikelet development, however the lack of significant difference in stage of development means a further repeat of these experiments would be needed for me to be confident of such a conclusion.

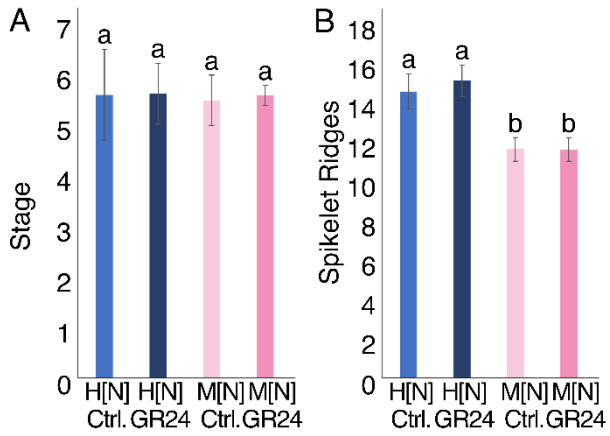

Figure 4.14: The effect of strigolactone treatment on wheat SAM development under nitrate restricted treatments.

All GR24 treated plants were injected with 0.33ml of 100nM once per week beginning 21 DaP until 35 DaP.

(A) Bar chart of mean stage of development per SAM **(B)** Bar chart of mean number of spikelet ridges per SAM.

Measurements taken at 35 DaP. High[N] plants are represented in blue, Mid[N] plants are represented in pink, GR24 treated plants in each treatment are represented in a darker shade and the control plants in a lighter shade. Error bars are 1 standard deviation from the mean. Different letters above bars indicates statistically significant difference between treatments (ANOVA, $P<0.05$, $n=5$-6).

Despite a lack of difference in the overall means between treatments, I attempted to discern if there were differences between tillers that could point to an expected developmental response to differences in nitrate and GR24 treatments. Mean rate of SAM development and spikelet ridge number were therefore calculated for tiller positions and compared.

The data shows little variation in ordinal position of first order tillers (Figure 4.15). The treatments produce tillers in exactly the same positions for the first 4 tillers. The only significant difference is at tiller 5, where the GR24 treatment results in the tiller emerging significantly earlier than in the control, suggesting a prioritisation of first order tillers, brought about by increased strigolactone.

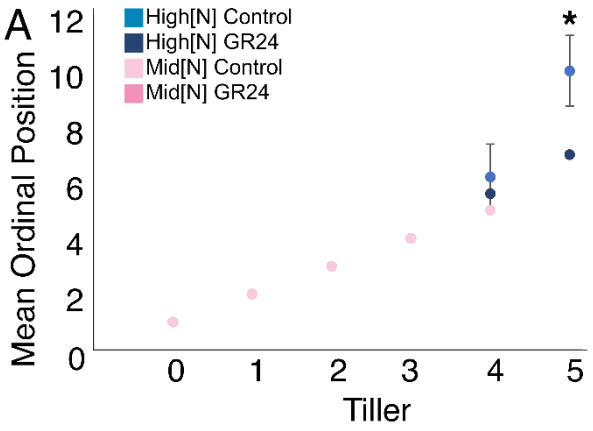

Figure 4.15: The effect of strigolactone treatment on wheat tiller emergence under nitrate restricted treatments.

All GR24 treated plants were injected with 0.33ml of 100nM once per week beginning 21 DaP until 35 DaP.

(A) Scatterplot of mean ordinal position of emergence, at each first order position of tiller emergence, taken at 35 DaP. High[N] plants are represented in blue, Mid[N] plants are represented in pink, GR24 treated plants in each treatment are represented in a darker shade and the control plants in a lighter shade. Error bars are 1 standard deviation from the mean. An asterisk above a point indicates statistically significant difference between treatments for that tiller (ANOVA, $P<0.05$, $n=5$-6).

Figure 4.16 reports data that aligns with that of Figure 4.14. there is no difference in stage of development at any tiller between all four treatments (Figure 4.16A), and there is a significant difference in spikelet ridge number between nitrate treatments but not GR24 treatments at all SAMs but the main shoot (Figure 4.16B).

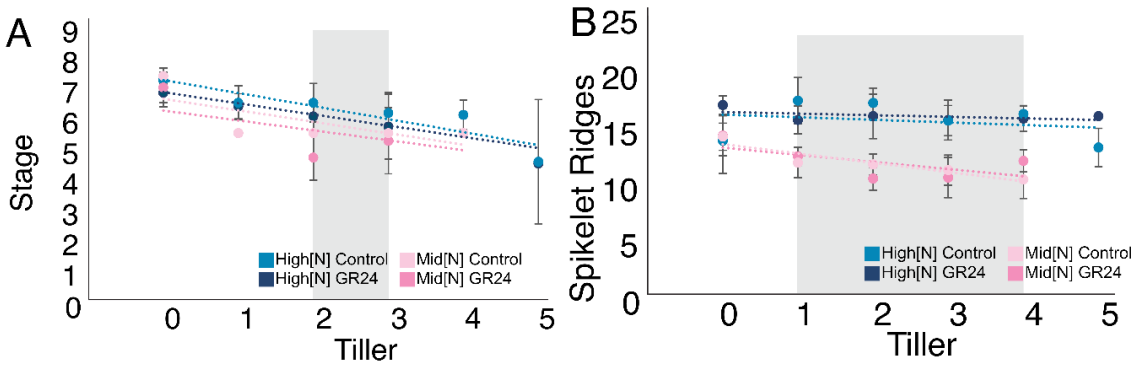

Figure 4.16: The effect of strigolactone treatment on wheat SAM development under nitrate restricted treatments, ordered by position of tiller emergence.

All GR24 treated plants were injected with 0.33ml of 100nM once per week beginning 21 DaP until 35 DaP.

(A) Scatterplot of mean stage of development per SAM, at each first order tiller. Grey square represents tillers where there is significant difference between High[N] Control and Mid[N] GR24. **(B)** Scatterplot of mean number of spikelet ridges per SAM, at each first order tiller. Grey square represents tillers where there is significant difference between both High[N] treatments and Mid[N] treatments. Measurements taken at 35 DaP. High[N] plants are represented in blue, Mid[N] plants are represented in pink, GR24 treated plants in each treatment are represented in a darker shade and the control plants in a lighter shade. Error bars are 1 standard deviation from the mean. Different letters above bars indicates statistically significant difference between treatments (ANOVA, $P<0.05$, n=5-6).

4.7 The effect of exogenous cytokinin treatment on nitrate restricted wheat

Sections 4.5 and 4.6 support the hypothesis that strigolactone is involved in coordinating wheat shoot developmental response to nitrate availability. However, plant developmental responses are often coordinated by multiple phytohormones. Furthermore, cytokinin is a known coordinator of shoot developmental response to nitrate availability in other species (Xu *et al.*, 2015; J. Wang *et al.*, 2018). Therefore, I investigated the additional hypothesis that cytokinin may also be involved in coordinating wheat shoot development, with perceived nitrate availability. Experiments utilised the hormone treatment protocol introduced in chapter 3.5, wherein the concentration of cytokinin is increased in the shoot system by injecting each emerged tiller with 0.33ml of 100µM of the synthetic cytokinin 6-BA once per week, slightly above the developing SAM, resulting in significant changes to wheat shoot architecture, in a manner that aligns with our current understanding of how cytokinin affects shoot development – such as an increase in tillering. Following this protocol, plants in both High[N] and Mid[N] treatments were treated with 6-BA. Tiller development was tracked up to 42 DaP, then compared between treatments.

The expected increase in tiller number is seen in both High[N] and Mid[N] treatments (Figure 4.17A). The data shows that this increase is proportionally similar between High[N] and Mid[N] plants (Figure 4.17B), and that the 6-BA treatment has no effect on the proportional increase in tillering between Mid[N] and High[N] treatments. If reduced cytokinin levels were responsible for reducing tillering in response to restricted nitrate levels in the control plants, I would expect to see a proportionally greater effect of the exogenous treatment on the Mid[N] plants, as the reduced endogenous cytokinin in their shoot system would mean the exogenous treatment was increasing cytokinin in the shoot by a proportionally greater amount.

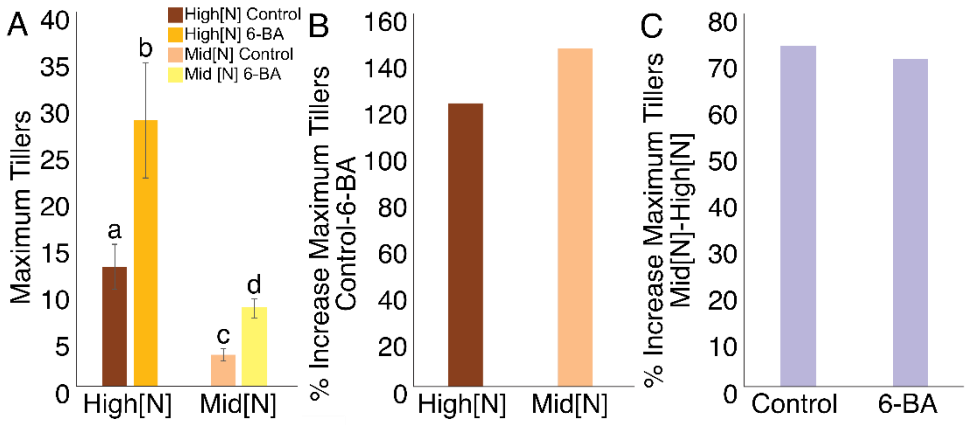

Figure 4.17: The effect of cytokinin treatment on wheat tiller development under nitrate restricted treatments.

Plants were treated with 0.33ml of 100µM 6-BA once per week from 21 DaP until 42 DaP.

(A) Bar chart of mean tiller number per plant, taken at 42 DaP. Control High[N] is represented in dark brown and Mid[N] in light brown; 6-BA treated High[N] is represented in orange, and Mid[N] in yellow. Error bars are 1 standard deviation from the mean. Different letters above bars indicates statistically significant difference between treatments (ANOVA, $P<0.05$, n=7-11). **(B)** Bar chart of percentage increase in mean number of tillers per plant, between the control and 6-BA treated plants, at 42 DaP. The High[N] plants are represented in dark brown; the Mid[N] are represented in light brown. **(C)** Bar chart of percentage increase in number of tillers per plant, between the Mid[N] and High[N] treatment, at 42 DaP.

To further investigate the way in which 6-BA treatment may influence shoot developmental response to nitrate availability, dissection experiments were conducted, to discern stage of SAM development and spikelet ridge number. The data shows a large reduction in stage of development (Figure 4.18A), resulting from the 6-BA treatment. This data continues to support the hypothesis introduced in section 3.9 that cytokinin delays SAM development in wheat. There is also a significant difference between the High[N] and Mid[N] 6-BA treated plants, suggesting that the Mid[N] treatment may have reduced endogenous quantity of cytokinin, and therefore SAM development is not delayed by as much by the same 6-BA treatment. No difference, however, is reported in the control treatments. This likely results from the difference expected between different nitrate treatments is no longer observed, because plants of both treatments have reached the end of reproductive development, and cytokinin may only affect rate of reproductive development, but affect later SAM and ear development in a different way. Future work would thus benefit from dissections at an earlier time point.

Additionally, the data shows a significant reduction in number of spikelet ridges in both treatments (Figure 4.18B), though the reduction is proportionally greater in the High[N] treatment (Figure 4.18D). However, one would expect the opposite to be the case if cytokinin was coordinating developmental response to nitrate. If wheat responded to the Mid[N] treatment by restricting shoot cytokinin levels, the exogenous treatment should be proportionally smaller in the High[N] shoot system and enact a proportionally smaller effect. This data therefore does not support the hypothesis that cytokinin coordinates shoot developmental response to nitrate availability in wheat.

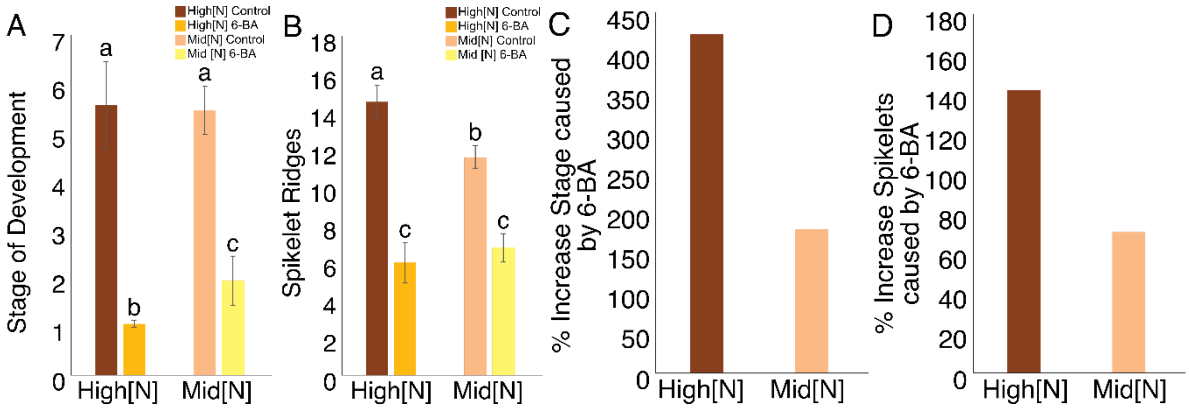

Figure 4.18: The effect of cytokinin treatment on wheat SAM development under nitrate restricted treatments.

Plants were treated with 0.33ml of 100µM 6-BA once per week from 21 DaP until 42 DaP.

(A) Bar chart of mean SAM stage of development. **(B)** Bar chart of mean number of spikelet ridges per SAM. Measurements taken at 42 DaP. Control High[N] is represented in dark brown and Mid[N] in light brown; 6-BA treated High[N] is represented in orange, and Mid[N] in yellow. Error bars are 1 standard deviation from the mean. Different letters above bars indicates statistically significant difference between treatments (ANOVA, $P<0.05$, n=7-11). **(C)** Bar chart of % increase in SAM stage of development caused by 6-BA treatment in High[N] and Mid[N] plants. **(D)** Bar chart of % increase in spikelet ridges caused by 6-BA treatment in High[N] and Mid[N] plants.

To better understand the differences observed in Figure 4.18, data for stage and spikelet ridges were compared between tillers, to discern if cytokinin affected how development was distributed among the shoot system. This data indicates that the control plants follow a similar trajectory between successive SAMs in the two nitrate treatments, as expected, given their lack of difference in overall mean stage of development (Figure 4.19A). Conversely 6-BA treated plants have a significant difference in the distribution of rate of development between successive SAMs between the two nitrate treatments . Whilst the High[N] 6-BA plants show very little difference from tiller to tiller (all being in a very young stage of development), the

Mid[N] plants show quite a strong decrease between SAMs. Whilst the development stage of tiller 3 is very similar between the two treatments, the SAM of the main shoot is in a significantly later stage in development in the Mid[N] treatment than the High[N] treatment. This suggests that CK generally delays the development of SAMs (as previously observed), but that in low nitrate treatments, the developmentally accelerated, first emerging SAMs – are 'immune' to this effect of cytokinin. If, as suggested above, strigolactone causes this developmental acceleration under nitrate restricted treatments, then this may suggest that strigolactone blocks the effect of CK on SAM development.

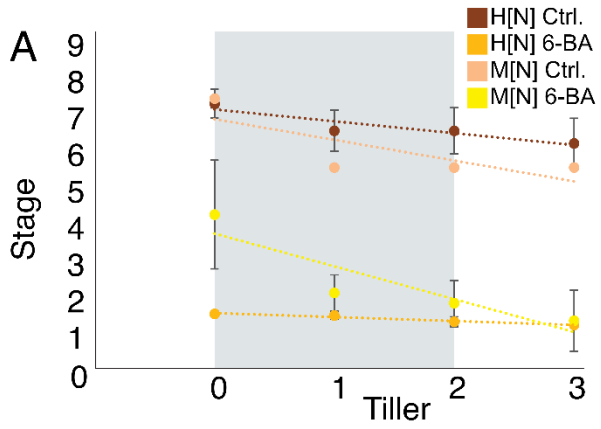

Figure 4.19: The effect of cytokinin treatment on wheat SAM development under nitrate restricted treatments, ordered by position of tiller emergence.

All GR24 treated plants were injected with 0.33ml of 100nM once per week beginning 21 DaP until 35 DaP.

(A) Scatterplot of mean stage of development per SAM, at each first order tiller. R^2 Values: High[N] Control = 0.84; High[N] 6-BA = 0.95; Mid[N] Control = 0.6; Mid[N] 6-BA = 0.82. At all tillers there is significant difference between High[N] and Mid[N] treatments. Grey square represents tillers at which there is significant difference between Mid[N] Control and Mid[N] 6-BA. Measurements taken at 35 DaP. Control High[N] is represented in dark brown and Mid[N] in light brown; 6-BA treated High[N] is represented in orange, and Mid[N] in yellow. Error bars are 1 standard deviation from the mean. Different letters above bars indicates statistically significant difference between treatments (ANOVA, $P<0.05$, n=7-11).

4.8 Measuring the effect of nitrate restriction on the relative expression of cytokinin signalling genes in wheat

The data presented in section 4.7 appears to disprove the hypothesis that cytokinin is involved in coordinating wheat shoot developmental response to nitrate restriction. To further confirm this, shoot apical meristems were harvested from the main shoot at 42 DaP, and RNA transcripts of cytokinin signalling genes were quantified via qPCR. These qPCR experiments were intended to determine whether transcription of canonical cytokinin signalling genes significantly changed under nitrate restriction. Wheat efp browser was used to identify transcripts of CKX (degradation) and RRA (signal perception) genes that were specifically highly expressed in the reproductive SAM (*Wheat eFP Browser*).

There is no significant difference in the expression of CKX3 or RRA1 (Figure 4.20). These results appear to suggest that the cytokinin signalling pathway undergoes little change in reaction to nitrate restriction in the SAM. However, the high level of variation in expression levels, especially for RRA1 allow for the possibility that the highly changeable transcriptome of the SAM may be hiding subtle changes in response to nitrate restriction.

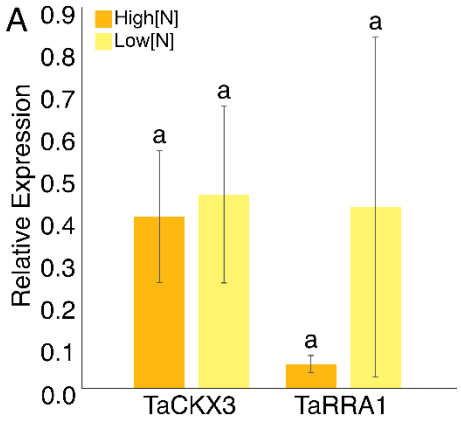

Figure 4.20: Relative expression of canonical cytokinin signalling genes in the shoot apical meristem of elite wheat Cadenza, under nitrate restricted treatments

(A) Bar chart showing the relative gene expression of TaCKX3 and TaRRA in the shoot apical meristem of elite wheat line Cadenza. Samples were collected from the shoot apical meristem of the main shoot, 42 DaP. Plants grown under High[N] treatments are shown in orange, plants grown under Low[N] treatments are shown in yellow. Error bars represent 1 standard deviation. Letters above bars represent statistical significance between treatments for that gene (n=3). Relative expression was determined from actin housekeeping gene TraesCS5A02G015600 (Borrill et. al., 2016).

4.9 Discussion

4.9.1 Nitrate affects wheat shoot development

The aim of this chapter was to study the shoot developmental response of wheat to nitrate availability, and subsequently investigate the involvement of strigolactone and cytokinin in the coordination of the observed effects.

There have been extensive studies on how nitrate sensing, assimilation and transport are conducted in wheat (Bajgain, Russell and Mohammadi, 2018; Wang *et al.*, 2020; Shi *et al.*, 2022). Some of the effect of nitrate availability on wheat shoot architecture is also well established, primarily a dosage dependent effect on tillering (Bauer and von Wirén, 2020) and final grain number (Oscarson, 2000). However, reporting on the effect on shoot apical meristem development remains sparse and inconclusive (Longnecker, Kirby and Robson, 1993). Furthermore, the effect on spikelet development is also underreported, though evidence for the communication of assimilated nitrogen to spikelets, suggests they are likely to be affected (Oscarson, 1996). This chapter aimed to address this deficit in understanding, by studying SAM and spikelet development, and more precisely mapping where and when changes in tillering occur.

Nitrate limitation resulted in a significant acceleration of the rate of reproductive development in the SAM (Figure 4.02A) and a significant reduction in spikelet development (Figures 4.02B-D), resulting from an increase in the difference in stage

and spikelet number between successive SAMs (Figures 4.05 and 4.06). The consequence of this was that a far greater proportion of the spikelets produced by the entire plant were produced on the main shoot (Figure 4.06B). Whilst successive SAMs – and subsequently ears – are expected to decrease in productivity under normal treatments (Wang, Cheng and Zhang, 2007; Jaenisch *et al.*, 2022), nitrate restriction resulted in the productivity being more heavily focused on a small number of early emerging tillers. Sparse evidence exists for nitrate affecting mean spikelets per ear (Oscarson, 2000), and it had previously been suggested that such an effect was unlikely (Maidl *et al.*, 1998). The evidence presented here for altered distribution of developmental effort between meristems suggests that wheat-nitrate response can be better understood through the study of individual tillers as well as whole plant response.

Furthermore, the observed reduction in tillering under nitrate restriction specifically resulted from a lack of higher order tillers (Figure 4.04). This finding aligns with evidence that suggests that treating rice with high N fertiliser causes a proportionally larger yield increase on later emerging tillers than the first tillers (Wang *et al.*, 2017). Responding to nitrate by primarily modulating later, higher order tillers may be a trait shared among cereals, and better understanding of this phenomenon could inform the breeding of improved yield varieties without the need for excessive fertiliser use. Whilst tiller number has been identified as an important aspect of wheat yield (Yao *et al.*, 2021; Jaenisch *et al.*, 2022), almost no work has been done studying the productivity gap between wheat tillers, either regarding its underlying mechanism or how it might be mitigated.

4.9.2 Shoot architecture response to nitrate is coordinated by strigolactone

There is a strong body of evidence for the phytohormone strigolactone acting as a coordinator of nutrient availability and shoot development. Primarily, it has been shown to modulate shoot development in response to phosphate availability in *Arabidopsis* and rice (Umehara *et al.*, 2010; Kohlen *et al.*, 2011). However, more recent work suggests they assume a similar role in nitrate response in rice

(Yoneyama *et al.*, 2012; Cui *et al.*, 2023) and it has been suggested they may also coordinate shoot nitrate response in wheat (Sigalas *et al.*, 2023). Furthermore, strigolactone is known to regulate tillering in wheat via *TaTB1* (Dixon *et al.*, 2018) and to have a less investigated, but potential effect on wheat spikelet development (Liu *et al.*, 2017a). Therefore, strigolactone was investigated as a potential coordinator of nitrate availability with the observed shoot developmental effects.

This work showed that the tillering response of mutant lines with reduced strigolactone perception was less sensitive to nitrate restriction than the wild type (Figure 4.07). Furthermore, the *d3* and *d14* mutants maintained a consistent reproductive effort between their meristems when nitrate was abundant (Figures 4.11A and 4.11C), but under nitrate restriction they did not exhibit the prioritisation for earlier tillers observed in wild type (Figures 4.05 and 4.06), but instead maintained a distribution similar to the High[N] treatment, only with greatly reduced productivity (Figures 4.11B and 4.11D).

These data support the hypothesis that strigolactone coordinates wheat developmental response to nitrate, contributing to the developing evidence for strigolactone as a nitrate-shoot response signal in cereals, in rice (Yoneyama *et al.*, 2012; Cui *et al.*, 2023) and proposed in wheat (Sigalas *et al.*, 2023). The most likely method through which this coordination is achieved would be by altering strigolactone synthesis in the root and transport to the shoot, thus reducing the shoot hormonal concentration. This approach has been well established for hormonal coordination of root treatments with shoot development (Takei *et al.*, 2004, p. 201; Umehara *et al.*, 2010; Müller *et al.*, 2015; Kapulnik and Koltai, 2016). However, in this study, nitrate restriction significantly increased expression of *D3* and *D14* in the SAM was observed, and hence likely an increase in sensitivity of strigolactone perception. Although this does not preclude the likelihood of strigolactone biosynthesis or root-shoot transport also increasing, it does suggest that at least part of the resultant developmental effects are engendered by expression changes which result in a shoot system more receptive to the effects of strigolactone. Expression analysis found that *TaD14* is expressed in many tissues and developmental stages,

including the developing shoot and spike (Liu *et al.*, 2021b), but the scale of expression varied significantly. Given its ubiquity as a strigolactone sensor, modulation of the timing and location of *TaD14* expression could be used to alter developmental response in addition to, or instead of, altering strigolactone concentration through biosynthesis and transport (Cui *et al.*, 2023).

4.9.3 The effect on rate of SAM development may relate to initiation of reproductive development

Here I have shown that strigolactone can act to accelerate wheat SAM development (Figure 3.28). This presents a likely method by which strigolactone enacts the observed acceleration in development under nitrate restriction (Figure 4.03B).

Whilst strigolactone mutants maintained an equivalent number of initiated meristems, the number of vegetative meristems increased significantly (Figure 4.10). This suggests a specific method by which strigolactone might affect rate of meristem development, by preventing or delaying the transition from vegetative to reproductive development. There has previously been little literature specifically connecting strigolactone with meristem rate of development or determinacy although recent work has implicated it in regulating spike size in wheat (Bai *et al.*, 2024). However, strigolactone's more established involvement in apical dominance (Domagalska and Leyser, 2011; Khuvung, Silva Gutierrez and Reinhardt, 2022), repressing initiation of tiller bud outgrowth suggests a general role in encouraging a preference for vegetative growth may exist and deserves further investigation.

4.9.4 Future work and Conclusions

The redistribution of reproductive effort under nitrate restriction may inform future efforts to develop high-yielding wheat lines that require reduced nitrate fertilisation. The possibility that strigolactone coordinates this response (potentially in part by regulating rate of meristem development), indicates that the way in which strigolactone coordinates meristem development is under-investigated.

Recently, an *Arabidopsis* fluorescent reporter line has been developed which allows for the examination of cellular strigolactone distribution, via confocal microscopy (Song *et al.*, 2022). This line could be highly useful in investigating the effect of nitrate availability on strigolactone distribution and activity in the plant shoot system. The developing SAMs of plants grown in High[N] and Low[N] treatments could be studied, to determine how nitrate availability affects the location and concentration of strigolactone. I predict that these lines would show the quantity of strigolactone decreasing between successive meristems and would show a greater discrepancy under nitrate restriction. More ideal, would be the generation of similar lines in wheat, to allow for species-specific investigation.

Strigolactone biosynthesis, transport and degradation have been studied particularly well in *Arabidopsis* (de Jong, Ongaro and Ljung, 2014) and rice (Yoneyama *et al.*, 2012; Cui *et al.*, 2023) and the canonical strigolactone signalling pathway is well defined (Mashiguchi, Seto and Yamaguchi, 2021). Highly specific expression profiling (species, gene, and condition specific) of genes involved in this signalling would be useful for better understanding how strigolactone signalling responds to nitrate availability. These genes could include those involved in strigolactone biosynthesis (*MAX3/D17* and *MAX4/D10*) (Waters *et al.*, 2012; Umehara *et al.*, 2015), transport (*PDR1*) (Kretzschmar *et al.*, 2012) or perception (*D53*) (Jiang *et al.*, 2013).

Also requiring investigation is the role (or lack of role) for cytokinin in coordinating nitrate response in wheat. Cytokinin is strongly supported as a coordinator of shoot development in response to nitrate availability in many species (Takei *et al.*, 2004; Müller *et al.*, 2015; Lin *et al.*, 2021), primarily through a mechanism of increased nitrate perception in the root upregulating biosynthesis of *trans*-Zeatin (*t*Z) cytokinins, which are then transported to the shoot where they enact known developmental effects, such as increasing tiller bud outgrowth (Takei *et al.*, 2004; Hirose *et al.*, 2008; Poitout *et al.*, 2018; Sakakibara, 2021). Natural plasticity in *Arabidopsis* nitrate sensitivity was shown to result from constitutively low cytokinin (de Jong *et al.*, 2019), and the identification of such a system in wheat could inform the breeding of nitrate

insensitive lines. There is a small amount of wheat-specific evidence that suggests that cytokinin may be involved in communicating nitrate levels between the root and shoot (Garnica *et al.*, 2010; Bauer and von Wirén, 2020) and the existence of such a system in other plants, including the *Poaceae* family, would make its absence in wheat surprising. Therefore, I cannot conclude that cytokinin is entirely uninvolved based on the evidence presented in sections 4.7-4.8. However, cytokinin may not be as essential to nitrate-mediated shoot developmental responses as in other plants. Cytokinin treatment was shown to mimic the effect of increased nitrogen availability on leaf senescence in wheat (W. Wang *et al.*, 2019), suggesting at least some involvement of nitrogen-cytokinin signalling in wheat.

Perhaps in wheat it has a role that affects leaf development more than tiller or spikelet development. Alternatively, cytokinin may be less important for coordinating response to nitrate in wheat, but instead for some other nitrogen form, such as ammonium. In rice, expression of auxin transporter *OsPIN9* responds to ammonium but not nitrate concentration (Hou *et al.*, 2021), showing how aspects hormone signalling that regulate both nutritional response and shoot architecture can become co-opted.

Finally, the evidence presented here and in chapter 3, for the ability of strigolactone to accelerate meristem development requires further investigation. There is currently little literature that implicates strigolactone in flowering time or meristem determinacy, however, other hormones that interact with strigolactone levels, such as auxin and cytokinin, do affect these (Whitewoods *et al.*, 2018; Kong *et al.*, 2024), and may do so in concert with strigolactone. A high-frequency time course of dissections of the mutant lines would likely grant further insight into how strigolactone affects rate of development within the context of nitrate response. The effect broadly identified here of strigolactone accelerating development would benefit from this more precise understanding.

4.10 References

Andrews, M., Raven, J. a. and Lea, P. j. (2013) ‘Do plants need nitrate? The mechanisms by which nitrogen form affects plants’, Annals of Applied Biology, 163(2), pp. 174–199.

Bai, J. et al. (2024) ‘Strigolactone and abscisic acid synthesis and signaling pathways are enhanced in the wheat oligo-tillering mutant ot1’, Molecular Breeding : New Strategies in Plant Improvement, 44(2), p. 12.

Bajgain, P., Russell, B. and Mohammadi, M. (2018) ‘Phylogenetic analyses and in-seedling expression of ammonium and nitrate transporters in wheat’, Scientific Reports, 8, p. 7082.

Bauer, B. and von Wirén, N. (2020) ‘Modulating tiller formation in cereal crops by the signalling function of fertilizer nitrogen forms’, Scientific Reports, 10, p. 20504.

Bennett, T. et al. (2016) ‘Strigolactone regulates shoot development through a core signalling pathway’, Biology Open, 5(12), pp. 1806–1820.

Cui, J. et al. (2023) ‘Fertilization controls tiller numbers via transcriptional regulation of a MAX1-like gene in rice cultivation’, Nature Communications, 14(1), p. 3191.

Dixon, L.E. et al. (2018) ‘TEOSINTE BRANCHED1 regulates inflorescence architecture and development in bread wheat (Triticum aestivum)’, Plant Cell, 30(3), pp. 563–581.

Domagalska, M.A. and Leyser, O. (2011) ‘Signal integration in the control of shoot branching’, Nature Reviews Molecular Cell Biology, 12(4), pp. 211–221.

Garnica, M. et al. (2010) ‘The signal effect of nitrate supply enhances active forms of cytokinins and indole acetic content and reduces abscisic acid in wheat plants grown with ammonium’, Journal of Plant Physiology, 167(15), pp. 1264–1272.

Hirose, N. et al. (2008) ‘Regulation of cytokinin biosynthesis, compartmentalization and translocation’, Journal of Experimental Botany, 59(1), pp. 75–83.

Hou, M. et al. (2021) ‘OsPIN9, an auxin efflux carrier, is required for the regulation of rice tiller bud outgrowth by ammonium’, New Phytologist, 229(2), pp. 935–949.

Jaenisch, B.R. et al. (2022) ‘Modulation of Wheat Yield Components in Response to Management Intensification to Reduce Yield Gaps’, Frontiers in Plant Science, 13, p.

Jiang, L. et al. (2013) ‘DWARF 53 acts as a repressor of strigolactone signalling in rice’, Nature, 504(7480), pp. 401–405.

de Jong, M. et al. (2019) ‘Natural variation in Arabidopsis shoot branching plasticity in response to nitrate supply affects fitness’, PLoS Genetics, 15(9).

de Jong, M., Ongaro, V. and Ljung, K. (2014) ‘Auxin and Strigolactone Signaling are Required for Modulation of Arabidopsis Shoot Branching by Nitrogen Supply’, Plant Physiology, 166(1), pp. 384–395.

Kapulnik, Y. and Koltai, H. (2016) ‘Fine-tuning by strigolactones of root response to low phosphate’, Journal of Integrative Plant Biology, 58(3), pp. 203–212.

Khuvung, K., Silva Gutierrez, F.A.O. and Reinhardt, D. (2022) ‘How Strigolactone Shapes Shoot Architecture’, Frontiers in Plant Science, 13, p. 889045.

Kohlen, W. et al. (2011) ‘Strigolactones are transported through the xylem and play a key role in shoot architectural response to phosphate deficiency in nonarbuscular mycorrhizal host arabidopsis’, Plant Physiology, 155(2), pp. 974–987.

Kong, S. et al. (2024) ‘Tradeoff between speed and robustness in primordium initiation mediated by auxin-CUC1 interaction’, Nature Communications, 15(1), p. 5911.

Kretzschmar, T. et al. (2012) ‘A petunia ABC protein controls strigolactone-dependent symbiotic signalling and branching’, Nature, 483(7389), pp. 341–344.

Lin, J. et al. (2021) ‘Nitrate restricts nodule organogenesis through inhibition of cytokinin biosynthesis in Lotus japonicus’, Nature Communications, 12(1), p. 6544.

Liu, J. et al. (2017) ‘miR156-Targeted SBP-Box Transcription Factors Interact with DWARF53 to Regulate TEOSINTE BRANCHED1 and BARREN STALK1 Expression in Bread Wheat’, Plant Physiology, 174(3), pp. 1931–1948.

Liu, R. et al. (2021) ‘Association of tad14-4d, a gene involved in strigolactone signaling, with yield contributing traits in wheat’, International Journal of Molecular Sciences, 22(7), pp.1-16.

Longnecker, N., Kirby, E.J.M. and Robson, A. (1993) ‘Leaf Emergence, Tiller Growth, and Apical Development of Nitrogen-Dificient Spring Wheat’, Crop Science, 33(1).

Luo, L., Zhang, Y. and Xu, G. (2020) ‘How does nitrogen shape plant architecture?’, Journal of Experimental Botany, 71(15), pp. 4415–4427.

Maidl, F.-X. et al. (1998) ‘Effect of Varied N-fertilization on Yield Formation of Winter Wheat under Particular Consideration of Mainstems and Tillers’, Journal of Agronomy and Crop Science, 180(1), pp. 15–22.

Mashiguchi, K., Seto, Y. and Yamaguchi, S. (2021) ‘Strigolactone biosynthesis, transport and perception’, The Plant Journal, 105(2), pp. 335–350.

Müller, D. et al. (2015) ‘Cytokinin is required for escape but not release from auxin mediated apical dominance’, Plant Journal, 82(5), pp. 874–886.

Oscarson, P. (1996) ‘Transport of Recently Assimilated15N Nitrogen to Individual Spikelets in Spring Wheat Grown in Culture Solution’, Annals of Botany, 78(4), pp. 479–488.

Oscarson, P. (2000) ‘The strategy of the wheat plant in acclimating growth and grain production to nitrogen availability’, Journal of Experimental Botany, 51(352), pp. 1921–1929.

Poitout, A. et al. (2018) ‘Responses to systemic nitrogen signaling in arabidopsis roots involve trans-zeatin in shoots’, Plant Cell, 30(6), pp. 1243–1257.

Sakakibara, H. (2021) ‘Cytokinin biosynthesis and transport for systemic nitrogen signaling’, Plant Journal, 105(2), pp. 421–430.

Shi, X. et al. (2022) ‘Comparative genomic and transcriptomic analyses uncover the molecular basis of high nitrogen-use efficiency in the wheat cultivar Kenong 9204’, Molecular Plant, 15(9), pp. 1440–1456.

Sigalas, P.P. et al. (2023) ‘Nutritional and tissue-specific regulation of cytochrome P450 CYP711A MAX1 homologues and strigolactone biosynthesis in wheat’, Journal of Experimental Botany, 74(6), pp. 1890–1910.

Song, C. et al. (2022) ‘Strigo-D2—a bio-sensor for monitoring spatio-temporal strigolactone signaling patterns in intact plants’, Plant Physiology, 188(1), pp. 97–110.

de Souza Campos, P.M. et al. (2019) ‘Phosphate acquisition efficiency in wheat is related to root:shoot ratio, strigolactone levels, and PHO2 regulation’, Journal of Experimental Botany, 70(20), pp. 5631–5642.

Sun, H. et al. (2023) ‘Strigolactone and gibberellin signaling coordinately regulate metabolic adaptations to changes in nitrogen availability in rice’, Molecular Plant, 16(3), pp. 588–598.

Takei, K. et al. (2004) AtIPT3 is a Key Determinant of Nitrate-Dependent Cytokinin Biosynthesis in Arabidopsis, Plant Cell Physiol, pp. 1053–1062.

Umehara, M. et al. (2010) ‘Contribution of strigolactones to the inhibition of tiller bud outgrowth under phosphate deficiency in rice’, Plant and Cell Physiology, 51(7), pp. 1118–1126.

Umehara, M. et al. (2015) ‘Structural Requirements of Strigolactones for Shoot Branching Inhibition in Rice and Arabidopsis’, Plant and Cell Physiology, 56(6), pp. 1059–1072.

Wang, F., Cheng, F. and Zhang, G. (2007) ‘Difference in Grain Yield and Quality among Tillers in Rice Genotypes Differing in Tillering Capacity’, Rice Science, 14(2), pp. 135–140.

Wang, J. et al. (2018) ‘Rice nitrate transporter OsNPF7.2 positively regulates tiller number and grain yield’, Rice, 11(1).

Wang, M. et al. (2020) ‘TaANR1-TaBG1 and TaWabi5-TaNRT2s/NARs Link ABA Metabolism and Nitrate Acquisition in Wheat Roots’, Plant Physiology, 182(3), pp. 1440–1453.

Wang, Wenqiang et al. (2019) ‘The involvement of cytokinin and nitrogen metabolism in delayed flag leaf senescence in a wheat stay-green mutant, tasg1’, Plant Science, 278, pp. 70–79.

Wang, Y. et al. (2017) ‘Effects of nitrogen and tiller type on grain yield and physiological responses in rice’, AoB Plants, 9(2).

Waters, M.T. et al. (2012) ‘Specialisation within the DWARF14 protein family confers distinct responses to karrikins and strigolactones in Arabidopsis’, Development, 139(7), pp. 1285–1295.

Waters, M.T. et al. (2017) ‘Strigolactone Signaling and Evolution’ Annual Reviews, 68, pp. 291-322.

Wheat eFP Browser. Available at: https://bar.utoronto.ca/efp_wheat/cgi-bin/efpWeb.cgi (Accessed: 22 July 2024).

Whitewoods, C.D. et al. (2018) ‘CLAVATA Was a Genetic Novelty for the Morphological Innovation of 3D Growth in Land Plants’, Current Biology, 28(15), pp. 2365-2376.

Xu, J. et al. (2015) ‘The interaction between nitrogen availability and auxin, cytokinin, and strigolactone in the control of shoot branching in rice (Oryza sativa L.)’, Plant Cell Reports, 34(9), pp. 1647–1662.

Yao, F.Q. et al. (2021) ‘Down-expression of TaPIN1s Increases the Tiller Number and Grain Yield in Wheat’, BMC Plant Biology, 21(1), p. 443.

Yoneyama, Kaori et al. (2012) ‘How do nitrogen and phosphorus deficiencies affect strigolactone production and exudation?’, Planta, 235(6), pp. 1197–1207.

Yuan, Y. et al. (2023) ‘Unlocking the Multifaceted Mechanisms of Bud Outgrowth: Advances in Understanding Shoot Branching’, Plants, 12(20), p. 3628.

Chapter 5

Coordination of Reproductive Shoot Architecture in Cereals with Soil Volume Availability

5.1 Chapter Aim

Predicted increases in global population and climate change-driven losses of arable land will require future crops to produce an increased yield on a reduced area of land (Alexandratos, 2012; Molotoks *et al.*, 2018). However, such a necessity runs counter to current understanding that resource restriction elicits a developmental response that restricts shoot architecture development, and thus yield potential (Conley *et al.*, 2009; Barbier *et al.*, 2019; de Jong *et al.*, 2019). Soil volume availability has been shown to have an influence on plant shoot architecture development, in a manner distinct from nutrient availability (Hess and De Kroon, 2007; Poorter *et al.*, 2012; Wheeldon *et al.*, 2020). Strigolactones have been shown to coordinate this response in part through their function as root exudates, which can be used by plants, including rice (Yoneyama *et al.*, 2022), to sense soil volume (Wheeldon *et al.*, 2022). However, strigolactones can also function as endogenous phytohormones, and I hypothesise that they may further coordinate this response by being transported to the shoot where they can modulate shoot development.

It has previously been reported that many plant species including tomato (Bar-Tal *et al.*, 1995), cotton (Yong *et al.*, 2010), bean (Carmi and Heuer, 1981), and pea (Wheeldon *et al.*, 2022) respond to soil volume availability by modulating shoot architecture and this response is an important factor in determining final reproductive effort. This response to soil volume availability (SVA) has also recently been shown in wheat (Wheeldon *et al.*, 2020). Exactly how perceived SVA is communicated into changes in wheat shoot development is poorly understood. Coordinating this response likely requires multiple interacting and tightly regulated processes, primarily, detection of SVA in the root, communication of this detection with the shoot and subsequently, proportional modulation of shoot development. Research has primarily focused on the initial step of how the root system detects soil volume availability (Hess and De Kroon, 2007; Poorter *et al.*, 2012; Wheeldon *et al.*, 2020). This chapter intends to investigate the later stages of SVA response in wheat and other cereals: how shoot architecture development changes in response to SVA and which molecules coordinate this process. Specific developmental responses to soil volume availability are studied and utilised to determine the wheat developmental

response to soil volume availability and the possible role of strigolactone in coordinating the observed effects is tested.

5.2 Comparing shoot architecture response to soil volume availability in elite wheat lines

I intended to investigate wheat SVA response primarily using the elite spring line Cadenza. However, wheat-SVA response is poorly reported and the extent to which different lines of wheat vary in their SVA response is not known. I hypothesised that the response, at least in modern elite varieties would be highly similar and thus the conclusions drawn from studying Cadenza would be broadly applicable to all modern elite wheat. However, it is possible that modern wheat has not been selectively bred to have a shared SVA response and lines may vary significantly in their shoot architecture-SVA response. Therefore, I conducted preliminary experiments growing Cadenza alongside the elite line Paragon. Both lines were grown in 100ml, 500ml and 2000ml soil volumes and their shoot development was measured to determine if the effect on shoot development between these similar wheat lines would differentiate significantly.

The response of the two elite wheat lines was highly similar, exhibiting a significant increase in maximum tiller and ear number at each increase in soil volume (Figure 5.01A-B). However, similar to previous reporting in wheat and other plant species, the response was not proportional to the increase in SVA (Fischer *et al.*, 2019; Wheeldon *et al.*, 2020). Whilst tiller number more than doubles for both lines between 100ml-500ml and 500ml-2000ml, this is in response to a 5-fold and 4-fold increase in resource availability.

Plants in both lines and all three soil volumes were grown to maturity and their final shoot architecture was studied. This data more strongly indicated the trends suggested by the analysis of tiller production – that SVA response can vary depending on the soil volumes being compared but is mostly similar between elite lines.

However, some measures of wheat shoot architecture do not appear to dependably increase in both lines between all SVA increases. Spikelet number increases with SVA in Cadenza, but in Paragon the increase in spikelet number between 500ml and 2000ml SVA is so small as to be statistically insignificant (Figure 5.01C), as was previously observed for the elite spring line Mulika (Wheeldon *et al.*, 2020). This result indicates that different lines (even very similar lines of elite spring wheat) can vary somewhat in their shoot developmental response, and that even a 4-fold increase in available soil can have no significant increase on the production of certain shoot architecture structures.

Both lines generally increase seed number per ear with increased SVA, except for Paragon between 500ml and 2000ml (Figure 5.01D), combined with the significant difference in ear number, this results in a large increase in seeds per plant (Figure 5.01E). However, the data shows that there is no difference in seed mass per ear between Cadenza plants grown in 100ml or 500ml and in Paragon there is no difference even between 100ml and 2000ml (Figure 5.01F), suggesting that elite wheat lines primarily respond to SVA by modulating number of ears and seeds on those ears, with a proportionally smaller effect on the size of those seeds.

Although there are some instances where the two lines differ in SVA response, taken as a whole, this data supports my hypothesis that within the same species, elite lines can be assumed to respond to SVA changes in the same manner and to the same order of magnitude.

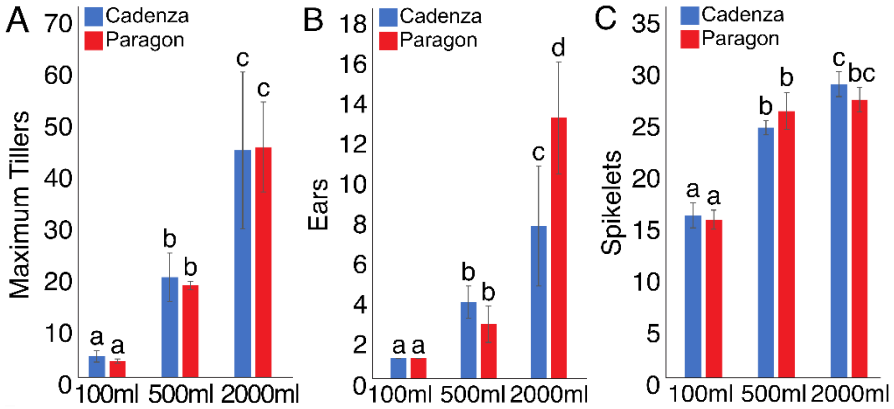

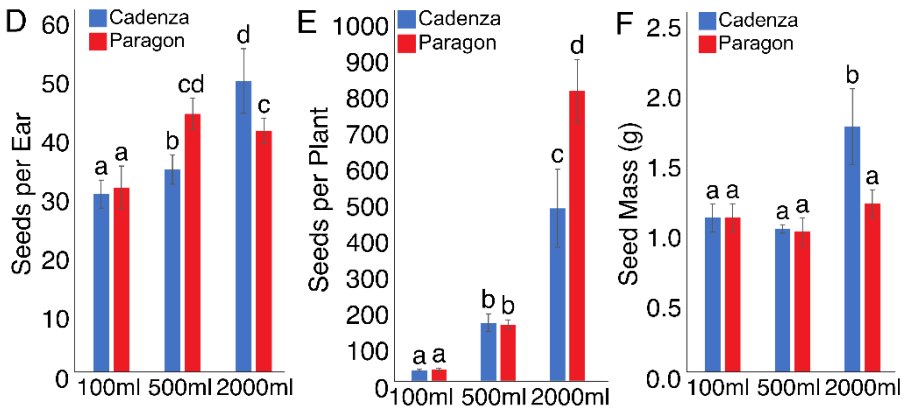

Figure 5.01: The effect of soil volume availability on elite wheat seed development.

(A) Bar chart of mean maximum number of tillers per plant **(B)** Bar chart of mean number of ears per plant **(C)** Bar chart of mean number of spikelets per ear **(D)** Bar chart of mean number of seeds per ear **(E)** Bar chart of mean number of seeds per plant **(F)** Bar chart of mean seed mass (g) per ear.

All measurements taken at end of plant life. Cadenza is represented in blue; Paragon is represented in red. Error bars are 1 standard deviation from the mean. Different letters above bars indicate statistically significant difference between treatments (ANOVA, $P<0.05$, $n=5$-6).

5.3 The effect of soil volume availability on distribution of reproductive effort between tillers

Important aspects of wheat shoot architecture are determined by the development of tillers and their meristems. I therefore hypothesised that key aspects of wheat shoot SVA response may result from differences in tiller and tiller meristem development. It is already established that SVA strongly affects tiller number (Wheeldon *et al.*, 2020) (Figure 5.01A), however I hypothesised that more detailed understanding regarding specifically where and when tillers developed on the plant, would be informative on precisely how wheat shoot development is affected by SVA. Additionally, spikelets per ear was shown to increase significantly in Cadenza between 500ml and 2000ml treatments (Figure 5.01C) but the scale of the increase was far smaller than that of tiller number (Figure 5.01A), increasing 19%, where tillering increased by more than 100%. Therefore, rate of spikelet development was

also studied, as I hypothesised this aspect of shoot development may respond to SVA differently to tiller development.

In chapter 3 of this thesis, I established that the location of tiller emergence on the wheat plant relates to rate of SAM development, and number of spikelets on the final ear. I hypothesised that soil volume may alter the location of tiller development as a way of responding to soil volume restriction. I therefore grew Cadezna plants in 500ml and 2000ml soil volumes and studied where and when they produced tillers, and how rate of development varied between soil volumes and between different tillers on the same plant.

Plants of the elite wheat variety Cadenza were grown in 500ml and 2000ml soil volumes. The emergence of the tillers of these plants was tracked for 7 weeks of growth, using the system detailed in Chapter 3, section 3.3 and illustrated in Figure 3.06. In this system, tillers are tracked by when they developed (ordinal tiller number) and where they developed relative to other tillers (position of emergence).

In section 3.3 I reported that cereal tiller development does not follow a fixed order of emergence, but general patterns of emergence can be identified. The same was observed in these experiments. However, here I also identified that SVA influences the pattern of which tillers the wheat plant produces and in what order. The 500ml plants showed significantly less variation in which tiller emerged at each ordinal position than the 2000ml plants. 60% or more of the 500ml plants produced the same tiller at each ordinal point (except for at positions 10 and 12) (Figure 5.02A). Whereas, after the first few tillers, there was almost never such a majority for a position in the 2000ml plants (Figure 5.02B). At later positions, this increased variation could be attributed to the fact that the 2000ml plants have produced a greater number of tillers and therefore there is a greater number of potential options for the location for a new tiller to emerge from. However, the mean tiller number for 500ml plants at the point of dissection was 10 and every plant made a minimum of 6 tillers. Even by the 6^{th} tiller a difference in variability is already evident between the SVA treatments, the 2000ml plants generally have more potential tiller options between the 6^{th} and 10^{th} tiller and these options appear to be more evenly split

between the samples dissected. This decreased variation in the 500ml treatment suggests a stronger regulation of tiller production. Wheat potentially responds to the reduced resource by prioritising certain tillers, as occurred in response to nitrate restriction (section 4.3).

The average ordinal position for first order tillers is very similar between the two treatments, with tillers 1, 2, and 3 appearing at the same early points in the order of tiller emergence (as ordinal tiller 2, 3 and 5.5 respectively) (Figure 5.02C-D).

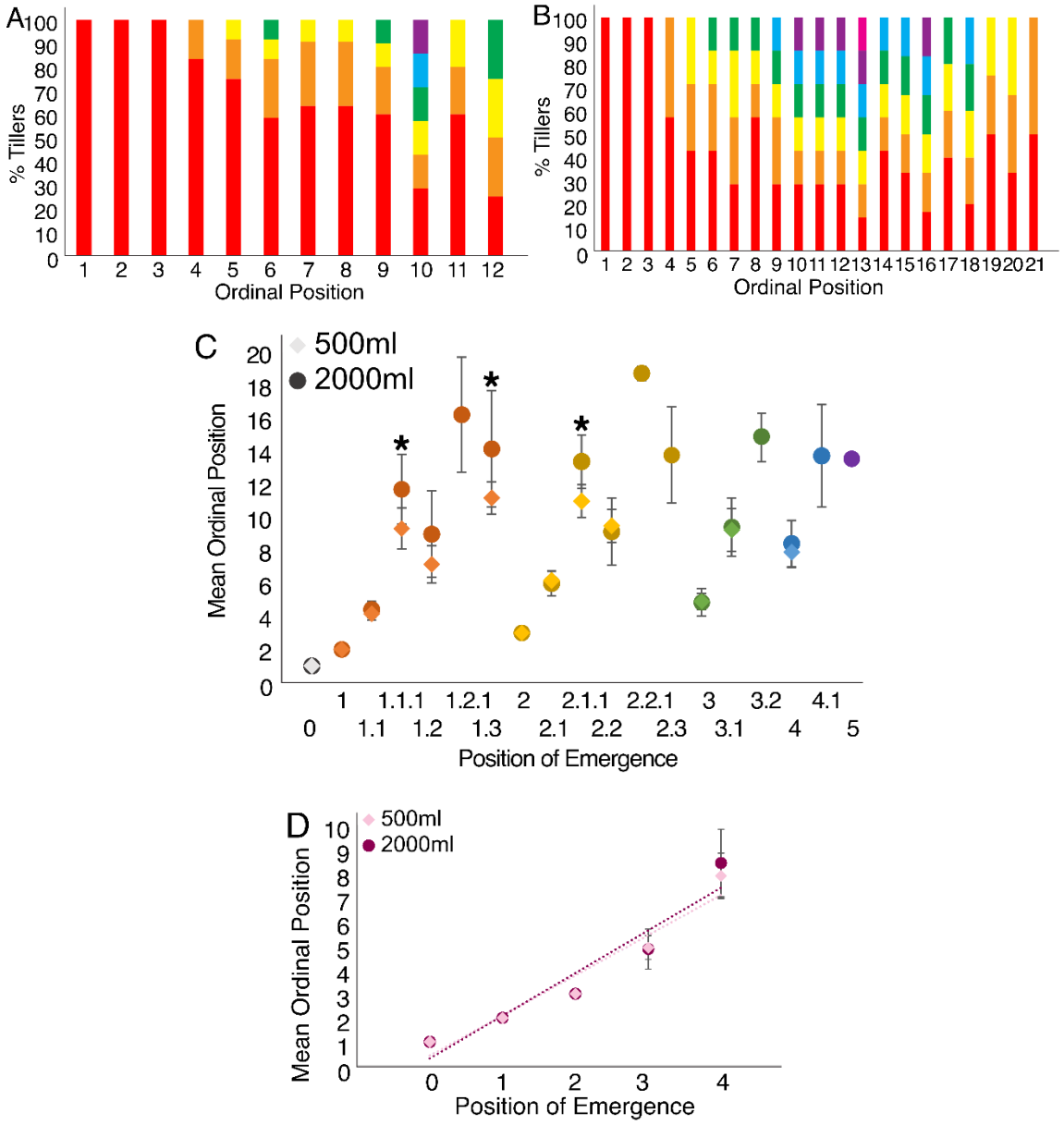

Figure 5.02: The effect of soil volume availability on tiller emergence in the elite wheat line Cadenza.

The notation used for labelling tillers is introduced and detailed in section 3.3, Figure 3.06.

(A) Bar chart of percentage distribution between different positions of emergence by ordinal tiller, taken at 42 DaP, for 500ml SVA treatments. Each different position of emergence found at each ordinal location is represented in a different colour and shown as a percentage of the total number of plants which produced that tiller at that ordinal position. **(B)** Bar chart of percentage distribution between different positions of emergence by ordinal tiller, taken at 42 DaP, for 2000ml SVA treatments. Each different position of emergence found at each ordinal location is represented in a different colour and shown as a percentage of the total number of plants which produced that tiller at that ordinal position. **(C)** Scatter plot of mean ordinal position of emergence of tillers by position of emergence on the plant, at 42 DaP. 500ml is represented in light coloured diamonds; 2000ml is represented in dark coloured circles. Error bars are 1 standard deviation from the mean. An asterisk above a point denotes statistically significant difference between SVA treatments for that tiller (two-tailed t-test, $P<0.05$, n=7-12). **(D)** Scatter plot of mean ordinal position of emergence of tillers by position of emergence on the plant, at 42 DaP. First order tillers only. 500ml is represented in light pink diamonds; 2000ml is represented in dark purple. Error bars are 1 standard deviation from the mean. An asterisk above a point denotes statistically significant difference between SVA treatments for that tiller (two-tailed t-test, $P<0.05$, n=7-12).

This data suggests that under more restricted soil volumes, when wheat reduces tiller production it initially prioritises lower order tillers, that emerge from shoot apical meristems developing on the main shoot. The ears that emerge from these tillers are typically more productive than higher order tillers, for instance, tillers 1, 1.1 and 1.1.1 produced on average 16.0, 10.4 and 6.0 spikelets respectively in 2000ml plants at the time of dissection (Figure 5.04C). This strategy further agrees with the

data presented in section 4.3 that, when resource limitation is sensed in the roots, wheat prioritises high productivity ears over the production of a greater number of tillers and ears.

However, this prioritisation may indicate a route for improving wheat productivity under restricted SVA, even if the species is already well adapted to these treatments. In 500ml plants, the control over tiller emergence weakens and higher order tillers, such as 1.1.1 and 2.1.1 were not only produced, but produced earlier on average than at the higher SVA. Taken together, these observations on tiller development imply a relatively strong level of control regarding tiller emergence that weakens with an increased number of tillers. This control maintains greater consistency under more restricted soil volume treatments. It is therefore reasonable to propose that, upon sensing a restriction in soil volume, the plant reduces tiller number by more strongly repressing tiller development and that this repressive effect more strongly affects higher order tillers.

In addition to tracking tiller emergence, the shoot apical meristem of each tiller was dissected to determine how changes to SVA could affect meristem development and where these changes could be observed.

The shoot apical meristems of wheat grown in the 500ml treatment were found to be developing at a significantly faster rate than those of the 2000ml plants. The mean stage of development for 500ml plants was 2.1, but only 1.6 for 2000ml (Figure 5.03A). The amount of time a meristem spends in reproductive development typically determines how productive the resultant ear is, as the meristem can spend more time producing spikelet ridges, which allows for an increased number of spikelets and subsequently florets and seeds per ear. Therefore, it makes sense that the additional SVA results in wheat slowing shoot apical meristem development. However, the data shows that it is not simply the mean that is affected by SVA (Figure 5.03A), but the difference in developmental stage between meristems on the same plant (Figure 5.03D). Generally, later emerging tillers will have meristems that are earlier in development, resulting in a gradient of meristem stage (and later in development a gradient in productivity, with the earlier tillers producing the most

productive ears). Interestingly, the meristems of 2000ml plants are not consistently earlier in development. In fact, some of the later meristems are actually later in development than the equivalent ordinal tiller in the 500ml treatment (Figure 5.03D). The difference in stage between successive meristems of the 500ml plants is greater than that of the 2000ml plants. Though the difference between that stage of the two treatments for each ordinal position was never significantly different (by two-tailed t-test, $P<0.05$), the difference between positions is different enough to result in evidently different gradients in decline. This result suggests that the emergence of the first 3-4 tillers is essentially the same between the two treatments (also seen in Figure 5.02C, where the tillers for ordinal tillers 1-4 are very similar) and plants in the different SVA treatments begins to diverge after this point, when the 500ml plant begins to limit shoot development in response to the perception of SVA limitation.

A similar trend is seen for spikelet ridge number, with the earlier tillers of plants in both treatments producing an equivalent amount, but the later tillers of 2000ml plants being more productive (Figure 5.03E). This does result in the finding that the 2000ml plants at this stage do not produce significantly more spikelet ridges than 500ml plants (Figure 5.03B). It should also be noted that whilst the spikelet ridge number is statistically equivalent, the 2000ml plants are earlier in development and have therefore produced the same number of ridges per meristem at an earlier point in development. When spikelet ridge number is compared as a proportion of developmental stage, the 2000ml plants have produced significantly more ridge relative to their stage in development (Figure 5.03F), suggesting that the greater SVA plants result in meristems that are producing spikelet ridges at a comparatively faster rate, which would eventually result in the small but significant increase in spikelets reported in the final architecture (Figure 5.03B).

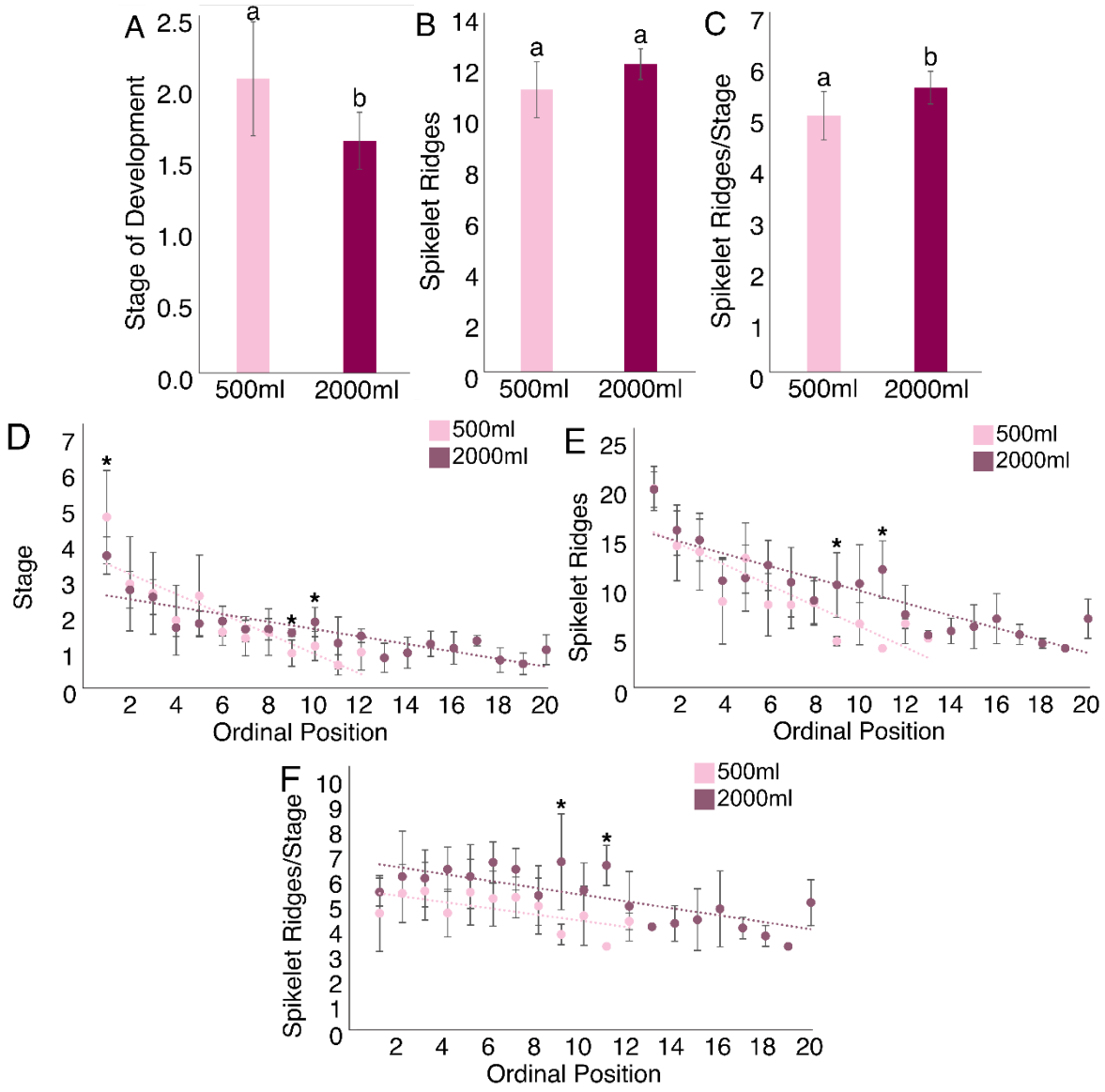

Figure 5.03: The effect of soil volume availability on SAM development in the elite wheat line Cadenza.

(A) Bar chart of mean stage of SAM development **(B)** Bar chart of mean number of spikelet ridges per SAM **(C)** Bar chart of mean number of spikelet ridges per stage. Different letters above bars indicate statistically significant difference between treatments (two-tailed t-test, P<0.05, n=7-12). **(D)** Scatter plot of mean stage of SAM development by ordinal tiller position **E)** Scatter plot of mean number of spikelet ridges per SAM by ordinal tiller position **(F)** Scatter plot of mean spikelet ridges per stage by ordinal tiller position.

Measurements taken at 42 DaP. 500ml is represented in light pink; 2000ml is represented in dark pink. Error bars are 1 standard deviation from the mean. An asterisk above a point denotes statistically significant difference between SVA treatments for that tiller (two-tailed t-test, $P<0.05$, $n=7$-12).

In addition to comparing rate of meristem development and spikelet ridge production by ordinal tiller position, the data was additionally compared by tiller position.

The data shows that the significantly later stage of development in 500ml meristems (Figure 5.03A) is predominantly the result of the lower order tillers (Figure 5.04A). Tillers 0 (the main shoot), 1, 2 and 3 all show the 500ml meristems at an equivalent or significantly later point in development, whereas all other, higher order, tillers are equivalent or (for tillers 1.2 and 1.3) significantly earlier in development. Despite the previously reported difference in gradient between meristems, the first order tillers of 500ml plants are consistently later in development than the 2000ml plants (Figure 5.04B).

Whilst there is a general trend of the 2000ml meristems producing more spikelet ridges, the difference is typically quite small, with only 1 or 2 spikelets more being produced (Figure 5.04C-D). However, when taken with the generally earlier average stage of 2000ml plants, this results in the plants growing at a higher SVA produce significantly more spikelets per stage at most tillers (Figure 5.04E). Interestingly the few exceptions include tillers 0, 1 and 2 (Figure 5.04F), the three most productive tillers on the plant by spikelet ridges (Figure 5.04A). This result suggests that plants growing at a more restricted soil volume prioritise the normal development over a small number of the most productive tillers, to maximise ultimate seed production and fitness.

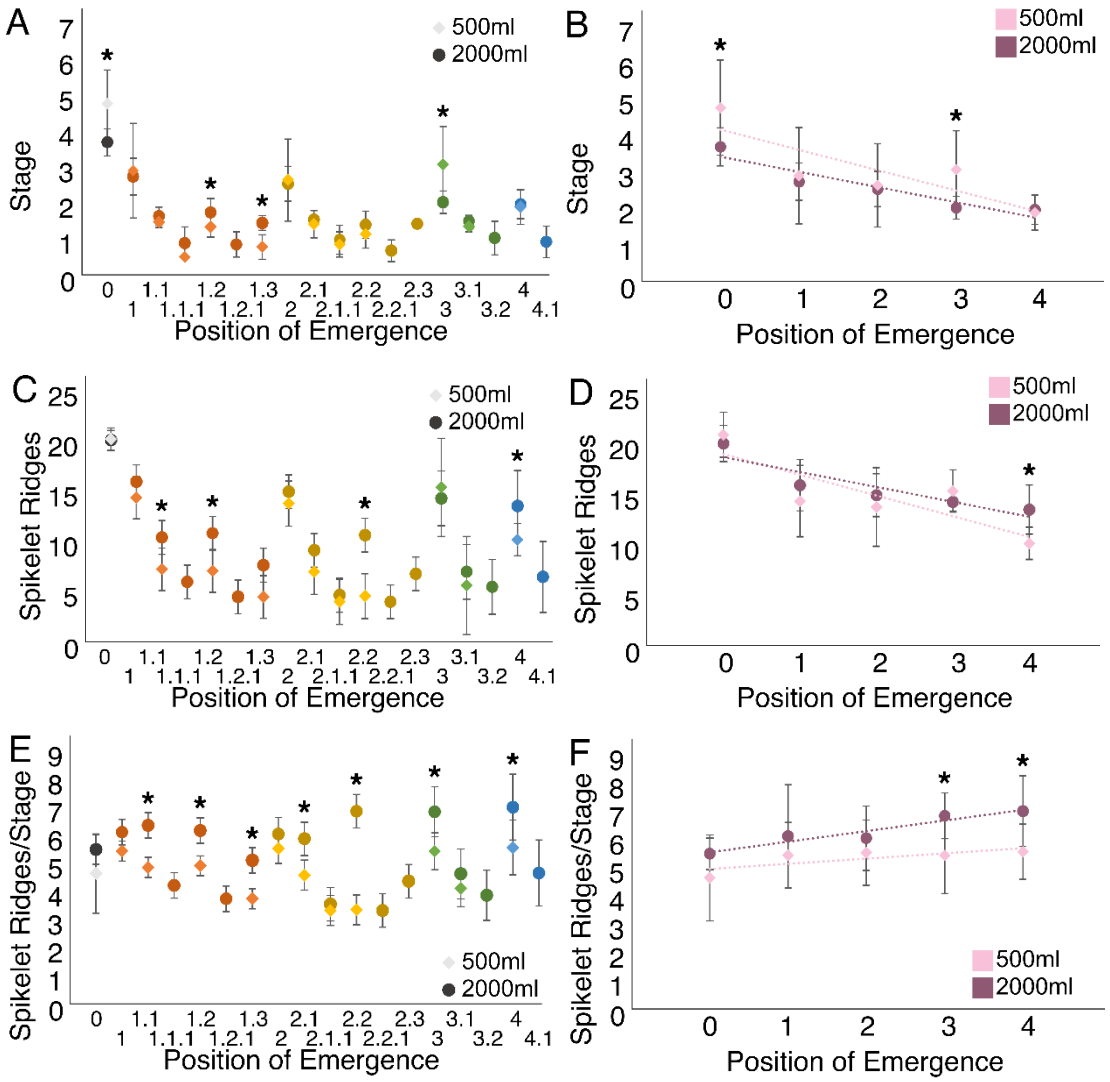

Figure 5.04: The effect of soil volume availability on SAM development at each tiller in the elite wheat line Cadenza.

The notation used for labelling tillers is introduced and detailed in section 3.3.6, Figure 3.06.

(A) Scatter plot of mean stage of SAM development by position of emergence on the plant, all tillers. **(B)** Scatter plot of mean stage of SAM development by position of emergence on the plant, first order tillers. **(C)** Scatter plot of mean number of spikelet ridges by position of emergence on the plant, all tillers. **(D)** Scatter plot of mean number of spikelet ridges by position of emergence on the plant, first order tillers. **(E)** Scatter plot of mean spikelet ridges per stage of SAM development by position of emergence

on the plant, all tillers. **(F)** Scatter plot of mean spikelet ridges per stage of SAM development by position of emergence on the plant, first order tillers.
Measurements taken at 49 DaP. 500ml is represented in light diamonds; 2000ml is represented in dark circles. Error bars are 1 standard deviation from the mean. An asterisk above a point denotes statistically significant difference between SVA treatments for that tiller (two-tailed t-test, $P<0.05$, $n=7$-12).

The data presented in section 5.2 established that wheat shoot development, including tiller and spikelet number are significantly affected by SVA. The data presented in this section better establishes *when* and *where* this significant difference in shoot architecture is brought about.

5.4 The effect of soil volume availability on wheat strigolactone and cytokinin related expression

The experimental data presented in sections 5.2-5.3 details establishing work that defines the developmental response to SVA. I hypothesised that one or more phytohormones were likely to coordinate the perception of SVA in the root system with changes to development in the shoot. I hypothesised that strigolactone and cytokinin were sensible candidates for investigation. Both are long distance molecules that can communicate information sensed in the root system, to cause developmental changes to the shoot reproductive architecture (Wang, Smith and Li, 2018; Wheeldon and Bennett, 2020; Guo *et al.*, 2024). I hypothesised that changes in the expression of genes related to their canonical signalling pathways might indicate the validity of further investigating these phytohormones. Therefore, qPCR experiments were conducted. In these experiments, RNA was extracted from either the shoot apical meristem of the main shoot and relative expression levels were determined and compared. Wheat efp browser was used to identify transcripts of signalling genes that were specifically highly expressed in the reproductive SAM (*Wheat eFP Browser*). Expression of *D3* and *D14* were tested to measure changes in strigolactone perception; *TB1* was tested to measure strigolactone and cytokinin

induced tillering change; *CKX9* was tested to measure rate of cytokinin degradation; *RRA1* was tested to measure cytokinin perception.

In 100ml, the expression of strigolactone signalling genes *D3* and *D14* are significantly increased (Figure 5.05). This result suggests that under more restricted SVA treatments, wheat shoot meristems become more sensitive to strigolactone, and therefore, likely its associated developmental effects (Umehara *et al.*, 2010; Kohlen *et al.*, 2011; Y. Liu *et al.*, 2023). In the same samples, expression of tillering repressor *TB1* was not affected, suggesting that an increase in strigolactone in the SAM of SVA restricted plants may not be responsible for the observed reduction in tillering, or if it is, it does not achieve this developmental change by strigolactone's known ability to upregulate *TB1*.

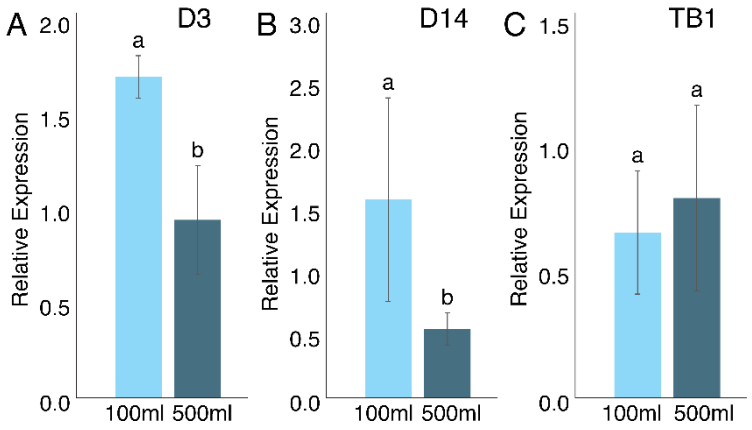

Figure 5.05: Gene expression of canonical strigolactone signalling genes in the shoot apical meristem of elite wheat Cadenza, under SVA restricted treatments

(A) Bar chart showing the relative gene expression of TaD3. **(B)** Bar chart showing the relative gene expression of TaD15. **(C)** Bar chart showing the relative gene expression of TaTB1.

Samples were collected from the shoot apical meristem of the main shoot, of Cadenza wheat at 42 DaP. Plants grown in the 100ml treatment are shown in light blue, plants grown in the 500ml treatment are shown in dark blue. Error bars represent 1 standard deviation. Letters above bars represent statistical significance between treatments for that gene (n=3). Relative expression was determined from actin housekeeping gene TraesCS5A02G015600 (Borrill et. al., 2016).

As outlined in Chapter 1, many known developmental effects are influenced by more than one phytohormone, cytokinin was also investigated. Neither of the tested cytokinin signalling genes significantly differed in expression between the two SVA treatments (Figure 5.06). Whilst the high degree of variation might indicate that further repeats could identify a difference that is statistically significant, these results did not encourage the further investigation of cytokinin as a key hormonal regulator of shoot developmental response to SVA in wheat. Therefore, the remaining work reported in this chapter primarily focuses on strigolactone as a candidate hormone. However, some investigation into cytokinin is reported in section 5.12.

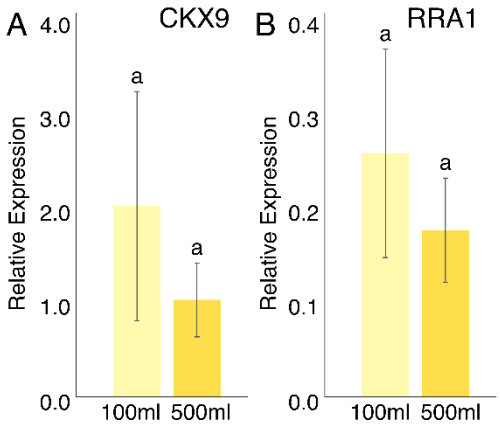

Figure 5.06: Gene expression of canonical cytokinin signalling genes in the shoot apical meristem of elite wheat Cadenza, under SVA restricted treatments

(A) Bar chart showing the relative gene expression of TaCKbarX3. **(B)** Bar chart showing the relative gene expression of TaRRA1.

Samples were collected from the shoot apical meristem of the main shoot, of Cadenza wheat at 42 DaP. Plants grown in the 100ml treatment are shown in light blue, plants grown in the 500ml treatment are shown in dark blue. Error bars represent 1 standard deviation. Letters above bars represent statistical significance between treatments for that gene (n=3). Relative expression was determined from actin housekeeping gene TraesCS5A02G015600 (Borrill et. al., 2016).

5.5 Characterising the shoot architecture of strigolactone signalling mutant wheat under soil volume restriction

Current literature suggests that strigolactone can act as a long-distance signal to communicate information in the roots to the shoot system and its presence in the shoot can enact significant developmental changes (Liu *et al.*, 2021b; Yuan *et al.*, 2023). Furthermore, the expression profiling reported in section 5.4 supports the hypothesis that strigolactone signalling is increased in the developing SAM of wheat under SVA restricted treatments. I thus hypothesised that strigolactone might be coordinating the observed wheat shoot developmental response to SVA.

To study the potential role of strigolactone in coordinating wheat shoot development in response to SVA, *d3* and *d14* null lines were investigated, which were insensitive to strigolactone levels. A third *tb1* null line was included in the experiments. This gene is known to regulate tiller production (Dixon *et al.*, 2018) and its inclusion was intended to act as a 'high tillering control' to contrast against the strigolactone signalling mutants.

These three lines and a wild-type control were grown in the same treatments, in 100ml and 500ml soil volumes. Tiller number was counted weekly and at final seed set shoot architecture parameters were measured including ears, spikelets and seeds.

In both soil volumes, the strigolactone mutants produced significantly more tillers than the wild type background, or even the *tb1* tillering mutant (Figure 5.07A). However, whilst the WT and *tb1* lines exhibit a large increase in tiller production under the higher SVA treatment, the strigolactone mutants show a far smaller increase (Figures 5.07A-B). The difference in tiller number between 100ml and 500ml SVA treatments was deemed to be statistically significant for the *d3* mutant line by two-tailed t-test ($P<0.05$), though the increase of only 25% was far smaller than those seen in the WT and *tb1* lines. The difference, however, was not significant for the *d14* mutant. This result indicates that strigolactone is required for the coordination of tiller development in response to soil volume availability.

Despite similar maximum tiller numbers, the strigolactone mutant lines do not produce tillers in the same way in the two SVA treatments. For both lines, tiller number was similar between soil volumes until around 21 DaP (Figure 5.07C). Then, between days 21 and 42 DaP, the 500ml plants produced tillers at a faster rate than the 100ml plants. However, after 42 days the 500ml plants stop producing tillers and some tillers senesced. Meanwhile, the 100ml plants produced tillers at a slower but more consistent rate, resulting in a final tiller number similar to the maximum tiller number reached by the 500ml plants. Whilst the similar tiller numbers in both soil volumes do implicate strigolactone in coordinating wheat shoot architecture with SVA, this difference suggests that it is not the only signalling molecule that regulates this process. The observed difference in tiller production may result from the activity of one or more other hormones initially influencing tiller development, though the similarity in the final result may indicate that strigolactone has a more influential role.

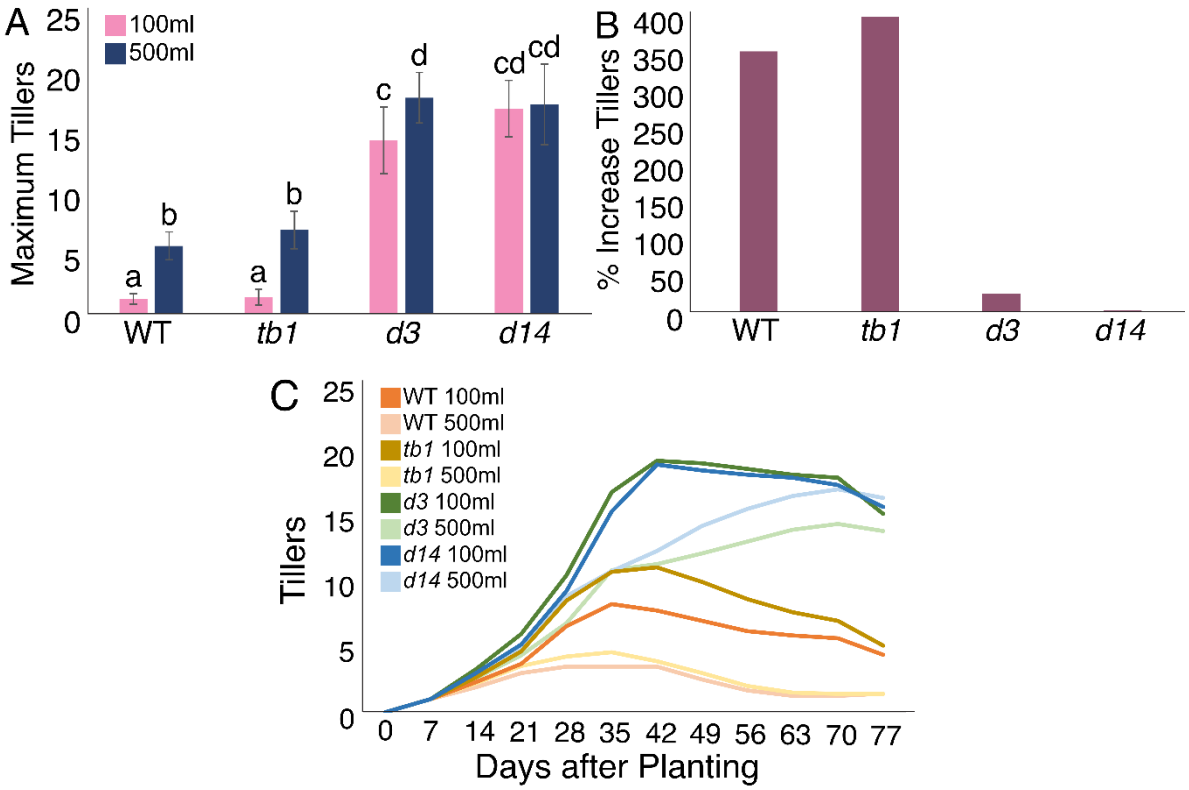

Figure 5.07: The effect of soil volume availability on tiller development in strigolactone signalling mutant wheat.

(A) Bar chart of mean maximum number of tillers per plant. The 100ml treatment is represented in pink; the 500ml treatment is represented in dark blue. Error bars are 1 standard deviation from the mean. Different letters above bars indicate statistically significant difference between treatments (ANOVA, $P<0.05$, n=10-12). **(B)** Bar chart of % increase in mean maximum number of tillers per plant. **(C)** Line chart of mean number of tillers per plant plotted against DaP. The 100ml treatments are represented in lighter shades; the 500ml treatments are represented in dark shades. Error bars are 1 standard deviation from the mean. Different letters above bars indicate statistically significant difference between treatments (ANOVA, $P<0.05$, n=10-12).

The greatly reduced tillering response observed in the *d3* and *d14* mutants was similarly observed for ear number. The mutant lines only increased ear number 17% and 39% in the 5-fold increase in SVA, compared with the wild type and *tb1* increases of 228% and 277% respectively (Figure 5.08A). Thus, it can be concluded that strigolactone is an important hormone in causing the observed reduction in ear number under SVA restricted treatments.

The two strigolactone mutants produced significantly fewer spikelets per ear than the wild type in both soil volumes (Figure 5.08B). However, contrary to the observed lack of sensitivity regarding tiller and ear number, the strigolactone mutants change their spikelet number by a greater extent than the wild type. This result is key in illustrating the complexity of hormonally regulated SVA response in wheat. Strigolactone does not act simply as a ‘make less under reduced SVA’ signal, but instead appears to act to redistribute growth amongst the shoot architecture. This data suggests that in wheat with functional strigolactone signalling, the developmental response to a limitation in SVA is to redistribute shoot development to prioritise spikelet production over the maintenance of a large number of tillers – hence these plants produce a small number of ears with a similar level of productivity to the 500ml treatment. In the mutant lines, a lack of functional strigolactone

signalling results in 100ml plants with a similar number of ears to the 500ml, with greatly reduced productivity.

The data shows that no difference in supernumerary spikelet production was observed between soil volumes or between mutants and wild type (Figure 5.08B), suggesting that whilst strigolactone is evidently involved in determining the number of rachis nodes that develop, it does not influence how many spikelets develop per node.

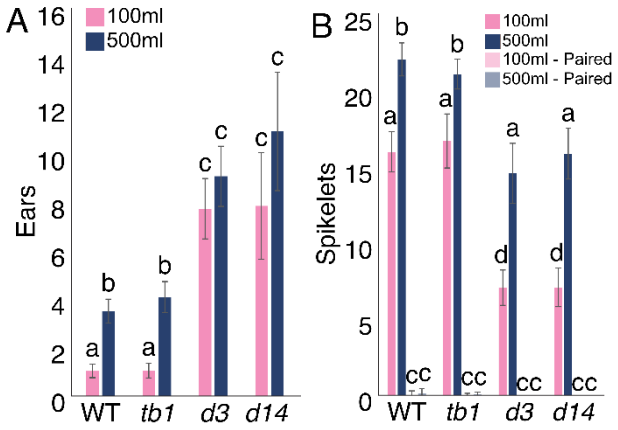

Figure 5.08: The effect of soil volume availability on shoot architecture development in strigolactone signalling mutant wheat.

(A) Bar chart of mean number of ears per plant. **(B)** Bar chart of mean number of spikelets and paired spikelets per ear.
Measurements taken at end of plant life. The 100ml treatment is represented in pink; the 500ml treatment is represented in dark blue. Error bars are 1 standard deviation from the mean. Different letters above bars indicate statistically significant difference between treatments (ANOVA, $P<0.05$, n=10-12).

Patterns in seed data all showed an increased sensitivity to SVA in the two strigolactone mutants. Whilst all four lines show an increased number of seeds per ear between the 100ml and 500ml treatments, the increase is far greater in the strigolactone mutants (Figure 5.09A). Seeds per ear increased 52% for the wild type, but 428% and 422% in the *d3* and *d14* mutants. Furthermore, seed mass per ear is a measurement that shows no statistically significant sensitivity to SVA change in

the wild type (Figure 5.09B), but in the strigolactone mutants seed mass per plant increases by 389% and 271%. These data appear to suggest that despite what may at first appear to be a developmental advantage in tiller and ear increase under SVA restriction, the increased number of ears is countered by an opposing reduction in spikelet and seed number. Predictably, SVA had a strong effect on total seed mass per plant in all lines (Figure 5.09C). This suggests that the previously observed wheat response to SVA, wherein tillering and seed number are highly affected and spikelet and seed mass per ear are not (Figure 5.01) is somewhat coordinated by strigolactone.

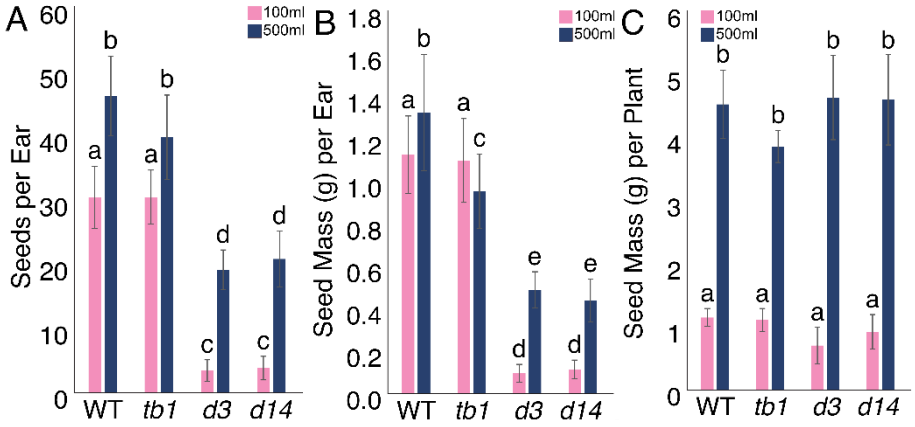

Figure 5.09: The effect of soil volume availability on seed development in strigolactone signalling mutant wheat.

(A) Bar chart of mean number of seeds per ear **(B)** Bar chart of mean seed mass (g) per ear **(C)** Bar chart of mean seed mass (g) per plant. Measurements taken at end of plant life. The 100ml treatment is represented in pink; the 500ml treatment is represented in dark blue. Error bars are 1 standard deviation from the mean. Different letters above bars indicate statistically significant difference between treatments (ANOVA, $P<0.05$, $n=10$-12).

The results reported in this section suggest that functional strigolactone signalling is essential for proper coordination of shoot architecture development with SVA. To further understand where and when these developmental differences occur, I conducted dissections of developing SAMs of the mutant lines in both SVA

treatments, to determine differences in rate of SAM development and spikelet production.

The data shows that stage of SAM development is significantly increased in the wild type over the strigolactone mutants in both treatments (Figure 5.10A), consistent with data presented in chapter 3 (discussed in section 3.17). The data further suggest that spikelet development in the mutant lines is insensitive to SVA (Figure 5.10B). In both lines there is no significant difference in spikelet ridges per SAM, whereas the wild type reduces spikelet ridges significantly in response to more restricted SVA, supporting the theory that strigolactone coordinates spikelet development in response to perceived SVA.

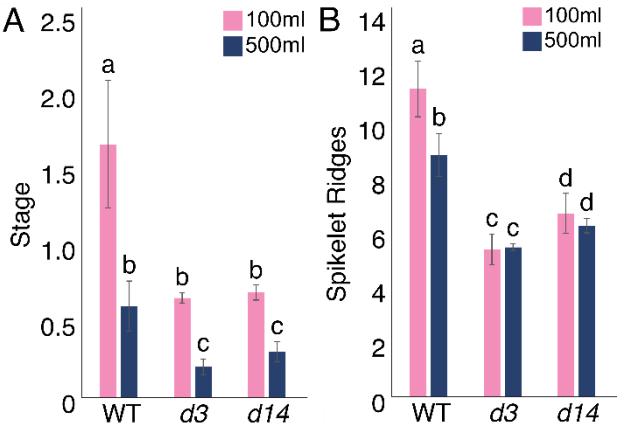

Figure 5.10: The effect of soil volume availability on SAM development in strigolactone signalling mutant wheat.

(A) Bar chart of mean stage of SAM development **(B)** Bar chart of mean number of spikelet ridges per SAM.

Measurements taken at 49 DaP. The 100ml treatment is represented in light blue; the 500ml treatment is represented in dark blue. Error bars are 1 standard deviation from the mean. Different letters above bars indicate statistically significant difference between treatments (ANOVA, $P<0.05$, n=3-5).

5.6 Characterising the shoot architecture of strigolactone mutant barley under soil volume restriction

The data presented in section 5.5 indicates a role for strigolactone signalling in coordinating wheat shoot development in response to SVA. There is little reporting on how wheat and other cereals coordinate their shoot development with perceived SVA. I hypothesised that barley, being closely related to wheat, would utilise similar mechanisms. I thus further hypothesised that strigolactone would play a similarly important role in barley. I investigated a *d14* null mutant line in barley, to test the hypothesis that the reduction in strigolactone sensitivity would affect barley shoot development in the same way as it does wheat. The *d14* mutant and the background control line were grown in the same treatments as the wheat in both 100ml and 500ml volumes. As with the wheat experiments in section 5.5, tiller number was taken weekly, and final architecture parameters were measured and compared between the two lines and the two soil volumes.

From 28 DaP, a statistically significant difference (two tailed t-test, $P<0.05$) in tiller number was observable between 100ml and 500ml plants in both lines (Figure 5.11A). From 35 DaP there was a significant difference between the two lines in the 100ml treatment, but not in the 500ml treatment. From 42 DaP until final seed set there was also a significant difference between the two lines in the 500ml treatment. As was reported in wheat (Figure 5.07A), the *d14* mutant produces more tillers under both SVA treatments, but unlike wheat, the *d14* response was proportionally similar to the WT. The *d14* mutant plants also produced significantly fewer spikelets per ear in both treatments than the wild type (Figure 5.11B). Interestingly, the increase in spikelet production between 100ml and 500ml treatments was similar in *d14* and WT plants (34% and 42% respectively) (Figure 5.11B). This result is different to wheat, where spikelet production in *d14* mutants exhibited greater sensitivity to differences in SVA (Figure 5.08B). This result appears to imply that strigolactone may have the same role coordinating ear and spikelet development in both species (i.e. maintaining a ratio of fewer, more productive ears), but is less important to maintaining this function under SVA restricted treatments in barley than it is in wheat.

The number of seeds per ear was significantly affected in both lines (Figure 5.11C), but seed mass per ear changed a small, but significant amount in *d14* and an insignificant amount in WT (Figure 5.11D). The wild-type response is highly similar to that observed in elite wheat (Figure 5.01D-F) and suggests that both species respond to SVA primarily by altering ear and seed number over seed size. Essentially, the *Triticeae* appear to broadly respond to SVA restriction by redistributing the development of their shoot architecture to favour a small number of highly productive ears. Reducing SVA results in relatively small reductions in spikelets per ear and seed mass per ear, but proportionally much larger ones in tiller number. In *d14* wheat this response is inverted and instead final tiller and ear number is maintained at a similar level, at the expense of a proportionally large reduction in spikelet and seed mass (Figures 5.08-5.09). However, in barley the *d14* line behaves much more similarly to the wild-type, suggesting a more important role for strigolactone in the coordination of this response in wheat than in barley.

SAM dissection further supports previous results that indicate strigolactone acts to accelerate SAM development that was identified in chapter 3, as the *d14* mutant is significantly earlier in development in both soil volumes (Figure 5.11E). Furthermore, both lines are significantly later in development under 100ml treatments compared with 500ml, suggesting that a reduction in strigolactone may cause this effect, alongside reduction in tillering and increased spikelet number.

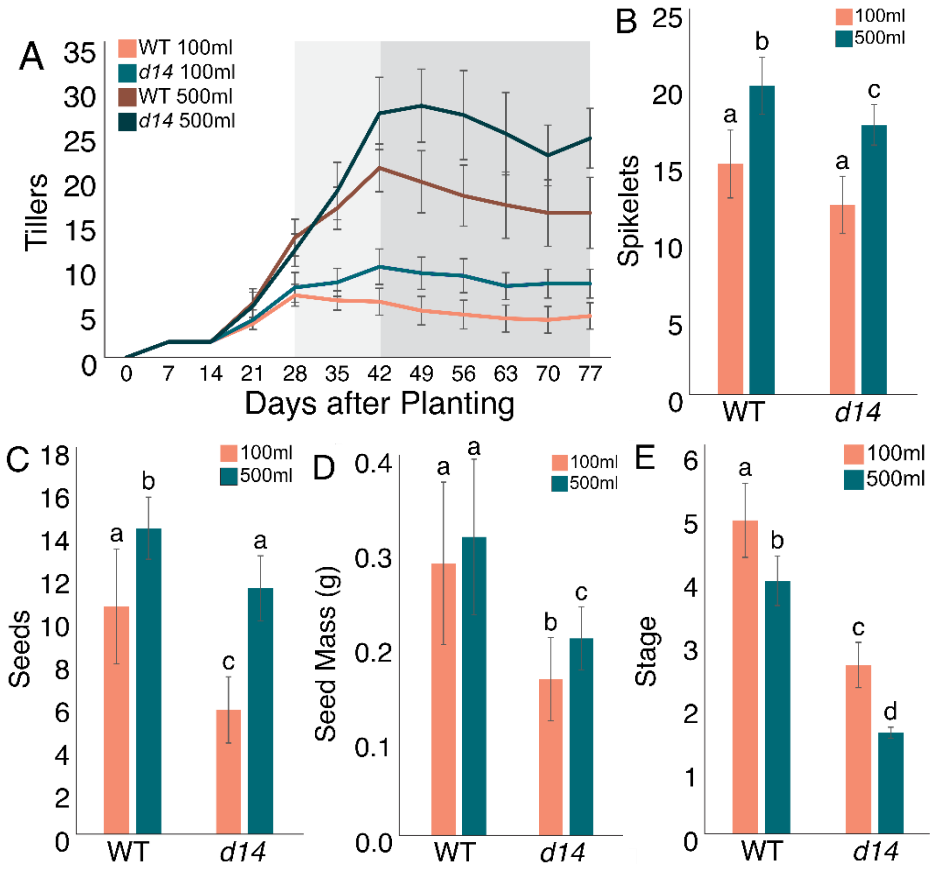

Figure 5.11: The effect of soil volume availability on SAM development in strigolactone signalling mutant barley.

(A) Line chart of mean number of tillers, plotted against DaP. Error bars are 1 standard deviation from the mean. Light grey represents timepoints at which there is a statistically significant difference between 100ml and 500ml; dark grey represents timepoints at which there is also a significant difference between WT and *d14* plants of the same SVA (ANOVA, P<0.05, n=3-5). **(B)** Bar chart of mean number of spikelets per ear, at end of plant life. **(C)** Bar chart of mean number of seed per ear **(D)** Bar chart of mean seed mass (g) per ear **(E)** Bar chart of mean stage of SAM development.

The 100ml treatment is represented in orange-pink; the 500ml treatment is represented in dark blue. Error bars are 1 standard deviation from the mean. Different letters above bars indicate statistically significant difference between treatments (ANOVA, P<0.05, n=3-5).

Almost every measurement in both lines in both species responds in the same way. The outlier where no change is seen in wheat *d14* tillering is likely due to the difference in tillering between the two lines, rather than a difference in strigolactone function. Therefore, the entire data set appears to support the hypothesis that wheat and barley have an equivalent response to SVA and that future insight from studies into one of the species can likely be applied to the other.

5.7 The effect of exogenous strigolactone treatment on wheat developmental response to soil volume availability

The experimental results presented in section 5.5 and 5.6 suggest that strigolactone may be responsible for coordinating shoot developmental response to soil volume availability in wheat and barley. To further test the validity of this theory, I hypothesised that an increase in perceived strigolactone would result in the opposite SVA response. I utilised the exogenous hormone treatment system first introduced in section 3.6 to study the effect of an increase in strigolactone, in comparison to the decrease in perceived strigolactone in the *d3* and *d14* mutant lines.

Therefore, plants of the elite wheat line Cadenza were grown in 100ml and 500ml soil volumes and treated with weekly injections of the synthetic strigolactone GR24 (following the protocol detailed in section 2.4.2). The effect of this treatment was studied by tracking tiller emergence. Further investigation was carried out by dissecting the meristems of emerged tillers and un-emerged buds to identify changes in rate of development and spikelet production.

In the 500ml treatment the GR24 treated plants show a significantly reduced tiller number at 42 DaP (Figure 5.12A). In the 100ml treatment GR24 treated plants shows a significantly reduced tiller number at 35 DaP, though this difference is no longer present at 49 DaP. Whilst both GR24 treated and control plants produce significantly more tillers in the 500ml treatment, in the GR24 treated plants, this increase is 275% compared with 364% in the control (Figure 5.12B). This result was unexpected, given that tillering of strigolactone insensitive plants was shown to be less sensitive to SVA than the control. This may have resulted from the 100ml plants

being so restricted by soil volume as to show no difference regardless of exogenous GR24 treatment. However, more promising was that the effect of the GR24 treatment was far more effective in 500ml plants, than in the 100ml plants, reducing tiller number by 24% in the former, but only 4% in the latter (Figure 5.12C). The lack of effect suggests the shoot system of 100ml plants already contains a high concentration of strigolactone, perhaps at a limiting ceiling, given the very low tiller development, which means a further increase has little additional effect.

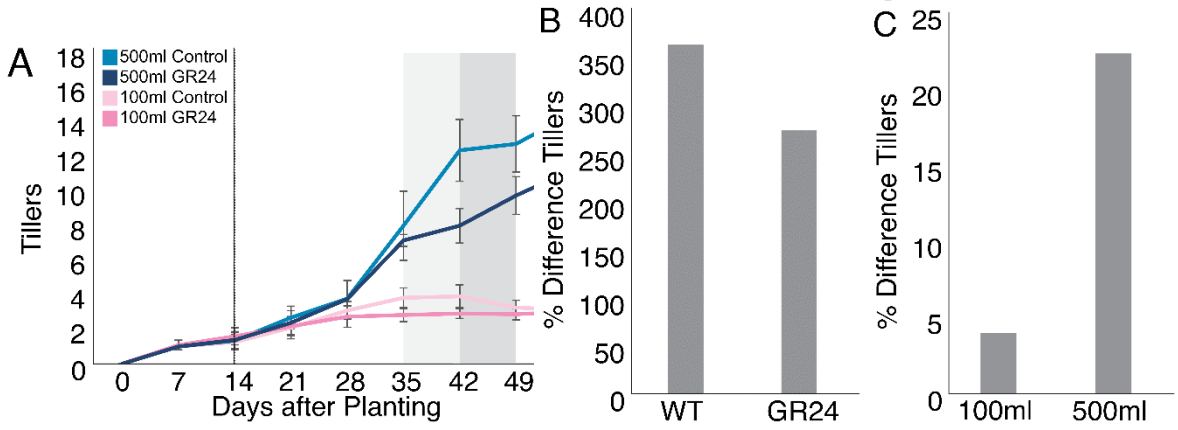

Figure 5.12: The effect of exogenous GR24 treatment on wheat tiller development in different soil volume availability treatments.

All GR24 treated plants were injected with 0.33ml per tiller of 100nM once per week beginning 14 DaP until 35 DaP.

(A) Bar chart of mean number of tillers, at 49 DaP. The 100ml treatment is represented in pink; the 500ml treatment is represented in blue; control plants are in the lighter shade, GR24 treated plants are in the darker shade. Error bars are 1 standard deviation from the mean. Different letters above bars indicate statistically significant difference between treatments at that time point (ANOVA, $P<0.05$, n=4-5). **(B)** Bar chart of % increase in number of tillers between 100ml and 500ml SVA treatments for WT and GR24 treated plants, at 49 DaP. (n=4-5). **(C)** Bar chart of % decrease in number of tillers between control and GR24 treated treatments, for 100ml and 500ml treated plants at 49 DaP. (n=4-5).

These results suggest a difference in response between the two soil volume treatments. However, the reduced response in the 100ml plants may be a result of their already highly restricted tiller number, leaving limited possibility for further tiller reduction. Hence, further experiments were carried out with the same soil volumes and treatments, in which the plant shoots were dissected, to further determine a difference in response.

The GR24 treatment has no effect on the number of unemerged meristems between plants in the same soil volume (Figure 5.13B). As a result of this, the total number of meristems was not found to be significantly different in either soil volume treatment (Figure 5.13C). Such a result implies that the effect on tiller number observed is solely the result of strigolactone's already reported function in modulating tiller bud outgrowth (Bennett *et al.*, 2016; Yuan *et al.*, 2023) rather than any specific role in modulating response to soil volume availability. This would explain the lack of tiller difference in the 100ml treatment, as in such plants tiller bud outgrowth is already highly restricted and therefore the increase in strigolactone in the shoot system can have little further effect.

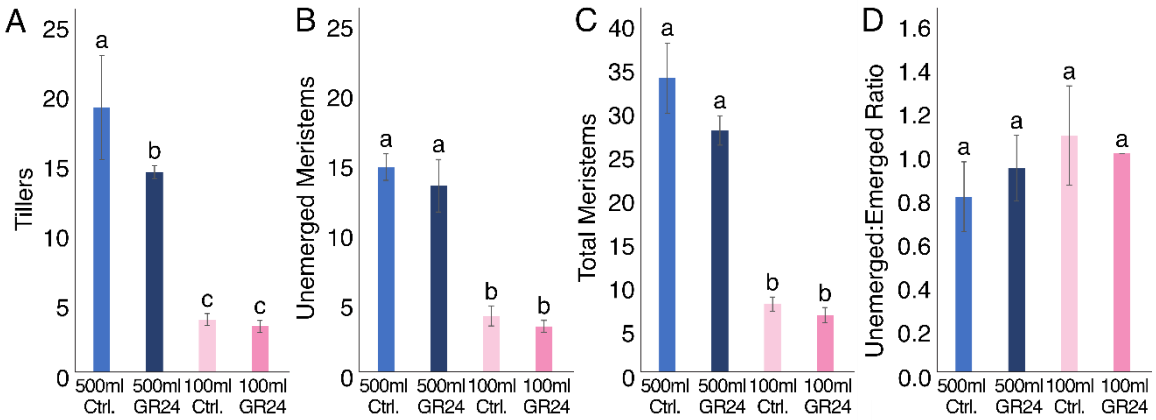

Figure 5.13: The effect of exogenous GR24 treatment on wheat tiller development and emergence in different soil volume availability treatments.

All GR24 treated plants were injected with 0.33ml per tiller of 100nM once per week beginning 14 DaP until 35 DaP.

(A) Bar chart of mean number of emerged tillers per plant **(B)** Bar chart of mean number of unemerged SAMs per plant. **(C)** Bar chart of mean number of total SAMs per plant. **(D)** Bar chart of mean ratio of unemerged to emerged SAMs.

Measurements taken at 49 DaP, calculated by dividing mean number of unemerged SAMs by mean number of emerged tillers. The 100ml treatment is represented in pink; the 500ml treatment is represented in blue; control plants are in the lighter shade, GR24 treated plants are in the darker shade. Error bars are 1 standard deviation from the mean. Different letters above bars indicate statistically significant difference between treatments (ANOVA, $P<0.05$, n=4-5).

As was first reported in Chapter 3 of this thesis, an increase in strigolactone appears to increase rate of shoot apical meristem development. However, as with tiller emergence, this effect is not seen in the 100ml plants (Figure 5.14A). It is possible that the lack of difference in the 100ml treatment is the result of an already increased quantity of strigolactone and therefore the GR24 treatment had a relatively smaller effect than in the 500ml plants. Furthermore, there is no significant difference in spikelet ridge number per meristem as a result of the GR24 treatment in either treatment (Figure 5.14B).

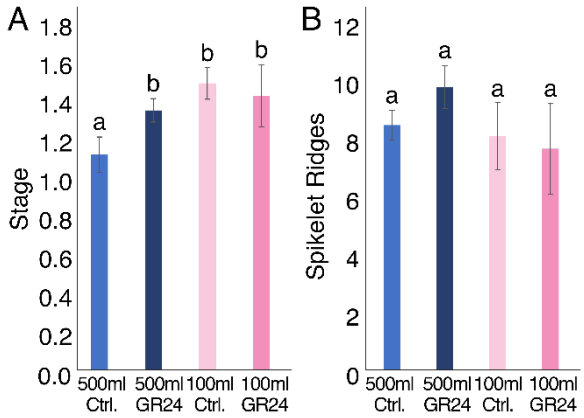

Figure 5.14: The effect of exogenous GR24 treatment on wheat SAM development and emergence in different soil volume availability treatments.

All GR24 treated plants were injected with 0.33ml per tiller of 100nM once per week beginning 14 DaP until 35 DaP.

(A) Bar chart of mean stage of SAM development **(B)** Bar chart of mean number of spikelet ridges per SAM.

Measurements taken at 49 DaP. The 100ml treatment is represented in pink; the 500ml treatment is represented in blue; control plants are in the lighter shade, GR24 treated plants are in the darker shade. Error bars are 1 standard deviation from the mean. Different letters above bars indicate statistically significant difference between treatments (ANOVA, $P<0.05$, $n=4$-5).

SAM stage of development and spikelet ridge number were ordered by tiller, to further investigate where changes between treatments may occur (Figures 5.15A-B). There is a clear difference in development between the two soil volume treatments, but no difference as a result of GR24 treatment. In both 100ml and 500ml plants, there is no significant difference between the control and GR24 treated plants at any tiller in either stage of development, or spikelet ridge number. There is however, a far stronger difference between tillers of the same plant in the 100ml treatments compared with the 500ml. On the main shoot SAM (tiller 0), there is no difference in stage or spikelet ridge number between the control 500ml and 100ml plants. However, a significant difference is seen for the later tillers, (Figure 5.15A),

which is the result of the later tillers of 100ml plants having progressively less productivity than in the 500ml plants.

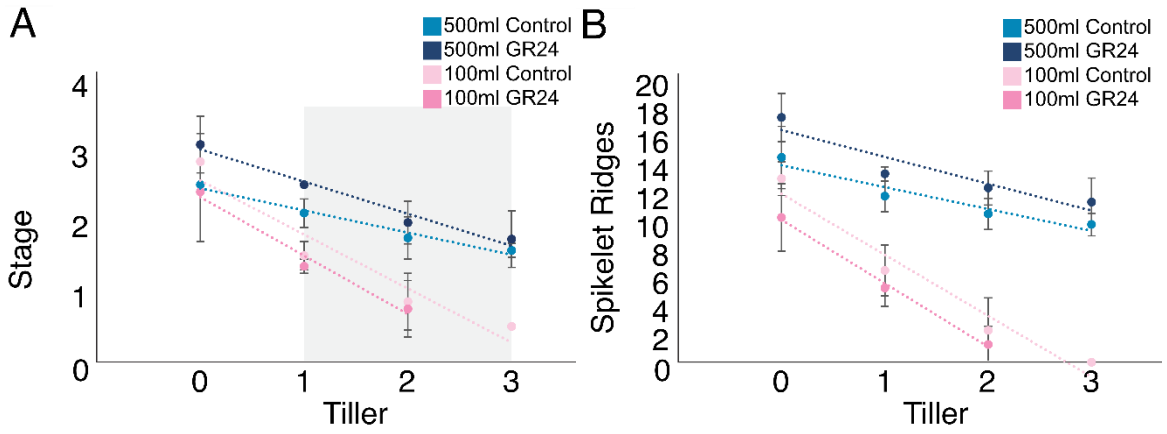

Figure 5.15: The effect of exogenous GR24 treatment on wheat SAM development by tiller in different soil volume availability treatments.

All GR24 treated plants were injected with 0.33ml per tiller of 100nM once per week beginning 14 DaP until 35 DaP.

(A) Scatter plot of mean stage of SAM development, at 49 DaP, at each first order tiller. The 100ml treatment is represented in pink; the 500ml treatment is represented in blue; control plants are in the lighter shade, GR24 treated plants are in the darker shade. Error bars are 1 standard deviation from the mean. Grey square indicates significant difference between 100ml and 500ml plants for control and GR24 at that tiller (ANOVA, $P<0.05$, n=4-5). **(B)** Scatter plot of mean number of spikelet ridges per SAM, at 49 DaP, at each first order tiller. The 100ml treatment is represented in pink; the 500ml treatment is represented in blue; control plants are in the lighter shade, GR24 treated plants are in the darker shade. Error bars are 1 standard deviation from the mean. At all tillers there is a significant difference between 100ml and 500ml plants for control and GR24 (ANOVA, $P<0.05$, n=4-5).

Taken together, these data are inconclusive in testing the hypothesis that strigolactone coordinates shoot development with SVA. However, this hypothesis is supported by the data in section 5.5 and therefore deserves further investigation.

5.8 Discussion

5.8.1 Effect of SVA on wheat development

The first aim of this chapter was to more thoroughly characterise the effect of soil volume availability on elite wheat shoot architecture.

SVA was shown to have the greatest effect on tiller and seed number (Figure 5.01A and 5.01D) with a smaller effect on spikelet number and seed mass per ear (Figure 5.01C and 5.0F). Planting density has previously been shown to affect grain filling in wheat, by specifically reducing the mass of grain in the middle spikelets (Liu, Liao and Liu, 2021). This report and my data suggest a complex interaction between SVA perception and seed mass that is poorly understood.

The shoot developmental response in both elite wheat lines was highly similar (Figure 5.01). A recent meta-analysis of wheat cultivars resulted in the suggestion that elite wheat cultivars have already been bred for relatively high tolerance to planting density (Postma *et al.*, 2021). In this context, the similarity between the two modern elite lines is not surprising. This confirms that future studies on one elite line are broadly applicable to others, but also might suggest that there is limited remaining space to improve wheat yield under denser planting conditions. It is possible that the perceived lack of effect on seed mass is the principal route through which elite wheat maintains relatively good yield under SVA restriction. Tiller and spikelet development are still highly sensitive to SVA and therefore better understanding how these develop in response to SVA may be a route for improving wheat yields.

Expression of central tillering coordinator *TaTB1* did not significantly change upon SVA restriction (Figure 5.05C). This suggests that the observed effect on tillering is enacted via some other pathway. For instance, through TaBA1 (BARREN STALK1) (Liu *et al.*, 2017a) or TaGRFs (Growth regulating factors) (J. Zhang *et al.*, 2021), both of which modulate wheat tillering. There is some evidence that TaGRFs are hormonally regulated by auxin and gibberellin, but there is currently no evidence that they are regulated by strigolactone (An *et al.*, 2019; J. Zhang *et al.*, 2021). Both of these hormones were shown to regulate tillering response to soil volume in *A.*

tauschii (Yu *et al.*, 2020) and could therefore also be key components in regulating wheat tillering response.

Investigation into how SVA affects tiller and SAM development revealed that the reduction in stage and spikelet production between successive meristems was increased by SVA restriction (Figure 5.03D-E) and that whilst SVA restriction significantly decreased spikelet number (Figure 5.01C), spikelet number did not decrease for the first order tillers (tillers 0-3) (Figure 5.04D). Together, this data suggests that wheat responds to perceived SVA limitation by shifting distribution of reproductive effort to maintain 'normal' productivity on the earliest and most productive tillers/ears.

5.8.2 Role of SL in coordination

Wheat *d3* and *d14* mutants showed almost no change in maximum tiller number in response to large changes in soil volume (Figure 5.07A-B) and qPCR analysis showed that in the wild-type, both genes were upregulated in response to SVA restriction (Figure 5.05A-B). These results strongly support my hypothesis that strigolactone has a role in modulating wheat tillering in response to SVA. Alongside other work which supports the involvement of strigolactone in SVA sensing in wheat (Wheeldon *et al.*, 2022; Y. Liu *et al.*, 2023), this presents strigolactone as an essential regulator of SVA response, both for volume perception and communicating perceived volume with the shoot system (Wheeldon *et al.*, 2022). However, changes in seed number and mass are still seen in the mutants, suggesting strigolactone only partially coordinates the response and other hormones such as auxin, gibberellin or cytokinin may be involved (He *et al.*, 2018; Yu *et al.*, 2020). Furthermore, *d14* mutants in barley showed a proportionally similar tillering response to SVA as the wild-type (Figure 5.11A), suggesting that strigolactone-mediated tillering response to SVA may not be shared by all *Triticeae.*

As shown throughout this thesis (Figure 3.37, 4.09 and 5.10A), strigolactone appears to have an acceleration effect on SAM development. Such an effect is seen as the result of SVA restriction (Figure 5.10A), suggesting increased strigolactone concentration in the shoot system in volume restricted plants. Furthermore,

exogenous GR24 treatment had little effect on highly restricted SVA plants, instead of the usual effect decreasing tillering and increasing rate of SAM development (Figure 3.36-3.37). This could suggest that these plants already have a high concentration of endogenous strigolactone in their shoot system, hence the treatment could have little further effect. However, these plants already produced a small number of tillers, which were often early in development. Future studies could resolve this using later dissections and higher tillering lines, to determine if there was still no effect from a further increase in strigolactone.

5.8.3 Future work and concluding remarks

The work presented in this chapter has described the developmental response of wheat shoot architecture to SVA and suggested that strigolactone coordinates the tillering response in a *TB1* independent manner. The null-mutants were insensitive to strigolactone throughout the entire plant system and the GR24 treatment specifically increased strigolactone in the shoot, therefore, it is unlikely that the observed results were simply the result of already reported method by which strigolactone influences SVA response as a volume sensing exudate in the root system (Reeves *et al.*, 2022; Wheeldon *et al.*, 2022).

It was recently proved that grafting can be successfully performed in monocots (including wheat). The use of such a technique could be used to graft *d3* and *d14* shoots onto wild-type roots, which could be studied to confirm the effect of strigolactone insensitivity on shoot development, but with unaffected function in the roots. Such work would be further supported by studies quantifying strigolactone levels in the shoot systems of plants growing in different soil volumes. The typically low concentration and high degradability of strigolactones have previously prohibited such studies, however recent mass-spectrometry based techniques have been developed that allow for strigolactone quantification (Rial *et al.*, 2020; Mi, Liew and Al-Babili, 2022). These could be used to determine if strigolactone levels are increased in the shoots of SVA restricted plants and even to study if concentration is increased in first order SAMs, to encourage the accelerated development of these over higher order tiller SAMs in SVA restricted wheat.

Whilst some evidence exists here and in the literature for strigolactone as a coordinator of tiller development with SVA (Figure 5.07), strigolactone also appears to have relatively little involvement in other aspects of response, including spikelet and seed number (Figure 5.08B and 5.09A). Other hormones should therefore be investigated as additional coordinators of SVA response. Auxin, gibberellin and cytokinin currently appear to be promising candidates (He *et al.*, 2018; An *et al.*, 2019; Yu *et al.*, 2020; J. Zhang *et al.*, 2021), given their reported ability to influence shoot development and interact with strigolactone (Hayward *et al.*, 2009; Rameau *et al.*, 2015) and the evidence that auxin and gibberellin concentration decreases in winter wheat under denser line spacing, and consequently modulating tillering (Y. Liu *et al.*, 2023).

5.9 References

Alexandratos, N. (2012) ‘World Agriculture towards 2030/2050: the 2012 revision’, Global Perspective Studies Team FAO Agricultural Development Economics Division.

An, J. et al. (2019) ‘The miRNA–mRNA Networks Involving Abnormal Energy and Hormone Metabolisms Restrict Tillering in a Wheat Mutant dmc’, International Journal of Molecular Sciences, 20(18), p. 4586.

Barbier, F.F. et al. (2019) ‘An Update on the Signals Controlling Shoot Branching’, Trends in Plant Science, 24(3), pp. 220–236.

Bar-Tal, A. et al. (1995) ‘Root restriction and N-NO3 solution concentration effects on nutrient uptake, transpiration and dry matter production of tomato’, Scientia Horticulturae, 63(3), pp. 195–208.

Bennett, T. et al. (2016) ‘Strigolactone regulates shoot development through a core signalling pathway’, Biology Open, 5(12), pp. 1806–1820.

Carmi, A. and Heuer, B. (1981) ‘The Role of Roots in Control of Bean Shoot Growth’, Annals of Botany, 48(4), pp. 519–527.

Conley, D.J. et al. (2009) ‘Controlling Eutrophication: Nitrogen and Phosphorus’, Science, 323(5917), pp. 1014–1015.

Dixon, L.E. et al. (2018) ‘TEOSINTE BRANCHED1 regulates inflorescence architecture and development in bread wheat (Triticum aestivum)’, Plant Cell, 30(3), pp. 563–581.

Fischer, R.A. et al. (2019) ‘Yield response to plant density, row spacing and raised beds in low latitude spring wheat with ample soil resources: An update’, Field Crops Research, 232, pp. 95–105.

Guo, F. et al. (2024) ‘Crosstalk between Brassinosteroids and Other Phytohormones during Plant Development and Stress Adaptation’, Plant and Cell Physiology, p. pcae047.

Hayward, A. et al. (2009) ‘Interactions between auxin and strigolactone in shoot branching control’, Plant Physiology, 151(1), pp. 400–412.

He, R. et al. (2018) ‘Quantitative Changes in the Transcription of Phytohormone-Related Genes: Some Transcription Factors Are Major Causes of the Wheat Mutant dmc Not Tillering’, International Journal of Molecular Sciences, 19(5), p. 1324.

Hess, L. and De Kroon, H. (2007) ‘Effects of rooting volume and nutrient availability as an alternative explanation for root self/non-self discrimination’, Journal of Ecology, 95(2), pp. 241–251.

de Jong, M. et al. (2019) ‘Natural variation in Arabidopsis shoot branching plasticity in response to nitrate supply affects fitness’, PLoS Genetics, 15(9).

Kohlen, W. et al. (2011) ‘Strigolactones are transported through the xylem and play a key role in shoot architectural response to phosphate deficiency in nonarbuscular mycorrhizal host arabidopsis’, Plant Physiology, 155(2), pp. 974–987.

Liu, J. et al. (2017) ‘miR156-Targeted SBP-Box Transcription Factors Interact with DWARF53 to Regulate TEOSINTE BRANCHED1 and BARREN STALK1 Expression in Bread Wheat’, Plant Physiology, 174(3), pp. 1931–1948.

Liu, R. et al. (2021) ‘Association of tad14-4d, a gene involved in strigolactone signaling, with yield contributing traits in wheat’, International Journal of Molecular Sciences, 22(7).

Liu, Y., Liao, Y. and Liu, W. (2021) ‘High nitrogen application rate and planting density reduce wheat grain yield by reducing filling rate of inferior grain in middle spikelets’, The Crop Journal, 9(2), pp. 412–426.

Liu, Yue et al. (2023) ‘Cytokinin-inducible response regulator SlRR6 controls plant height through gibberellin and auxin pathways in tomato’, Journal of Experimental Botany, p. erad159.

Mi, J., Liew, K.X. and Al-Babili, S. (2022) ‘Ultrahigh-Performance Liquid Chromatography–Mass Spectrometry Analysis of Carotenoid-Derived Hormones and Apocarotenoids in Plants’, Current Protocols, 2(2), p. e375.

Molotoks, A. et al. (2018) ‘Global projections of future cropland expansion to 2050 and direct impacts on biodiversity and carbon storage’, Global Change Biology, 24(12), pp. 5895–5908.

Poorter, H. et al. (2012) ‘Pot size matters: a meta-analysis of the effects of rooting volume on plant growth’, Functional Plant Biology, 39(11), p. 839.

Postma, J.A. et al. (2021) ‘Dividing the pie: A quantitative review on plant density responses’, Plant, Cell & Environment, 44(4), pp. 1072–1094.

Qi, J. et al. (2024) ‘The role of strigolactones in resistance to environmental stress in plants’, Physiologia Plantarum, 176(4), p. e14419.

Rameau, C. et al. (2015) ‘Multiple pathways regulate shoot branching’, Frontiers in Plant Science, 5, p. 741.

Reeves, G. et al. (2022) ‘Monocotyledonous plants graft at the embryonic root–shoot interface’, Nature, 602(7896), pp. 280–286.

Rial, C. et al. (2020) ‘Quantification of Strigolactones’, in M. Rodríguez-Concepción and R. Welsch (eds) Plant and Food Carotenoids: Methods and Protocols. New York, NY: Springer US, pp. 199–208.

Umehara, M. et al. (2010) ‘Contribution of strigolactones to the inhibition of tiller bud outgrowth under phosphate deficiency in rice’, Plant and Cell Physiology, 51(7), pp. 1118–1126.

Wang, B., Smith, S.M. and Li, J. (2018) ‘Genetic Regulation of Shoot Architecture’, Annual Review of Plant Biology 69, pp.437-468.

Wheat eFP Browser (no date). Available at: https://bar.utoronto.ca/efp_wheat/cgi-bin/efpWeb.cgi (Accessed: 22 July 2024).

Wheeldon, C.D. et al. (2021) ‘Wheat plants sense substrate volume and root density to proactively modulate shoot growth’, Plant Cell and Environment, 44(4), pp. 1202–1214.

Wheeldon, C.D. et al. (2022) ‘Environmental strigolactone drives early growth responses to neighboring plants and soil volume in pea’, Current Biology, 32(16), pp. 3593-3600.e3.

Wheeldon, C.D. and Bennett, T. (2020) ‘There and back again: An evolutionary perspective on long-distance coordination of plant growth and development’, Seminars in Cell and Developmental Biology, 109(2021), pp. 55–67.

Yoneyama, K. et al. (2022) ‘Supra-organismal regulation of strigolactone exudation and plant development in response to rhizospheric cues in rice’, Current Biology, 32(16), pp. 3601-3608.

Yong, J.W.H. et al. (2010) ‘Effects of root restriction on growth and associated cytokinin levels in cotton (Gossypium hirsutum)’, Functional Plant Biology, 37(10), pp. 974–984. .

Yu, H. et al. (2020) ‘Effects of plant density on tillering in the weed grass Aegilops tauschii Coss. and its phytohormonal regulation’, Plant Physiology and Biochemistry, 157, pp. 70–78.

Yuan, Y. et al. (2023) ‘Unlocking the Multifaceted Mechanisms of Bud Outgrowth: Advances in Understanding Shoot Branching’, Plants, 12(20), p. 3628.

Zhang, J. et al. (2021) ‘Key wheat GRF genes constraining wheat tillering of mutant dmc’, PeerJ, 9, p. e11235.

Chapter 6

General Discussion

6.1 Relevance of tiller location and timing on final productivity

It is already established that successively emerging cereal tillers have a ‘productivity gap’ (Mohapatra and Kariali, 2008), in which the meristems and ears of later emerging tillers are less productive, leading to the suggestion that high yield cereal ideotypes would produce only a small number of the most productive tillers (Wang, Smith and Li, 2018; Senapati and Semenov, 2019). However, there has been very little work on how this productivity gap is affected by resource availability, though one paper has suggested that increased nitrate availability reduces the gap in rice (Wang *et al.*, 2017).

The overall focus of this thesis has been to investigate how internal and external stimuli are coordinated with the development of reproductive shoot architecture in cereals. To develop a more detailed understanding of this coordination, I consistently gathered data on when and where each tiller emerged. Such experiments revealed that upon resource restriction, the gap in productivity between successive meristems increases, whether resource restriction resulted from nitrate restriction (Figure 4.06), soil volume restriction (Figure 5.03) or increased demand from high spikelet number (Figure 3.04). For all three, the negative correlation between order of tiller emergence and rate of meristem and spikelet development increased. My work suggests that this shoot developmental response to resource availability is under-investigated. Improved understanding of how resource availability is communicated to successive meristems, and how resource perception interacts with correlative inhibition and flowering time in cereals might inform efforts to produce cereals with improved yield, by specifically improving late tiller yields (Figure 6.01).

The observed approach might have evolved as a mechanism for optimising whole plant productivity under resource restriction. However, plants have also likely evolved to be conservative with resources in a method that is perhaps advantageous in a wild context but is limiting in an agricultural one. This further utilisation may allow for crops with a reduced productivity gap between tillers, in both resource restricted and abundant contexts (Figure 6.01).

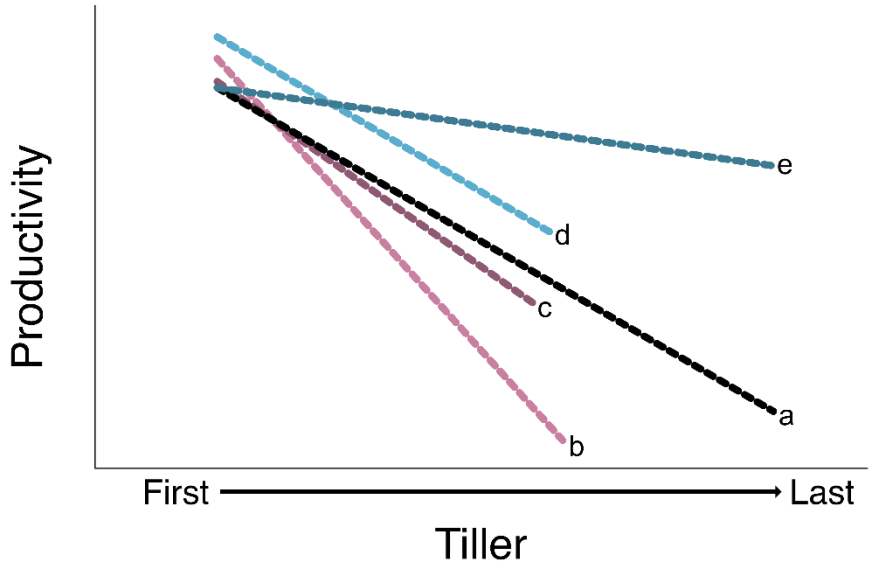

Figure 6.01: Illustrative comparison of observed and theoretical ideal trends in successive tiller productivity

a) A hypothetical average trajectory for successive tillers gradually reducing productivity (e.g. rate of development, spikelet number) under resource abundant conditions; b) The observed effect on the trend upon resource restriction; c) A theoretical 'resource restriction insensitive' ideotype, in which the productivity of later tillers is maintained under resource restriction, to maintain a total output similar to that under resource abundance; d) The trajectory of previously proposed cereal ideotype, in which the later, less productive tillers are not produced, allowing the plant to direct reproductive effort to the highly productive earlier tillers, resulting in improved total yield; e) An alternative ideotype, in which the productivity gap between successive tillers is reduced, resulting in later tillers with productivity levels similar to those of earlier tillers, resulting in overall productivity increase.

6.2 Rate of shoot meristem development

Cytokinin and strigolactone have been studied as known signals coordinating resource availability and shoot architecture (Takei *et al.*, 2004; Umehara *et al.*, 2008; de Jong, Ongaro and Ljung, 2014; Müller *et al.*, 2015; Yeh *et al.*, 2015; Liu *et al.*, 2021b; Wheeldon *et al.*, 2022; Ai *et al.*, 2024). A previously unreported effect that was repeatedly observed in my work was the ability for cytokinin to delay (Figure 3.19A) and strigolactone to accelerate (Figure 3.28A) SAM development

respectively. These hormones are already known to affect tiller and spikelet development (Liu *et al.*, 2021b; Ai *et al.*, 2024; Bai *et al.*, 2024) and rate of meristem development is a major determinant of final productivity in many plants (Park *et al.*, 2012; Brambilla *et al.*, 2017; Goldshmidt *et al.*, 2022), including cereals. Their modulation of rate of development may be an additional mechanism through which they influence shoot architecture, though these are likely interrelated phenomena.

Tuning of cytokinin and strigolactone levels in specific tissues and time points has already been proposed as a promising pathway for improving crop yields (Chen *et al.*, 2020; Kelly, Tucker and Brewer, 2023; Rathore *et al.*, 2024). The ability for these hormones to regulate rate of SAM development further supports this idea, and suggests that specifically, manipulation of rate of SAM development could be utilised as a pathway for yield improvement. Furthermore, it is possible that the productivity gap, discussed in section 6.1, results from altered strigolactone and cytokinin availability in the shoot system for later emerging tillers. Future work using recently developed techniques (Rial *et al.*, 2020; Mi, Liew and Al-Babili, 2022) quantifying hormonal levels in successive meristems on the same plant could therefore be highly informative in elucidating how hormonal sink-source relationships result in the observed productivity gap and its change in response to resource restriction.

6.3 Response to soil-based resource restriction

Chapters 4 and 5 of this thesis were dedicated to investigating the coordination of wheat shoot development with nitrate availability and soil volume availability. Whilst volume and nutrient sensing elicit distinct responses (Poorter *et al.*, 2012; Wheeldon *et al.*, 2020), they are highly related and in field conditions restriction of soil volume is likely to coincide with restriction of nutrient availability. The observed effects of restriction of nitrate or soil volume individually resulted in reduction in tiller and spikelet number and increase in stage of meristem development (Figures 4.03 and 5.03). Additionally, wheat responded to both restrictions with a shift in reproductive effort towards maintaining productivity in the earliest emerging tillers (as discussed in section 6.1). Strigolactone was identified as a major coordinator of the

developmental changes in response to both, despite the more well-established role for cytokinin in nitrate response in other plants (Takei *et al.*, 2004; Müller *et al.*, 2015). These data support the theory that strigolactone functions as a general response coordinator, integrating several points of environmental information regarding soil volume, nitrate availability and phosphate availability (Kapulnik and Koltai, 2016; de Souza Campos *et al.*, 2019), to influence cereal shoot architecture development accordingly. These roles make it a possible candidate for not only coordinating distinct responses of shoot development with nitrate and soil availability, but a response that integrates the two. For instance, increased wheat planting density has been shown to alter nitrogen uptake (Dai *et al.*, 2014). Future work might investigate whether strigolactone is involved in such developmental feedback.

	Resource restriction	**Cytokinin**	**Strigolactone**
Tiller number	↓	↑	↓
Spikelet number	↓	↑	-
Rate of SAM development	↑	↓	↑

Figure 6.02: Generalised effects of resource restriction on wheat

Table summarising the observed effects of resource limitation, cytokinin and strigolactone on wheat. Green arrows indicate an increase, red arrows indicate a decrease, grey indicates a lack of conclusive evidence.

Taken together, resource restriction (either nitrate or soil volume availability) resulted in a reduction in tiller and spikelet number, an increase in mean rate of SAM development and a larger decrease in rate of SAM development and spikelet number between successive meristems (Figures 4.05, 4.06 and 5.03). These physiological changes are highly similar to the effects of strigolactone and opposite to the effects of cytokinin (Figure 6.02), presented both in this work (Figures 4.17, 4.18, 5.07 and 5.10) and the literature (Umehara *et al.*, 2008; Yeh *et al.*, 2015; Liu *et al.*, 2021b; Ai *et al.*, 2024). I therefore hypothesise that both cytokinin and

strigolactone are important coordinators of wheat shoot development with nitrate and soil volume availability. Further work could confirm this by quantifying endogenous hormone levels in the developing shoot of resource abundant and restricted plants.

6.4 Conclusion

Here I have presented details regarding shoot architecture developmental response to resource restriction, within several ‘resource’ contexts. The data implicates cytokinin and strigolactone in the underlying mechanism by which the physiological responses are coordinated. This work may act as a base for future investigations into correlative inhibition and resource response in wheat and other cereals. In particular, I identify the alteration of productivity in later emerging tillers and the potential involvement of strigolactone in this as particularly promising future lines of inquiry.

6.5 References

Ai, G. et al. (2024) ‘Dissecting the molecular basis of spike traits by integrating gene regulatory networks and genetic variation in wheat’, Plant Communications, 5(5), p. 100879.

Bai, J. et al. (2024) ‘Strigolactone and abscisic acid synthesis and signaling pathways are enhanced in the wheat oligo-tillering mutant ot1’, Molecular Breeding : New Strategies in Plant Improvement, 44(2), p. 12.

Brambilla, V. et al. (2017) ‘The Importance of Being on Time: Regulatory Networks Controlling Photoperiodic Flowering in Cereals’, Frontiers in Plant Science, 8.

Chen, L. et al. (2020) ‘Cytokinin dehydrogenase: a genetic target for yield improvement in wheat’, Plant Biotechnology Journal, 18(3), pp. 614–630.

Dai, X. et al. (2014) ‘Increased plant density of winter wheat can enhance nitrogen–uptake from deep soil’, Plant and Soil, 384(1), pp. 141–152.

Goldshmidt, A. et al. (2022) ‘Tuning of meristem maturation rate increases yield in multiple Triticum aestivum cultivars’, Plant Direct, 6(11), p. e459.

de Jong, M., Ongaro, V. and Ljung, K. (2014) ‘Auxin and Strigolactone Signaling are Required for Modulation of Arabidopsis Shoot Branching by Nitrogen Supply’, Plant Physiology, 166(1), pp. 384–395.

Kapulnik, Y. and Koltai, H. (2016) ‘Fine-tuning by strigolactones of root response to low phosphate’, Journal of Integrative Plant Biology, 58(3), pp. 203–212.

Kelly, J.H., Tucker, M.R. and Brewer, P.B. (2023) ‘The Strigolactone Pathway Is a Target for Modifying Crop Shoot Architecture and Yield’, Biology, 12(1), p. 95.

Liu, R. et al. (2021) ‘Association of tad14-4d, a gene involved in strigolactone signaling, with yield contributing traits in wheat’, International Journal of Molecular Sciences, 22(7).

Mi, J., Liew, K.X. and Al-Babili, S. (2022) ‘Ultrahigh-Performance Liquid Chromatography–Mass Spectrometry Analysis of Carotenoid-Derived Hormones and Apocarotenoids in Plants’, Current Protocols, 2(2), p. e375.

Mohapatra, P.K. and Kariali, E. (2008) ‘Time of emergence determines the pattern of dominance of rice tillers’, Australian Journal of Crop Science, 1(2), pp. 53-62.

Müller, D. et al. (2015) ‘Cytokinin is required for escape but not release from auxin mediated apical dominance’, Plant Journal, 82(5), pp. 874–886.

Park, S.J. et al. (2012) ‘Rate of meristem maturation determines inflorescence architecture in tomato’, Proceedings of the National Academy of Sciences of the United States of America, 109(2), pp. 639–644.

Poorter, H. et al. (2012) ‘Pot size matters: a meta-analysis of the effects of rooting volume on plant growth’, Functional Plant Biology, 39(11), p. 839.

Rathore, R.S. et al. (2024) ‘Concurrent improvement of rice grain yield and abiotic stress tolerance by overexpression of cytokinin activating enzyme LONELY GUY (OsLOG)’, Plant Physiology and Biochemistry, 211, p. 108635.

Rial, C. et al. (2020) ‘Quantification of Strigolactones’, in M. Rodríguez-Concepción and R. Welsch (eds) Plant and Food Carotenoids: Methods and Protocols. New York, NY: Springer US, pp. 199–208.

Senapati, N. and Semenov, M.A. (2019) ‘Assessing yield gap in high productive countries by designing wheat ideotypes’, Scientific Reports, 9(1).

de Souza Campos, P.M. et al. (2019) ‘Phosphate acquisition efficiency in wheat is related to root:shoot ratio, strigolactone levels, and PHO2 regulation’, Journal of Experimental Botany, 70(20), pp. 5631–5642.

Takei, K. et al. (2004) AtIPT3 is a Key Determinant of Nitrate-Dependent Cytokinin Biosynthesis in Arabidopsis, Plant Cell Physiol, pp. 1053–1062.

Umehara, M. et al. (2008) ‘Inhibition of shoot branching by new terpenoid plant hormones’, Nature, 455(7210), pp. 195–200. Available at: https://doi.org/10.1038/nature07272.

Wang, B., Smith, S.M. and Li, J. (2018) ‘Genetic Regulation of Shoot Architecture’, Annual Review of Plant Biology 69, pp.437-468.

Wang, Y. et al. (2017) ‘Effects of nitrogen and tiller type on grain yield and physiological responses in rice’, AoB Plants, 9(2).

Wheeldon, C.D. et al. (2021) ‘Wheat plants sense substrate volume and root density to proactively modulate shoot growth’, Plant Cell and Environment, 44(4), pp. 1202–1214.

Wheeldon, C.D. et al. (2022) ‘Environmental strigolactone drives early growth responses to neighboring plants and soil volume in pea’, Current Biology, 32(16), pp. 3593-3600.

Yeh, S.Y. et al. (2015) ‘Down-Regulation of Cytokinin Oxidase 2 Expression Increases Tiller Number and Improves Rice Yield’, Rice, 8(1), pp. 1–13.